Preface

On March 29 and 30, 2011, the European VLBI Group for Geodesy and Astronomy (EVGA) held its 20th meeting on the invitation of the Max Planck Institute for Radio Astronomy, Bonn, Germany. Starting 31 years ago on the initiative of Prof. James Campbell this series of conferences can look back to an impressive record. Today, EVGA has firmly settled for a two-year sequence of its meetings. Starting in Bonn in 1980 the venue has come back to its initial location at 2011 again, though at a different institute. In the meantime, many different groups have hosted the meetings at various places in Europe as can be read from the table to the right.

Table 1 Previous meetings

Bonn, Germany	April	1980
Madrid, Spain	December	1981
Delft, Netherlands	November	1983
Onsala, Sweden	June	1985
Wettzell, Germany	November	1986
Medicina, Italy	April	1988
Madrid, Spain	October	1989
Dwingeloo, Netherlands	June	1991
Bad Neuenahr, Germany	October	1993
Matera, Italy	May	1995
Onsala, Sweden	August	1996
Hönefoss, Norway	September	1997
Viechtach, Germany	February	1999
San Pietro, Italy	September	2000
Barcelona, Spain	September	2001
Leipzig, Germany	May	2003
Noto, Italy	April	2005
Vienna, Austria	April	2007
Bordeaux, France	April	2009
Bonn, Germany	March	2011

As with the other 19 meetings before, the occasion was dedicated to the presentations of the current status and of recent results in the form of oral and poster presentations. With 80 participants from Europe as well as from overseas, the meeting was one of the biggest clearly indicating that geodetic and astrometric VLBI in Europe is an important cornerstone of worldwide VLBI research. The number of contributions has increased to an impressive 41 talks and 13 posters with many exciting new results and ideas. We are grateful to all authors who have submitted their manuscripts for publication in these proceedings and hope that many more readers will draw interesting information from the papers.

Walter Alef, Simone Bernhart, Axel Nothnagel

Bonn, July 2011

Contents

Past and present EVGA activities

New technological developments

Status and development reports

VLBI2010

Analysis reports and strategies

Solutions and interpretations of VLBI results

Observational programs

Progress and outlook in VLBI applications

EVGA - Looking back at the early beginnings

J. Campbell

Abstract On the occasion of the 20th EVGA meeting, 31 years after the first European VLBI meeting for Geodesy and Astrometry in April 1980 in Bonn, Germany, it seems appropriate to take a look back at the early beginnings of a cooperative European effort to establish a regional geodetic VLBI network. It was mainly devoted to geodetic, or rather geodynamic, and astrometric research, but was open also to subjects of general interest that were relevant to VLBI. The paper traces the early developments in some detail and refers to the continuing series of Workshop Proceedings for events of the more recent past.

Keywords EVGA, History

1 Introduction

In the early 1970's the news about the first successful VLBI experiments carried out by leading teams in the US and Canada quickly spread to interested scientific communities around the globe. For geodesists in particular, the technical developments at Haystack Observatory and MIT (Dept. of Earth and Planetary Sciences, Shapiro et al. 1974 and 1976) raised special interest: the Mark I bandwidth synthesis method was aimed at high group delay resolution in order to resolve the baseline-source geometry with the highest possible precision. In Europe, in the mid-seventies, the Onsala Space Observatory in Sweden became partner to the US for the first transatlantic baselines measured to decimeter precision (Robertson 1975, Herring et al. 1981).

At the Geodetic Institute of the University of Bonn contacts with the Max-Planck-Institute for Radio Astronomy in Bonn (MPIfR) were established in 1974 and a baseline calibration software (VLBASCAL, written by I. Pauliny-Toth on the basis of Cohen and Shaffer 1971) was modified and expanded to become the nucleus of the Bonn Geodetic VLBI data analysis system (Schuh 1986). Subsequently (1977 and 1979) two successive research grants were obtained from the German Science Foundation (Deutsche Forschungsgemeinschaft DFG) in cooperation with the Astronomical Institute of the Bonn University (P. Brosche), to explore the possibilities of performing specially designed geodetic and astrometric VLBI experiments using existing radio telescopes in Europe. These grants included the development of geodetic VLBI software and the organisation of a global astro-geodetic pilot experiment. Several trips to the US in 1979 and 1980 were essential to establish personal contacts with leading VLBI scientists at both the East Coast (Haystack-MIT, NASA/GSFC and NRL (Naval Research Laboratory)) and West Coast (NASA-JPL, Caltech) VLBI centers. The new MkIII data acquisition system developed in a cooperative effort of Haystack-MIT and NASA Goddard Space Flight Center on the East Coast and the use in the DSN of the less costly MkII bandwidth synthesis system by JPL on the West Coast could be studied on-site. Close contacts were also made with the operational center of the newly established POLARIS Earth rotation network of NOAA-National Geodetic Survey (NGS) at Rockville, MD.

In order to bring together interested groups from all parts of Europe two working meetings were organised at Bonn (AGRAM 1 and 2 - meetings in

James Campbell
Rheinische Friedrich-Wilhelms Universität Bonn, IGG, Nußallee 17, D-53115 Bonn, Germany

March 9, 1977 and November 6, 1978), which may be considered as precursors to the first truly European geodetic VLBI meeting in April 1980. At the second AGRAM (Astronomisch-geodätische Nutzung Radiointerferometrischer Methoden) meeting in 1978 the now familiar goals of a 'cooperative European VLBI activity' were laid down (original text):

I. Permanent network of fixed stations:
observations on a regular basis (minimum two 48-hour periods every month) for
- astrometry (extragalactic inertial system, precession, nutation, positions)
- Earth rotation (polar motion & UT1-variations)
- Earth tides
- crustal motions (plate stability
- reference observations for mobile stations

II. Mobile stations:
observations in selected active regions, reference for satellite and terrestrial techniques
- crustal motions in the Mediterranean and Turkey

III. Participation in cross-Atlantic experiments
- continental drift

At the same time, the need for advanced VLBI equipment was recognised, although ways for optimal use of the existing MkII technology had to be found as a first step for learning to set up and carry out dedicated astro-geodetic VLBI experiments in European and intercontinental networks. For global space-geodetic measurements, around 1980, the technological situation was quite fluent with Doppler satellite tracking in decline, the NAVSTAR-GPS coming on stage and high accuracy mobile satellite laser ranging systems (SLR) being deployed in the Eastern Mediterranean. These SLR campaigns actually produced the first evidence of ongoing crustal motion with site displacements of up to 2.5 cm/yr (WEGENER-MEDLAS Project, Wilson 1989). In this scenario, complementary techniques of similar or even higher accuracy such as VLBI were welcomed in order to obtain independent checks of the observed phenomena. It soon became clear that VLBI had significant advantages over the other competing techniques: i.e. weather independence, stable terrestrial monumentation, ties to the extragalactical celestial reference frame, and self-calibrating primary observables (group delays).

The outcome of the second AGRAM meeting in November 1978 was to start with regular European VLBI working meetings of informal character in order to coordinate joint activities that would eventually lead to an operational European geodetic VLBI network, i.e. defining the primary goals, suitable instrumentation and coordinated observing programs.

2 Early astrometric and geodetic VLBI activities in Europe

In the late seventies, the primary motive for radio astronomy observatories to afford observing time for geodetic VLBI experiments was to generate station positions, i.e. improved terrestrial coordinates of the telescope sites, which in turn would lead to better source imaging and more precise relative positioning of close source pairs (references in Porcas 2010). This argument did have its merit obtaining a share of the chronically short supply of observing time for radio astronomy.

In hindsight, it appears that 1980 was the crucial year when the more specific scientific goals of astro-geodetic VLBI in Europe began to take shape. The research subjects that crystallized in the fields of astronomy and geodesy were:

Astronomy (Astrometry):
- Determination of new/improved radio source positions
- Identification of optical counterparts of compact radio sources

Astronomy and Geodesy:
- Investigation of tidal effects in VLBI time series of UT1 & Polar motion
- Tests of effects of special and general relativity by VLBI

Geodesy:
- Establishment of a fundamental network of precise geodetic station positions in Europe
- Comparison of results with other space techniques, such as Doppler satellite positioning, the upcoming GPS and Satellite Laser Ranging
- Measurement of local ties at the telescope sites, vector baselines between different telescopes at the same site, connections to the terrestrial geodetic network and to points occupied by other space techniques.

- Modeling tropospheric path delays and further development of water vapour radiometry (WVR)

With these subjects in mind a number of astro-geodetic VLBI experiments were planned, partly embedded in global projects and partly as pure European based activities (Table 1). The first VLBI experiments conducted by the Bonn astro-geodetic VLBI group led by J. Campbell, M. Bonatz and P. Brosche under the support of the German Science Foundation had to take into account the then available VLBI equipment at European radio observatories and institutions.

Around 1980 the VLBI instrumentation at the European radio observatories was still mostly based on the NRAO MkII recording and processing system and many observatories could not yet afford to equip their stations with MkIII backends. Moreover, the commonly used frequencies for radio astronomy were concentrated on the 18cm, 6cm and 2.8 cm bands, while the NASA-owned Deep Space Network had been running on the S/X frequency pair (13 and 3.8 cm). Therefore, the Bonn geodetic VLBI group put a proposal to the MPIfR program committee in 1979 for a 48h astro-geodetic 18cm (1.67GHz) global MkII single 2MHz channel experiment 'JOEN' with 4 stations, Onsala, Effelsberg, Greenbank (NRAO) and Johannesburg (HARTRAO, former NASA DSN station) in South Africa (Fig. 1). This pilot experiment (MPI program number 25-79) became the first step towards active involvement in VLBI observing and was successfully carried out on 19-21 Feb. 1980 (see original documents on the EVGA web site). In this context, the South-African extension of the network was to become a special bonus of intercontinental VLBI activities originating in Europe. It was due in a substantial part to the transfer of A. Nothnagel to HartRAO, where he worked as a geodetic assistant to the station's director G.D. Nicolson. Thus, in 1984 South Africa rose to an important station in the IRIS Earth rotation network (Carter et al. 1988; Nothnagel et al. 1992).

The largest purely European-based campaign before the new MkIII technology had fully taken hold in Europe was the ERIDOC project, which included a network of 6 European radio observatories and 18 Doppler stations (Fig. 2), requiring the cooperation of more than 30 individuals from 10 different European countries and the US (Beyer et al. 1982). F. Brouwer of the Delft Technical University brought up the idea and was the driving force all through the entire project

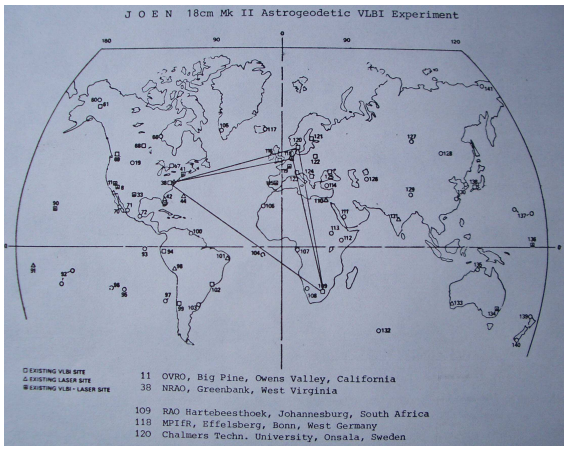

Fig. 1 The JOEN South Africa network in 1980

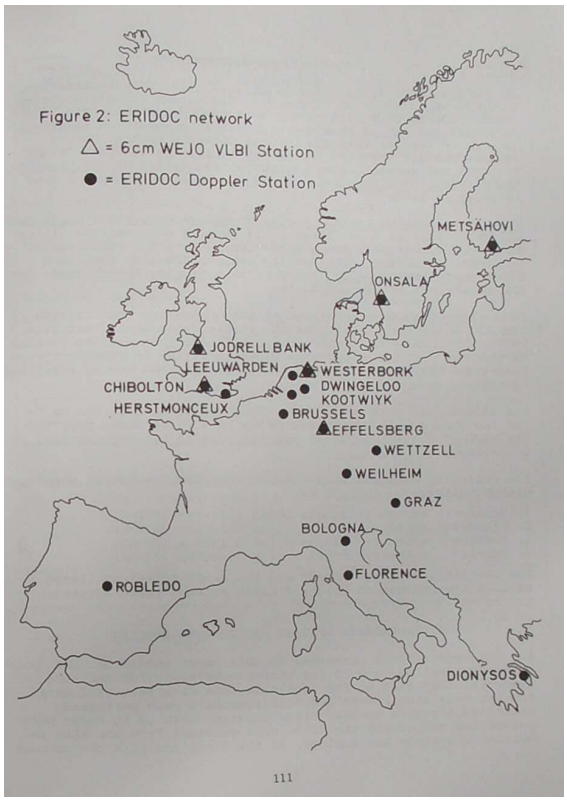

Fig. 2 The ERIDOC network 1980/81 (combined VLBI and Doppler campaign)

(Final report in Brouwer et al. 1987). It was clear from the start that the accuracy of the geodetic coordinates would not exceed the decimeter-level, because at that time most of the instrumental requirements for high group delay precision could not be met, meaning e.g.

Table 1 Early VLBI experiments in Europe with astro-geodetic background

Date	Proposed and set up by	Network	Remarks
European baselines			
24 - 26 Nov. 1979	Haystack-MIT, Onsala, MPIfR (+ Bonn geodetic VLBI group)	Effelsberg-Onsala-Haystack-Greenbank-Owens Valley	First full MkIII S/X Continental Drift experiment
19 - 21 Feb. 1980	Bonn astro-geodetic VLBI group	Effelsberg-Onsala-Green Bank -Johannesburg	MkII 18 cm astro-geodetic pilot experiment 'JOEN'
26 - 27 July 1980	Haystack-MIT, Onsala, MPIfR (+ Bonn geodetic VLBI group)	Effelsberg-Onsala-Haystack -Fort Davis-Owens Valley	Second MkIII S/X Continental Drift experiment
26 July 1980	Bonn geodetic VLBI group	Effelsberg - Onsala - Madrid	MkII-X-band BWS 'MEO 1' experiment
26 -29 Sept. 1980	Haystack-MIT, Onsala, MPIfR (+ Bonn geodetic VLBI group)	Effelsberg-Onsala-Haystack -Fort Davis-Owens Valley	First intercontinental MkIII S/X 'MERIT preliminary short campaign' Earth Rotation experiment
26 -27 Sept. 1980	Bonn geodetic VLBI group	Effelsberg - Onsala - Madrid	MkII-X-band BWS'MEO 2'experiment
4 Oct. 1980	Bonn geodetic VLBI group, Haystack-MIT, NASA GSFC	Werthhoven - Haystack	MkIII- X-band fast slewing experiment (test of Werthhoven facility (FGAN))
5 - 6 Oct. 1980	Bonn geodetic VLBI group	Effelsberg-Westerbork -Jodrell Bank-Metsähovi	MkII-6 cm BWS experiment'WEJO 1' (Project ERIDOC)
12-13 Apr. 1981	Bonn geodetic VLBI group +Geodetic Institute Delft)	Effelsberg-Onsala-Westerbork -Jodrell Bank-Chilbolton	MkII-6 cm BWS experiment 'WEJO 2' (Project ERIDOC)
20 July 1983	Bonn geodetic VLBI group, Haystack-MIT, NASA GSFC	First baseline Wettzell-Onsala	MkIII-X-band experiment
Local baselines			
15 Nov. 1979/81/82	NASA/JPL + INTA + IGM	Madrid DSN Complex, DSS-61, DSS-62, DSS-63	MkII S/X and S-only BWS experiments
13 Jan. 1981	Onsala VLBI team	600m baseline between OSO 26.5m and OSO 20m	Mk III X-band

no dual frequency ionospheric calibration, no instrumental phase/delay calibration and rubidium clocks instead of H-masers at three of the six stations. Nevertheless, a lot of experience could be gained from this effort, both in technical as well as in logistical respect.

In this connection, it may be of interest to add that five years later the French VLBI group of the Institut Géographique National ran a MkII BWS campaign to connect new stations (Nancay in France and Atibaia in Brazil) to the existing global VLBI network (Post VEGA Project, GRIG-2 of 29 June and 4 July 1985, G. Petit 1987).

A first bid to reach mm-accuracy on European ground was performed by the Onsala VLBI group determining the 601 m baseline between the 26.5m antenna and the 20m antenna at the OSO site with formal errors of 1.5 mm (Aug 25, 1980) and 0.3 mm (Jan 13, 1981) for the group delay solutions (Lundqvist 1983). The data were taken with the MkIII system at X band only, but otherwise all instrumental high performance requirements were fulfilled. This impressive demonstration as well as the transatlantic MkIII experiments of the MERIT preliminary campaign of Sept/Oct. 1980 made it quite clear for the geodetic community which way to go in the future.

More local site activities include the analysis of earlier MkII BWS data from the late seventies at the Madrid DSN complex of Robledo between three different antennas (Rius and Calero, 1983) and vector links between the Effelsberg antenna reference point, the terrestrial control network and Doppler satellite antenna marker for the ERIDOC campaign.

In the early European working group proceedings, a significant number of papers deal with the efforts to improve atmospheric path delay modelling, in particular the wet component, where the Onsala team lead the development of water vapour radiometry (Elgered 1993).

In those days, the development of geodetic VLBI software formed an important part of the activities of

virtually all of the VLBI groups. Aside from the Bonn geodetic VLBI software (BVSS, Schuh 1986), the software DEGRIAS (Brouwer 1985) was developed in Delft, Holland, while most of the groups also used software from the US, such as VLB3 (MIT, Robertson 1975), Masterfit (Fanselow 1983) and CALC/SOLVE (Ryan et al. 1985).

3 Further Development of the geodetic European VLBI network

The introduction in 1979 of the two major geodynamical observation programs, i.e. the NASA Crustal Dynamics Project (CDP, Coates et al. 1985) and the NOAA/NGS Polaris Network for Earth rotation monitoring (later extended internationally to IRIS) as well as the IAU/IAG Project of Earth rotation monitoring and intercomparison of techniques (MERIT) proved to be most important to speed up the advance of geodetic VLBI in Europe. Thus, the decision in 1980, to build a dedicated geodetic VLBI telescope at the satellite observing station of Wettzell (Schneider et al. 1983) set the stage for an upsurge of geodetic VLBI in Europe and brought about a burst of geodetic VLBI activities in a number of European countries. In view of the high investment costs, however, only a few countries managed to enter the era of MkIII technology and had difficulties to open up effective funding sources for longer term participation in geodetic observing programs.

At the heart of each radiointerferometric network the correlator and postprocessing systems are essential to produce the primary interferometric observables, phase, amplitude and, most importantly for geodesy, the group delays. Near the end of 1977 the MPIfR in Bonn had installed a copy of the NRAO MkII correlator, which was helpful introducing the geodesy newcomers to the inner secrets of VLBI (D. Graham, R. Porcas and other MPIfR staff members). In November 1982, the first version of the MkIII correlator became operational and cooperation between the Geodetic Institute of the University of Bonn (H. Seeger) and MPIfR (P.G. Mezger, K.I. Kellerman) grew ever more intensive and fruitful leading to increasing financial support from the geodesy side (employment of personnel at correlator group, procurement of additional tape drives and further upgrade of the MkIII correlator for extended use in the correlation of geodesy experiments). Thus, a fifth tape drive was procured in 1985 by the SFB 78 'Satellite Geodesy' (M. Schneider, H. Seeger) This special research group formed by members of the Technical University of Munich, the University of Bonn and the Institute for Applied Geodesy (IfAG), Frankfurt, has been responsible for a major part of the development and support of the Wettzell station in the time frame 1979 to 1986.

Fig. 3 June 1983: mounting of the S/X paramp receiver (on loan from Haystack) at the Wettzell radio telescope with R. Kilger (middle) and R. Zeitlhöfler (right) (Wettzell), G. Reichert (middle left) (Geod. Inst. Univ. Bonn), O. Lochner (left) (MPIfR Effelsberg)

The opening of the Wettzell 20m telescope, which had its first baseline observed in July 1983 with Onsala OSO20 in a 12h X-band run, marked the beginning, too, of the operations of the European geodetic MkIII network. Figure 3 bears witness to the strong support provided by NASA/GSFC (T.A. Clark, N. Vandenberg and others) as well as technical assistance by MPIfR (W. Zinz, O. Lochner and others) to bring sys-

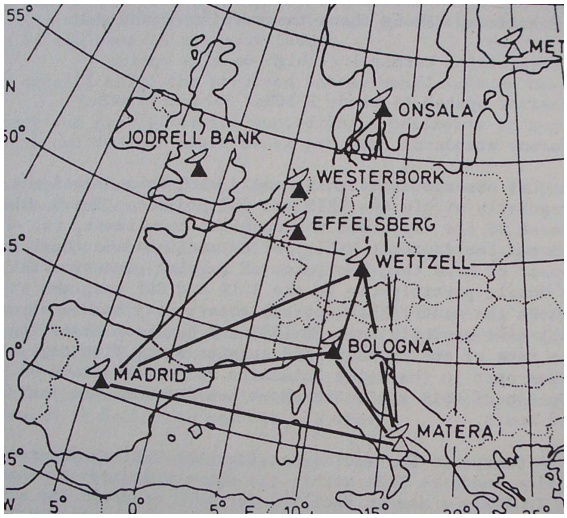

Fig. 4 The European geodetic VLBI net around 1987

Observatory	Antenna	Receiver status	Terminal	Field system	Frequency standard
Onsala	20 m dual feed az-el	S-X cooled	Mk III	HP 1000F	H-maser
Wettzell	20 m dual feed az-el	S-X cooled	MK III MK IIIA	HP 1000F	2 H-masers
Medicina	32 m dual feed az-el	S-X uncooled	Mk III	HP 1000F	2 H-masers
Madrid (DSS 65)	34 m dual feed az-el	S-X cooled	Mk III (1988)	IBM PC	H-maser
Effelsberg	100 m az-el	X cooled	MK III	IBM PC	H-maser
Westerbork	25 m equat.	--	MK III	HP 1000F	H-maser
Jodrell Bank (Mk-2)	25 m az-el	--	MK III	HP 1000F	Rubidium
Matera (under constr.)	20 m dual feed az-el	S-X	MK III	?	H-maser
Noto (under constr.)	32 m dual feed az-el	S-X	Mk III	?	H-maser

Tab. 1: Status of European VLBI observatories

Fig. 5 Equipment status of the European geodetic VLBI net 1987

tems up and running. With the VLBI facility in place, the satellite observing station of Wettzell became the first Geodynamic Fundamental Station. The concept of fundamental stations co-locating different geodetic space techniques at one site originated in the introductory phase of the Crustal Dynamics Program (Coates et al. 1985). It required considerable means for investment and operations, which could not have been realized without the sustained commitment of the BKG (former IfAG) Frankfurt (H. Seeger).

Only a short while after the start of Wettzell in summer 1983, the inauguration of the Bologna 32m telescope (located at Medicina) took place in September that same year. Italy, affected strongly by the mediterranean tectonics, was able to set up a national geodynamics program as a complement to the ongoing radio astronomy research at Istituto di Radioastronomia (IRA) and realize a network of three VLBI stations, two shared observatories (Medicina and Noto) belonging to IRA/CNR (Setti 1980) and a dedicated geodetic telescope at the SLR station of Matera (ASI), which then (1990) also became a full fundamental station, the second one in Europe next to Wettzell (Sylos-Labini, Zerbini 1985). First regular observations on European baselines with the complete high accuracy MkIII geodetic VLBI equipment began in November 1983, when both Onsala and Wettzell participated in the first IRIS Earth rotation measurements. When the Bologna 32m telescope obtained its own S/X receiver in Feb. 1987 and the Madrid NASA DSN antenna was equipped with a MkIII terminal by the end of that same year, a nucleus of the European VLBI net was ready to embark on regular observations (Fig. 4 and 5). In 1993 the network reached its definitive size and shape with 10 stations operating together in five to six common 24-h-sessions per year. First signs of crustal motion were detected two years after regular observations began on the baseline Wettzell-Noto (Sicily) in 1990 with a shortening of 5.9 ± 2.4 mm/yr (Campbell et al. 1993)

Operational funding for two consecutive 3-year periods from 1993 to 2000 was obtained under the EU-Framework Programmes ”Science” and ”Training and Mobility”, allowing employment of 6 post-doc scientists in the participating EU countries, helping to pass on the know-how in the field of VLBI to the younger generation. An overview as well as an in-depth report on the geodynamic results of this funding phase of the geodetic European VLBI network are presented in Campbell and Nothnagel 2000 and Campbell, Haas, Nothnagel 2002.

The further progress of the European geodetic VLBI network and its achievements have been and continue to be extensively documented in the series of proceedings of the European Working Group for geodetic and astrometric VLBI (Fig. 6). The lasting interest in the data from the European VLBI network, which have contributed to the realization of the ITRF

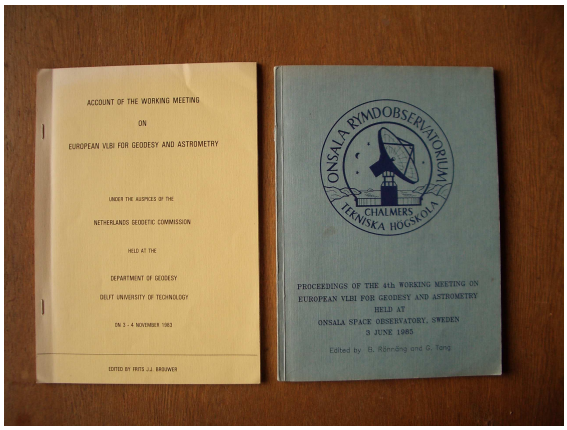

Fig. 6 :No. 3(Delft 1983) and No. 4 (Onsala 1985) of the series of proceedings of the Working meetings on European VLBI for geodesy and astrometry. The facsimile minutes of the first and second meetings (Bonn, 1980 and Madrid 1981) are included in the appendix of the present meeting.

Fig. 7 Attendants of the 4^{th} European meeting in Onsala, June 1985

and EUREF terrestrial reference frames, has prompted the setting up of a formal status for this regional network: At the 17th meeting at Noto in 2005, the European VLBI Group for Geodesy and Astrometry (EVGA) was created as part of the IVS paving the way for a healthy and active future.

To conclude this review one of the earlier photos of participants at a European VLBI meeting (Onsala 1985) is reproduced here (Fig. 7a), together with a slide taken at that same occasion by J. Campbell (Fig 7b).

4 Acknowledgements

On behalf of all members of EVGA the author wishes to extend many thanks to all individuals and institutions that have contributed in one way or another to the achievements of the European Geodetic VLBI Network and whose names appear in the text or are included in the references of this review.

5 References

W. Beyer, J. Campbell, F. J. Lohmar, H. Seeger, A. Sudau, F. J. J. Brouwer, G. J. Husti, G. Lundqvist, B. O. Rönnäng, R. T. Schilizzi, R. S. Booth, P. Richards, S. Tallquist: Project ERIDOC (European Radiointerferometry and Doppler Campaign) Proc. IAG Symposium No. 5: Geodetic Applications of Radio Interferometry, Tokyo, May 1982, NOAA Techn Rep. NOS 95 NGS 24, Rockville, MD, 1982, p. 105 - 119

F. J. J. Brouwer: On the principles, assumptions and methods of geodetic Very Long Baseline Interferometry. PhD Thesis, Technical University of Delft, May 1985

F. J. J. Brouwer, G. J. Husti, W. Beyer, J. Campbell, B. Hasch, F. J. Lohmar, H. Seeger, G. Lundqvist, B. O. Rönnäng, A. van Ardenne, R. T. Schilizzi, B. Anderson, R. S. Booth, P. N. Wilkinson, P. Richards, S. Tallquist: Data Analysis of Project ERIDOC. In: VLBI- and Doppler- Papers 1983-1987, Mitteilungen Geod. Inst. Rhein. Friedr.-Wilh. Universität Bonn, Nr. 72, p. 1 - 37, 1987

J. Campbell: European VLBI for Geodynamics. In: Proc. 3rd int. Conf. on the WEGENER/MEDLAS Project, Bologna, May 25-27, 1987 Eds. P. Baldi, S. Zerbini, Univ. of Bologna, Soc. Editrice Esculapio Bologna 1988, p. 361-374

J. Campbell, H. Hase, A. Nothnagel, H. Schuh, N. Zarraoa, A. Rius, E. Sardon, V. Tornatore, P. Tomasi: First Results of European Crustal motion Measure-

ments with VLBI. AGU Geodynamics Series, vol. 23, p. 397-405, 1993

J. Campbell, R. Haas, A. Nothnagel, eds.: Measurement of vertical crustal motion in Europe by VLBI. European Commission, TMR Networks Publication, Cat.-No. KI-NA-20-084-ENC, Bonn, 2002

W. E. Carter, D. S. Robertson, A. Nothnagel, G. D. Nicolson, H. Schuh, J. Campbell: IRIS-S: Extending Geodetic VLBI Observations to the Southern Hemisphere; Journal of Geophysical Research, Vol. 93, No. B12 S. 14947 - 14953, 1988

R. J. Coates, H. Frey, G. D. Mead, J. M. Bosworth: Space-Age Geodesy: The NASA Crustal Dynamics Project. IEEE Transactions on Geoscience and Remote Sensing, Vol. GE-23 No. 4, July 1985, p. 360-367

M. Cohen, D. Shaffer: Positions of radio sources from very long baseline interferometry. Astron. Journal, vol. 76, 1971

G. Elgered: Tropospheric radio-path delay from ground-based microwave radiometry. In: Atmospheric remote sensing by microwave radiometry, chapter 5, ed. M. A. Janssen, 1993

J. L. Fanselow: Observation model and parameter partials for the JPL VLBI Parameter Estimation Software MASTERFIT V1.0 . JPL-Publication 83-39, Jet Propulsion Laboratory, Pasadena, California, 1983

T. A. Herring, B. E. Corey, C. C. Counselman III, I. I. Shapiro, B. O. Rönnäng, O. E. H. Rydbeck, T. A. Clark, R. J. Coates, C. Ma, J. W. Ryan, N. R. Vandenberg, H. F. Hinteregger, C. A. Knight, A. E. E. Rogers, A. R. Whitney, D. S. Robertson and B. R. Schupler: Geodesy by Radio Interferometry: Intercontinental distance determinations with subdecimeter precision. Journ. Geophys. Res. Vol. 86 No. B3, P. 1647-1651, 1981

G. Lundqvist: Precision surveying at the 1-mm level. In: Techniques d'interférométrie à très grande base, Toulouse Aug/Sept 1982, CNES, CEPAUDES-Editions, Toulouse, 1983 p. 209-215

A. Nothnagel, G. D. Nicolson, J. Campbell, H. Schuh: Radiointerferometric polar motion observations with high temporal resolution. Bull. Géod. ,Vol. 66, p. 346-354, 1992

G. Petit: Preliminary Results of the Post-VEGA MkII-VLBI Experiments (GRIG-2). Proc. of the 5th Working Meeting on European VLBI for Geodesy and Astrometry at Wettzell 7-8 Nov. 1986, Mitt. Geod Inst. Univ. Bonn, No. 71, p. 73-76, Bonn 1987

R. W. Porcas: A History of the EVN: 30 Years of Fringes. 10th European VLBI Network Symposium and EVN Users Meeting: VLBI and the new generation of radio arrays. Sept. 20-24, 2010, Manchester, UK, publ. in Proceedings of Science, http://pos.sissa.it/

A. Rius, E. Calero: Comparison of VLBI and conventional surveying of the Madrid Deep Space Network antennas. In: Techniques d'interférométrie à très grande base, Toulouse Aug/Sept 1982, CNES, CEPADUES-Editions, Toulouse, 1983 p. 33-38

D. S. Robertson: Geodetic and astrometric measurements with very-long-baseline interferometry. Ph.D. thesis, Mass. Inst. of Technol., Cambridge, 1975

J. R. Ryan, D. Gordon, C. Ma: CALC 6.0 Memorandum, Goddard Space Flight Center, Greenbelt MD, USA, 1985

M. Schneider, R. Kilger, K. Nottarp, E. Reinhart, J. Campbell, H. Seeger: Status report on the new radiotelescope for the Wettzell station. P.73-81, In: Techniques d'interférométrie à très grande base, Toulouse Aug/Sept. 1982, CNES, CEPADUES Editions, Toulouse 1983

H. Schuh: Die Radiointerferometrie auf langen Basen zur Bestimmung von Punktverschiebungen und Erdrotationsparametern. DGK-Reihe C, Heft Nr. 328, 1986

G. Setti: The Italian VLBI Project: A Status Report. CSTG-Bulletin, p. 21-22, 1981

I. I. Shapiro, D. S. Robertson, C. A. Knight, C. C. Counselman III, A. E. E. Rogers, H. F. Hinteregger, S. Lippincott, A. R. Whitney, T. A.Clark, A. E. Niell, and D. J. Spitzmesser: Transcontinental baselines and the rotation of the Earth measured by radio interferometry. Science vol. 186 p. 920-922, 1974 and vol.191, p. 451, 1976

G. Sylos-Labini, S. Zerbini : The Italian contribution to the study of the dynamics of the Earth's crust in the mediterranean region by means of space techniques. CSTG-Bulletin No. 8, p. 163-174, Nov. 1985

P. Wilson: The WEGENER program. Lecture Notes in Earth Sciences, eds. I.I. Mueller, S. Zerbini, Vol. 22, p. 275-286, 1989

Geodetic VLBI Intensive Scheduling based on Singular Value Decomposition

J. Pietzner, A. Nothnagel

Abstract An automatic scheduling process for VLBI Intensive sessions based on singular value decomposition is developed. Beginning with a simple starting configuration, the observations are selected successively by analyzing the Jacobian matrix at each step of the scheduling process. Indicators on the geometry of the measurement derived of the singular value decomposition are used for the selection of the sources to be observed with the purpose of improving the dUT1 determination. The formal errors of dUT1 deduced from the normal equation, which can be created just from the geometry of a schedule, serves as an assessment criterion of the scheduling method. The new scheduling method shows promise for improvements of the dUT1 determination by IVS Intensive observing sessions.

Keywords Earth Rotation, Scheduling, Intensives

1 Introduction

The scheduling of Very Long Baseline Interferometry (VLBI) observing sessions is a crucial step to obtain reliable results with the best possible accuracy. At present, there is no clear strategy for the scheduling of VLBI Intensive sessions for the purpose of dUT1 determination except of trying to spread the observations as evenly as possible over the sky at each telescope. Here, a new approach for scheduling one hour long Intensive VLBI sessions is presented based on singular value decomposition (SVD).

Judith Pietzner and Axel Nothnagel
Rheinische Friedrich-Wilhelms Universität Bonn, IGG, Nußallee 17, D-53115 Bonn, Germany

As shown, e.g., in Vennebusch et al. (2009) the SVD is suitable as part of regression diagnostics for any geodetic adjustment problem and, therefore, for geodetic VLBI as well. The SVD can be used to derive indicators which contain information on the geometry of the design with respect to the influence of observational errors. Therefore, it can be used for planning the design of the measuring process (Förstner, 1987). In this paper a method for automatic scheduling of VLBI observing sessions is presented taking into account the geometry of an experiment by investigating the design matrix of the associated adjustment problem at each step of the scheduling process by using SVD. Furthermore, preliminary results of the scheduling method accomplished for VLBI Intensive sessions focusing on dUT1 determinations are presented. The only geodetic target parameter of those sessions is dUT1. In addition, three clock parameters for one station (clock offset CL_0, clock rate CL_1 and frequency drift CL_2 w.r.t. the other clock) and one atmospheric parameter per station (atmospheric zenith wet delays AT_A at station A and AT_B at station B) complete the functional VLBI model.

2 Singular value decomposition

The SVD is a tool that enables a detailed analysis of an $m \times n$ matrix $\mathbf{X}$ with rank r by the factorization into three matrices

$$\mathbf{X} = \mathbf{U} \cdot \mathbf{S} \cdot \mathbf{V}^T \tag{1}$$

(Lay, 2003). The first r diagonal entries of $\mathbf{S}$ ($m \times n$) are the singular values σ_i of $\mathbf{X}$, which are (usually) arranged in descending order $\sigma_1 \geq \sigma_2 \geq \ldots \geq \sigma_r > 0$,

$$\mathbf{S} = diag\left(\sigma_1\ \sigma_2\ \ldots\ \sigma_r\ 0\ \ldots\ 0\right). \tag{2}$$

The columns of the $m \times m$ orthogonal matrix $\mathbf{U}$ are called left singular vectors $\mathbf{u}_i$ corresponding to the order of the singular values σ_i

$$\mathbf{U} = \left(\begin{array}{ccccccc} \vdots & \vdots & & \vdots & \vdots & & \vdots \\ u_1 & u_2 & \ldots & u_r & u_{r+1} & \ldots & u_m \\ \vdots & \vdots & & \vdots & \vdots & & \vdots \\ \underbrace{}_{\mathbf{U}_r} & & & & \underbrace{}_{\mathbf{U}_0} & & \end{array} \right), \tag{3}$$

where the first r columns $\mathbf{U}_r = \{\mathbf{u}_1, ..., \mathbf{u}_r\}$ span a basis for the column space $R(\mathbf{X})$ of the matrix $\mathbf{X}$. The columns of the $n \times n$ orthogonal matrix $\mathbf{V}$ are called right singular vectors $\mathbf{v}_i$

$$\mathbf{V} = \left(\begin{array}{ccccccc} \vdots & \vdots & & \vdots & \vdots & & \vdots \\ v_1 & v_2 & \ldots & v_r & v_{r+1} & \ldots & v_n \\ \vdots & \vdots & & \vdots & \vdots & & \vdots \\ \underbrace{}_{\mathbf{V}_r} & & & & \underbrace{}_{\mathbf{V}_0} & & \end{array} \right), \tag{4}$$

where the first r columns $\mathbf{V}_r = \{\mathbf{v}_1, ..., \mathbf{v}_r\}$ span a basis for the row space $R(\mathbf{X}^T)$ of the matrix $\mathbf{X}$. In sense of a least-squares adjustment, interpreting the Jacobian matrix $\mathbf{X}$ as a mapping from the space of the model parameters into the data space, the subspace $\mathbf{U}_r$ is related to the data space and the subspace $\mathbf{V}_r$ is related to the model space of $\mathbf{X}$ (Scales et al., 2001). For further detail of the SVD see e.g. Golub et al. (1965), Lay (2003) or Strang (2003).

A data resolution matrix $\mathbf{H}$ (also known as 'Hat Matrix') being an $m \times m$ projection operator onto the data space of $\mathbf{X}$ can be computed by

$$\mathbf{H} = \mathbf{U}_r \mathbf{U}_r^T. \tag{5}$$

Since the elements of the data resolution matrix indicate how much weight each observation has on the adjusted observations (Scales et al. (2001) or Menke (1984)), the main-diagonal elements of $\mathbf{H}$ are called impact factors $\mathbf{h} = diag(\mathbf{H})$. The impact factors are closely related to partial redundancies (Förstner, 1987). The redundancy numbers $r_i = 1 - h_i = (\mathbf{I} - \mathbf{H})_{ii}$ (for $\mathbf{P} = \mathbf{I}$) indicate how far errors in an observation show up in the corresponding residuals of the least-squares fit. Observations with large impact factors and thus weakly controlled observations are called high leverage points. On the one hand, it is difficult to locate gross errors at observations with small redundancy numbers. On the other hand, high leverage points being no gross errors significantly affect the accuracy of the estimated parameters and are necessary to avoid a defect of the configuration (Niemeier, 2002).

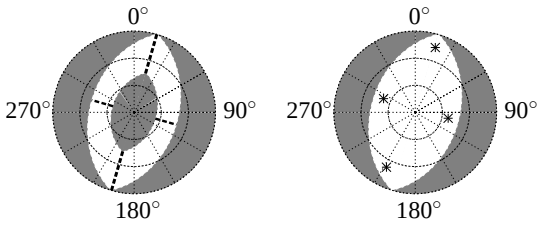

Fig. 1 Locations of the initial sources depicted at the sky plot of the baseline's mid point (left); example of four initial observations (right).

3 Scheduling Concept

The scheduling process occurs in two general steps. First, the initial four sources to be observed are chosen subject to special spatial consideration. The second step is the main scheduling process, where the subsequent observations are selected by criteria following from the SVD.

Initial observations

Fig. 1 (left) shows a sky plot of the baseline's mid point view, where the white area and the inner gray area is the common visibility of both radio telescopes. The dashed lines lie in the direction of the baseline and orthogonal to it. In order to start the schedule with a relative stable geometry, four initial observations are selected with minimal distances to the dashed lines. Additionally, the elevations of these observations are constricted to the lower half of the common visibility of the telescopes, which is indicated by the white area in fig. 1 (left). Fig. 1 (right) shows an example of four sources which are selected with this concept.

Main schedule

The main scheduling process starts at a time t defined by the last initial observation. If the time since the start

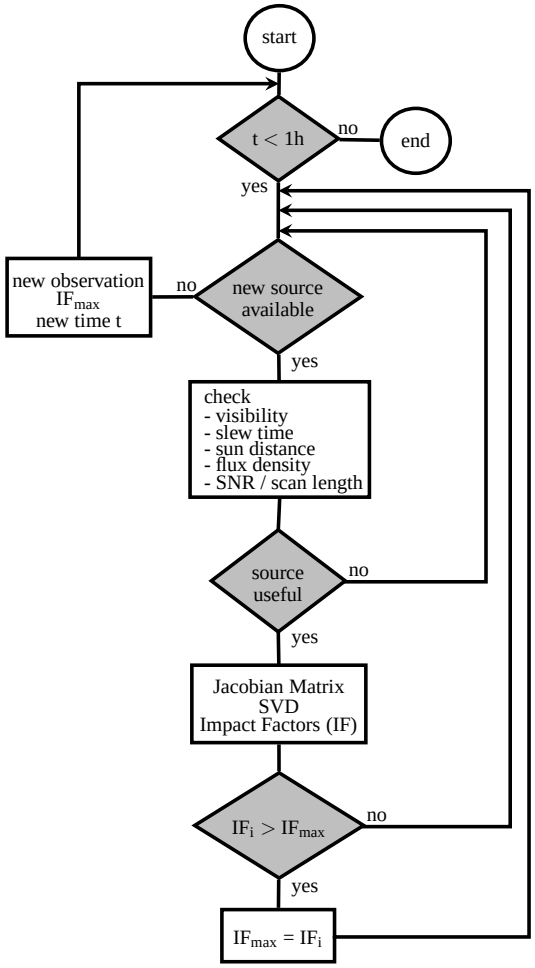

Fig. 2 Procedure of the automatic scheduling method based on the SVD for one hour long VLBI Intensive sessions.

of the scheduling process is less than one hour - following the VLBI Intensive concept - all sources are checked for their suitability at this time. If a source is useful, the Jacobian Matrix is built and the impact factors are computed. If the impact factor of the new source is larger than that of all previous sources of the loop, the source will be earmarked as the new observation. When all sources are checked the new observation with the largest impact factor is found. With the slew time of the radio telescopes and the scan length of the observation, a new time is computed. While this new time is less than one hour, the process of finding the next observation with the largest impact factor is repeated. The algorithm is depicted in Fig. 2.

In this work two different criteria are used. The first criterion is, that in each case the observation with

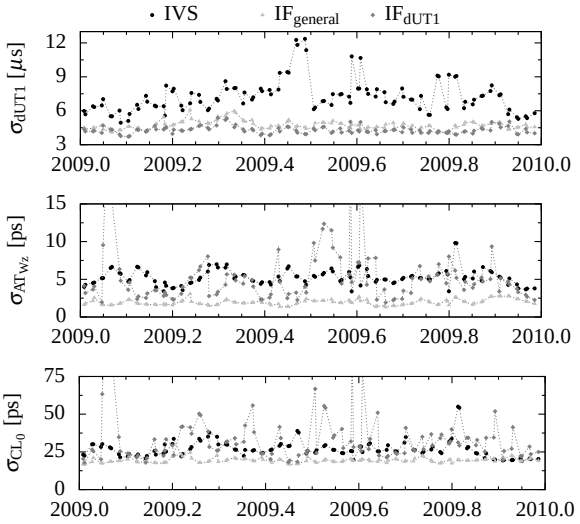

Fig. 3 Formal errors of dUT1 (top), the atmospheric zenith wet delay AT of the station Wettzell (middle) and the clock offset CL_0 of the station Wettzell (bottom) for Ts-Wz Intensive schedules in 2009. IVS: standard schedules of the IVS, $IF_{general}$: SVD schedules with general impact factors, IF_{dUT1}: SVD schedules with dUT1 impact factors.

the largest impact factor for all parameters, the general impact factor, is selected. The second criterion is the largest impact factor for the parameter dUT1 only.

4 Simulation Results

The described procedure was applied for the Intensive baseline Tsukuba – Wettzell (INT2) with both selection criteria. For comparison, standard schedules of the International VLBI Service for Geodesy and Astrometry (IVS, Schlüter and Behrend, 2007) were analyzed in the same manner as the SVD schedules. For the purpose of a direct comparison, the SVD schedules are generated for the same time windows as the IVS schedules for the year 2009.

Formal errors

The resulting formal errors of dUT1 received from the normal equations of the three different cases assuming a variance of unit weight of 1, are shown in fig. 3 (top). It should be noted that the resulting formal errors purely represent the geometry produced by the ob-

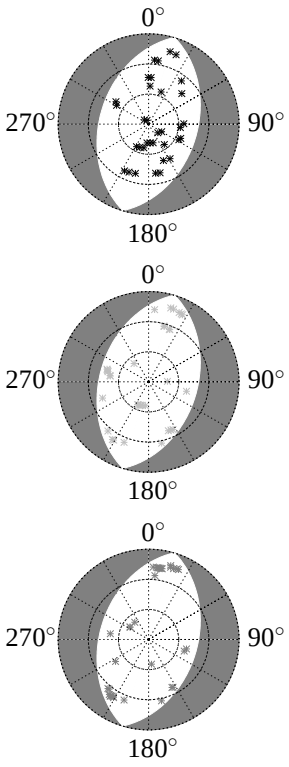

Fig. 4 Mid point sky plots for a Ts-Wz schedule (k09150) for the three different cases. Top: standard schedule of the IVS, bottom left: SVD schedule with general impact factors, bottom right: SVD schedule with dUT1 impact factors.

serving schedules still neglecting the post fit scatter of the observations. Obviously, the formal errors of the SVD schedules are clearly lower than those of the IVS schedules. Furthermore, the SVD schedules with the impact factors computed for dUT1 alone show the best results. For the other parameters, the SVD schedules with the general impact factors exhibit the lowest formal errors, whereas the SVD schedules with the dUT1 impact factors have a similar magnitude as the IVS schedules as shown by the example of the atmospheric parameters and the clock offsets in Fig. 3 (middle and bottom).

Example of sky plots

Figure 4 shows the mid point sky plots of a single session (k09150) for the three cases with the positions of the observed sources. It is obvious that the distribution of the sources for both SVD schedules is less homogeneous as for the IVS schedule. The observations of the SVD schedules are arranged in clusters instead. Particularly, sources with low elevations are observed more often and in more rapid succession for both SVD schedules. The sources in the cusps of the sky plot are those with the lowest common elevations for both radio telescopes. Those observations seem to be important for the determination of dUT1 as they represent the major difference between the two scheduling methods. Furthermore, the number of different sources is lower for both SVD schedules as for the IVS schedule (see Tab. 1).

	IVS	$IF_{general}$	IF_{dUT}
# observations	34	33	33
# sources	18	14	16

Table 1 Number of observations and number of sources of the three different Intensive schedules in Fig. 4.

Example of correlations

The correlation matrices of the same session for the three cases described above are shown in Fig. 5. In comparison to the IVS schedule, the SVD schedule with the general impact factor exhibits lower correlations of dUT1 with all other parameters, while the correlations of the other parameters almost remain constant. Within the SVD schedule with the impact factor for dUT1, the clustered observations with low elevations cause a significant decorrelation of dUT1, whereas the other parameters are higher correlated.

The correlation matrices of the other sessions of the year 2009 show a very similar relation. So, the correlation matrices in Fig. 5 are representative for the year 2009.

5 Conclusions

In this work preliminary results of an automatic scheduling method for the optimization of the geometry of VLBI Intensive sessions are presented. The scheduling method based on the singular value decomposition shows promise for VLBI Intensive dUT1 sessions.

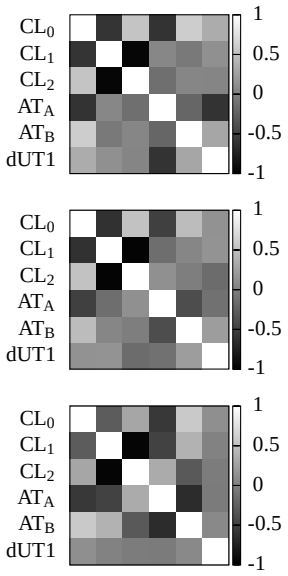

Fig. 5 Correlation matrices of the parameters w.r.t. the three cases depicted in Fig. 4. Top: standard schedule of the IVS, bottom left: SVD schedule with general impact factors, bottom right: SVD schedule with dUT1 impact factors.

The formal errors of dUT1 from regular IVS Intensive schedules and simple cofactor analysis without taking the variance of unit weight into account is 7.3 μs on average for the year 2009. The formal errors of dUT1 of the SVD schedules is on average 4.7 μs for the general impact factor schedules and 4.3 μs for the dUT1 impact factor schedules. Thus, regarding the target parameter dUT1, both SVD schedules yield an improvement in its determination. The formal errors of the atmospheric parameters average 6 ps for both the IVS schedules and the SVD schedules with the dUT1 impact factor. Here, only the SVD schedule with the general impact factor improves the formal errors to an average of 2 ps. The determination of the clock parameters even shows a degradation for the SVD schedules with the dUT1 impact factor compared to the IVS schedules. The average formal error of the clock offset amounts to 27 ps for the IVS schedules and 34 ps for the SVD schedules with the dUT1 impact factor. Again, the SVD schedules with the general impact factor show the best result with an average formal error of 19 ps.

Regarding the correlations between the estimated parameters, both SVD schedules promise a more reliable determination of the target parameter dUT1. So far, the formal errors are computed only from the co-factor matrix still neglecting the variance of unit weight. It remains to be seen how these numbers compare to a more sophisticated simulation with synthesized o-c, vectors. This is the next step on the way of applying this scheduling method to real observations.

References

W. Förstner. Reliability analysis of parameter estimation in linear models with applications to mensuration problems in computer vision. Computer Vision, Graphics, and Image Processing 40:273-310. 1987

G. Golub and W. Kahan. Calculating the singular values and pseudo-inverse of a matrix. J. SIAM Numer. Anal. 2:205-224. 1965

D. Lay. Linear algebra and its applications. Addison-Wesley, New York. 2003

W. Menke. Geophysical data analysis: discrete inverse theory. Academic Press, Orlando. 1984

W. Niemeier. Ausgleichungsrechnung. de Gruyter, Berlin New York. 2002

J. Scales, M. Smith and S. Treitel. Introductory geophysical inverse theory. Samizdat Press, Golden. 2001

W. Schlüter and D. Behrend. The International VLBI Service for Geodesy and Astrometry (IVS): current capabilities and future prospects. 81(6):379–387, 2007. doi: 10.1007/s00190-006-0131-z.

G. Strang. Lineare Algebra. Springer, Berlin. 2003

M. Vennebusch, A. Nothnagel and H. Kutterer. Singular value decomposition and cluster analysis as regression diagnostics tools for geodetic applications. *Journal of Geodesy*, 83:877–891, 2009. doi: 10.1007/s00190-009-0306-5.

IVS Live: All IVS on your desktop

A. Collioud

Abstract IVS Live is a new tool that can be used to follow the observing sessions organized by the International VLBI Service for Geodesy and Astrometry (IVS), navigate through past or coming sessions, or search and display specific information related to sessions, sources (especially the most recent VLBI images) and stations. The IVS Live user interface and all its functionalities are accessible at this Web address: http://ivslive.obs.u-bordeaux1.fr/.

Keywords IVS activities, dynamic Web site

1 Introduction

In the framework of the International Year of Astronomy 2009 (IYA), the International VLBI Service for Geodesy and Astrometry (IVS) organized the largest 24-hour astrometric session ever conducted. 35 radiotelescopes located all around the world observed 243 out of the 295 ICRF2 defining sources. The Laboratoire d'Astrophysique de Bordeaux built for the occasion a dynamic Web site allowing one to follow in real time the progress of the session. This page also provided the most recent VLBI images for each source, as well as ancillary information about sources and stations. This Web page was a nice success with almost a thousand connections throughout the session.

Arnaud Collioud
CNRS, UMR 5804, Laboratoire d'Astrophysique de Bordeaux, Université de Bordeaux, Observatoire Aquitain des Sciences de l'Univers, 2 rue de l'Observatoire, BP 89, 33271 Floirac Cedex, France

IVS Live is a generalized version of the IYA2009 dynamic Web site, developed to provide an easy access to the entire IVS observing plan. IVS Live is accessible by pointing your favorite Web browser to http://ivslive.obs.u-bordeaux1.fr/. The major capabilities of the IVS Live Web site, along with screenshots, are presented in the next section.

2 IVS Live capabilities

The IVS Live Web site was designed to achieve three main goals: follow all IVS sessions in real time, navigate through past or coming sessions, and search specific information related to sessions, sources or stations. To make it fully dynamic, IVS Live was developed in javascript (using the desktop Web application framework "ExtJS") and PHP, with a MySQL database as back-end. The Web site and the associated database are hosted on a dedicated server at the Laboratoire d'Astrophysique de Bordeaux.

2.1 Follow sessions in real-time and look at source images

The main reason for the existence of the IVS Live Web site is the monitoring of IVS sessions. Session schedules are routinely and automatically added to the IVS Live database as soon as they are available on one of the IVS data center servers. The database at present contains 750 sessions (starting from 1 January 2010), 723 sources and 47 stations, and the amount of data is constantly growing. Once into the database, these ses-

sions become accessible in IVS Live. The homepage automatically loads the ongoing IVS session (if there is any) or counts down to the session to come. All IVS Live functionalities are accessible through a single user interface, which is divided into several subpanels (Figure 1). One contains the schedule of the session, which may be sorted by time, source name, or scan duration. The main panel provides an overview of the session: dates and session type (intensive or non-intensive), source list, and an interactive network map. While the session is running, IVS Live is automatically updated thanks to a synchronization procedure with the displayed master clock. A new tab is created in the main panel for each source once a new observation begins. This tab regroups information related to this specific scan: the latest VLBI images available for the source extracted from one of the VLBI image databases (the Bordeaux VLBI Image Database, Collioud and Charlot, 2009, the Radio Reference Frame Image Database or the VLBA Calibrator Survey data), the observing network (along with static station details, pictures and webcam links, if available), and some scheduling information about this observation and source (Figure 2). The source names within tab titles and schedule are color-coded according to the source observation status (completed, ongoing, or to come).

2.2 Navigate through IVS sessions and master schedules

If you are looking for another session than the one automatically loaded, you can easily change the active session in the IVS Live interface. The links to the previous and next sessions are directly selectable from the main page. If you need a more elaborate tool to look for specific IVS sessions, you may use the IVS Live "Calendar". This tool provides a quick and convenient graphical visualization of all IVS master schedules (from 1979 to 2011 thus far). It provides daily to monthly to yearly views, as well as basic information about each session such as duration or observational network (Figure 3) and a direct link to load the session in the main interface (if the schedule is available in IVS Live database).

2.3 Search for specific sessions, sources, or stations

In addition to be a monitoring tool for IVS activities, IVS Live may also help you to retrieve specific information about a given session, source, or station. By using search forms, you may query the IVS Live database using several search criteria. For example, a session may be queried by its code (e.g., rdv86, i10023), time span (06 through 25 May 2011), and/or type (Intensive, non-Intensive). Each such query leads to a window with the result list. In the case of a session search, you will see the list of matching sessions along with the links for directly loading a session into IVS Live (Figure 4). Source and station queries (Figure 5 and Figure 6) result in a list of matching sources or stations with links to additional details (e.g., position, images, map location, webcam link, and list of sessions with the selected source or station).

3 Conclusions

The IVS Live dynamic Web site allows the user to follow IVS sessions in real-time, navigate through IVS sessions and master schedules, and search specific information about sessions, sources (especially the most recent VLBI images) and stations. Thanks to IVS Live, you should now be able to easily and conveniently answer simple questions such as which IVS session is currently running, which stations are observing, or which source is being observed? IVS Live will be regularly updated and extended in order to maintain and increase its value for the entire IVS community.

References

A. Collioud and P. Charlot. The Bordeaux VLBI Image Database. In G. Bourda, P. Charlot and A. Collioud, editors, *Proceedings of the 19th European VLBI for Geodesy and Astrometry Working Meeting*, Bordeaux, 2009.

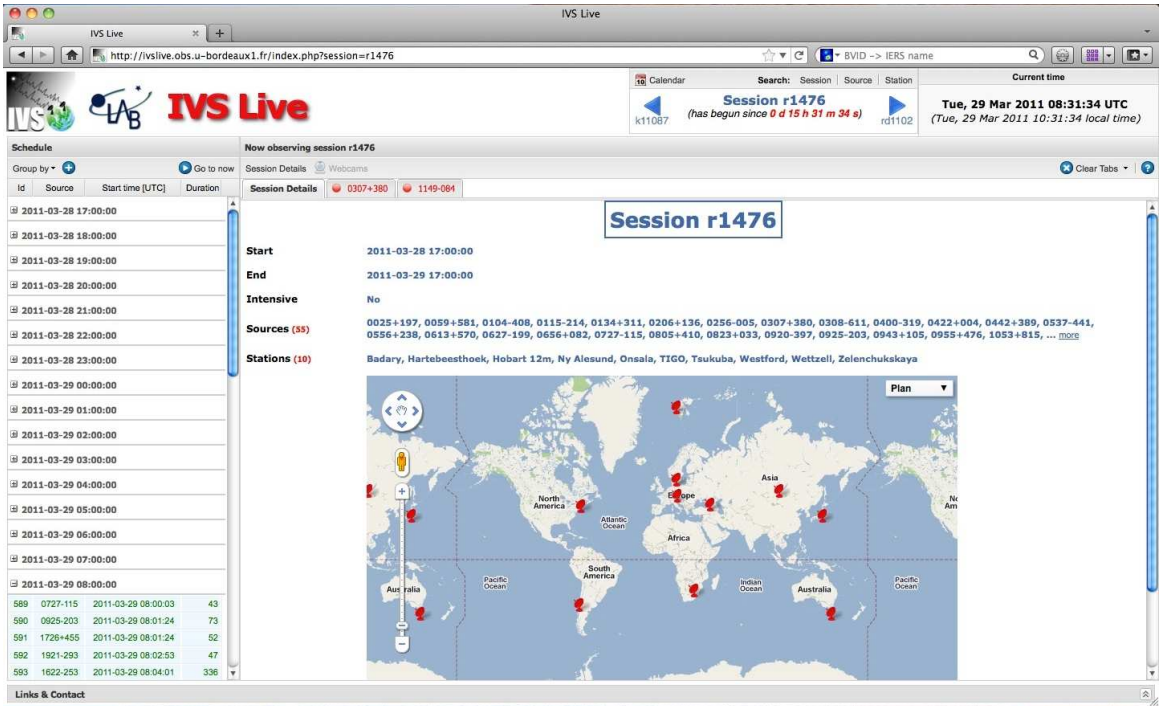

Fig. 1 The IVS Live main interface during the session R1476 (29 March 2011). The interface is organized in several subpanels: the clock and navigation panel (top), the schedule panel (left-hand side) and the main panel which contains a short introduction of the active session (right-hand side).

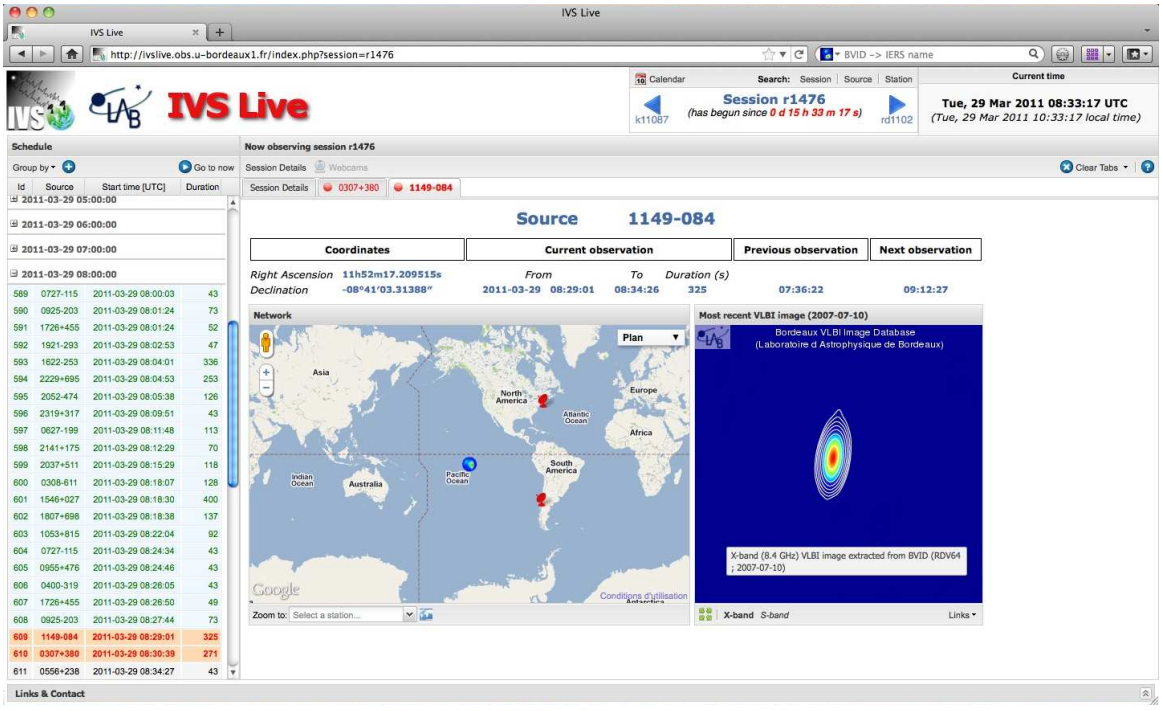

Fig. 2 One observation tab for the source 1149-084. It displays specific information about this scan and source, an interactive map of the observing network and the most recent X- and S-band VLBI images of this source, extracted from the Bordeaux VLBI Image Database (BVID; http://www.obs.u-bordeaux1.fr/BVID/).

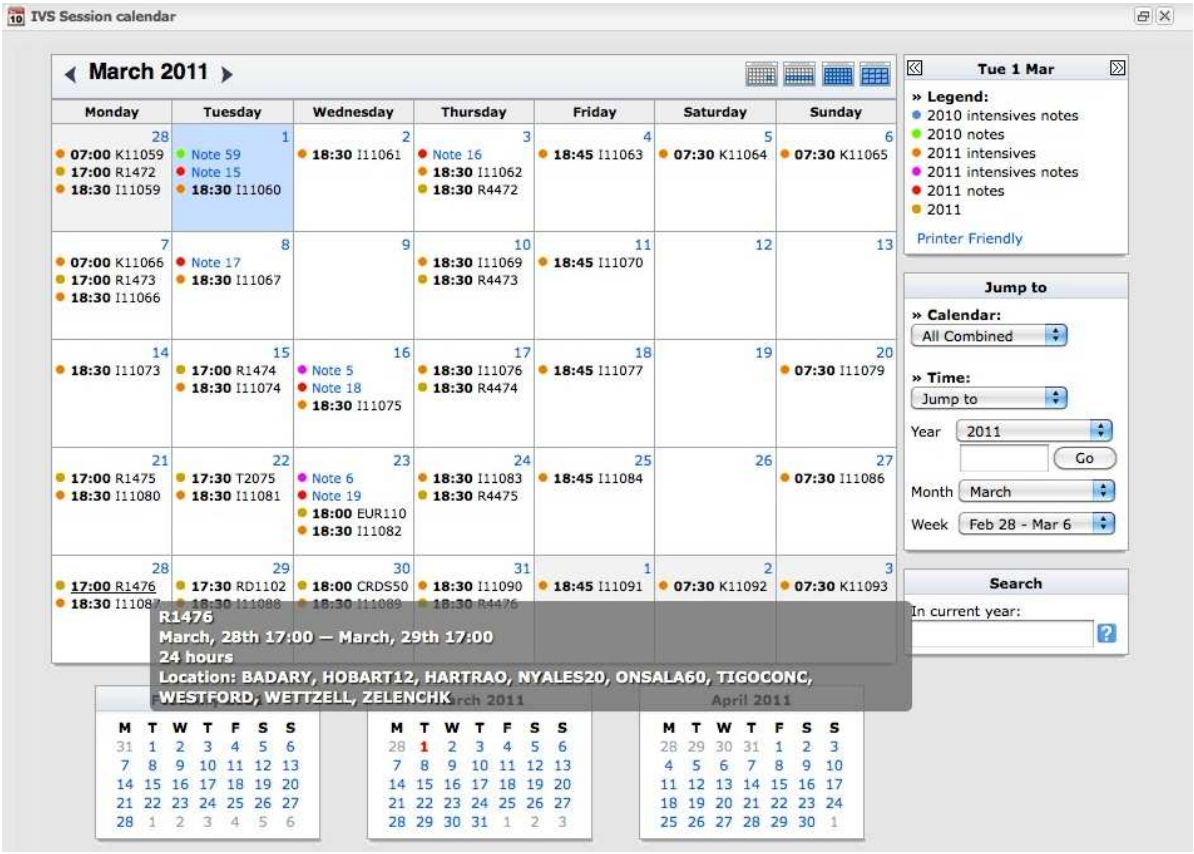

Fig. 3 The IVS Live Calendar tool provides several views of the IVS master schedules (e.g., the monthly view here), useful navigation tools and basic information about each session by clicking on or mousing over the session name (R1476 in this case).

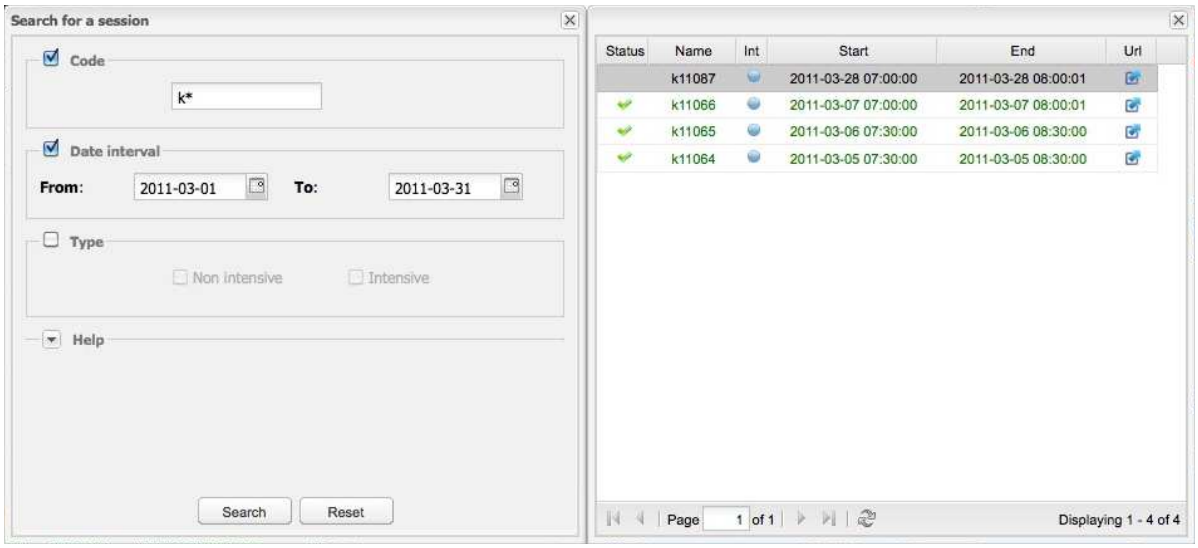

Fig. 4 Example of a session search: we looked for all March 2011 sessions with a code that begins with a “k” (query forms are located in the left-hand side window). As displayed in the result window (right-hand side), four sessions matched these criteria (k11064, k11065, k11066 and k11087). By clicking on the corresponding url icon, you will load the session into the IVS Live interface .

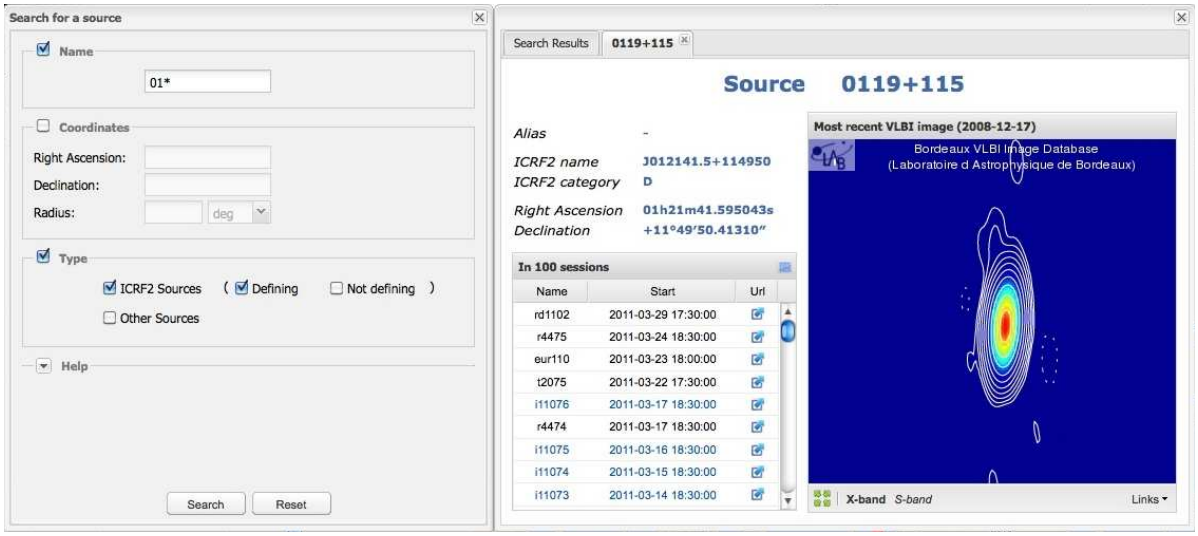

Fig. 5 Example of a source search: we looked for all ICRF2 defining sources with a name that begins with "01". Among the list of the 12 matching sources, we selected the source 0119+115. The associated tab comprises specific information about this source, the list of the sessions which contain the source, and the most recent VLBI images extracted from the Bordeaux VLBI Image Database.

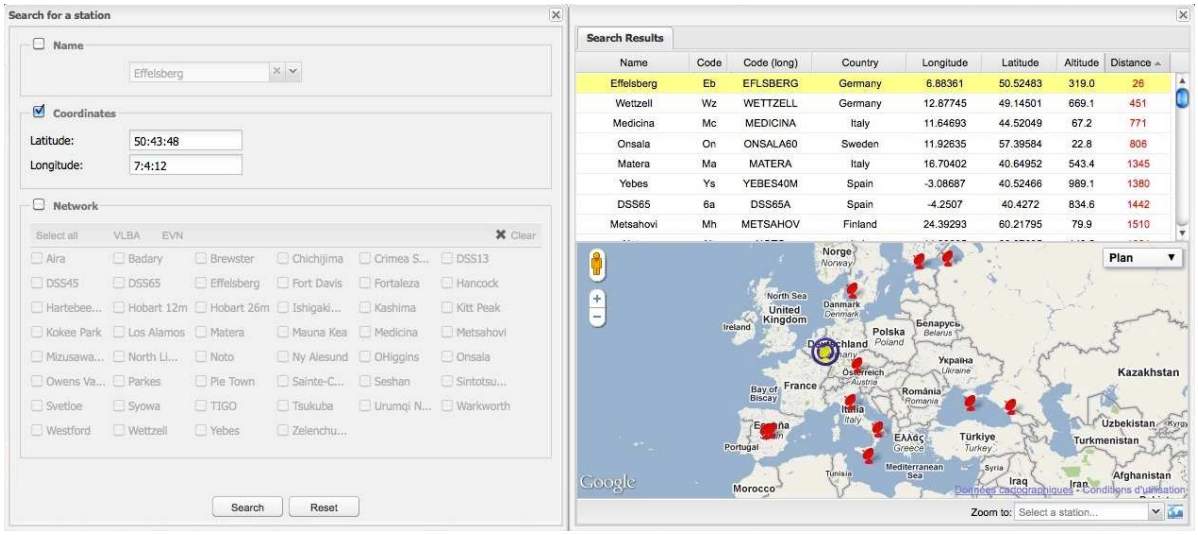

Fig. 6 Example of station search: we are interested in the closest station from the Max Planck Institute for Radio Astronomy at Bonn, Germany (MPIfR coordinates are approximatively 50°43′48″N, 7°4′12″E). As the resulting list is ordered by distance, we found that the closest station is Effelsberg (26 kilometers away). More information may be displayed by clicking on the station name: details about the station (coordinates, webcam link, if available), the list of the sessions in which the station participated and a location map.

DBBC3

G. Tuccari

Abstract The DBBC backend is crossing a new phase because an important bandwidth and data rate growth is required for both geodetic and astronomical observations. Current state of the art technologies offer the opportunity for a significant improvement in the overall sensitivity and in the delay determination. This suggested a new project named DBBC3 that represents the third generation of the DBBC backends.

Keywords DBBC, Digital Backend, Digital Receiver

1 Background

The DBBC development as an entire system started in 2004. Preliminary experiments with the first prototypes indeed had demonstrated as it could have been achieved the possibility to condensate the functionality included in the entire MK4 VLBI analogue terminal in the numerical domain, converting immediately the signal available as IF from the receiver. The entire process in the time was proved to be a challenge for the wide band and the high frequencies involved. The DBBC project so has had an evolution that can be summarised like:

- DBBC1 2004 - 2008
  in: 4 x IF-512MHz
  out: DDC 16xbbc(1-2-4-8-16MHz)@32MHz
  1.024Gbps

- DBBC2 2007 - now
  in: 4 x IF-1024MHz
  out: DDC 16xbbc(1-2-4-8-16MHz)@32MHz
  PFB 4 x 16 x 32MHz@64MHz
  8.192Gbps = 4 x 2048Mbps

- DBBC2010 2009 - now
  in: 8 x IF 512/1024MHz
  out: PFB 8 x 16 x 32MHz@64MHz
  16.384Gbps = 8 x 2048Mbps

The first version was a replacement one to one of the existing VLBI terminal at its most evolved performance, while starting with the DBBC2 together with such possibility there were also included observing modes not existing in the analogue backend. This has been still enhanced with the VLBI2010 that is a backend able to accomplish the VLBI2010 observing mode, the coming next generation of geodetic VLBI backend system.

VLBI2010 operates in a single wide band ranging approximately between 2 and 14 GHz. Inside this range a number of 512 or 1024 MHz wide pieces of band are selected in order to optimise a band synthesis translated in a much wider portion of spectrum with the respect to the present one. A so wide portion of band is also of great interest for astronomy because of the significant increase of sensitivity. Having the chance to process an entire piece of band wide 14 GHz could then represent an actual quantum leap in the digital radioastronomy data acquisition. This is the goal for the DBBC3.

Gino Tuccari
INAF, Istituto di Radioastronomia, via Gobetti 101, I-50100 Bologna, Italy

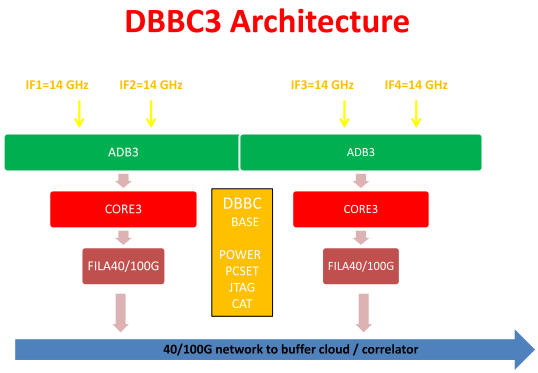

Fig. 1 DBBC3 Architecture

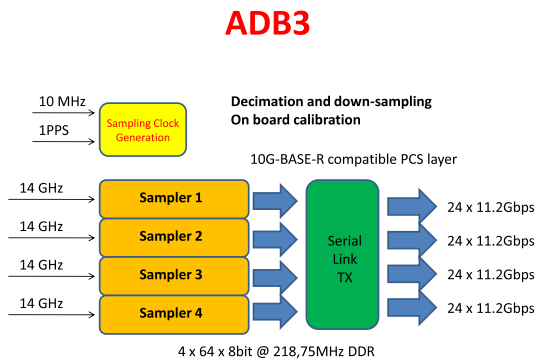

Fig. 2 The Sampler Board ADB3

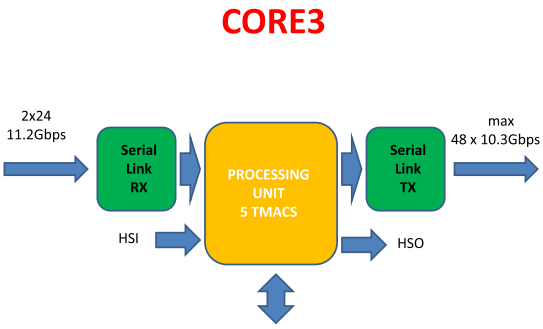

Fig. 3 The Processing Board CORE3

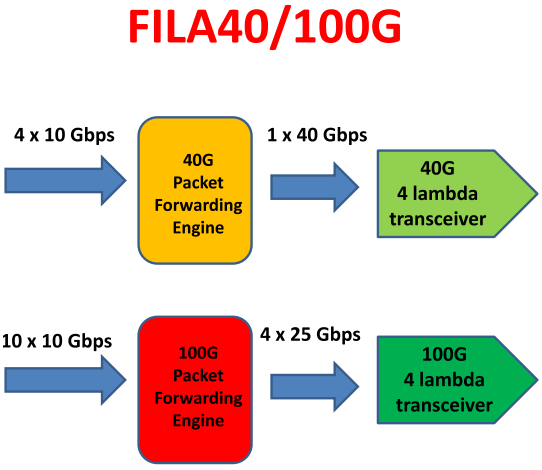

Fig. 4 The Network Board FILA40G

2 DBBC3 Performance and Structure

The DBBC3 has to accomplish some mandatory requirements, some of them looking at the past and so at the existing system, some in the direction of a near future.

In order to be compatible with the existing structures, the new hardware needs to be 'socket compatible'. This aspect is useful because existing DBBC terminals on the field can just be upgraded to meet the new performance. Moreover elements proper of the DBBC3 can be adopted in the existing DBBC2 and DBBC2010 to improve the capability with additional functionalities.

The much higher performance on the other hand requires new elements in the hardware parts that will be then specific to support the advanced functionalities. The main features of the new system are:

- Number of Wide Input IF: 4
- Instantaneous bandwidth in each IF : more than 14 GHz
- Sampling representation: 8 bit
- Processing capability 2 x 5 TMACS (multiplication-accumulation per second)
- Output data rate: max 896 Gbps
- Compatibility with existing DBBC environment.

In the figures are represented the main schematic components of the DBBC3: overall architecture, the ADB3 structure, the Core3 structure, FILA40G concept.

The structure of the system is straightforward. Four IFs 14 GHz wide are sampled with 8-bit representation. Such impressive functionality is performed by a state of the art device at present available in some prototype units. Data coming from the samplers board ADB3 are routed using the high speed input lanes (HSIL) bus to the processing board CORE3. Such last board process data in polyphase filter bank fashion to produce a large number of down-converted portions of band. From such pool of potential channels a selection is per-

formed in order to accomplish the actual output data rate through the high speed output lanes (HSOL) bus. Band synthesis can then realized, with an appropriate choice of such channels dividing the band, as desired by the VLBI2010 requirements and limited by the RFI constraints.

Data from the converted bands are then transferred to the network board FILA40G that is then routing with the required data rate at the final destination using standard transmission in packets. Such final point could be a VLBI correlator so as a buffer cloud if required.

A direct data conversion is possible in the digital domain for the full 14 GHz band, without a need for a preliminary analogue conversion. This can represent a very important step ahead in the simplification and in the performance improvement of the VLBI2010 electronics so as a reduction of the system cost. The same term backend could be not anymore adequate due to the typical functionality of a front-end this system would represent.

The first evaluation and simulation suggest to consider a full input band 14.336 GHz wide that after processing generates a block of 256 channels spanned in the entire 14 GHz range, each of them wide 56 MHz. Other options suggest 128 channels each 112 MHz wide. The output band selection is then the last logical stage in the data definition for band synthesis or to fit the maximum actual data transfer or correlation capabilities.

3 First Measurements

Some preliminary evaluations are underway and a first prototype of ADB3-like has been considered. Such prototype is including two samplers in one board and the support for determining the basic performance.

It was then possible to perform the first measurements in April 2011 adopting in particular the direct acquisitions with a full input bandwidth of 14 GHz. A zero baseline cross-correlation was realized with the samples at the entire 8-bit data representation coming from the two samplers both fed with the same signal. Results are shown in the figure, and it can be seen as the amplitude and phase behave pretty well. This even if preliminary test is a very encouraging result.

Additional tests will be performed with a second prototype with completely independent internal local

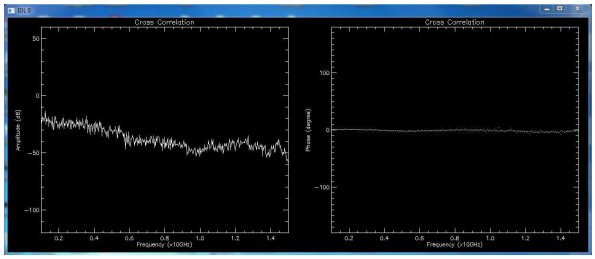

Fig. 5 ADB3 Preliminary correlation results in zero baseline cross-correlation

oscillators, of course locked with a common low frequency reference. This test is planned for June 2011.

4 Development Plan and Team

The project has been financed by Radionet and in 2012 the first formal activities will start. In this previous year the structure in detail will be defined, including those simulations critical for the architecture definition. The team collaborating to the project is composed by INAF Istituto di Radioastronomia and Osservatorio di Arcetri in Italy, Max-Planck-Institut für Radioastronomie in Germany and Chalmers Onsala Space Observatory in Sweden.

Concepts for continuous quality monitoring and station remote control

M. Ettl, A. Neidhardt, H. Rottmann, M. Mühlbauer, C. Plötz, E. Himwich, C. Beaudoin, A. Szomoru

Abstract In the newly funded Novel EXploration Pushing Robust e-VLBI Servicesproject (NEXPReS) the Technische Universität München realize concepts for continuous quality monitoring and station remote control in cooperation with the Max-Planck-Institute for Radioastronomy, Bonn. NEXPReS is a three-year project aimed at further developing e-VLBI services of the European VLBI Network (EVN), with the goal of incorporating e-VLBI into every astronomical observation conducted by the EVN. This project focus on developments of an operational e-control system with authentication and authorization. It includes an appropriate role management with different remote access states for future observation strategies. To allow a flexible control of different systems in parallel sophisticated graphical user interfaces are designed and realized. It requires also a session oriented data management. Because of the higher degree of automation additional system parameters and information is collected with a new system monitoring. The whole system for monitoring and control is fully compatible to the NASA field system as extension. The concept will be proofed with regular tests between Wettzell and Effelsberg.

Keywords NEXPReS, VLBI, e-VLBI, remote control, e-RemoteCtrl, e-SysMon, rpc, idl2rpc, middleware, GGOS, NASA field system, Wettzell, Tigo, ssh, authentication, authorization, Geodetic Observatory Wettzell, Geodesy, fundamental station, system monitoring, EVN

M. Ettl and A. Neidhardt
Geodetic Observatory Wettzell (FESG)
Sackenrieder Strasse 25
D-93444 Bad Kötzting, Germany

M. Mühlbauer, C. Plötz and R. Dassing
Geodetic Observatory Wettzell (BKG)
Sackenrieder Strasse 25
D-93444 Bad Kötzting, Germany

H.Rottmann
Max-Planck-Institut für Radioastronomie
Auf dem Hügel 69
53121 Bonn

E.Himwich
National Aeronautics and Space Administration/Goddard Space Flight Center,
Mail Code 698.2
Greenbelt, MD 20771

C. Beaudoin
MIT Haystack Observatory
Off Route 40
Westford, MA 01886-1299

A. Szomoru
Joint Institute for VLBI in Europe
Postbus 2
7990 AA Dwingeloo

1 Station remote control strategies

At the Geodetic Observatory Wettzell several possible observations strategies were detected (fig. 1). The standard case is, that an observer controls a VLBI observation locally on site at the telescope (local observation). But with new remote control technologies it is not necessary anymore that the operator is on location. He can control the system from remote (remote observation). This technology can also be used to run more than one telescope by a single operator. This kind of control-sharing between operators is called shared ob-

servation. At Wettzell also completely unattended observations have been done especially for the weekend sessions for over 2 years now. For these the antenna runs completely autonomous and automatic without an operator (unattended observation). Especially remote and shared observations offers a lot of new possibilities: A passive data access can be granted for live monitoring. There are possibilities for tele-working with full control access where specialists can assist the local operators by remote. Very remote telescopes as at Antarctica can be controlled from remote over large distances. And shared observations can reduce the manpower for shifts or help to react on current research needs.

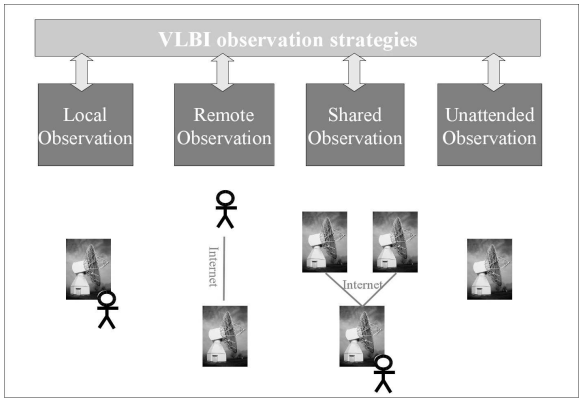

Fig. 1 VLBI Observation strategies

2 Authentication and authorization

The current software generator (`idl2rpc.pl`) version used for creating the communication layer automatically, does not support authentication and authorization techniques as well as role management. This means that in the current development state, a remotely connected user has complete access and control rights on the radio telescope system. For a future usage within an international collaboration of different, proprietary telescopes of different institutions the access rights must be definable and dedicated to the individual institution permits. This requires different access rights to the telescope, definable on a fine grained level by the site administration. Therefore a basic user authentication with user name and password is needed as a low-level individualization. This must be directly assignable with operating system users to use standard system features. During the first phase of this milestone it is necessary to compare possible methods, as given by the operating system or by data encryption standards from remote procedure call generators. A suitable solution must be integrated into the `idl2rpc.pl` generator. The general encryption is already given by Secure Shell (SSH) usage.

3 Role management

The live monitoring strategy is especially helpful for coordinating a session. For instance, if there are changes in the schedule, the scheduler has the possibility to check all telescopes pointing to the correct source. This requires a sophisticated role management where each client that is allowed to access the telescope is associated with a dedicated role. A possible set of roles are depicted in fig.2. The following fine grained access levels (roles) are possible candidates:

- *Observer*
  The *observer* is passively monitoring the system state without having any control or influence to the running system. This is the default associated role.
- *Notifier*
  Having this role, signals can be sent, e.g. if a session scheduler or a correlator detects problems during observations, but has no rights to control the telescope, it can push a notification to the local staff in real-time.
- *Scheduler*
  A *scheduler* is capable of manipulating observation schedules and whole events. Therefore a responsible person for a dedicated session can change the schedule relevant parts and inject it into the field system. During the run he can change complete sequences to replace sources or change frequencies. An extension to the NASA field system is needed to realize these dynamic scheduling possibilities (`drudg` adaption).
- *Agent*
  An *agent* can change dedicated procedures during observations, where specific observer tasks are used. This role has a reduced access to system specific procedures, directly involved to the current session.

- *Operator*
  An Operator has all rights for NASA Field System on location of the telescope which is similar to a remote version of a current operator on site.
- *Superuser*
  The *superuser* has complete access to the computer system. Normally only the telescope staff should have these exclusive permissions.

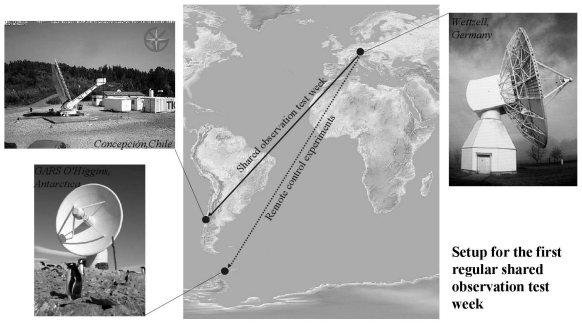

Fig. 2 Associated roles

4 e-RemoteCtrl features

The graphical user interface (GUI) has been developed using wxWidgets[1]. It is a well tested and popular platform independent development kit for the C++ programming. The current version of this GUI was mainly developed for Linux systems. Following an overview about a few new features is given:

- *Logging window and user input (see fig. 3)*
  Compared to the classic version of the NASA field system user interface, the new design has a built-in filter mechanism where the user can search for patterns. This is very helpful, because during a session the logfile can become very big and searching the logfile for a specific keyword was time consuming in the past. Furthermore the logfile can be recorded to a file at the remote computer, an alarm beep is implemented to warn the user when an error is reported from the field system. The user interface has a command line history, similar to the well known Linux command line.
- *Mark 5 capacity (see fig. 4)*
  This window has been extended to a more graphical layout, compared with to the classic version. Now, the current available Mark 5 disc space is visualized using pie charts. An additional feature for printing the labels, needed for shipping discs has also been implemented.
- *System Temperature (see fig. 5)*
  In the classic window the current system temperature values according the associated frequency was shown. In the new design a graphical window has been created, capable of plotting changes of the system temperatures over time. Here, the user can select the frequency which should be displayed over observation time. Furthermore the observation time interval can be set manually or scaled by simply using a slider.

In the new version of the GUI, the classic and the new view can be selected by the user.

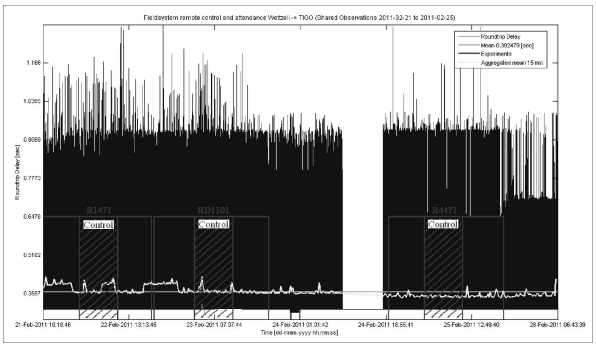

Fig. 3 The logging window

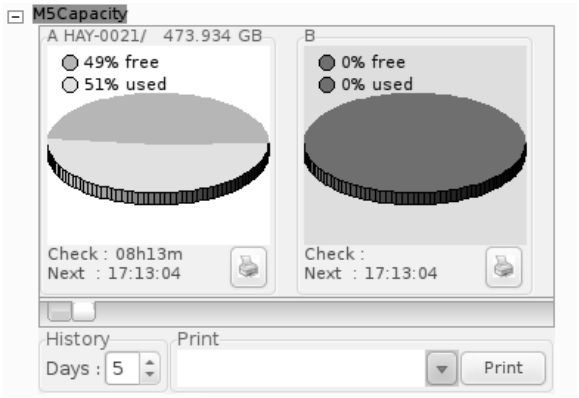

Fig. 4 The Mark5 capacity window

[1] available at http:://www.wxwidgets.org

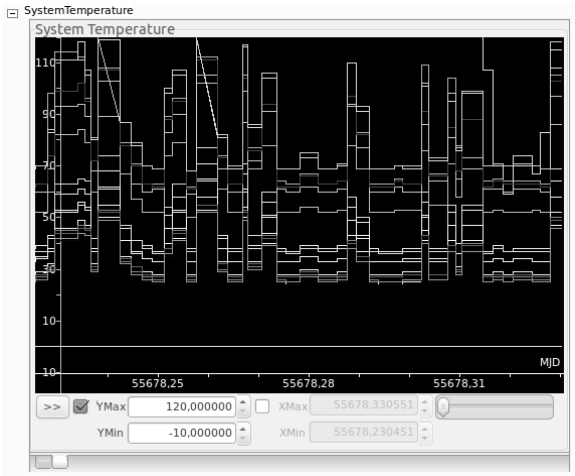

Fig. 5 The system temperature window

5 Conclusion

During the next three years the e-RemoteCtrl software will be extended about authentication and authorization features. Furthermore, this software will be part of the upcoming NASA field system release which is planned for summer 2010. This especially is a great advantage, having so many stations available for testing and verification of the software and its features. In addition, the system monitoring concept will be further refined within the VLBI MCI collaboration group[2]. Having a standardized monitoring concept is vital for station wide system monitoring and remote control. This is the first step towards the realization of a global geodetic observation system (GGOS[3]) in case of system monitoring and remote control.

References

Hans Peter Plag, Michael Pearlman (Eds.) Global Geodetic Observing System - Meeting the Requirements of a Global Society on a Changing Planet in 2020 *Axel Spring Verlag, 2009, ISBN 978-3-642-02686-7*

[2] more information at https://groups.google.com/group/vlbi2010-mci-collaboration?hl=de

[3] more information at http://www.ggos.org/ and Plag and Pearlman (2009)

New technical observation strategies with e-control (new name: e-RemoteCtrl)

A. Neidhardt, M. Ettl, H. Rottmann, C. Plötz, M. Mühlbauer, H. Hase, W. Alef, S. Sobarzo, C. Herrera, C. Beaudoin, E. Himwich

Abstract New remote control technologies for VLBI observations offer the possibilities of remote and unattended observations. This means that an operator has not to be on location of the telescope all the time but has full access from remote (remote observation). This also allows to control more than one telescope by one operator (shared observation). At Wettzell also completely unattended observations have been done especially for the weekend sessions for over three years now. The development goal is to simplify operational workflows in combination with general control structures. These new observation control strategies are not limited to VLBI. They can also be applied to other geodetic space techniques such as SLR which are necessary to realize the Global Geodetic Observing System (GGOS). The demand for continuous and reliable observations requires to disburden inconvenient night and weekend shifts. Remote controlled and autonomous observations will become more and more important in the future. State-of-the-art software for control and monitoring, developed by a team at the Geodetic Observatory Wettzell, is publicly available for testing and further developments. The most recent software release integrates several new and comfortable features to support the daily work of an operator. Cooperations as the Monitoring And Control Interface Collaboration Group as part of the VLBI2010 Working Group of the International VLBI Service for Geodesy and Astrometry work on standardizations in these developments.

Keywords e-RemoteCtrl, remote control, technical observation strategies, GGOS

A. Neidhardt, M. Ettl
Forschungseinrichtung Satellitengeodäsie, Technische Universität München, Geodätisches Observatorium Wettzell, Sackenrieder Str. 25, D-93444 Bad Kötzting, Germany
C. Plötz, M. Mühlbauer, H. Hase
Bundesamt für Kartographie und Geodäsie, Geodätisches Observatorium Wettzell, Sackenrieder Str. 25, D-93444 Bad Kötzting, Germany
H. Rottmann, W. Alef
Max-Planck-Institut für Radioastromonie, Auf dem Hügel 69, 53121 Bonn, Germany
S. Sobarzo, C. Herrera
Universidad de Concepción, Camino Einstein Km 2,5., Casilla 4036, Correo 3, Concepción, Chile
C. Beaudoin
MIT Haystack Observatory, Off Route 40, Westford, MA 01886-1299, USA
E. Himwich
National Aeronautics and Space Administration/Goddard Space Flight Center, Greenbelt, MD 20771, USA

1 Introduction

Personnel from the Geodetic Observatory Wettzell operate not only the 20 meter radio telescope at Wettzell. In cooperation with other institutes they also run the 9 meter radio telescope at the German Antarctic Receiving Station (GARS) O'Higgins, Antarctica and the 6 meter radio telescope of the Transportable Integrated Geodetic Observatory (TIGO) Concepción, Chile for geodetic VLBI experiments. In near future also the currently build TWIN radio telescopes at Wettzell must be operated in parallel with the same staff.

In the future similar situations will appear also in other observatories as the scientific visions for future sites propose an increased number of worldwide sites and telescopes. For example the designers of the Global Geodetic Observing System (GGOS) sug-

gest several globally distributed observatories with co-located, different space techniques (Plag and Pearlman, 2009). What GGOS for the geodetic science is the Square Kilometer Array (SKA) for the VLBI astronomy. The planners propose hundreds of telescopes for different frequency bands distributed over one continent (Australia or Africa) with a timeline of different phases until the year 2024 (Adams et. al., 2010).

All these developments have to deal with the same technical challenges. They touch not only the mechanical constructions. Also new technical control strategies, optimized workflows and additional system monitoring parameters must be considered. This offers a wide range for applied computer science and a team at the Geodetic Observatory Wettzell has started to investigate on realizations. Parts of them are funded by the European Union via the Frame Program 7 within the ”Novel EXplorations Pushing Robust e-VLBI Services (NEXPReS)” project (Ettl et. al., 2010).

2 New technical operation control strategies

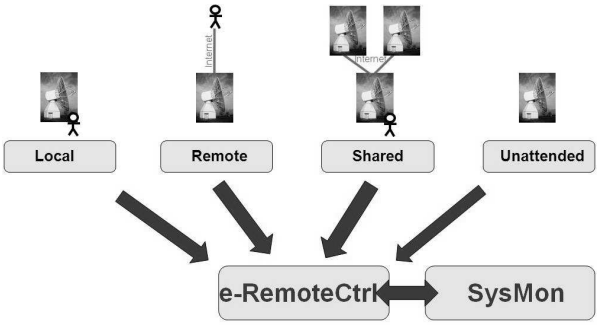

Fig. 1 Classification of the technical observation strategies.

The standard case to control operations of a radio telescope is that an observer controls a VLBI session locally on site at the telescope (local observation). He has direct access to the control system, the hardware and the telescope itself. In case of an error the operator can directly interact and stop the system manually. It is important that well educated personnel can detect problems immediately by using all human senses. But this operation mode is also the most time consuming one, because for future visions three shifts in 24 hours seven days a week must be planned.

With new remote control technologies it is no longer necessary for the operator to be on location (see 1). The operator can control the system from remote (remote observation). On stable internet connections and with intelligent and self-controlling mechanisms on location of the radio telescopes critical situations can automatically be detected. Autonomous, redundant systems can check system states and stop the operation in case of an error. The important system information can be transfered to responsible operators over the internet to each place all over the world. As the operator just gets the information which is offered by the system, an additional monitoring on location of the telescope must replace the senses of a local operator. These monitoring data allow the automatic detection of critical states and situations, either automatically taking action or informing the remote operator.

This technology can also be used to control more than one telescope by one operator. The control can be shared between different operators on different sites (shared observation). Hierarchically arranged control structures are needed to give one operator the possibility to attend and control several observations on different sites in parallel. A sophisticated graphical user interaction is as important as reliable communication systems. Communication losses must be detected, reestablished and proofed. During blackouts the systems must be able to run autonomously.

At Wettzell also completely unattended observations have been done especially for the weekend sessions for over three years now. For these the antenna runs completely autonomous and automatic without an operator (unattended observation). Well maintained and stable telescopes are needed. It is also helpful to have an on-call service, where especially trained staff can be activated on time to react on critical, automatically or from remote not solvable situations. The most important implementation of the system to detect such situations is a functional and detailed system monitoring ((Neidhardt et. al., 2010).

These remote and shared observations offer many possibilities: A passive data access can be granted for live monitoring. There are possibilities for teleworking with full control access or specialists can assist local operators by remote. Very remote telescopes such as those in Antarctica can be controlled from large distances. Further, shared observations can re-

duce the manpower for shifts or help react to current research needs. These shared observations are not restricted to systems of one dedicated space technique but can partly be arranged over system borders. Tests are already proceeded at Wettzell, where student operators at the laser ranging system also take care of the weekend sessions at the radio telescope. With clear on-call structures in case of a problem the shared observations between personnel of the two systems work quite well.

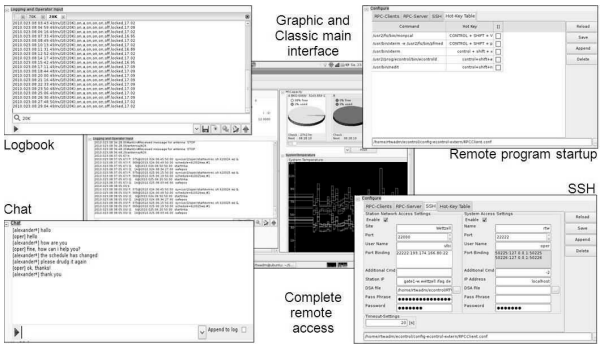

Fig. 2 The graphical user interface of e-RemoteCtrl.

3 A possible state-of-the-art solution for the new strategies: e-RemoteCtrl

Even in times of modern web-service based architectures a reliable control should base on low-level, reliable, well-known and from large software packages independent socket communications. In combination with a simple, already under Linux available middleware based on Sun Remote Procedure Calls (RPC) a classic client-server-model can be implemented. It uses the extensive functionality of the existing NASA field system (FS) and extends it with a remote interface. In the case of the FS an additional, automatically generated communication is defined using a software generator ”idl2rpc.pl”. This is also a development from Wettzell.

The main driver in the given design is a strict separation of control, communication and presentation logic. The complete arithmetic and workflow control logic reside in the server, defined as device control code. It is an autonomous working process which interacts with the remote controlled device (here at this level, the FS). The communication code independently connects the server to the outer world for requesting clients. The clients are only used to realize more or less sophisticated graphical user interfaces (see 2) with a presentation of the server processed elements. This is also the connection point to convert into possible web-services.

Overall the server acts completely autonomously. It can check system status information independently and decide what to do to keep stable and safe states. Such controlling utilities can be defined as autonomous process cells. The generated watchdog process keeps it alive and an automatic safety device allows to register if a responsible client is connected. After a breakdown of the communication to the client the server can operate completely autonomously until a critical situation (e.g. increase of wind speed to a level which is critical for the telescope) forces it to run into a safe state (Neidhardt et. al., 2010).

4 Needed information about system states

A big difference between the classic operation method with an operator on location of the telescope and a remote operator is that the remote operator can’t see all of the system states. Current hardware normally only signals errors or operation states with LEDs or on local monitors. Therefore it is difficult for a remote operator to evaluate given situations during an observation when there are no additional outputs in the FS log. Also some important information are not yet collected in the FS, as power distribution parameters or safety and emergency details.

A newly founded Monitoring and Control Interface (MCI) Collaboration Group deals with these needs and works iteratively on new standards. One result of their work is a compiled list of monitoring data collected by different monitoring nodes distributed over the telescope, its monument and the operation building. A classification of monitoring points defines three categories: data for science and analysis, data for system operations and data for diagnosis.

As some of the data are also relevant for the analysis to optimize the scientific output of the VLBI data, dedicated sets should be offered to the analysts. These data are normally low-sampled information (means within a few seconds or minutes/hours) as meteorolog-

ical data, clock offsets, strain meter measurements or water vapor radiometer values. Currently they are included to the log file which is transfered to the analysts after a session. In future selective information can also be streamed during the session. This might be especially interesting for upcoming e-VLBI transfers and real-time correlations.

Other data are mostly needed for operators, controlling the session locally or from remote. These data, as power distribution values and currents, wind speeds, emergency stops and safety parameters or rack and computer temperatures, are sampled with medium data rates (human reaction times up to a few seconds; just for info: the emergency interlocks work independently from the display much faster using hardware switches). The data are displayed over hierarchically and location tagged monitoring interfaces. Some of those states together with data for analysis can also be used to give a real-time support of the IVS Live service from the University of Bordeaux (Collioud , 2010). Some of the data also needed to be archived to identify long-term trends, as given for deformations or simple things as fan speeds, which gives hints about aging fans. Some of the sensors need activations, as given for noise diodes, so that necessary control possibilities must also be implemented.

Sometimes it is necessary to offer higher sampled (far below milliseconds to milliseconds) data for diagnosis purposes. The data mainly overlaps with the information collected for operation. But not all sensors need to offer this high sampling rates, as e.g. rack temperatures wont change rapidly . The high sampling rate for predefined sensors, as servo currents or contouring errors, can be switched on for a dedicated short time period as the produced data volumes might be enormous. The data then can be used for maintenance decisions.

On the basis of a wide range of sensor nodes autonomous systems can run there decisions combining the states logically. A sophisticated collection and upgrade of existing hardware is essential to get a reliable system which protects humans as well as the telescope hardware itself. In the suggested e-RemoteCtrl interfaces for such MCI nodes are already included and can be filled after the node installation. Such nodes should consist of simple fan-less and robust computers, with self-identifying data sets and flexible hierarchical sensor sets.

5 Identifying and optimizing operation workflows

Essential is also to think about optimizations of the current workflows. Higher observation loads need more convenient procedures for the setup, the run and the finishing of sessions on the different shared telescopes. The operator must be supported by dedicated protocol logs, showing directly checklists and giving graphs of historic data sets of the monitoring data, e.g. cable delays or clock references. In general the different communication needs within the phases for setup, run and finishing can be planned to receive data for the observation (schedules and also quality feedbacks) or to send results to correlators and analysis centers. The main modules of the workflows normally can be found in similar ways in all the systems of the geodetic space techniques with more or less extensive subsections. The main workflow parts for VLBI observations can be seen in fig. 3. To support th operator with needed monitoring information about systems states it is important to present the checklist details and check results in an ergonomic way.

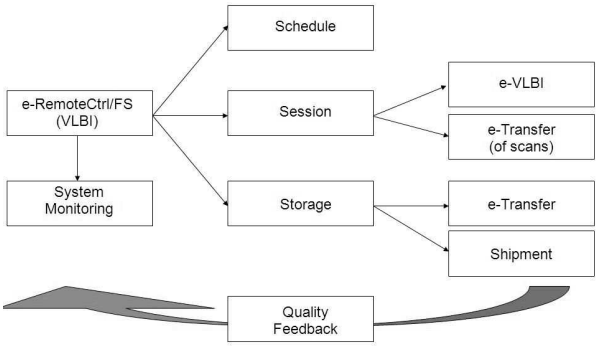

Fig. 3 Main parts of the current VLBI workflow structure.

An example of a current experiment setup checklist can be found in the notes of the Technical Operations Workshop described as ”Experiment Pre-Checks for Mark IV and VLBA Systems” (a list of suggested, manually done quality pre-checks to run an experiment including detailed information, Strand et. al., 2011):

- Prepare experiment SNAP and procedure files
- Check the computer control especially the NASA field system
- Check the station timing and time standard offsets

- (Check feed polarization)
- Check receiver status and parameters
- Check Intermediate Frequency (IF) distributor, IF3 module and IF upconverter or downconverter
- Check video or baseband converters
- (Check antenna focus)
- Check antenna pointing using a dedicated pointing fit
- Check System Equivalent Flux Density (SEFD)
- Check system temperatures
- Check phase calibration signal
- Check cable calibration
- Check and prepare Mark5A data acquisition system for data recording
- Check meteorological sensors
- Send 'Ready' message
- If necessary run additional, extensive testing

Some of the checks are more significant if the historic data are visible, e.g. for SEFD, pointing or cable delays. Other checks give a current snapshot of the system states. But most of the checks can be (semi-)automated offering a resulting protocol logbook. It should include all necessary information in manageable, graphically oriented presentations and plots. For the systems at the observatory Wettzell such improvements allow to run several parallel sessions with several worldwide telescopes in parallel controlled by one operator, who has a complete, immediate overview over and feeling for the controlled systems.

6 Conclusion

In general the new technical observation strategies allow to increase the observation load to support future scientific needs. In times of limited recourses it is essential to use the synergies over system borders especially at the observatories with co-located techniques. The observations itself are more or less time consuming and allow (semi-)automated scenarios to disburden the operators work. The solutions from the applied computer science should therefore also include investigations on workflows and operator interactions with the system. Maybe it is also possible to combine technical solutions and workflows for GGOS with those at the future SKA.

References

B. Adams. The Square Kilometre Array (SKA). SKA web page, Jodrell Bank Centre for Astrophysics, The University of Manchester, http://www.jodrellbank.manchester.ac.uk/research/ska/, 2011 (Download 2011-05-29).

A. Collioud. IVS Live Observing Sessions Come Alive... In: D. Behrend, H. Hase, H. Johnson (eds.). IVS Newsletter, Issue 28, http://ivscc.gsfc.nasa.gov/publications/newsletter/issue28.pdf, 2010.

M. Ettl, A. Neidhardt, C. Plötz, M. Mühlbauer, R. Dassing, H. Hase, C. Beaudoin, E. Himwich. SysMon, a monitoring concept for VLBI and more. 10th European VLBI Network Symposium and EVN Users Meeting: VLBI and the new generation of radio arrays, 10th EVN Symposium, PoS(10th EVN Symposium)025, http://pos.sissa.it/archive/conferences/125/025/10th%20EVN%20Symposium_025.pdf, 2010 (Download 2011-05-29).

A. Neidhardt, M. Ettl, C. Plötz, M. Mühlbauer, H. Hase, S. Sobarzo, C. Herrera, W. Alef, H. Rottmann, E. Himwich. Interacting with radio telescopes in real-time during VLBI sessions using e-control. 10th European VLBI Network Symposium and EVN Users Meeting: VLBI and the new generation of radio arrays, 10th EVN Symposium, PoS(10th EVN Symposium)024, http://pos.sissa.it/archive/conferences/125/024/10th%20EVN%20Symposium_024.pdf, 2010 (Download 2011-05-29).

H.-P. Plag, M. Pearlman. Global Geodetic Observing System. Meeting the Requirements of a Global Society on a Changing Planet in 2020. Springer, 2009.

R. Strand, M. Poirier. Experiment Pre-Checks for Mark IV and VLBA Systems. Notes of the 6th IVS Technical Operations Workshop, MIT Haystack Observatory, 2011.

Mark 6: A Next-Generation VLBI Data System

A. R. Whitney, D. E. Lapsley, M. Taveniku

Abstract The Mark 6 system is being jointly developed by Haystack Observatory and XCube Communications as a next-generation disk-based VLBI data system, and is designed to support sustained data rates to 16Gbps writing to an array of disks. Begun as a collaborative project in late 2010, the system is based completely on COTS hardware and has demonstrated 16Gbps sustained recording (to 32 disks) from digital-backend systems based on the Casper ROACH board; zero-baseline data of broadband correlated noise have been successfully recorded and correlated on the Haystack DiFX software correlator. The Mark 6 system is expected to be tested in several VLBI experiments in mid-2011 and be available to the general VLBI community in late 2011.

Keywords VLBI, VLBI2010, VLBI recording, VLBI instrumentation

1 Introduction

The demand for increasing data rates for VLBI observations is particularly acute in two disciplines: 1) mm-VLBI observations, which are typically starved for sensitivity, as well as the need to gather as much data as possible during the atmospheric coherence period of 30-60 seconds, and 2) geodetic-VLBI observations, which must gather as much data as possible over a multi-GHz bandwidth in a period of 5-15 seconds. Both of these disciplines are eager to capture data at 16-64Gbps and record to disk. The Mark 5 series of VLBI data systems is limited to a maximum of 4Gbps (Mark 5C) and cannot support 16 Gbps and higher data rates without many systems operating in parallel, which is both expensive and cumbersome. The Mark 6 system, based fully on commercial-off-the-shelf (COTS) hardware, is being jointly developed by MIT Haystack Observatory and XCube Communications, Inc to fulfill these needs. A prototype Mark 6 system has demonstrated VLBI data recording at sustained 16Gbps, with burst-capture capability to $\sim$32Gbps.

A.R. Whitney, D.E. Lapsley
MIT Haystack Observatory, Westford, MA 01886, USA
Michael Taveniku
XCube Comminications, Inc., Nashua, NH, 03060, USA

2 Origin of the Mark 6 system

The basis of the Mark 6 system is derived from a disk-based data-logging system developed by XCube Communication of Nashua, NH for testing automated-driving systems for the automotive industry. Cars to be tested are outfitted with XCube 'loggers' to capture real-time technical data from the automobile, as well as from numerous car-mounted HD video cameras pointing in all directions to continuously capture the complete environment around the vehicle; this allows thorough examination of the environment surrounding the vehicle to understand reactions of the automated-driving software, and to diagnose unexpected actions. The sustained data-rate requirement for this application is $\sim$6 to 12 Gbps, with the recording equipment mounted in the trunk of a moving automobile that must operate properly while absorbing all the usual bumps and motions of driving. As a result, the XCube 'logger' was specifically designed to sustain required recording

Fig. 1 Front view of Mark 6 controller with disk module

Fig. 2 Rear view of Mark 6 controller with disk module

rates in the face of disks whose performance may be degraded by this harsh environment.

Though VLBI-data disks do not typically suffer a bumpy ride during recording, they often suffer a bumpy trip from correlator to station, which sometimes has a negative effect on the recording performance of some disks; use of such affected disks can threaten required sustained recording rates if used in ordinary RAID disk arrays, which are insensitive to real-time requirements. The techniques used in the XCube 'logger' have been extended to the Mark 6 VLBI data system, but at much higher data rates. Both the XCube 'logger' and the Mark 6 system are based completely on high-end COTS hardware with highly specialized control software.

3 Main Characteristics of the Mark 6 system

3.1 Hardware

As indicated above, the Mark 6 controller incorporates only COTS hardware, though components are carefully selected for performance and compatibility with other system elements. A high-end motherboard, CPU and RAM memory are used to maximize performance; a standard Mark 6 system is outfitted with ∼12GB of high-speed RAM memory, though up to ∼128GB can be accommodated for burst-mode applications. The Mark 6 prototype system is shown in Figures 1 and 2.

3.2 Software

The Mark 6 system operates under an Ubuntu Linux OS, though with some modified kernel code and drivers for efficient memory and disk management. Application software is written primarily in C++ and Python. The Mark 6 performance arises from a technique decoupling network and disk datastreams with elastic buffers and kernel-bypass DMA for data transfer.

3.3 Input

The Mark 6 can accommodate up to four 10GigE data-input ports, each operating at up to ∼7Gbps. Each input may operate at a different data rate. Normally, data are transmitted to the Mark 6 in a UDP packet stream to minimize load on the Mark 6 Ethernet NIC cards and sustain the highest possible data rate.

3.4 Disks, disk modules and connection to disks

The Mark 6 system supports only SATA-interface disks; furthermore, it has been discovered that not all disk vendors implement the SATA interface in exactly the same way, which causes some vendors disks to operate more capably with the chosen disk-interface card. As a result, for maximum performance, it is currently necessary to specify particular disk vendors, though low-cost commodity (i.e. non-enterprise) disks from these vendors are acceptable.

Mark 6 disk modules are similar to Mark 5 disk modules (8 disks per module) except that Mark 6 disk modules connect to the controller via COTS external-SATA cables. Each external-SATA cable supports 4 disks, so that a module requires the connection of two such cables plus one power cable. Any cable may be connected to any disk module; the controller sorts out which disks it is connected to. XCube also offers a

module that houses 16 2.5-inch disks that requires the connection of four external-SATA cables. All XCube modules include an internal fan.

We are investigating the feasibility of developing a conversion kit that will permit existing Mark 5 disk modules to be modified to operate with the Mark 6 system, allowing significant cost recovery of the original module expense (though existing PATA modules will need to be outfitted with SATA disks). A conversion kit would include a new module backplane, plus a new front panel with appropriate connectors. Because the Mark 5 modules do not include built-in cooling, an external cooling fan must be provided, which could be provided by an (otherwise idle) Mark 5 chassis or a simple chassis that accepts the modules and provides fan cooling.

The use of standard external-SATA cables to connect the Mark 6 controller to the modules is different from Mark 5 but is quite workable. The heaviest wear is on the cable ends connecting to the modules. Cables can be reversed to double their lifetime (projected $\sim$500 connect/disconnect cycles for each cable end). When a cable connector wears out, the cable is easily and inexpensively replaced.

3.5 Monitor & Control and disk management

A VSI-S command set has been specified for the Mark 6 and is being built as a layer on top of the native XML interface provided by XCube.

Depending on recording data rate, different numbers of simultaneously-operating disk modules are required. A single 8-disk module with modern disks will support 4Gbps; two modules (16 disks) are required for 8Gbps, 4 modules (32 disks) are required for 16Gbps. In order to accommodate these different requirements, the concept of a ‘volume’ has been created to identify the collection of one or more disk modules needed to support a particular observing requirement. A ‘volume is created by ‘bonding’ a specified set of modules together for the duration of existence of a particular data set. When that data set is erased, the constituent modules become individual volumes again.

In the case that multiple volumes are simultaneously mounted to the Mark 6 (for example, four volumes of single 8-disk modules, or two volumes of two 8-disk modules), they are organized into a logical ‘volume stack that specifies the order of usage; when the currently active (recording) volume nears capacity, the Mark 6 can automatically re-direct subsequent scans to the next volume in the ‘volume stack’. The full volume may be then disconnected and a new empty volume attached and added to the volume stack, all while recording continues on the active recording volume. Enhancements have had to be made to the XCube software in order to support this mode of operation required for VLBI operations.

Care is being taken to continuously collect disk-performance statistics to identify the module and disk serial-number of poor-performing disks so that such disks can be easily physically identified and replaced.

3.6 Data format on disks; playback

The Mark 6 writes a single standard Linux file to each data disk for each input data stream. The data stream from each Ethernet interface is gathered into a buffer of order 64MB before attempting to write that data to the next disk in a round-robin sequence; if a disk is not ready at the time the data buffer is ready to be written, the write request is immediately diverted to the next disk in the sequence; this allows data distribution among disks according to their individual performance. Each buffer is identified by a header with a sequence number that, on replay, allows properly ordered data to be reconstructed from the multiple files to which is has been scattered.

Software is being written that, on replay, represents the data from each recorded data stream as a single Linux file; this greatly simplifies interfacing the Mark 6 to a software correlator.

In order to maintain the maximum recording-rate capability, the Mark 6 records the entire Ethernet packet from all data streams and is oblivious to the format of the actual data frame within the Ethernet packet. On replay, Ethernet header and trailer data are normally stripped so that the user sees only the actual payload packet (VDIF or Mark 5B, etc).

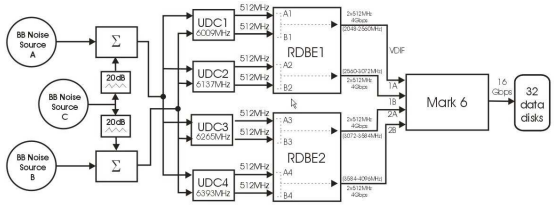

Fig. 3 System used for 16Gbps Mark 6 demonstration

3.7 e-VLBI capabilities

Full e-VLBI capabilities are planned for the Mark 6.

4 16 Gbps Mark 6 demonstration at Haystack TOW meeting

On the occasion of the VLBI Technical Operations Workshop (TOW) held at Haystack Observatory in May 2011, a demonstration of the Mark 6 system was held. Figure 3 shows the schematic of the system setup for recording. Two broadband correlated noise sources are fed into a set of four up-down converters (UDC). Each UDC selects a different 512MHz slice of spectrum from each of the two correlated noise sources and translates it to 512-1024MHz (second Nyquist zone) for input into two RDBE digital backend units (based on the ROACH general-purpose signal-processing board developed at Berkeley, NRAO and South Africa, with firmware developed at Haystack Observatory). The output of each RDBE is two 10GigE data streams, each at 4Gbps, for an aggregate data rate into the Mark 6 of 16Gbps. Data were recorded to a set of 32 disks for several minutes.

Following recording ∼1 second of data were reconstructed from the Mark 6 disks and transferred to a standard Linux file for correlation on the Haystack DiFX software correlator (see Figure 4). The correlation (from the 'fourfit' fringe-fitting program) results from one 512MHz slice of the recorded bandwidth are shown in Figure 5, and are as expected. Ripples on the cross-correlation bandpass amplitude and phase are due to both non-flatness of the noise sources and differences in analog filters along the parallel signal-processing paths across the 512MHz channel bandwidth.

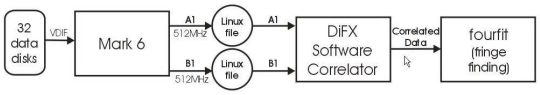

Fig. 4 System used for replay and correlation of 16Gbps data

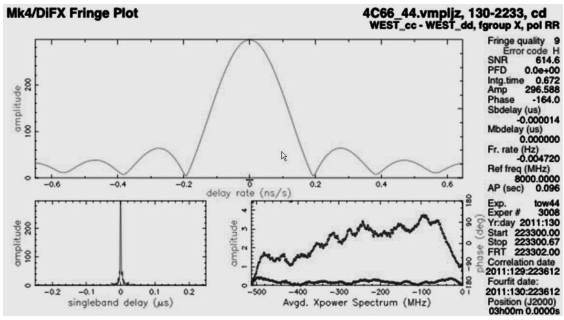

Fig. 5 Cross-correlation results through 'fourfit' fringe-fitting program

5 Summary

The Mark 6 VLBI data system is a major step forward in data-rate capability over previous VLBI data systems, and is the first high-performance system to use fully COTS hardware. The high-performance and low-cost of the Mark 6 system, as well as future improvements due to the normal progress of COTS technology, will help to maintain its long-term viability. In the short term, mm-VLBI and geodetic VLBI will be the major beneficiaries of the new capability, but in the longer term will also enable much higher sensitivity over a board range of VLBI observations.

More information about the Mark 6 system is available at http://www.haystack.edu/tech/vlbi/mark6/index.html. The Mark 6 system is expected to be available to the general VLBI community in late 2011.

Experiences with regular remote attendance towards new observation strategies

M. Ettl, A. Neidhardt, M. Mühlbauer, C. Plötz, H. Hase , S. Sobarzo, C. Herrera, E. Oñate, P. Zaror, F. Pedreros, O. Zapato

Abstract Current VLBI observations are controlled and attended locally at the radio telescopes on the basis of pre-scheduled session files. Operations dealing with system specific station commands and individual setup procedures. Neither the scheduler nor the correlator nor the analyst get a real-time feedback about system parameters during a session. Remotely induced changes in schedules after the start of a session are impossible. For future scientific applications more flexibility in the session control would optimize the station resources. Therefore a proposed shared-observation control of the global network of radio telescopes will be an advantage. Remote attendance/control as well as completely unattended-observations will become a necessity for VLBI2010 observation programs. To approach the goal of remote controlled VLBI operation the Geodetic Observatory Wettzell in cooperation with the Max-Planck-Institute for Radio Astronomy in Bonn are developing a software extension for remote control to the existing NASA Field System. The status of this developments allow already regularly remote controlled observations at Wettzell. The software extension was also tested in both ways in geodetic VLBI session between Wettzell, Germany and Concepción, Chile. The Intensive-sessions during weekends from Wettzell with Tsukuba are regularly operated remotely. The experiences gathered by these different session setups have led to new features like automatic connection reestablishment and internet performance measurements. Future developments for an authentication and user role management will be subject of the upcoming NEXPRES[1] project.

Keywords NEXPReS, VLBI, remote control, remote attendance, GGOS, geodetic observation strategies, e-RemoteCtrl, rpc, idl2rpc, middleware, GGOS, NASA-Fieldsystem, Wettzell, TIGO

M. Ettl and A. Neidhardt
Geodetic Observatory Wettzell (FESG)
Sackenrieder Strasse 25
D-93444 Bad Kötzting, Germany

M. Mühlbauer, C. Plötz and H. Hase
Geodetic Observatory Wettzell (BKG)
Sackenrieder Strasse 25
D-93444 Bad Kötzting, Germany

S. Sobarzo, C. Herrera, E. Oñate, P. Zaror, F. Pedreros and O. Zapato
Universidad de Concepción
Camino Einstein Km 2,5., Casilla 4036, Correo 3, Concepción, Chile

1 VLBI observation strategies

At the Geodetic Observatory Wettzell several possible observations strategies were detected (fig. 1). The standard case is, that an observer controls a VLBI observation locally on site at the telescope (local observation). But with new remote control technologies it is not necessary anymore that the operator is on location. He can control the system from remote (remote observation). This technology can also be used to run more than one telescope by a single operator. This kind of control-sharing between operators is called shared observation. At Wettzell also completely unattended observations have been done especially for the weekend sessions for over 2 years now. For these the antenna

[1] http://www.nexpres.eu/

runs completely autonomous and automatic without an operator (unattended observation). Especially remote and shared observations offers a lot of new possibilities: A passive data access can be granted for live monitoring. There are possibilities for tele-working with full control access where specialists can assist the local operators by remote. Very remote telescopes as at Antarctica can be controlled from remote over large distances. And shared observations can reduce the manpower for shifts or help to react on current research needs.

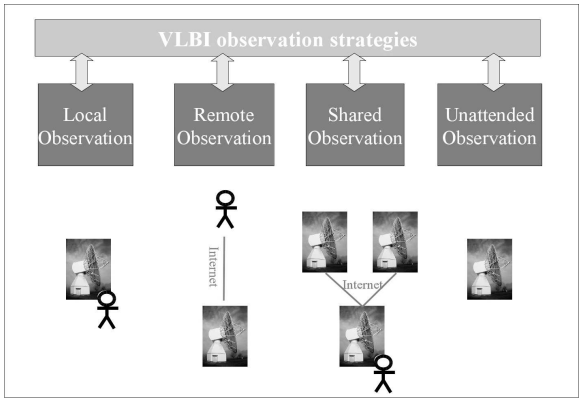

Fig. 1 VLBI Observation strategies

2 Regular shared observation test week

Wettzell develops a software extension for remote control to the existing NASA Field System (FS) in cooperation with the Max-Planck-Institute for Radio Astronomy (Bonn). The software, called e-RemoteCtrl, uses remotely accessible, autonomous process cells as server extension to the FS on the basis of Remote Procedure Calls (RPC)[2]. Based on this technology several remote control and attendance tests were successfully shown with telescopes at Germany, Chile, Antarctica and also at foreign sites as Hobart[3]. The latest test between Wettzell and Concepción on February 21th to 25th demonstrated a regular shared observation week. Wettzell took over complete night shifts from Concepción while running the own observation sessions. Therefore Wettzell operated the sessions **R1471**, **RD1101** and **R4471** at the Chilean telescope remotely between 2:00UT and 10:00UT. For security reasons, the whole communication was tunneled using Secure Shell (SSH) with automatic connection control. It (re-)establishes broken SSH tunnel without user interaction. During the session local operators were available on both sides to be prepared in case of malfunctions. The integrated chat functionality and a web cam live view gave additional feedback.

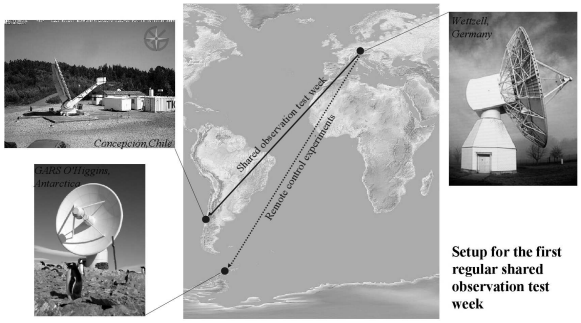

Fig. 2 Geographic locations and setup

3 The results

During the shared observation the roundtrip delays (time for sending a request and receiving the response) of commands were captured for almost a whole week. For a better interpretation an aggregated mean calculation for 15 minute intervals over the round-trip delays is used. Therefore higher network loads can be seen, influencing the remote control. The mean roundtrip delay to Chile and back is about 0.39 seconds. This means that each command takes a third second from sending to the response. With this one week lasting regular observation test very important conclusions could be made: (1) The used SSH-stabilization without a human interaction worked quite well without large control gaps (the longer time without transfer was caused while the system was not active). (2) The telescopes use very proprietary setup procedures and antenna commands. Even with the standardizing FS it is quite difficult to know all of these specifics. This means, that standardized pro-, mid- and post-session procedures must be designed on the basis of checklists and with (graphical) logbook reports. (3) Additional system monitoring

[2] see more at Neidhardt (2009) and Bloomer (1992)

[3] see more at Ettl (2010) and Neidhardt (2010)

data is necessary to get a better overview of the system status from remote.

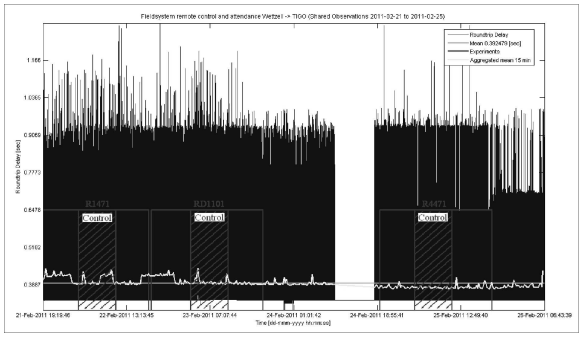

Fig. 3 Roundtrip delay results during remote control session

References

J. Bloomer *Power Programming with RPC* O'Reilly, 1992, ISBN 0-937175-77-3

M. Ettl, A. Neidhardt, R. Dassing, H. Hase, C. Sobarzo Guzmán, C. Herrera Ruztort, C. Plötz, M. Mühlbauer, E. Onate, P. Zaror, First proof of concept of remote attendance for future observation strategies between Wettzell (Germany) and Concepción (Chile) *Proceedings of Science (PoS) - 10th European VLBI Network Symposium and EVN Users Meeting: VLBI and the new generation of radio arrays, EID PoS(10th EVN Symposium)075, Scuola Internazionale Superiore di Studi Avanzati (SISSA), 2010*

A. Neidhardt Manual for the remote procedure call generator *idl2rpc.pl Geodetic Observatory Wettzell, 2009*

A. Neidhardt, M. Ettl, C. Plötz, M. Mühlbauer, H. Hase, S. Sobarzo Guzmán, C. Herrera Ruztort, W. Alef, H. Rottmann, E. Himwich: Interacting with radio telescopes in real-time during VLBI sessions using e-control *Proceedings of Science (PoS) - 10th European VLBI Network Symposium and EVN Users Meeting: VLBI and the new generation of radio arrays, EID PoS(10th EVN Symposium)025, Scuola Internazionale Superiore di Studi Avanzati (SISSA), 2010*

Experiment of Injecting Phase Cal ahead of the Feed: New Results

D. Ivanov, A. Vytnov

Abstract The phase calibration system has been developed for the Russian VLBI network of new generation. The speciality of this phase calibration system is to radiate phase cal impulses from a special broadband feed located ahead of the receiving feed. The main advantage of injecting phase cal ahead of the receiving feed is in putting most of the VLBI signal path into the phase calibration loop. The research carried out in 2009 showed the absence of multipath effects in the external radiation phase cal signal. In 2010 the long-period phase stability was investigated with broadband TEM horn. The results of last experiments are considered.

Keywords Phase calibration system, TEM horn

The primary goal of the phase calibration system is to monitor the instrumental phase delay. For this purpose a spectrally pure reference signal is transmitted by cable to the mirror room of radio telescope where it synchronizes generator of very short impulses of about 40 ps duration. In current phase calibration system the impulses are injected through direction coupler into the input of receiver before the first LNA and passed with the received signal through receiver and data acquisition devices to digitization, after which the phases of the tones are extracted.

The phase calibration system has been developed for the Russian VLBI network of new generation (Finkelstein et al., 2010). The speciality of this phase calibration system is to radiate phase cal impulses from a special broadband feed located ahead of the receiving feed. The main advantage of injecting phase cal ahead of the receiving feed is in putting most of the VLBI signal path into the phase calibration loop (Ivanov et al., 2010).

Dmitrij Ivanov, Alexander Vytnov
Institute of Applied Astronomy of RAS, 10, Kutuzova emb., 191187 Saint Petersburg, Russia

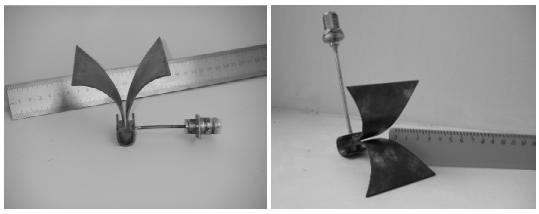

Fig. 1 Photos of the manufactured TEM horn feeds.

Frequency, GHz	Level of side lobes, dB		Width of directional pattern, deg	
	E-plane	H-plane	E-plane	H-plane
2	−12	−15	68.5	61
5	−13	−15.3	50.1	52.3
8	−11.1	−17.5	48.2	49.1
14	−16.3	−13.7	40.5	36.2

Table 1 The characteristic of radiation pattern of the TEM horn feed

For emitting phase cal we have used transverse electromagnetic (TEM) horn antennas. TEM horn antennas have the advantages of wideband, no dispersion, unidirectional and easy construction (Mallahzadeh et al., 2010). Some samples of TEM horn antenna with TEM double-ridged transition for the 2–14 GHz frequency band was made in IAA (Fig. 1). These samples are differed by method of manufacturing.

The characteristic of VSWR and radiation pattern of the feed are measured (see Fig. 2 and table 1). Characteristics of TEM horn feed obtained show feasibility of using it for emitting phase cal signal.

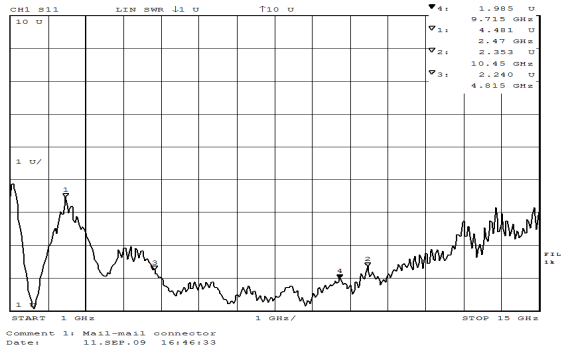

Fig. 2 The characteristic of VSWR of the TEM horn feed.

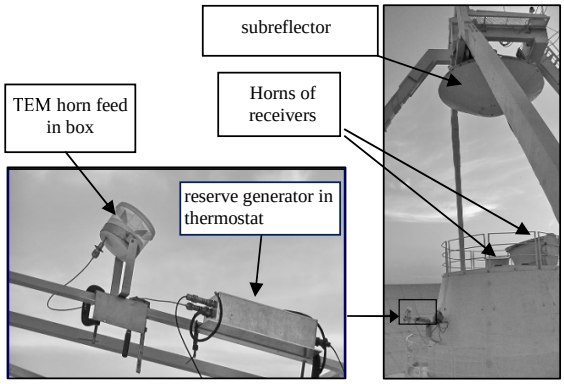

Fig. 3 Experiment with TEM horn feed in the observatory "Svetloe".

Fig. 4 Oscillogram of output signal for S-band receiver.

In the mid 2010 a few experiments with TEM horn feed were carried out in the observatory "Svetloe" on the Russian VLBI-network Quasar (Fig. 3). A feed connects to reserve generator which synchronized by reference 5 MHz signal.

The phase cal impulses being transmitted from regular generator and emitted through TEM horn feed were simultaneously observed by oscillograph Agilent DSO 6102A on outputs of the receivers *S*, *L*, *X* bands. The output oscillograms are shown on Fig. 4. These experiments showed the absence of multipath effects in the external radiation phase cal signal.

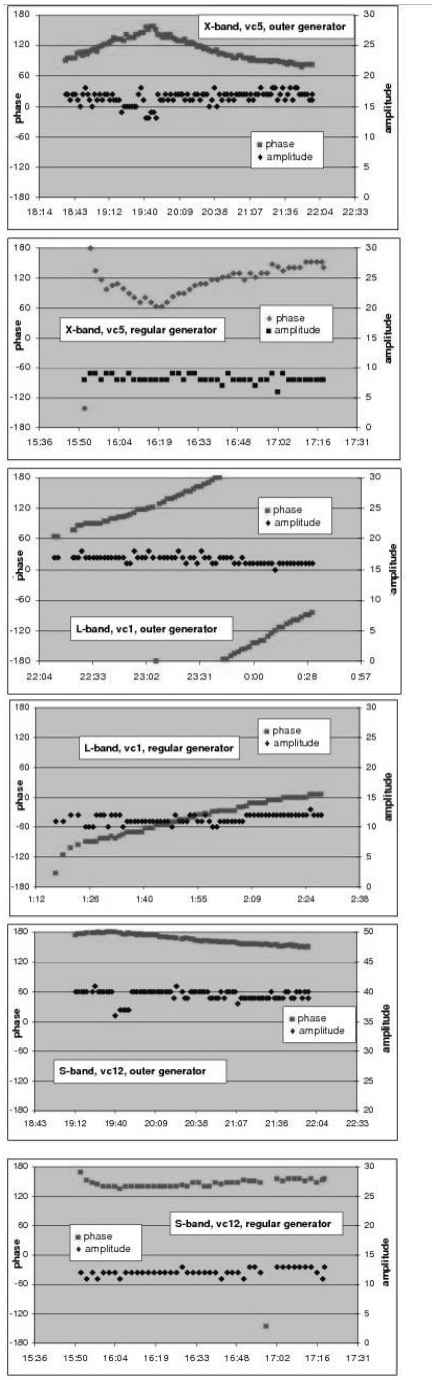

Fig. 5 Amplitude and phase of a signal of phase calibration on outputs of video converters.

The long-term phase stability was investigated by phase cal system with outer radiate impulse for receiving systems of *S*-, *L*-, *X*- bands. The results obtained

are similar to that of regular phase cal system (Fig. 5). Hence, such method doesn't bring additional phase instability.

Conclusions

The research carried out shown the possibility to use TEM horn feed for wideband emitting of phase calibration into a reception path of the radiotelescope. It is planned to investigate influence of weather conditions on phase stability of the method presented.

References

A. Finkelstein, A. Ipatov, S. Smolentsev, V. Mardyshkin, L. Fedotov, I. Surkis, D. Ivanov, I. Gayazov: The New Generation Russian VLBI Network, IVS 2010 General Meeting Proceedings, p. 106–110.

D. Ivanov, A. Maslenikov, A. Vytnov: Experiment of Injecting Phase Cal Ahead of the Feed: First Results, IVS 2010 General Meeting Proceedings, p. 429–433.

R. Mallahzadeh, F. Karshenas: Modified TEM horn antenna for broadband application Progress In Electromagnetics Research, PIER 90, 2009 p. 105–119.

Next-Generation DAS for the Russian VLBI-Network

E. Nosov

Abstract The Data Acquisition System (DAS) R1002M was developed by Institute of Applied Astronomy for upgrading radio interferometric network "Quasar" (Grenkov et al., 2010). The new DAS uses digital signal processing on video frequencies and provides enhanced performance. It is compatible with existing analog DASs and is intended for their replacement. The system consists of 16 Base Band Converters (BBC), IF-distributor, Clock Generator, Data Stream Combining Board (DSCB) and auxiliary units (Fig. 1). It has four IF-inputs which can be electronically connected to the BBCs in required way by IF-distributor unit. The BBCs' output data streams are combined in DSCB and available on its output in VSI-H format with up to 2048 Mbps data rate. The DAS is well suited to work with Mark 5B+ recording system but it can also work with Mark 5B in case of 1024 Mbps and lower data rate. For properly synchronizing the DAS is required for 1 PPS and 5 or 10 MHz signals. The clock generator automatically determines which input reference frequency (5 or 10 MHz) is used.

Keywords DAS, DBBC, Quasar network, FPGA

1 Base Band Converter

The main purpose of the BBCs is to cut a part of the input IF-signal in required frequency range and translate it to a baseband, separate side bands, form desired bandwidth and execute 2-bits quantizing in compliance with VSI-H format (Grenkov et al., 2009). In R1002M the translation to baseband is performed by high quality analog mixer and local oscillator (LO). The output signals of the mixer are then digitized and all subsequent processing is implemented by an FPGA (Fig. 2). The digitizing is performed by 2-channels analog-to-digital converter (ADC) with sample rate of 64 Msps. To separate the side bands it is necessary to inject phase shifting of 90° between digitized input signals. A special multirate filter bank with complex-valued coefficients was developed and realized in FPGA for this purpose. It contributes precise phase shift of 90° in the whole bandpass started from as low as 10 kHz (-6 dB level achieved at 5 kHz). It gives an opportunity to use the usual phase calibration signal of 10 kHz for correlation processing and makes the R1002M DAS fully compatible with existing analog DASs. At the same time the use of this technique allows achieving relatively high image rejection rate. Its typical value for the digital BBC is $-40 \div -45$ dB (at frequencies below 16 MHz) while for existing analog BBCs the typical value is about $-20 \div -25$ dB.

Fig. 1 Block1 of R1002M DAS.

E. Nosov
Institute of Applied Astronomy of RAS, 10, Kutuzova emb., 191187 Saint Petersburg, Russia

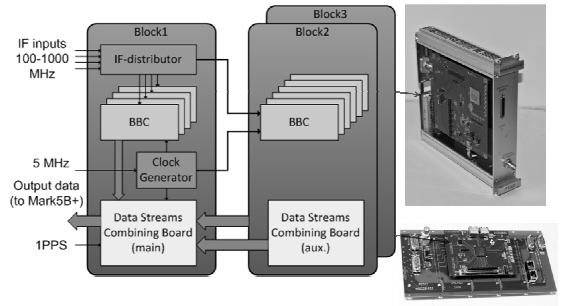

Fig. 2 Simplified structure of R1002M DAS and pictures of the BBC and DSCB.

A few additional switchable FIR-filters are used for forming six possible bandwidths: 0.5, 2, 4, 8, 16 and 32 MHz. The resulting amplitude-frequency characteristics of the digital BBCs are made similar to those of BBCs of existing analog DASs for improving compatibility between the systems. Furthermore, the bandwidths of 4 and 16 MHz have variants with close-to-square characteristics. It could improve the sensitivity of radio interferometer a bit more in case it is only the digital DASs that work on each station. The using of digital signal processing allows to achieve almost complete identity over the channels and thus it allows to avoid associated sensitivity loss of the interferometer.

2 Control

There are three possible ways to connect the R1002M DAS to control computer of radiotelescope. RS-232, RS-485 and 100/10 Ethernet interfaces could be used for this purpose. Normally, the DAS is controlled by Field System software, but the special control software under Windows OS is also available. Besides regular functions of control and monitoring it provides a few additional useful futures mainly intended for testing and service goals. First, it allows on the fly computing of 128-points 2×2-bits correlation function between any channels of the DAS. The computing itself realized in the FPGA of DSCB and the software just does some post-processing and graphic representation of the result. Second, the software could find the power spectrum density or cross-spectrum by using an FFT of received correlation function. Finally, the program displays counted by DSCB 2-bits distribution of quantized output signals.

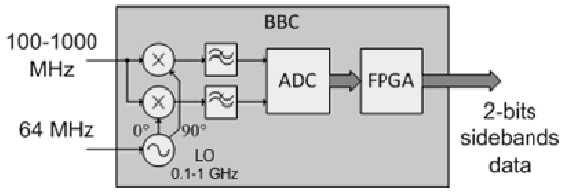

Fig. 3 Simplified structure of the BBC.

3 Field tests

The DASs R1002M have been installed in Svetloe and Zelenchukskaya observatories and have been used in the following observations: Ru-E090, Ru-E096 and Ru-U133. The systems operated in parallel with regular DASs (Mark IV in Svetloe and VLBA4 in Zelenchukskaya). Correlation processing of these observations proves compatibility between the digital and the analog DASs. Furthermore, using R1002M on both stations gave appreciable increase of SNR on the correlator output. Ratio of SNRs in case of digital-to-digital and analog-to-analog channels correlation is counted and averaged over 215 scans (Fig. 3). In average over the session the digital DASs gave an improving of about 36on each station of radio interferometer. The Multi-band delay (MBD) error was decreased as well (Fig. 4).

4 Summary

The channels of R1002M DAS have high repeatability, high rate of image noise rejection, low LO phase noise, low ripple of amplitude-frequency response and linear phase-frequency response. It allows minimizing degradation of radio interferometer sensitivity contributed by DAS. Wide control and monitoring futures makes it handy for using. Due to reprogrammable FPGAs the DAS functionality could be easy upgraded and new futures could be added. The tested observations prove advantages of created DAS and its compatibility with existing analog DASs. The third R1002M DAS is ready for installing in Badary observatory and after additional testing the R1002M DASs will be accepted as a regular DAS for all telescopes of “Quasar” network.

Input frequency range	$100 \div 1000$ MHz
Number of IF-inputs	4
Number of channels (BBCs)	16
Selectable bandwidths	0.5, 2, 4, 8, 16, 32 MHz
Separated sidebands	Both lower and upper
Image rejection rate (typ.)	$-40 \div -45$ dB
Commutation of input and output signals	Electronically
Local oscillators phase noise (rms)	$\leq 0.7^\circ$ (measured from 30 Hz to 30 MHz)
Ripple of amplitude-frequency response of the BBCs	≤ 0.3 dB
Output data format	VSI-H
Output data rate	Up to 2 Gbps
Available control interfaces	RS-232, RS-485, 100/10 Ethernet
Total dimension (three 19″ subracks)	$445 \times 950 \times 315$ mm

Table 1 R1002M DAS specification

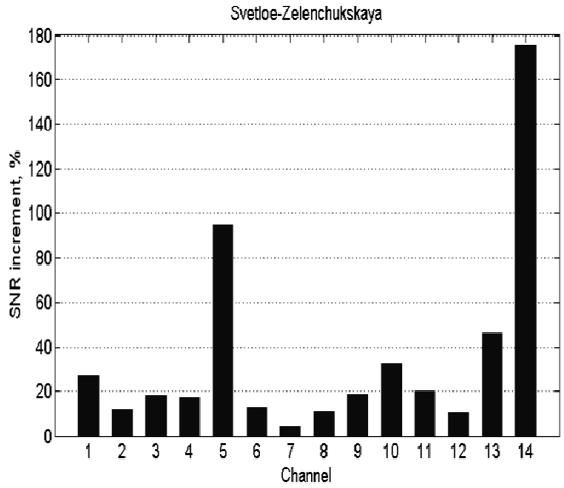

Fig. 4 SNR increment in the digital system in compare to the analog systems. Average over 215 scans. Base: Svetloe–Zelenchukskaya.

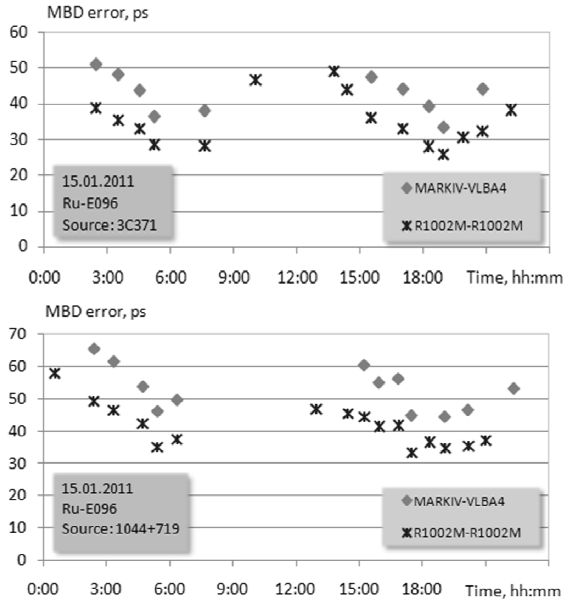

Fig. 5 MBD error for MarkIV-VLBA4 and R1002M-R1002M cases during RU-E096 observation session for 1044+719 and 3C371 sources. Base: Svetloe-Zelenchukskaya.

References

S. A. Grenkov, E. V. Nosov, L. V. Fedotov, N. E. Kol'tsov A Digital Radio Interferometric Signal Conversion System. *Instruments and experimental techniques.* Vol. 53. No. 5. 2010.

S. A. Grenkov, N. E. Kol'tsov, E. V. Nosov, L. V. Fedotov A Digital Signal Converter for Radio Astronomical Systems. *Instruments and experimental techniques.* Vol. 52. No. 5. 2009.

Status and future plans for the VieVS scheduling package

J. Sun, A. Pany, T. Nilsson, J. Böhm, H. Schuh

Abstract In order to exploit the full power of the future VLBI2010 system and derive the best possible geodetic parameters, a new scheduling package (VIE_SCHED) has been developed since 2010 at the Institute of Geodesy and Geophysics (IGG) of the Vienna University of Technology. It is one part of the Vienna VLBI Software (VieVS). To test the newly developed scheduling algorithms, thorough and realistic simulations have been carried out. The schedules for 24-hour continuous VLBI2010 observations are prepared with the software packages VIE_SCHED and SKED respectively, which are compared in terms of scheduled sources, number of observations, idling percentage, sky coverage, and station position repeatabilities. Results of similar quality are achieved. Finally some future work is also listed.

Keywords VLBI, VLBI2010, scheduling, Monte Carlo simulation

1 Introduction

The goals of the next generation VLBI (Very Long Baseline Interferometry) system, VLBI2010, are to achieve 1 mm position accuracy over a 24-hour observing session and to carry out continuous observations, i.e. observing the Earth Orientation Parameters (EOP) seven days per week. Initial results shall be delivered within 24 hours after taking the data. To fulfill the requirements of VLBI2010, the various new facets have been investigated within the International VLBI Service for Geodesy and Astrometry (IVS) including small fast-moving antennas, broadband frequency observations (2-14 *GHz*), and two or more antennas at a site (Petrachenko et al., 2009). At Goddard Space Flight Center (GSFC), Greenbelt (USA), the SKED software (Vandenberg, 1999) has been updated for VLBI2010 scheduling. Furthermore, a new scheduling package (VIE_SCHED) has been developed and used at the Institute of Geodesy and Geophysics (IGG) of the Vienna University of Technology. It is part of the Vienna VLBI Software (VieVS) (Boehm et al., 2009), and similar to VieVS it is based on MATLAB script files. The requirements of VLBI2010 have been studied in detail and the new scheduling algorithms were designed to fully exploit the possibilities of the future VLBI2010 system.

Considering a more uniform network (than the current one) of fast moving antennas we focus on the increase of observation density which is the critical factor for the accuracy of the estimated parameters. So far we have been concentrating on station dependent scheduling (Petrachenko et al., 2009), i.e., we optimize the sky coverage for short intervals taking into account the rapid atmospheric variability, partly at the expense of the total number of observations. For the purpose of cross-checking and convenient interface, VIE_SCHED reads the same catalogues of sources, stations, and observing modes as the SKED software from GSFC. It also writes .skd file, which contains a complete description of the session, the schedule, and the additional information used in scheduling the session. The cable wrap algorithms have also been developed to calculate the slewing time. Furthermore, models of source structure and elevation-dependent sensitivity are used to calculate the duration of the scan. The VIE_SCHED

Institute of Geodesy and Geophysics, Vienna University of Technology, 1040 Vienna, Austria, jing.sun@tuwien.ac.at

software offers the possibility to the user to optimize the schedule according to different criteria. Thus, the selection of the next source to be observed depends on the selected optimization criteria.

The simulation process is repeated 25 times, each time creating new values for zenith wet delay, clocks, and observation noise, to obtain a sample of output parameters that can be analyzed statistically.

2 VLBI2010 simulations

2.1 Network

The same VLBI2010 network of 18 stations plotted in Figure 1 is used for SKED and VIE_SCHED. This is an interim VLBI2010 network consisting of antennas expected to be outfitted with VLBI2010 observing systems in the near future (2013), and also considering political, infrastructural, and economical aspects. The interim network includes legacy antennas (stars) and new fast slewing antennas (circles).

Table 1 Characteristics of the 18 stations used for the simulations. The numbering of the stations (station indices) in the table corresponds to the numbers in Figures 2-5. The slewing rates given are just exemplificative values used for the simulations and do not always agree with the real or projected specifications of the antennas.

Sta Index	Sta Name	Slew Rate AZ (deg/min)	Slew Rate EL (deg/min)
1	*HARTRAO	120	60
2	*KOKEE	120	120
3	*NYALES20	120	120
4	*GOLD2010	180	60
5	*URUMQI	180	60
6	*WARKWORT	180	60
7	*TSUKUB32	180	180
8	oARECIBO	300	75
9	oFORTLEZA	300	75
10	oGGAO2010	300	75
11	oKATH12M	300	75
12	oMT_PLSNT	300	75
13	oYARRA12M	300	75
14	oKOREA	300	300
15	oAZOR2010	720	360
16	oCNARY_IS	720	360
17	oWETZ2010	720	360
18	oYEBE2010	720	360

2.2 Schedule parameters

1. The 24-hour continuous observing session is considered and compared. When creating a schedule for an experiment, VIE_SCHED and SKED read the same catalogue system files for the selection of sources, stations, and observing modes.
2. Source structure models (elliptical Gaussian models) are also used in VIE_SCHED to calculate the predicted observed flux on each baseline of a scan. The minimum of observed flux is 0.3 Jy. A pair of sources (at least 120 degrees apart) is scheduled.
3. The generation of the schedules is done assuming that the observations are carried out with the current S/X system. The recording rate is 7 $Gbps$ (number of channels 14, bandwidth 128 MHz, sample rate 256 MHz and 2 bits quantization). The minimum Signal-to-Noise Ratios (SNR) are 20 (X band) and 15 (S band), respectively. The cut-off elevation angle is 5 degrees.
4. The 18 stations are divided into two groups (11 fast antennas plus 7 slow antennas) according to slew rates. We pay more attention to the antennas with fast slew rate. The slow antennas take part in the experiment only if they can arrive at the next source in time.

2.3 Simulation parameters

To support the development of new scheduling algorithms, realistic VLBI2010 simulations have been carried out at the IGG and at the GSFC to investigate the new geodetic VLBI system thoroughly and systematically. VIE_SCHED is directly connected to VieVS to provide feedback on the quality of the schedule. After scheduling the observations with the software packages SKED and VIE_SCHED comparably, they are transformed to NGS format and used as input to the VieVS simulator (VIE_SIM). VIE_SIM sets up the o-c vector (observed minus computed) of the least-squares adjustment with simulated values of zenith wet delays, clocks, and observation noise at each epoch. The output of VIE_SIM is transformed to databases in NGS format, and thus can be analysed by VieVS as well as by other software packages. It is absolutely necessary to define standard interfaces (like NGS files) to be able to cross-check the result.

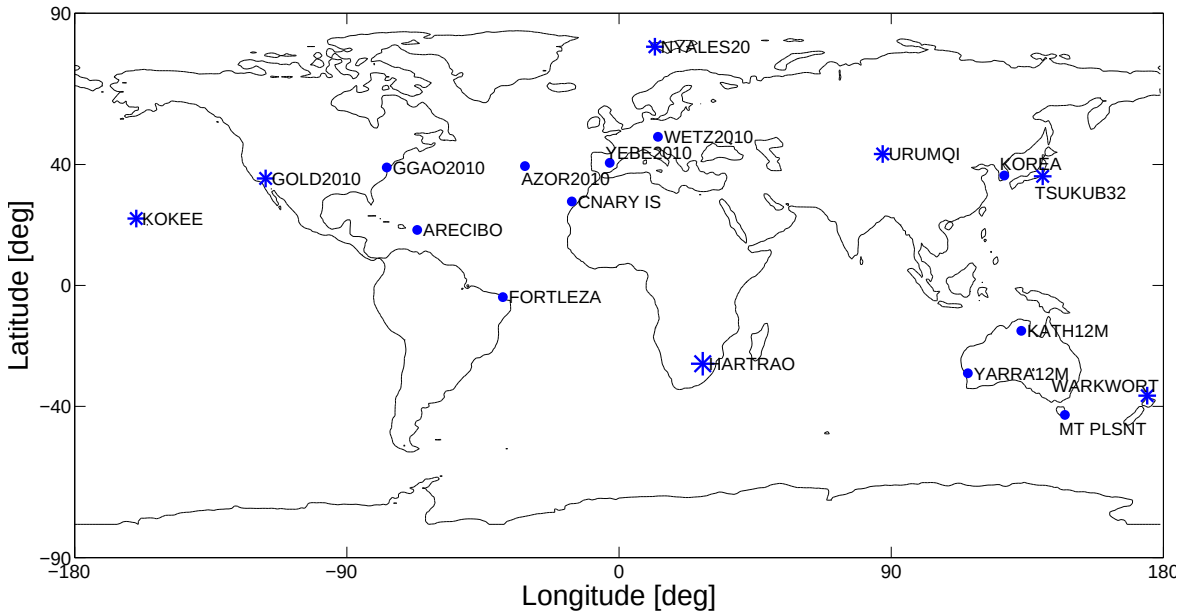

Fig. 1 18 stations network used for the VLBI2010 simulations. Stars denote legacy antennas, circles new fast slewing antennas.

The simulation values listed were chosen by the VLBI2010 Committee (V2C) to provide comparability between the simulations done at IGG Vienna and those done at GSFC (Petrachenko et al., 2009). The parameters include the refractive index structure constant C_n ($2.5 * 10^{-7} m^{-1/3}$), the effective height of the wet troposphere H (2000 *m*), and the wind velocity vector v (8.0 m/s) towards east (see Nilsson and Haas, 2010; Pany et al., 2011). The stochastic variations of station clocks are computed as sum of a random walk and an integrated random walk, with a power spectral density corresponding to an Allan Standard Deviation (ASD) of 10^{-14} @ 50 *min*. A white noise of 16 *ps* per baseline observation is added.

2.4 Estimated parameters

The simulated NGS data files are entered into the software package VieVS, which computes a classical least-squares solution. The parameters to be estimated are troposphere parameters, clock parameters, and station position residuals (with No-Net-Rotation (NNR) and No-Net-Translation (NNT) on all stations), as well as daily EOP. The tropospheric slant wet delay is modeled with a zenith wet delay and superimposed gradients as proposed in the IERS Conventions 2010 (Petit and Luzum, 2010). The troposphere parameters to be estimated are zenith wet delays and gradients, all of which are parameterized as piecewise linear offsets. The variations between the offsets are constrained to zero by introducing pseudo observations. Station clocks are modeled with a second order polynomial and superimposed piecewise linear offsets. The components of station position are treated as offsets and are estimated once per 24-hour session.

The parameters used to estimate troposphere parameters, clock parameters, and station positions are listed below.

1. NNR/NNT for all a priori station coordinates; source coordinates fixed to ICRF2.
2. EOP offsets for each 24-hour session.
3. Quadratic function plus 60 *min* piecewise linear function for clocks with relative constraints of 42 *ps*.
4. 6 *min* piecewise linear function for zenith wet delays with relative constraints of 19 *ps*.
5. 10 *min* piecewise linear function for gradients with 1.4 *mm* relative constraints and 1 *mm* absolute constraints.

Table 2 Statistics of the different schedules

	From SKED	From VIE_SCHED
Number of scheduled sources	200	225
Number of scans	4000	4138
Number of observations	99371	84398

3 Results

Schedules for 24-hour continuous observation are prepared with the software packages SKED and VIE_SCHED, respectively. These are compared in terms of scheduled sources, observation number, idling percentage, and sky coverage. The estimated station position repeatabilities are also compared.

1. The number of observations is shown in Table 2 and Figure 2.

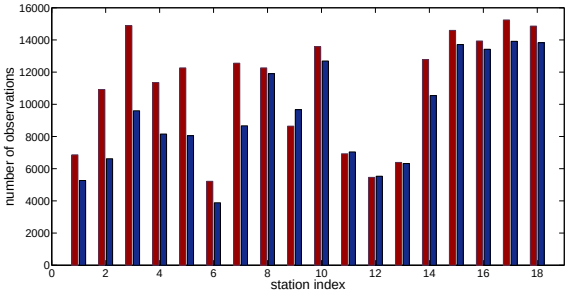

Fig. 2 Distribution of observations. Results from SKED are shown with left bar (red), and results from VIE_SCHED are shown with right bar (blue). The station indices are consistent with increasing slew rate.

2. The characteristics of the antenna in the schedule are summarized in Figure 3. One of the most striking features is how little time is actually spent on observing. The rest of the time is spent slewing and idling. Using fill-in mode (Gipson, 2010), the idling precentage is less than slewing precentage in the results from SKED at slow stations.
3. One possible method to clearly define uniform sky coverage and to get a corresponding statistical number is to divide the sky above the station in 13 segments and count the segments which contain at least one observed source in a certain time interval (Wresnik et al., 2007). If for one station the schedule has 13 observations per hour distributed over all 13 segments, the sky coverage is of category 13: the best possible sky coverage. Figure 4 shows the difference of mean sky coverage per 20 minutes from the two schedules. Because of less observations, the stations with slow slewing rates (low station indices) have worse sky coverage comparably.

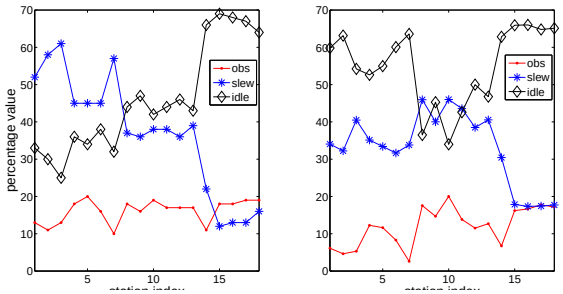

Fig. 3 Idling, slewing, and observing percentage. Results from SKED are shown left, results from VIE_SCHED are shown right.

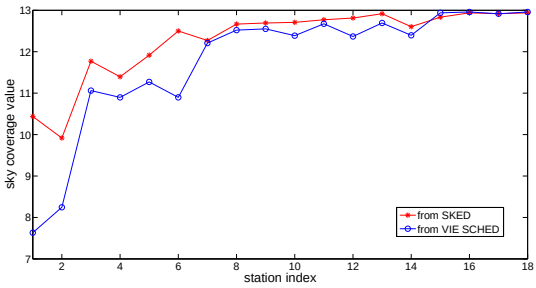

Fig. 4 Sky coverage distribution for 20 min intervals. For definition of sky coverage, see section 3.

4. Figure 5 shows station position repeatabilities obtained from the simulations. The median station position repeatabilities derived from SKED and VIE_SCHED are 3.29 *mm* and 3.72 *mm*, respectively. The median station position repeatabilities of 7 slow stations are 3.36 *mm* (from SKED) and 4.29 *mm* (from VIE_SCHED), respectively. And the median station position repeatabilities of 11 fast stations are 3.25 *mm* (from SKED) and 3.36 *mm* (from VIE_SCHED). As a consequence of the difference in terms of observations distribution, idling percentage, and sky coverage distribution, the station position repeatabilities from VIE_SCHED are a little worse than those from SKED at stations with low station indices, i.e., slow slewing rates.

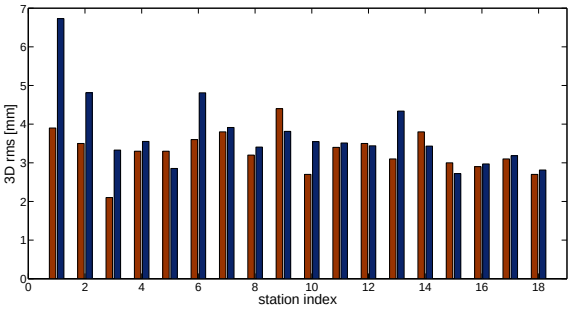

Fig. 5 Station position repeatabilities obtained from the simulations. Results from SKED are shown with left bar (red), and results from VIE_SCHED are shown with right bar (blue).

4 Conclusions and prospects

The schedules for 24-hour continuous observation are prepared with the software packages VIE_SCHED and SKED respectively, which are compared in terms of scheduled sources, number of observations, idling percentage, sky coverage, and station position repeatabilities. Results of similar quality are achieved.

There is still work needed to complete the VIE_SCHED software. It includes considerations of antenna maintenance and power saving mode. Variance and covariance analysis and even a dynamic optimization process will be considered to select the next source, which allows the successful separation of the various geodetic parameters in large multi-parameter adjustments. Schedules of sites with multiple antennas will also be considered.

Acknowledgements

The authors would like to thank the Austrian Science Fund (FWF) for supporting this work (P21049-N14). Andrea Pany is a recipient of a DOC-fFORTE fellowship of the Austrian Academy of Sciences at the Institute of Geodesy and Geophysics, Vienna University of Technology. Tobias Nilsson likes to acknowledge financial support from the German Research Foundation (DFG) (Project SCHU 1103/3-2).

References

J. Boehm, H. Spicakova, L. Plank, K. Teke, A. Pany, J. Wresnik, S. Englich, T. Nilsson, H. Schuh, T. Hobiger, R. Ichikawa, Y. Koyama, T. Gotoh, T. Kubooka, T. Otsubo. Plans for the Vienna VLBI Software VieVS. *Proceedings of the 19th Workshop Meeting on European VLBI for Geodesy and Astrometry*, Bordeaux, 24-25 March 2009.

J. Gipson An introduction to Sked. *IVS 2010 General Meeting Proceedings*, p.77-84, 2010.

A. Niell, A. Whitney, B. Petrachenko, W. Schlueter, N. Vandenberg, H. Hase, Y. Koyama, C. Ma, H. Schuh, G. Tuccari. VLBI2010: Current and Future Requirements for Geodetic VLBI Systems. *2005 IVS Annual Report*, 13-40, 2006.

T. Nilsson, R. Haas. The impact of atmospheric turbulence on geodetic very long baseline interferometry. *J Geophys Res*, 115:B03407. doi:10.1029/2009JB006579, 2010.

A. Pany, J. Boehm, D. MacMillan, H. Schuh, T. Nilsson, J. Wresnik. Monte Carlo simulations of the impact of troposphere, clock and measurement errors on the repeatability of VLBI positions. *J. Geodyn.*, 85:39–50, 2011.

G. Petit and B. Luzum. IERS Conventions (2010). IERS Technical Note No. 36.

B. Petrachenko, A. Niell, D. Behrend, B. Corey, J. Boehm, P. Charlot, A. Collioud, J. Gipson, R. Haas, T. Hobiger, Y. Koyama, D. MacMillan, Z. Malkin, T. Nilsson, A. Pany, G. Tuccari, A. Whitney, J. Wresnik. Design Aspects of the VLBI2010 System. Progress Report of the IVS VLBI2010 Committee, *IVS Annual Report*, 2009.

N. Vandenberg. Interactive/Automatic Scheduling Program. Program Reference Manual, NASA/Goddard Space Flight Center, NVI, Inc., 1999.

J. Wresnik, J. Boehm, A. Pany, H. Schuh. Toward a new VLBI system for geodesy and astrometry. *Adv Geosci*, AOGS 2007 A6(13):167180 2009.

The Quasar Network Observations in e-VLBI Mode

I. Bezrukov, A. Finkelstein, A. Ipatov, M. Kaidanovsky, A. Mikhailov, A. Salnikov, V. Yakovlev

Abstract This paper describes activity of the Institute of Applied Astronomy in developing real-time VLBI-system using high speed digital communication links.
Now e-VLBI sessions are carried out routinely within domestic VLBI-programs for UT1-determination. Observational data of 1-hour sessions are transmitted simultaneously from “Svetloe”, “Zelenchukskaya” and “Badary” observatories to the IAA Data Processing Center in Saint-Petersburg through fiber lines at 50–70 Mbps via Tsunami-UDP protocol.
Within these experiments observation data recorded by Mark 5B recorder are transmitted to the buffer server during time interval when an antenna pointed from one source to another. This procedure allows us to reduce total time of obtaining final result by 30 %.

Keywords e-VLBI, Quasar Network, Tsunami-UDP protocol

1 Introduction

Institute of Applied Astronomy of the Russian Academy of Sciences performs regular observations on Quasar Network within international and domestic programs. There are two types of domestic observational sessions: 24-hour Ru-E series for EOP determination and 1-hour Ru-U sessions for UT1 evaluation in near real-time mode (Finkelstein et al., 2008). Both series are carried out weekly. Real-time VLBI-technology is being used at IAA since 2007 when the first experiment was successfully done with Haystack observatory (Bezrukov et al., 2009; Salnikov et al., 2009). All observatories are equipped with Mark 5B recording terminals. The observations are correlated in the IAA Control and Processing Center in Saint-Petersburg. Now e-VLBI sessions are carried out routinely within domestic VLBI-programs for UT1-determination. Observational data of 1-hour sessions are transferred simultaneously from “Svetloe”, “Zelenchukskaya” and “Badary” observatories to the IAA Data Processing Center in Saint-Petersburg through fiber lines at 50–70 Mbps via Tsunami-UDP protocol http://tsunami-udp.sourceforge.net. In September 2010 few scans were successfully transferred from Quasar-Network observatories to Correlator Center at Shanghai observatory and vice-versa from Shanghai observatory to Correlator of RAS. The developing of advanced algorithm for automation of the data transfer process from the recorder to Correlator is in progress. The goal of activity of the Institute of Applied Astronomy in developing real-time VLBI-system is to achieve the requirements of VLBI-2010 Program.

Ilia Bezrukov, Andrey Finkelstein, Alexander Ipatov, Michael Kaidanovsky, Andrey Mikhailov, Alexander Salnikov, Vladislav Yakovlev
Institute of Applied Astronomy of RAS, 10, Kutuzova emb., 191187 Saint Petersburg, Russia

2 Communications

In 2007 all observatories of the VLBI Network “Quasar” were linked by optical fiber lines to provide both e-VLBI modes for determining Universal Time within intensive 1-hour sessions and real-time remote monitoring each part of the Network. All observatories of the Network “Quasar” were equipped with UNIX servers for data buffering. Now the observato-

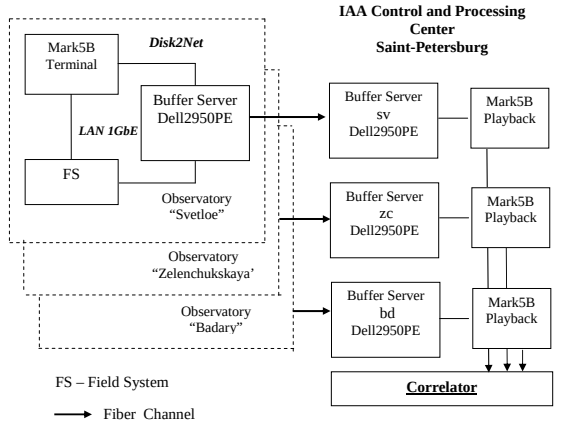

Fig. 1 Block-scheme of data transferring within e-VLBI mode with buffering: Mark 5B – LAN – Buffering Server – the Internet – Buffering Server – LAN – Mark 5B – Correlator.

ries Badary, Zelenchukskaya and Svetloe have communication channels 'last mile' at 1 GbE and via the Internet at 100 Mbps rate. Intensive sessions for determining the Universal Time in e-VLBI mode in network "Quasar" on baselines "Svetloe" – "Badary" and "Zelenchukskaya" –"Badary" observatories have been started in 2009 year. The Block-scheme of data transferring from three observatories within e-VLBI mode with buffering is presented on Fig. 1

3 Algorithm for data transfer in the e-VLBI mode

In the first phase a very simple algorithm (Fig. 2) was implemented — all actions were carried out sequentially. The data had been copied to buffering servers in observatories after the whole session, and then it had been transferred to the buffering server in the Control and Processing Center (CPC).

The second phase of the e-VLBI algorithm realization has provided:

- copying of all the scans to buffering servers in the observatories during pauses between session scans;
- simultaneous data transfer to the buffering server at the CPC as it becomes available from the three observatories in parallel with observations.

Automated data transfer software includes the following components:

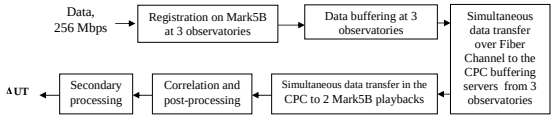

Fig. 2 Algorithm for data transfer in the e-VLBI mode from observatories of the "Quasar" Network.

1. Module that writes session scans to the buffering server at a observatory:
   - software module that provides synchronization of data transfer with observation session schedule. It is integrated with software that is installed on the radio telescope control computer (Field System computer);
   - software module installed on the buffering server at observatory that receives data from the Mark 5B. It is developed on the basis of standard utility Net2File.
2. Module that transfers data between observatories and the CPC:
   - control module provides startup, control and logging information about the session;
   - data transfer module. It consists of two parts that are launched on the buffering servers at observatory and at the CPC respectively. Buffering servers are combined into a "logical pair". They interact with each other and the control module;
   - operator interface that displays information about the current session, list of participating stations, transferring and already received scans, errors etc.

Due to its modular design, the data transfer system can be easily extended by adding a new "logical pair" (Observatory — CPC), installing necessary software on the new servers and adding corresponding information to the configuration files.

Automated data transfer system runs under the Linux operating system, is developed using Python language and uses Tsunami-UDP network protocol.

Within these experiments observation data recorded by Mark 5B terminal are transferred to the buffer server during time interval when an antenna pointed from one source to another. This procedure allows us to reduce total time of obtaining final result by 30 % (Fig. 3). Implementation of these actions has reduced the total time of transfer data to 2 hours. The next step for increasing efficiency in obtaining ΔUT is the integrated automation of the entire process

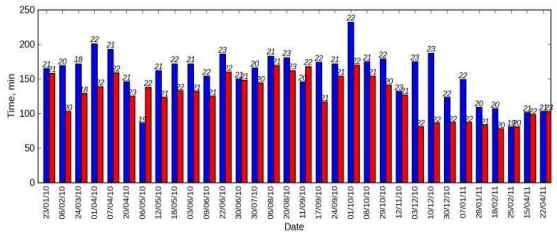

Fig. 3 Total time transfer data of intensive session from 2 observatories ("Badary" — dark grey color and "Zelenchukskaya" — light grey color) with automation process transfer to the CPC buffering servers. (Number of scans is top.)

of data transfer and processing, from registration to correlation. In particular, copying data to the playback terminal as they occur on the server at the CPC and alternating copy and correlation processes. In this case, time from the beginning of the session to obtaining the ΔUT is a little more than two hours.

4 Our Nearest Future

We plan to develop an algorithm to automate the overall data transfer process from Mark 5B recorders on observatories to the Control and Processing Center. By the end of 2011 the Quasar Network observatories and the Control and Processing Center of IAA RAS will be supplied VLBI data transfer rates of at least 1 Gbps from all observatories.

References

I. A. Bezrukov, A. G. Mikhailov, and A. I. Sal'nikov Preliminary Tests of High-Speed Data Communications Protocol on the KVAZAR-KVO Radio Interferometric System Institute of Applied Astronomy, Russian Academy of Sciences, nab. Kutuzova 10, St. Petersburg, 191187 Russia Received December 23, 2008 ISSN 00204412, Instruments and Experimental Techniques, 2009, Vol. 52, No. 5, p. 678–685. ©Pleiades Publishing, Ltd., 2009.

A. Finkelstein, A. Ipatov, S. Smolentsev The Network "QUASAR": 2008–2011. "Measuring the Future". Proc. of the Fifth IVS General Meeting, A. Finkelstein, D. Behrend (eds.), "Nauka", St. Petersburg, 2008, p. 39–46.

A. Salnikov, A. Finkelstein, A. Ipatov, M. Kaidanovsky, I. Bezrukov, A. Mikhailov, I. Surkis and E. Skurikhina "e-VLBI Technology in VLBI Network "Quasar" PoS(EXPReS09)098. http://pos.sissa.it/cgi-bin/reader/conf.cgi?confid=82: The 8th International e-VLBI Workshop, Madrid, Spain / 22-26 June 2009

Recent Developments at the Joint Institute for VLBI in Europe (JIVE)

S. Mühle, R. M. Campbell, A. Szomoru

Abstract After an overview of the European VLBI Network (EVN), including new stations and upgrades at existing stations, and of the core services that JIVE provides, the status and capabilites of the correlators at JIVE are reviewed. The transition phase from the Mark IV hardware correlator to the locally developed software FX correlator (SFXC) has now reached the point where the first user experiments correlated on the SFXC have been distributed. As of March 2011, more than 100 science observations have been carried out with real-time e-VLBI and this observing mode now adds considerably to the overall available EVN network hours. Ftp fringe tests, performed at the beginning of each EVN observing block have helped to improve the performance of the EVN during the user experiments.

Keywords European VLBI Network (EVN), Joint Institute for VLBI in Europe (JIVE), correlators, e-VLBI, ftp fringe-test

1 Introduction: The EVN and JIVE

The European VLBI Network (EVN) is a network of radio telescopes that conducts VLBI observations for astronomical research. Its was established in 1980 by five major radio astronomy institutes in Europe and the (then) Geodetic Department of the University of Bonn, and has grown significantly ever since. Besides eleven telescopes in EU countries, the network today includes the 305-m telescope in Arecibo (Puerto Rico), a station in Hartebeesthoek (South Africa) and two Chinese stations (for a complete list of EVN stations and their telescopes, please refer to `www.evlbi.org`). The three 32-m telescopes from the Russian VLBI Network KVASAR at Svetloe, Zelenchukskaya and Badary participated in EVN experiments for the first time in October 2009 and are now fully integrated into the network as EVN member stations. In China, a new 64-m telescope is being built at Shanghai station and the telescopes at Kunming and Miyun have participated in an EVN experiment in August 2009. The station at Kunming recently acquired a Mark IV recorder and plans to extend its suite of receivers. On Sardinia, the Sardinia Radio Telescope (SRT), a 64-m dish that is to be equipped with a full suite of receivers from P-band to W-band, is currently under construction.

The Joint Institute for VLBI in Europe (JIVE) is located in Dwingeloo, the Netherlands. Its core services comprise the correlation of EVN and global VLBI data — including infrastructure, logistics and quality assurance — user support and the support and development of the EVN. Besides hardware and software maintenance and development in connection with its operational tasks, JIVE hosts the EVN data archive, conducts real-time e-VLBI correlations and performs tests for the verification and development of the network.

2 Correlators at JIVE

With sixteen station units and the same number of Mark5A or Mark5B playback units, the Mark IV hard-

S. Mühle, R.M. Campbell, A. Szomoru
Joint Institute for VLBI in Europe, Postbus 2, 7990 AA Dwingeloo, The Netherlands

Fig. 1 The control station in the JIVE correlator room. The climate controlled row of racks in the background houses sixteen Mark5A or Mark5B units with corresponding stations units as well as the software FX correlator (central racks).

ware correlator is still at the heart of operations at JIVE (s. Fig. 1). Processing 1-bit or 2-bit sampled data with observed rates of up to 1024Mbit per second, the correlator can offer full-Stokes polarization output, an integration time as low as an eighth of a second and/or up to 2048 frequency points per subband and polarization. Experiments with more than 16 stations can be accommodated through multiple correlation passes and multiple MERLIN outstations recorded on one disk pack can be treated as separate EVN antennas. The correlator also supports real-time e-VLBI operations as well as special modes like oversampling and recirculation. The processed data that can be downloaded from the EVN archive along with diagnostic plots and the products of an automated data reduction are in the user-friendly IDI-FITS format.

The correlator can be configured in many different modes, depending on the aims of each experiment. The total correlator capacity is given by

$$N_{\rm sta}^2 \cdot N_{\rm sb} \cdot N_{\rm pol} \cdot N_{\rm frq} \leq 131072 \cdot R$$

$N_{\rm sta}$	$N_{\rm sb}$	$N_{\rm pol}$	$N_{\rm frq}$	comments
5-8	1	1	2048	a common spectral-line mode
5-8	1	4	512	all polarization products
9-16	1	1	512	spectral-line with more stations
9-16	1	2	512	with recirc. (8 MHz filters)
9-16	1	2	2048	with recirc. (2 MHz filters)
9-16	8	4	16	a common continuum mode

Table 1 Example configurations of the Mark IV correlator.

where $N_{\rm sta} = (4,8,12,16)$ is the number of stations, $N_{\rm sb}$ the number of subbands, $N_{\rm pol} = (1,2,4)$ the number of polarisations, $N_{\rm frq} \leq 2048$ the number of frequency points, and $R \leq 16\,{\rm MHz/BW_{sb}}$ the recirculation factor ($\rm BW_{sb}$ = bandwidth of a subband), with the additional constraints that $N_{\rm sb} \cdot N_{\rm pol} \leq 16$ and the minimum integration time $t_{\rm int} \leq R \cdot 1/8\,{\rm sec}$. Table 1 lists a few examples of popular configurations of the Mark IV correlator. Table 2 gives an overview of the achievable velocity resolution for frequently observed spectral lines corresponding to 2048 frequency points per subband.

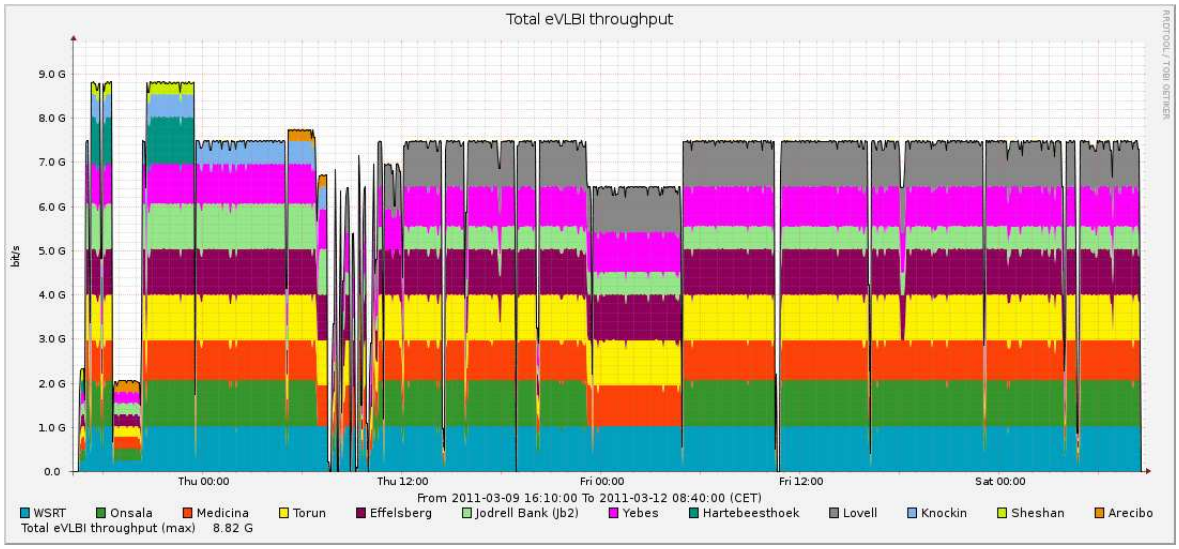

Fig. 2 Data throughput of the e-VLBI run on 9-12 March 2011. The data stream of each participating station is color-coded

BW_{sb} (1)	Δv (2)	Δv_{1420} (3)	Δv_{1665} (4)	Δv_{6668} (5)	Δv_{22235} (6)
16	7813	1651	1408	351	105
2	977	206	176	44	13
0.5	244	52	44	11	3.3

Table 2 The maximal velocity resolution of the Mark IV correlator for frequently observed spectral lines. Columns: (1) bandwidth of a subband in MHz, (2) spectral resolution in Hz, if $N_{frq} = 2048$, (3) – (6) velocity resolution in m/s for the HI (3), OH (4), methanol (5) and water (6) spectral lines at the frequencies given in MHz in the index.

JIVE now also operates a locally developed software FX correlator (SFXC) that takes the same input as the Mark IV correlator and offers a much wider range of correlation configurations, because the SFXC has essentially no hard limit for the number of frequency points or the integration time. Its special modes include the correlation of multiple phase centers in parallel and pulsar gating/pulsar binning. The software has been used for ftp fringe tests since 2007 and for user experiments since 2010. The SFXC currently runs on a dedicated 16-node, 128-core cluster, which allows real-time processing of data from 9 stations recorded at 512 Mbit per second with 1024 frequency points. This capacity is to be doubled in 2011.

3 Applications: Real-time e-VLBI

For astronomical research projects that require urgent observations on short notice, a rapid turn-around from observations to results or a denser time-sampling than the regular EVN observing sessions that are held three times a year can accommodate, the EVN offers real-time e-VLBI operations. For example, flares of X-ray binaries or just-exploded supernovae need to be observed as soon as their transient status is known, while monitoring campaigns, e.g. of binary stars at specific orbital phases, require frequent high-resolution observations. e-VLBI runs are usually 24-hour observing periods on fixed dates, for which time can be requested by submitting a proposal of the scientific project before the regular deadlines on 1 February, 1 June and 1 October of each year. Thanks to the development of the EVN network in recent years under the auspices of the EXPReS project, almost all EVN stations now have dedicated high-speed network connections to the Mark IV correlator at JIVE that enable sustained observations and real-time correlation with a data rate of 1024 Mbit per second from each station.

The e-VLBI run on 9-12 March 2011 set a new record with real-time e-VLBI observations running almost continuously for 64.5 hours. Fig. 8 shows the total e-VLBI throughput, i.e. the amount of data streaming

into the correlator at JIVE, as a function of time. Almost all participating stations sent 1024 Mbit of data per second, adding up to a sustained influx of 7.5 Gbit per second and a peak data rate of 8.82 Gbit per second. Lower data rates were chosen during setup times and tests. For example, the low data rates during the first hours of the observing run correspond to the clock-searching phase, where the restriction of the correlation to one subband allows for wider delay search windows. The only major problem during this run was the loss of the data stream from Onsala due to a power outage in Hamburg on early Friday morning.

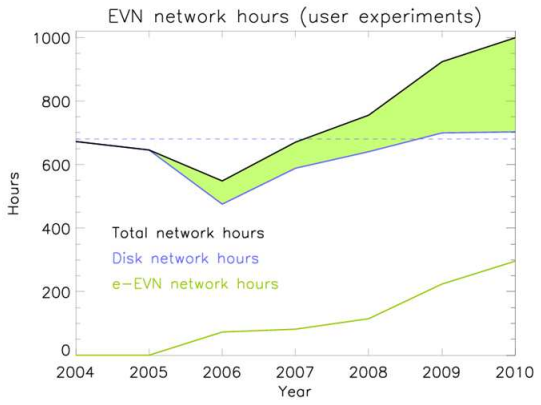

Fig. 3 Overview of the EVN network hours spent on disk-based and on e-VLBI observations. While the disk-based observations are limited to three times three weeks per year, the time for real-time e-VLBI observations has grown continuously.

To date (March 2011), 113 science observations have been carried out, including observations triggered by transient phenomena ("triggered proposals"), exploratory observations ("short proposals") and observations of transient objects of very high priority ("target of opportunity proposals") that are scheduled as soon as sufficient resources (stations) become available. Fig. 3 shows the number of EVN network hours dedicated to user experiments over the last seven years. Except for a small dip in 2006, when many projects were postponed at the request of their principal investigators because Effelsberg could not participate in the observations in session 3 of that year, the number of network hours spent on disk-based observations remains at a constant level, a consequence of the fixed time allocation for this mode of EVN observations of three times three weeks per year. In contrast to that, the number of network hours dedicated to user experiments done by e-VLBI has grown considerably along with the increased capabilities of this mode of operations. In 2010, real-time e-VLBI comprised about 30% of the total EVN network hours.

4 Applications: FTP Fringe Tests

For the three-week sessions of disk-based EVN and global VLBI observations that take place three times a year, the user experiments are grouped into blocks according to the receiver(s) requested. At the beginning of each block, i.e. after each change of receivers, a few hours are dedicated to network monitoring experiments to ensure that all stations perform at their optimum and to carry out tests in the development of new observing modes or for the inclusion of new stations or new hardware. The most important part of this technical time are the ftp fringe tests. The feature autoftp in sched leads to a small part of a scan being written to a file instead of to the disk-pack and sent by ftp to a specified location. During an ftp fringe test, the data designated for the test are sent to JIVE, where they are correlated in near real-time on the software FX correlator. The large number of automatically produced diagnostic plots and numerical results from fringing are provided on a webpage that is publically available shortly after the termination of the correlation and allows a quick and thorough inspection of the performance of each station (see `www.evlbi.org/tog/ftp_fringes/ftp.html`). Fig. 4 shows the uppermost part of a webpage generated during the network monitoring experiment at C-band (5 cm) on 1 March 2011. At one glance, the table allows the stations to check the status of each of their baseband channels — a green field indicates that a fringe has been found with a good signal-to-noise ratio, whereas red signifies no fringe or a fringe with a low signal-to-noise ratio. In Fig. 4, the two red fields on the baseline between Effelsberg and Medicina indicate a problem with the video converter #02 at Medicina. The values shown in blue are links to plots of the autocorrelation amplitudes or to plots of the fringes, amplitudes and phases of the baselines. The signal-to-noise ratios and the sampler statistics of the 2-bit sampled data listed further down on the page allow an estimate of the current sensitivity and

Vex file -- Integration time: 4s -- Start of the integration: 2011y060d14h13m56s0ms

N11M1	Auto correlations									Cross correlations							
	Ef	Hh	Jb	Mc	On	Sh	Tr	Wb	Ys	Ef-Hh	Ef-Jb	Ef-Mc	Ef-On	Ef-Sh	Ef-Tr	Ef-Wb	Ef-Ys
6640.52MHz, LSB, Rcp-Rcp	2	2	2	2	2	1	1	2	1	89.67 A P offset: -1	133.4 A P offset: -1	8.47 A P offset: -148	143.4 A P offset: -10	60.98 A P offset: -1	282.9 A P offset: 0	105.7 A P offset: 0	397.7 A P offset: -1
6640.52MHz, LSB, Rcp-Lcp	Cross hands									5.584 A P offset: -1	4.691 A P offset: 102	4.656 A P offset: 91	18.96 A P offset: -10	4.22 A P offset: -33	5.674 A P offset: 31	4.228 A P offset: -117	46.93 A P offset: -1
6640.52MHz, LSB, Lcp-Lcp	1	1	1	1	1	2	2	1	2	85.26 A P offset: -1	127.4 A P offset: -1	225.6 A P offset: -1	143.9 A P offset: -10	58.36 A P offset: -1	287.5 A P offset: 0	117 A P offset: 0	393.9 A P offset: -1
6640.52MHz, LSB, Lcp-Rcp	Cross hands									4.164 A P offset: 95	6.372 A P offset: -1	5.647 A P offset: -31	14.97 A P offset: -10	6.141 A P offset: -5	25.97 A P offset: 0	6.055 A P offset: -74	19.67 A P offset: -1
6640.52MHz, USB, Rcp-Rcp	2	2	2	2	2	1	1	2	1	88.54 A P offset: -1	139.6 A P offset: -1	3.582 A P offset: 59	134.9 A P offset: -10	62.31 A P offset: -1	267.3 A P offset: 0	99.44 A P offset: 0	370.7 A P offset: -1
6640.52MHz, USB, Rcp-Lcp	Cross hands									6.649 A P offset: -1	4.557 A P offset: 10	3.999 A P offset: 122	20.58 A P offset: -10	4.594 A P offset: -24	6.581 A P offset: 0	5.607 A P offset: -77	40.4 A P offset: -1
6640.52MHz, USB, Lcp-Lcp	1	1	1	1	1	2	2	1	2	101.8 A P offset: -1	117.9 A P offset: -1	212.2 A P offset: -1	135.2 A P offset: -10	50.28 A P offset: -1	292.2 A P offset: 0	109.4 A P offset: 0	399 A P offset: -1
6640.52MHz, USB, Lcp-Rcp	Cross hands									4.169 A P offset: 50	8.147 A P offset: -1	4.87 A P offset: 17	17.55 A P offset: -10	3.942 A P offset: -2	28.69 A P offset: 0	4.92 A P offset: -67	26.12 A P offset: -1
6656.52MHz, LSB, Rcp-Rcp	4	4	4	4	4	3	3	4	3	72.66 A P offset: -1	134 A P offset: -1	206.9 A P offset: -1	140.6 A P offset: -10	62.49 A P offset: -1	297.3 A P offset: 0	101.3 A P offset: 0	356.1 A P offset: -1
6656.52MHz, LSB, Rcp-Lcp	Cross hands									6.054 A P offset: -2	4.143 A P offset: -118	4.397 A P offset: -17	22.51 A P offset: -10	5.378 A P offset: -124	5.012 A P offset: -11	3.747 A P offset: -79	33.12 A P offset: -1
6656.52MHz, LSB, Lcp-Lcp	3	3	3	3	3	4	4	3	4	90.4 A P offset: -1	96.2 A P offset: -1	186.1 A P offset: -1	140.3 A P offset: -10	53.68 A P offset: -1	305.4 A P offset: 0	113 A P offset: 0	384 A P offset: -1
6656.52MHz, LSB, Lcp-Rcp	Cross hands									7.451 A P offset: -1	4.948 A P offset: 7	9.365 A P offset: -1	15.71 A P offset: -10	4.644 A P offset: 101	32.09 A P offset: 0	4.772 A P offset: 15	22.69 A P offset: -1
6656.52MHz, USB, Rcp-Rcp	4	4	4	4	4	3	3	4	3	78.33 A P offset: -1	135.9 A P offset: -1	208.3 A P offset: -1	135.2 A P offset: -10	59.11 A P offset: -1	283.8 A P offset: 0	103.7 A P offset: 0	335.3 A P offset: -1
6656.52MHz, USB, Rcp-Lcp	Cross hands									8.361 A P offset: -1	4.504 A P offset: -44	4.008 A P offset: 54	19.9 A P offset: -10	4.912 A P offset: 13	10.6 A P offset: 0	5.414 A P offset: -10	36.28 A P offset: -1
6656.52MHz, USB, Lcp-Lcp	3	3	3	3	3	4	4	3	4	89.67 A P offset: -1	89.81 A P offset: -1	173.4 A P offset: -1	145.7 A P offset: -10	51.94 A P offset: -1	280.2 A P offset: 0	109.6 A P offset: 0	368 A P offset: -1
6656.52MHz, USB, Lcp-Rcp	Cross hands									4.871 A P offset: -1	7.416 A P offset: -1	10 A P offset: -1	17.06 A P offset: -10	5.364 A P offset: -9	28.52 A P offset: 0	4.816 A P offset: 33	20.05 A P offset: -1
6672.52MHz, LSB, Rcp-Rcp	6	6	6	6	6	5	5	6	5	86.15 A P offset: -1	133.5 A P offset: -1	176.8 A P offset: -1	131.7 A P offset: -10	57.01 A P offset: -1	282.9 A P offset: 0	103.9 A P offset: 0	358.4 A P offset: -1
6672.52MHz, LSB, Rcp-Lcp	Cross hands									5.27 A P offset: 27	4.232 A P offset: -95	3.931 A P offset: -180	25.37 A P offset: -10	5.404 A P offset: -79	8.527 A P offset: 0	4.333 A P offset: 113	27.67 A P offset: -1
6672.52MHz, LSB, Lcp-Lcp	5	5	5	5	5	6	6	5	6	93.65 A P offset: -1	119.8 A P offset: -1	203.6 A P offset: -1	128.7 A P offset: -10	50.92 A P offset: -1	280.2 A P offset: 0	102.6 A P offset: 0	377 A P offset: -1

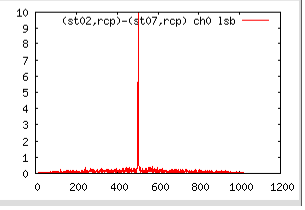

Fig. 4 Some results of the C-band ftp fringe test at 5cm in March 2011.

attenuation settings of each baseband channel.

Each network monitoring experiment at the beginning of an observing block includes several ftp fringe tests, with the results of each test and the URL of the corresponding webpage communicated to the stations via a skype text chat before the start of the next ftp test. This rapid feedback allows stations to quickly address and fix the diagnosed problems and to iteratively optimize their setup. By limiting the data transfer to a few seconds of data per test, even stations with a slow internet connection can participate and profit from the ftp fringe tests. Due to the wide variety of setups requested by astronomers and the continuous development of both the EVN and new observing modes, there are usually a number of problems at various stations that are found and fixed during these ftp fringe tests, leading to a much improved performance of the EVN during the user experiments.

Acknowledgements The European VLBI Network is a joint facility of European, Chinese, South African, and other radio astronomy institutes funded by their national research councils. e-VLBI research infrastructure in Europe is supported by the European Union's Seventh Framework Programme (FP7) under grant agreement 261525 (NEXPReS) and the European Union's Sixth Framework Programme (FP6) under grant agreement 026642 (EXPReS).

References

R. M. Campbell, 2011, *e-VLBI and Other Developments at the EVN Mk IV Data Processor at JIVE*, In: 10th EVN Symposium Proceedings, PoS(10th EVN Symposium)034, `pos.sissa.it/cgi-bin/reader/conf.cgi?confid=125`

M. Kettenis, A. Keimpema, D. Small, D. Marchal, 2009, *e-VLBI with the SFXC correlator*, In: proceedings of The 8th International e-VLBI Workshop, PoS(EXPReS09)045, `pos.sissa.it/cgi-bin/reader/conf.cgi?confid=82`

A. Szomoru, 2011, *NEXPReS*, In: 10th EVN Symposium Proceedings, PoS(10th EVN Symposium)035, `pos.sissa.it/cgi-bin/reader/conf.cgi?confid=125`

Bonn Correlator Status Report

W. Alef, H. Rottmann, A. Bertarini, A. Müskens

Abstract We present the status of the Bonn MPIfR/BKG[1] VLBI correlator center including a field report on how the MK IV hardware correlator was replaced by the DiFX software correlator.

Keywords correlator, software correlator, VLBI, geodetic VLBI, techniques: interferometric, instrumentation: interferometers

1 Introduction

The Max Planck Institute for Radio Astronomy has been operating five generations of VLBI correlators since 1978 — MK II, MK III, MK IIIA, MK IV (Whitney et al., 2004) and since about 2007 DiFX. The DiFX (Distributed FX) correlator (Deller et al., 2007) is the first software correlator used at MPIfR. The first geodetic correlations at Bonn date back to about 1979.

In 1993 MPIfR and BKG signed an MoU to build and operate a MK IV correlator on a 50/50 basis. The MK IV correlator was operational at Bonn for astronomy and geodesy between 2000 and 2010. Other common MPIfR/BKG projects were

- support of the Mark 5 development at MIT Haystack,
- upgrading the Mark 5A units at the correlator to Mark 5B
- and implementation and test of the DiFX software correlator for geodesy (2008/2009).

Walter Alef, Helge Rottmann
Max Planck Institute for Radio Astronomy, Auf dem Hügel 69, D-53121 Bonn, Germany
Alessandra Bertarini, Arno Müskens
Rheinische Friedrich-Wilhelms Universität Bonn, IGG, Nussallee 17, D-53115 Bonn, Germany

[1] MPIfR: Max Planck Institute for Radio Astronomy. BKG: Bundesamt für Kartographie und Geodäsie

2 Correlator usage in 2010

Up to December 2010, geodetic observations were still correlated with the MK IV hardware correlator. A total of 72 R1s, EUROs, T2s and OHIGs were correlated, as well as 44 of the three station INT3 e-VLBI observations of one hour duration each. All astronomical observations were processed with the DiFX software correlator. The 27 user experiments were comprised of up to 15 stations.

3 Requirements for DiFX for geodetic correlation

During the first tests of DiFX for geodesy in 2008 it was found that certain preconditions and requirements for a switchover from the MK IV correlator to DiFX had to be fulfilled:

- Phase-cal extraction had to be implemented.
- A translation program from the DiFX native output format to the MK IV correlator data format was needed to allow the HOPS fringe-fitting software to be used. DiFX had a data path into FITS format only, which requires the AIPS software (Greisen et al., 1990) for data analysis. In the standard geodetic analysis with AIPS fringes are searched in each sub-band (IF) separately which raises the fringe detection threshold, so that in the geodetic observations a significant fraction of good detections with low SNR are lost.
- A detailed comparison between DiFX and MK IV correlated data was also required. This includes tests with phase-cal extraction, DiFX data conversion into MK IV-format and subsequent usage of the standard analysis path.

3.1 Phase-cal tone extraction

The phase-cal extraction was coded 2009/2010 by F. Jaron (IGG Uni Bonn), J. Morgan (MPIfR, Curtin), J. Wagner (Metsähovi, MPIfR), and A. Deller (NRAO) with input from W. Brisken

(NRAO), W. Alef (MPIfR), and S. Pogrebenko (JIVE). R. Capallo (Haystack) added improvements for VLBI2010 frequency setups. The phase-cal algorithm extracts all possible tones within each sub-band and accumulates them with the same integration time as the data. It has been published in Jaron's bachelor thesis (2010).

3.2 MK IV interface

The format conversion program `difx2mk4` was written by R. Capallo with improvements added by others. Initial tests were done in autumn 2010 and at the time of this report very few issues remain.

3.3 Geodetic testing of DiFX

The first geodetic comparison of DiFX correlated data to the same data generated with the the MK IV correlator was reported at the 19^{th} EVGA meeting at Bordeaux by Alef et al. (2009) and by Tingay et al. (2009).

First tests with phase-cal extraction were done by J. Morgan during a visit to Bonn. In October 2010 the software delivered stable and reasonable results. A DiFX – MK IV comparison of a full geodetic observation was analysed at the IGG, University of Bonn. Other comparisons were done at Haystack. While the phase-cal extracted phases agreed well the extracted amplitudes were different, a problem which was fixed recently.

In order to test the new export path from DiFX native formatted data to MK IV format, selected single fringe-fits of the same scans were compared. Special care has to be taken to select the exact time range of data. For this the standard integration time of 2 s at the MK IV correlator had to be reduced to 1 s, as DiFX and MK IV use different algorithms to decide the reference time of each accumulation period; for 2 s integrations the reference times could disagree by 1 s. The primary observables for geodesy agreed to within the noise.

Next the R1 observations R1448 and R1456 were compared at the IGG, University of Bonn, with encouraging results, although it was noted that fewer good detections had been delivered by DiFX. This was due to a scaling problem of the interferometer amplitudes in `difx2mk4` which was fixed sometime later.

An independent investigation was carried out by L. Petrov. It has been published on his web page[2]. He analysed R1456, R1457 and R1459 with his analysis software PIMA which reads FITS formatted DiFX data. Phase-cal could not be applied at the time of his investigations. He found that the differences are at the level of 1σ. In addition he found two bugs and one omission in DiFX.

Other comparisons of DiFX with MK IV were done by Haystack, USNO, J. Morgan and possibly others. NRAO has been correlating geodetic observations with DiFX since early 2010 so far with good success — none of the analysis centers have reported problems with the DiFX data.

4 DiFX status at Bonn

DiFX is installed on a HPC[3] cluster which was acquired in 2008/2009. It consists of 60 nodes with a total of 480 compute cores. DiFX is executed and controlled on its own head node. 60 TB of disk space are available in 3 Raid systems mostly for storing raw recorded data. The cluster interconnect is realised with Gigabit Ethernet and 20 Gbit-Infiniband.

Astronomy observations have been correlated with DiFX exclusively since summer 2009. Initially DiFX version 1.5x was implemented at Bonn with `fusemk5a`[4] which makes data on disk modules available as read-only file systems. These file systems were made available to the DiFX correlator via NFS.

In November/December 2010 DiFX 2.0 (trunk version) was installed and `fusemk5a` was abandoned. The Mark 5 disk modules are accessed now in the so-called native mode developed and used by NRAO for the VLBA. With the native mode the 14 Mark5 units connected to the cluster become cluster datastream nodes and free up to 14 nodes for computations. DiFX 2.0 can extract the phase-cal signal and the data can be exported to MK IV format.

In the following months the geodetic correlation was more streamlined and quality control was built into the data reduction path. Batch processing of the correlation is handled via scripts, and all Mark 5 related tasks are done with the NRAO Mark 5 software.

During the ensuing period all 14 Mark 5A/B/C units were upgraded to the latest Conduant Software (SDK 9.1). In addition the operating systems were upgraded to a newer Linux kernel version, but problems were encountered which forced us to go back to the old 2.6.18 kernel[5]. To further integrate the Mark 5s into the cluster, both 1 Gb network connections are now directly connected to the cluster, and all Mark 5s have been included in the automatic cluster installation system. Since then playback rates of up to 1.5 Gbps can be achieved. If more than about 3 playback units are involved the data rate drops which might be due to an issue with the 1 Gbit switch used.

5 DiFX geodetic correlation

In December 2010 the MK IV correlator broke and could not be repaired with a passable effort. Geodetic correlation had to be switched over to DiFX within less than a week. With a major effort at the Bonn correlator the R1 and INT3 observations could

[2] http://astrogeo.org/petrov/discussion/corr_comp/

[3] High Performance Computing

[4] http://fusemk5a.sourceforge.net/

[5] The Linux distribution was changed also from Debian to CentOS.

be delivered to the analysis centers although with some delays. Since early 2011 geodetic correlation has become routine at the Bonn correlator.

The DiFX correlator has a number of advantages over the MK IV:

- Creation of the correlator control files is much simpler and faster. It takes now about 20 minutes per geodetic observation.
- The wall-clock time for the correlation proper has shrunk from about 30 hours for a 24 hour observation with 6 stations to less than 5 hours if the correlation runs without problems. It is presently limited by the maximum playback data rate and the stability of the Mark 5 units.
- Data from any variety of Mark 5 system (A/B) can be played back on any unit at the correlator, as the data is sent through the host system (and Ethernet) and not via the Mark 5A/B I/O cards. This is a big problem at MK IV correlators!
- All modules are checked in a Mark 5 unit at arrival at the correlator. In this process each scan is opened and the data is checked. A detailed directory listing is made and saved and serves as input to the correlator control files. This allows to detect problems with playback early so that the correlation during the night and weekends is less prone to failures.

For quality control a sufficient number of utilities are available, although further improvements are planned.

Of course the new system still has a number of problems. Most notably the Mark 5 units crash more often than on the hardware correlator. This is presently under investigation. A severe problem is also that missing tracks will lead to the loss of all the data which is due to the way the data decoding routines are written. At present the data is "fixed" with an offline program which replaces the broken track with a neighbouring one. Such a problem is fortunately rare but causes delays in correlation.

Online diagnostics for failures is not optimal still and should be improved. For instance a graphical display would make it easier for operators to recognise problems. Delays in the correlation are also caused by Mark 5 units which don't "close" the files which are being read for correlation. A few months ago a workaround was implemented.

NRAO have integrated into DiFX their own commercial data base which is also used for the global "track"-ing of module shipments. MPIfR will instead implement a MySQL data base. It should hold all experiment control files, disk modules, shelf locations, logs, clocks, archiving info, etc.

To ease the work of the operators the GUI which NRAO has developed needs to be adapted to the typical operation mode at Bonn and other correlators.

6 DiFX highlights at Bonn

The new capabilities of DiFX lead to new possibilities for scientists. Outstanding was the correlation of a VLBA observation where 97 positions in the field of view of the 25m VLBA antennas were processed in one correlation run. The execution time was only about a factor of two longer than for a single position.

Several pulsar observations have been correlated already using pulsar gating which was never implemented in the MK IV correlator. Most pulsar observations were scheduled for astrometric purposes, some of them in phase-reference mapping mode because the pulsars were too weak for a detection in the coherence time of the VLBI interferometer.

Millimetre-VLBI observations with the GMVA (Global Mm-VLBI Array) which previously required up to four correlation passes with the MK IV correlator are now done in a single pass, in less than the duration of the observations.

For the future we are planning to look at the transient detection mode of the DiFX correlator. Transient phenomena which produce sufficient radio flux can be detected in the data streams of each station on the fly during correlation. This could lead to very interesting science that might get extracted from data to be correlated nearly for free. NRAO is using this technique for all their production correlation already.

7 Conclusions

The Bonn correlator center was the first of the MK IV correlators to switch over to the DiFX software correlator completely. The switchover was successful and went fairly smoothly considering that it had to happen in a hurry and earlier than anticipated. The advantages of the new system like faster correlation, or no multipass correlation are real benefits. On the downside are the need for further development work and stability problems of the Mark 5 units.

References

W. Alef, H. Rottmann, D.A. Graham, A. Müskens, J. Morgan, S.J. Tingay, A.T. Deller MPIfR/BKG correlator report. In, Proc. 19th EVGA Working Meeting, eds. G. Bourda, P. Charlot & A. Collioud, Bordeaux France, 24-25 Mars 2009, 74-78.

A.T. Deller, S. J. Tingay, M. Bailes & C. West, DiFX: A Software Correlator for Very Long Baseline Interferometry Using Multiprocessor Computing Environments PASP, 2007, 119, 318-336

E.W. Greisen, G. Longo & G. Sedmak (Eds.) The Astronomical Image Processing System. Acquisition, Processing and Archiving of Astronomical Images, 1990, 125-142

S. J. Tingay, W. Alef, D.A. Graham, A.T. Deller, 2009. Geodetic VLBI correlation in software. I. Feasibility of using the DiFX software correlator for geodetic VLBI. *J. Geodesy*, 2009, 83 (11), 1061-1069.

A.R. Whitney, R. Cappallo, W. Aldrich, B. Anderson, A. Bos, J. Casse, J. Goodman, S. Parsley, S. Pogrebenko, R. Schilizzi & D. Smythe. Mark 4 VLBI correlator: Architecture and algorithms Radio Science, 2004, 39, 1007-+

First steps of processing VLBI data of space probes with VieVS

L. Plank, J. Böhm, H. Schuh

Abstract The Vienna VLBI Software (VieVS) will be extended by a VLBI tracking module, which is capable to process VLBI data received from transmitters within the solar system, e.g. space probes. Up to now, the processing has been realized for two mission scenarios, first for same-beam differential VLBI data from the Japanese lunar mission SELENE, and second for tracking GNSS satellites with VLBI antennas. In the case of SELENE first results are comparable to those published by the mission team but do not match the expected accuracy yet. For the satellite tracking, the effects of clock drift and troposphere delays on the determined satellite position were determined by using simulated observations.

Keywords VieVS, VLBI for space applications

1 Introduction

The Vienna VLBI Software (VieVS, Böhm et al., 2011) has been developed by the VLBI group at the Institute of Geodesy and Geophysics (IGG) of the Vienna University of Technology since 2008. It is capable to process and simulate geodetic VLBI data (Nilsson et al., 2011), perform a so-called global solution (Spicakova et al., 2011), and to schedule VLBI observations for actual and future antenna networks (Sun et al., 2011).

VLBI has been used for spacecraft navigation for more than 40 years (e.g., Thornton and Border, 2003). In recent years the interest in VLBI for space applications has strongly increased, coming along with dedicated programs by the big space agencies (e.g. ESA, NASA, JAXA): several new space missions using various methods of VLBI for tracking assistance have been recently proposed. With the goal of the geodetic usage of such mission data, primarily concerning frame ties between the dynamic reference frame of a space probe and the kinematically defined International Celestial Reference Frame (ICRF), we intend to upgrade VieVS for the possibility of processing VLBI tracking data of transmitters within the solar system. Our main focus is the delay modelling of moving sources at finite distance and its implementation in VieVS. The important tasks of

a. specifying the system configuration in terms of signal type and observation mode (single source vs. differential) as well as
b. observation and correlation

are not treated in this contribution. In the following we present work we have done for two mission scenarios so far, describe the computation of the theoretical delay in VieVS, show some results, and present our ideas for future work.

Lucia Plank, Johannes Böhm, and Harald Schuh
Vienna University of Technology, IGG, Gußhausstraße 27-29, 1040 Vienna, Austria
E-mail: lucia.plank@tuwien.ac.at

2 VLBI for space applications

Speaking of *Spacecraft VLBI*, it is meant that VLBI observations to sources other than far distant quasars are performed. Instead, signals from space probes, e.g. interplanetary spacecrafts, celestial bodies' orbiters, or Earth satellites are observed. Due to the finite distance between the antenna and the transmitter, the usual assumptions of a plane wave front and stable sources over time are not valid any more. As shown in figure 1, the source vectors $\mathbf{k_1}$ and $\mathbf{k_2}$ from antenna 1 and antenna 2 are not parallel and the curvature of the wave front must be included in the delay model. Another difficulty is the determination of the location of the space probe SC_{t_0} at the time of signal emission t_0, when the probe is moving with the velocity vector $\mathbf{v_{SC}}$ during the signal travel time. This is accounted for by iterating the light time according to:

$$t_0(i+1) = t_0(i) - \frac{SC_{t0} - St1_{t1}}{c} - \tau_{grav} \qquad (1)$$

Thus, the time of emission t_0 can be determined iteratively by subtraction of the signal travel time between the source and the antenna from the time of signal reception at antenna 1 t_1. The travel light time is obtained by the distance between the spacecraft at the time of signal emission SC_{t_0} and the position of antenna 1 at the time of signal reception $St1_{t_1}$, divided by the speed of light c. τ_{grav} is the gravitational bending effect on the signal ray path due to gravitating bodies like the Sun, Moon, and

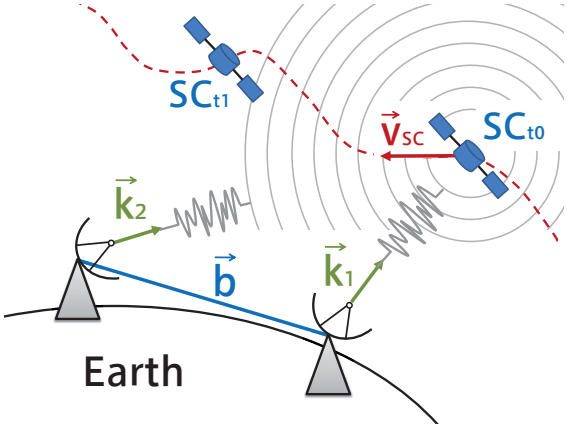

Fig. 1 Concept of spacecraft VLBI.

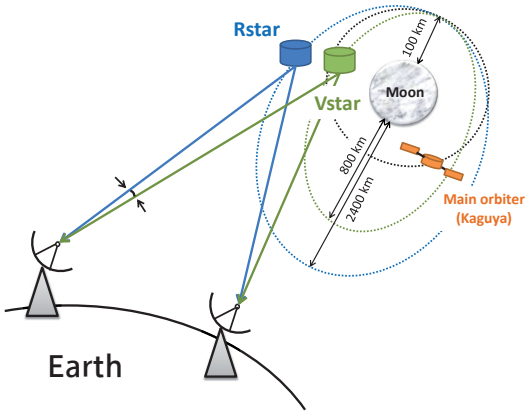

Fig. 2 Same-beam D-VLBI observations within the SELENE mission.

planets. If we set $t_0(1)$ to t_1, the iteration converges very rapidly. Special care when modelling spacecraft delays has to be taken on the choice of coordinate and time systems and the correct transformation and relativistic scaling between them.

3 Differential VLBI (D-VLBI) for SELENE

First steps into processing spacecraft VLBI data in VieVS were done with data from the Japanese lunar mission SELENE (SELenological and ENgineering Explorer, e.g., Kato et al., 2006). Designed for improved determination of the lunar gravity field, especially on the far side of the Moon, one of the key techniques to improve the stability of the orbital parameters was the differential VLBI (D-VLBI) method. SELENE consists of three orbiters, the main orbiter in a circular orbit and two sub-satellites Rstar and Vstar which were used to relay a signal to the main orbiter above the far side of the Moon. Rstar and Vstar were transmitting S- and X-Band signals that could be observed in same-beam D-VLBI mode by VLBI antennas on Earth (figure 2). By differencing the single delays from Rstar and Vstar, many error sources like station displacements, clock errors, or propagation delays due to the atmosphere are mostly cancelled out. D-VLBI observations can be done in switching or same-beam mode. In the first, the antennas alternately observe source 1 and source 2, in the latter the angular distance between both sources is small enough that they can be received within one antenna beam width. In the case of SELENE, both methods were performed, depending on the satellite constellation. The observable is the differential phase delay $\Delta\tau$, which can be extracted from the observed signals using the multi-frequency technique as described by Kikuchi et al. (2009). With $St \rightarrow transmitter$ denoting the travel light time calculated by using the positions of antennas 1 and 2 at the time of their signal reception and of spacecrafts Rstar and Vstar at the time of signal emission, the observable can be written as:

$$\begin{aligned}\Delta\tau = \tau_{Rstar} - \tau_{Vstar} = \\ [(St2 \rightarrow Rstar) - (St1 \rightarrow Rstar)] \\ - [(St2 \rightarrow Vstar) - (St1 \rightarrow Vstar)]\end{aligned} \quad (2)$$

In VieVS, the delay model for sources at finite distance according to Sekido and Fukushima (2006) was implemented, including the light time iteration (eq. 1) and accounting for the curvature of the wave front by using the so-called pseudo direction vector **k**, representing the geometric mean of the directions $\mathbf{R_i}$ from station i to the source *SC*.

$$\mathbf{k} = \frac{\mathbf{R_1}(t_1) + \mathbf{R_2}(t_1)}{R_1(t_1) + R_2(t_1)} \quad (3)$$

For our investigations, the RISE group from the National Astronomical Observatory of Japan (NAOJ) in Mizusawa provided S-band same-beam data from October 19, 2008, 17-19 UT. At that time the four antennas Mizusawa, Iriki, Ishigaki, and Ogasawara of the Japanese VERA network were observing the two sub-satellites, giving us a maximum of 6 baselines at a time. In figure 3 we show the residuals $\Delta\tau_{observed} - \Delta\tau_{computed}$ plotted separately per baseline. Though the nominal accuracy of S-band data is 1 mm Kikuchi et al. (2009), the residuals are about one order of magnitude bigger. Nevertheless, our results are in good agreement with those from the RISE group, as e.g. published by Goossens et al. (2010).

4 GNSSVLBI

In a second experiment, "*GNSSVLBI*" a completely different approach of VLBI spacecraft tracking is realized. The goal is to process data from the experiment performed by Tornatore and Haas (Tornatore et al., 2010). Hereby, GLONASS satellites are tracked with standard geodetic VLBI antennas by observing the signal that is normally used for GNSS observations. Different to the procedure of the previous section, observations are now done

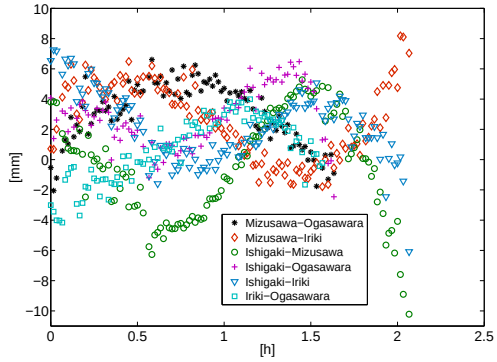

Fig. 3 Residuals plotted per baseline of SELENE same-beam D-VLBI data from Oct. 19, 2008.

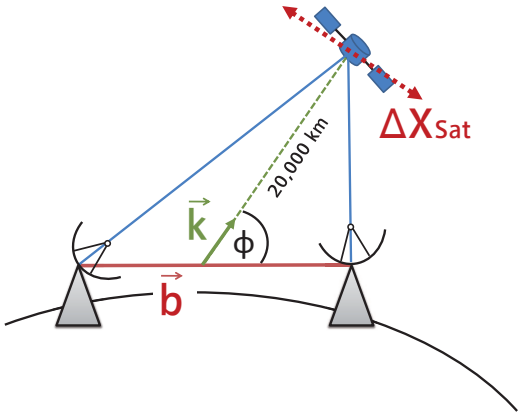

Fig. 4 GNSSVLBI experiment setup.

in single source VLBI mode. Due to the fact that the GLONASS orbits are provided in a geocentric reference frame, we decided to model the delay in a geocentric system as well, as proposed by Klioner (1991, chapter 6). This eases the computation, as many of the relativistic transformations that were needed in the approach above can then be omitted. As we do not have real observation data yet, we investigated the effect of non-modelled tropospheric delay and clock drift on the estimated position of the satellite by simulations. Therefore, we used the module Vie_sim of VieVS, which is based on Monte Carlo simulation following the procedure described by Pany et al. (2011). The simulations were set up for the experiment of August 16, 2010, when the VLBI antennas Medicina (Italy) and Onsala (Sweden) observed three GLONASS satellites (PR11, PR21, PR13). The observations were performed between 12 and 13:45 UT, in 20 seconds intervals. With only a single baseline observing, there is only one observable at each measurement epoch. For a start we set up a very simple model, simulating the variation $d\Phi$ of the parameter Φ, representing the direction of the pseudo source vector **k** (eq. 3) as can be seen in figure 4. By multiplication with an approximate satellite height of 20,000 km we can determine the

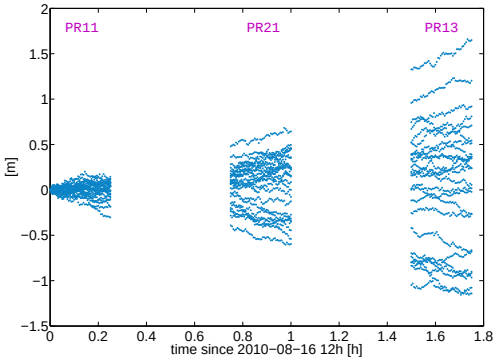

Fig. 5 Simulated effect of clock drift on the satellite positions; simulated 25 times.

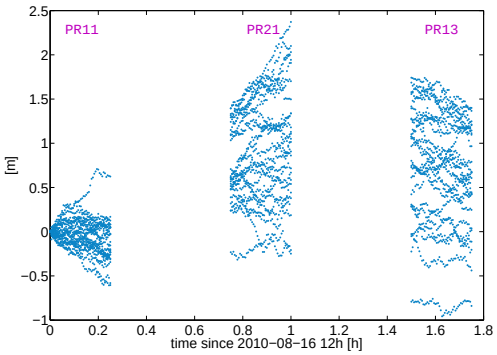

Fig. 6 Simulated effect of the slant wet delay on the satellite positions; simulated 25 times.

C_n	=	$2.5 \cdot 10^{-7}\, m^{-3}$	refractive index structure constant
H	=	$2,000\, m$	effective height of wet troposphere
wzd_0	=	$150\, mm$	reference equivalent zenith wet delay
v_n	=	$0\, m/s$	wind velocity in north direction
v_e	=	$8\, m/s$	wind velocity in east direction

Table 1 Simulation parameters for the troposphere.

corresponding satellite position error in the plane of the baseline.

$$\Delta \mathbf{X}_{Sat} = d\Phi \cdot 20,000\ km \tag{4}$$

Assuming a clock stability of $1 \cdot 10^{-14}$ within 50 minutes, which can be easily achieved with today's hydrogen masers, the satellite position error was simulated 25 times. Figure 5 shows the accumulating effect of up to 1.5 metres, when the clock drift is neglected during 1.8 hours of observations. In figure 6 we simulated the error caused by non-modelled slant wet delays. Simulation of the troposphere was done with the help of turbulence theory (Nilsson and Haas, 2010), using the parameters given in table 1. With about $1-2$ metres, this effect has the same order of magnitude as the clocks.

5 Summary and outlook

We reported about our activities to use VieVS for modelling delays of spacecraft VLBI. Successful processing was done for same-beam D-VLBI data from the Japanese lunar mission SELENE. Additionally, VieVS is ready to process GNSSVLBI tracking data. Concerning parameterization, a simple estimation tool (vie_sim_sc, vie_sim_gnss) for the two observation setups exists and can be used for simulations.

Our upcoming work covers an improvement for the estimation part. Due to mostly low redundancy, the parameterization needs to be reviewed. We need to clarify, which parameters the measurement setup actually senses, and how to incorporate them best in the modelling. Further, for precise orbit determination, the treatment of the transmitters' coordinates in VieVS has to be revised. While currently a set of three-dimensional coordinates is created for each measurement epoch, in future we might work with orbital arcs or directly estimate the orbital elements of the trajectory. Our goal is to continue the work with real measurement data from various missions; this will help to validate and improve the correct implementation of the delay model in VieVS. Once we achieve better accuracies, we also intend to take care of remaining propagation delays in D-VLBI, e.g. by applying GNSS derived ionospheric corrections and tropospheric delays obtained by ray-tracing.

6 Acknowledgements

The authors are thankful to the colleagues from the RISE group at NAOJ Mizusawa, for providing data from the SELENE mission and for introducing us into the processing of same beam D-VLBI data. We also want to thank Vincenza Tornatore and Rüdiger Haas for giving us insight to their project of observing GNSS satellites with VLBI.

References

J. Böhm, S. Böhm, T. Nilsson, A. Pany, L. Plank, H. Spicakova, K. Teke, H. Schuh. The new Vienna VLBI Software VieVS. In: S. Kenyon, M. C. Pacino, U. Marti (eds), *Proceedings of the 2009 IAG Symposium*, Buenos Aires, *Series: International Association of Geodesy Symposia Series*, vol 136 in press, Springer, 2011, ISBN 978-3-642-20337-4.

S. Goossens et al.. Lunar gravity field determination using SELENE same-beam differential VLBI tracking data. *J Geodesy*, Springer-Verlag 2010. doi: 10.1007/s00190-010-0430-2.

M. Kato, S. Sasaki, K. Tanaka, Y. Ijima, and Y. Takizawa. The Japanese lunar mission SELENE: Science goals and present status. *Advances in Space Research*,42, pp 294-300, 2008. doi: 10.1016/j.asr.2007.03.049.

F. Kikuchi et al.. Picosecond accuracy VLBI of the two subsatellites of SELENE (KAGUYA) using multifrequency and same beam methods. *Radio Sci*, 44, RS2008, 2009. doi: 10.1029/2008RS003997.

S. A. Klioner. General Relativistic Model of VLBI Observables. In: Carter W. E. (ed), *Proceedings of the AGU Chapman Conference on Geodetic VLBI: Monitoring Global Change*. NOAA Technical Report NOS 137 NGS 49, American Geophysical Union, Washington, D. C., pp 188-202, 1991.

T. Nilsson, J. Böhm, S. Böhm, M. Madzak, V. Nafisi, L. Plank, H. Spicakova, J. Sun, C. Tierno Ros, and H. Schuh. Status and future plans for the Vienna VLBI Software VieVS. In: *Proceedings of the 20th EVGA Meeting* in press (this volume), 2011.

T. Nilsson and R. Haas. The impact of atmospheric turbulence on geodetic very long baseline interferometry. *J Geophys Res*, 115, B03407, 2010. doi: 10.1029/2009JB006579.

A. Pany, J. Böhm, D. MacMillan, H. Schuh, T. Nilsson, and J. Wresnik. Monte Carlo simulations of the impact of troposphere, clock, and measurement errors on the repeatability of VLBI positions. *J Geodesy*, 85, pp 39-50, 2011. doi: 10.1007/s00190-010-0415-1.

M. Sekido and T. Fukushima. A VLBI delay model for radio sources at a finite distance. *J Geodesy*, 80, pp 137-149, 2006. doi: 10.1007/s00190-006-0035-y.

H. Spicakova, L. Plank, T. Nilsson, J. Böhm, and H. Schuh. Terrestrial reference frame solutions with the Vienna VLBI Software VieVS. In: *Proceedings of the 20th EVGA Meeting* in press (this volume), 2011.

J. Sun, A. Pany, T. Nilsson, J. Böhm, and H. Schuh. Status and future plans for the VieVS scheduling package. In: *Proceedings of the 20th EVGA Meeting* in press (this volume), 2011.

C. L. Thornton and J. S. Border. Radiometric tracking techniques for deep space navigation. J. H. Yuen (ed), *JPL Deep Space Communications and Navigation Series*, J. Wiley and Sons, Inc., Hoboken, New Jersey, 2003. ISBN 0-471-44534-7.

V. Tornatore, R. Haas, G. Molera, and S. Pogrebenko. Planning of an Experiment for VLBI Tracking of GNSS Satellites. In: D. Behrend and K.D. Baver (eds), *International VLBI Service for Geodesy and Astrometry 2010 General Meeting Proceedings*, pp 70-74, 2010.

Near real-time monitoring of UT1 with geodetic VLBI

R. Haas, T. Hobiger, M. Sekido, Y. Koyama, T. Kondo, H. Takiguchi, S. Kurihara, K. Kokado, D. Tanimoto, K. Nozawa, J. Wagner, J. Ritakari, A. Mujunen, M. Uunila

Abstract We give a short overview on the current status of near real-time monitoring of UT1 with geodetic VLBI. The use of real-time data transfer together with automated correlation and data analysis makes it possible to derive final dUT1-results with very low latency. The agreement with IERS C04 results is on the level of 30 μsec. It is even possible to determine time series of dUT1 during ongoing 24 h IVS-sessions. The concept is highly relevant for future VLBI2010 operations.

Keywords near real-time UT1, e-VLBI, VLBI2010

1 Introduction

In 2007 the VLBI research groups at Onsala (Sweden), Metsähovi (Finland), Kashima (Japan) and Tsukuba (Japan) started the Fennoscandian-Japanese ultra-rapid dUT1-project. The overall goal of this project is to determine dUT1 with very low latency using e-VLBI and automated data processing (Sekido et al., 2008). Figure 1 shows a map with the VLBI stations involved and the long and almost parallel east-west baselines that can be formed.

Different kind of observing sessions were and are performed in the project. In the beginning during 2007 and 2008, the focus was on dedicated 1-baseline intensive-style sessions that lasted about 1 to 1.5 hours. Since 2009 the focus moved to 24 h long sessions during standard IVS-sessions when Tsukuba and Onsala are participating. During these network sessions the baseline Tsukuba-Onsala is used during 24 hours for dUT1-determination on one baseline. Additionally, several hour long intensive-style sessions are scheduled and observed when additional observing time is available after standard IVS-sessions.

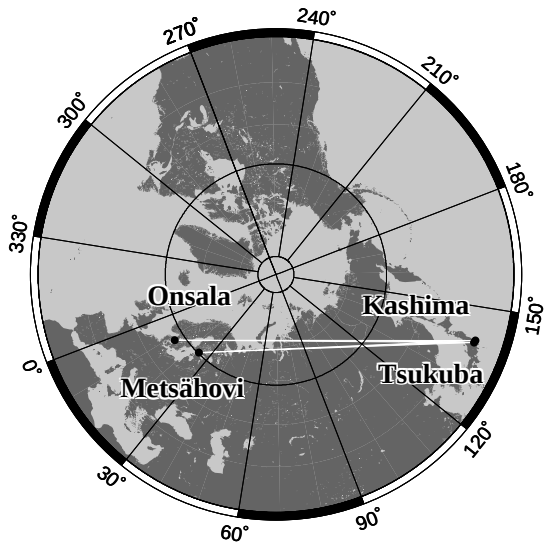

Fig. 1 The network of four stations used for the ultra-rapid dUT1-sessions

The project tried to address the effect of different data rates on the dUT1-results and the question of consistency of dUT1-results that are determined simultaneously on almost parallel baselines.

Figure 2 gives a schematic description of the ultra-rapid setup. The Fennoscandian VLBI stations acquire data with the Mark4 data acquisition system. The observational data are recorded on Mark5 units and PCEVN computers, and in parallel send the data in real-time via optical fibre to the correlator station in Japan where the data are also recorded. The real-time data transfer uses the Tsunami data transfer protocol. The

Rüdiger Haas
Chalmers University of Technology, Onsala Space Observatory, Onsala (Sweden)
Thomas Hobiger, Mamoru Sekido, Yasuhiro Koyama, Tetsuro Kondo, Hiroshi Takiguchi
National Institute of Information and Communications Technology, Koganei (Japan)
Shinobu Kurihara, Kensuke Kokado, Daisuke Tanimoto
Geospatial Information Authority of Japan, Tsukuba (Japan)
Kentarou Nozawa
AES Co.,Ltd., Tsukuba (Japan)
Jan Wagner, Jouko Ritakari, Ari Mujunen, Minttu Uunila
Aalto University, Metsähovi Radio Observatory, Metsähovi (Finland)

Japanese VLBI stations acquires data with the VSSP system and record on K5-recorders, and transfer the data to the correlator. At the correlator the Fennoscandian VLBI data are first converted from Mark4-format to K5-format, and than correlated with the Japanese data. The whole process chain is automatized, as well as the post-processing of the correlation results (Hobiger et al., 2010).

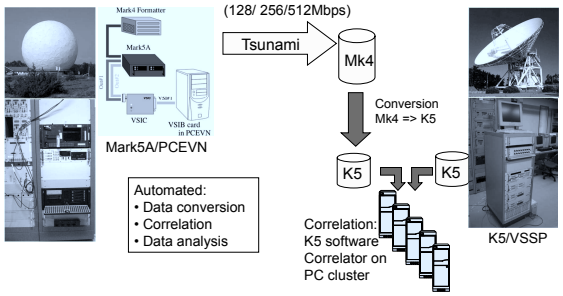

Fig. 2 Schematic description of the setup for ultra-rapid dUT1-sessions.

2 Ultra-rapid intensive-style dUT1-sessions

The series of ultra-rapid intensive-style dUT1-sessions started in March 2007. During 2007 and 2008 in total 41 successful 1 hour long sessions were conducted, see e.g. Haas et al. (2010). The latency of the final dUT1-results improved dramatically from several hours to a couple of minutes after end of observations. The world record was achieved in February 2008 on the baseline Onsala-Tsukuba when the final dUT1-results were derived within 3.5 minutes after the end of the observing session (Matzusaka et al., 2008).

The comparison to IERS C04-results show that the ultra-rapid dUT1 values show the same level of agreement with C04 as the IERS-rapid solutions (about 30 μsec) (Haas et al., 2010). However, the latency of the ultra-rapid dUT1 results is much lower.

Unfortunately there were only very few simultaneous sessions on almost parallel baselines. The reasons were that it was difficult to get telescope time and/or that equipment failed. However, for one session in July 2007 we found an RMS-agreement of 16.7 μsec.

The majority of the sessions was observed with a data rate of 256 Mbps. Only a few session did use 128 or 512 Mbps, so that a rigorous assessment of the effect of data rates on the precision of the dUT1-results was not easy possible. However, there is some indication that higher data rates give lower formal error for the dUT1-results, which might indicate a higher precision.

Since the intensive-style ultra-rapid sessions were successful and reduced the latency of the dUT1-results significantly, the concept was adopted for the standard IVS sessions INT-2 and INT-3. The data transfer for these sessions also used offline or real-time data transfer, and the INT-2 sessions correlated at Tsukuba are since 2010 done in ultra-rapid mode.

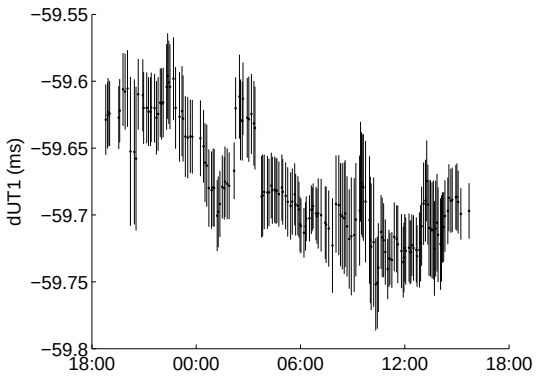

Fig. 3 Ultra-rapid 24 h dUT1 during R1.450 on September 27/28, 2010.

3 Ultra-rapid 24 h dUT1-sessions

Since 2009 almost all standard 24 h IVS-sessions where both Onsala and Tsukuba are involved are operated as ultra-rapid sessions. The sessions include e.g. R1-, RD- and T2-experiments. The observational data from Onsala are real-time transferred to the Tsukuba correlator where the data are converted and correlated. Once 35 scans are collected, a data analysis is performed and dUT1 determined. During the 24 h session the data are analyzed in a sliding-window-approach. This means that when a new scan comes in the oldest is left out and a new analysis is performed. The results is a time series of dUT1 that is produced during the ongoing IVS-session. The results are available with very low latency and the progress of the analysis can be monitored on the webpage `http://www.spacegeodesy.go.jp/vlbi/dUT1/`.

The data are analyzed in an automatic mode with two independent software packages, an automated version of OCCAM, and the software C5++ (Hobiger et al., 2010). The results are close and do for most cases agree within their formal errors, but they are so far not identical. Figure 3 shows as an example the ultra-rapid 24 h dUT1-results during R1.450 on September 27/28, 2010.

Figure 4 depicts the residuals with respect to the IESR C04 dUT1 values. Shown are the residuals of the INT-series as analyzed by BKG, the IVS-R-series as analyzed by BKG, the combined IVS-results of the IVS-R-series, and the ultra-rapid 24 h observations. The agreement expressed in bias and RMS is depicted in Figure 5. The ultra-rapid results show a larger bias than the other series and the RMS scatter is on the same level as the IVS-INT results. The larger bias is probably due to that

the observing schedules of standard 24 hour network session are not optimized for one-baseline determination of dUT1. A degradation of the dUT1-results is thus to be expected compared to dedicated one-baseline experiments. Furthermore, is the 'sliding-window' analysis approach probably not the best strategy to analyze the data. A filter-based analysis strategy promises to give more robust results.

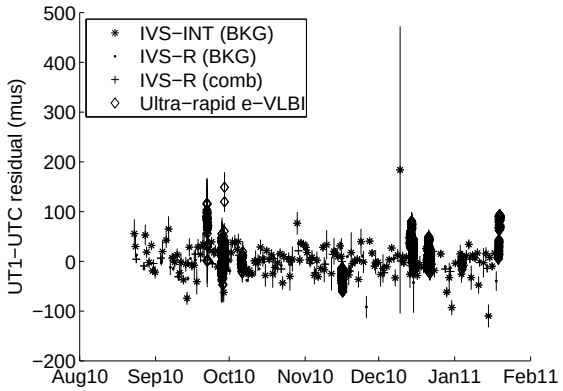

Fig. 4 Residuals with respect to IERS C04 series.

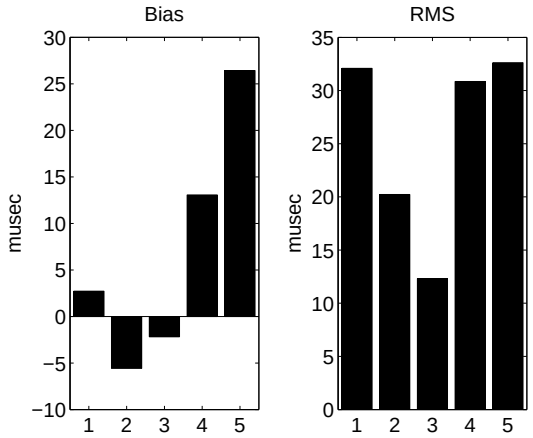

Fig. 5 Bias (left) and RMS-scatter (right) for the comparison with IERS C04. Presented are bias and RMS-scatter for 1 – IVS-INT (BKG), 2 – IVS-R (BKG), 3 – IVS-R (IVS combined), 4 – ultra-rapid (OCCAM), 5 – ultra-rapid (C5++).

4 Summary and outlook

Real-time e-VLBI including near-real-time correlation and data analysis is possible. Low latency for dUT1-results can be achieved, even within minutes after the end of the observations. The agreement with C04 on the same level as the IERS rapid solutions.

Simultaneous observations on almost parallel baselines agree on the order of better than 16.7 μsec. There is an indication that higher data rates give reduced formal errors of the dUT1-results.

The results from ultra-rapid-24h sessions show a larger biases with respect to C04 than dedicated INT-sessions. This is probably due that the 24 hour network schedules are not optimized for one-baseline dUT1-determination. The RMS-agreement with respect to C04 is comparable to standard INT-sessions. The INT-2 and INT-3 series have thus adopted the ultra-rapid approach, respectively e-transfer, to achieve low latency dUT1-results. This is important since low latency has been shown to improve dUT1-predictions considerably (Luzum and Nothnagel, 2010).

The sliding-window analysis approach of the ultra-rapid 24 h dUT1-sessions is not ideal. A filter-based analysis strategy is under development (Hobiger, 2011). The results from the two software packages used for the automated data analysis do not agree completely, but for most of the cases within the formal errors. It appears that a unified analysis strategy is necessary and currently the IVS Task Force for Intensives is working on this topic.

The plans for 2011 are to perform the complete CONT11 in a ultra-rapid mode and to determine dUT1 continuously for 15 days. Additionally, we want to continue with the 24 h ultra-rapids and 'long-intensives'.

For the future one can expect that the ultra-rapid concept will be well suited for VLBI2010. It is plausible that VLBI201 could be operated with distributed correlation. Single baselines could be correlated in near real-time already during the ongoing sessions. Complete databases that include all individual baselines could be merged and complete networks could be analyzed partly already during or latest directly after the end of an observing session. This will allow to determine all EOP in near-real-time.

References

R. Haas, M. Sekido, T. Hobiger, T. Kondo, S. Kurihara, D. Tanimoto, K. Kokado, J. Wagner, J. Ritakari, A. Mujunen (2010) Ultra-Rapid DUT1-Observations with E-VLBI. *Artificial Satellites*, **45**, 75–79.

T. Hobiger, T. Otsubo, M. Sekido, T. Gotoh, T. Kubooka, H. Takiguchi (2010) Fully automated VLBI analysis with c5++ for ultra-rapid determination of UT1, *Earth Planets Space*, **45(2)**, 75–79.

T. Hobiger (2011) personal communication.

B. Luzum, A. Nothnagel (2010) Improved UT1 predictions through low-latency VLBI observations, *Journal of Geodesy*, doi: 10.1007/s00190-010-0372-8.

S. Matsuzaka, H. Shigematsu, S. Kurihara, M. Machida, K. Kokado, D. Tanimoto (2008) Ultra Rapid UT1 Experiment with e-VLBI, In: A. Finkelstein, D. Behrend (eds.) *Proc. 5th IVS General Meeting*, 68–71.

M. Sekido, H. Takiguchi, Y. Koyama, T. Kondo, R. Haas, J. Wagner, J. Ritakari, S. Kurihara, K. Kokado (2008) Ultra-rapid UT1 measurements by e-VLBI, *Earth Planets and Space*, **60**, 865–870.

VLBI2010 - Current status of the TWIN radio telescope project at Wettzell, Germany

A. Neidhardt, G. Kronschnabl, T. Klügel, H. Hase, K. Pausch, W. Göldi, VLBI team Wettzell

Abstract The Twin radio Telescope Wettzell (TTW) is a project of the Bundesamt f"ur Kartographie und Geod"asie (BKG, Federal Agency for Cartography and Geodesy) for the period of 2008 to 2011. The design of the TTW is based on the concept of an VLBI2010 Working Group of the International VLBI Service for Geodesy and Astrometry (IVS). The TTW consists of two equivalent fast moving, broadband radio telescopes. During the first project year the final design was fixed after numerous simulations to meet the technical specifications needed for the VLBI2010 concept. For the construction of the radio telescopes at the Geodetic Observatory Wettzell a thorough soil analysis was made in order to define the most suitable locations. Since 2009 the construction work is ongoing and close to its end. In parallel several acceptance tests of different telescope parts had been conducted, e.g. azimuth bearings. Therefore the construction is on time. For the last project year the design of the receiver parts need to be finished and their construction, assembly and installation are on the agenda.

Keywords VLBI2010, TWIN, radio telescope, Wettzell

A. Neidhardt
Forschungseinrichtung Satellitengeodäsie, Technische Universität München, Geodätisches Observatorium Wettzell, Sackenrieder Str. 25, D-93444 Bad Kötzting, Germany
G. Kronschnabl, T. Klügel, H. Hase
Bundesamt für Kartographie und Geodäsie, Geodätisches Observatorium Wettzell, Sackenrieder Str. 25, D-93444 Bad Kötzting, Germany
K. Pausch
Vertex Antennentechnik GmbH, Baumstr. 46-50, D-47198 Duisburg, Germany
K. Pausch
Vertex Antennentechnik GmbH, Baumstr. 46-50, D-47198 Duisburg, Germany
W. Göldi
Mirad Microwave AG, Hofstetstr. 6, CH-9300 Wittenbach, Switzerland

1 Introduction

On the basis of the requirements for geodetic radio telescopes, published by the International VLBI Service for Geodesy and Astrometry (IVS), the Bundesamt für Kartographie und Geodäsie (BKG, Federal Agency for Cartography and Geodesy) has launched the TWIN project at Wettzell (Hase et. al., 2009). Within this two rapidly moving radio telescopes are built, which will be equipped with a broadband receiving system including the two geodetic used frequency bands S and X. Both telescopes have been designed for continuous operations over 24 hours 7 days per week. As array both telescopes can be additively interconnected, so that the effective receiving surface corresponds approximately to that of the current 20m radio telescope at the Wettzell observatory. The radial symmetric reflector concept combines the advantages of a dual offset antenna, as low noise temperature, with the advantages of a Cassegrain or Gregory antenna regarding the mechanical stability, the control possibility and the weight.

The technical data of the telescopes are:

- Diameter of main reflector: 13.2m
- Diameter of sub-reflector: 1.48m
- Ring focus design with f/D = 0.29
- Surface quality of the reflectors: < 0.2 mm RMS
- Path length error : < 0.3 mm
- Surface quality of the panel: < 0.065 mm RMS
- ALMA mounting with angular velocities of 12°/s in azimuth and 6°/s in elevation
- Acceleration: Az, El = $3^\circ/s^2$
- Ranges of rotation: Azimuth 540°, Elevation 0-115°
- Balanced reflector mounting
- High mechanical quality for gears, motor servos, bearings, etc.
- 27Bit Encoder: 0.0003° resolution
- Sub-reflector is adjustable using a hexapod
- Lifetime of more than 20 years

Goal of these new, highend antennas is to support the very fast generation and distribution of the IVS products as the continuous and precise UT1 monitoring for the determination of UT1-UTC and the regular evaluation of the International Celestial Reference Frame (ICRF). Therefore it is possible to monitor the Earth Orientation Parameter with shorter generation rates,

which might be a sufficient support of the future Global Geodetic Observing System (GGOS). In addition the position of each telescope should be quantified with relative positions better than 1 mm per year.

2 Locations of the new telescopes

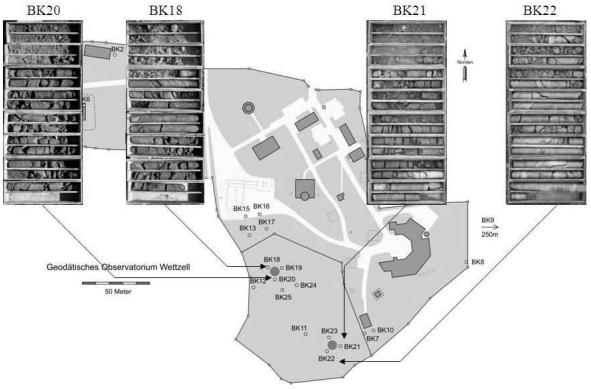

Fig. 1 The locations of the new telescopes and drilling core examples.

To find the ideal location for the two telescopes extensive soil specimens and geological surveys were done. The goal was to find two locations for the two telescopes which offer the same good geological stability as given at the 20m radio telescope. This has an extraordinarily low azimuth axis deviation. In total more than 12 drillings were made to determine the geological conditions of the new sites (see fig. 1). Special attention was turned to set the height of the elevation axis onto the same level for an additional system monitoring. A suitable location was found close to the observatory, which simplifies the connection of the new telescopes according to the local survey, the infrastructure and the operational tasks.

3 The ring focus design

The specially designed reflector uses a radial symmetric design. The advantage of this ring focus antenna (see fig. 2) is a reflection of the rays from the outer main reflector regions into the center of the sub-reflector giving a better illumination of the feed horn. This design is properly suited for broadband feed horns, which need a wider opening angle. Therefore the feed must be positioned close to the sub-reflector. This design offers not only a higher efficiency of the dish it also prevents more or less from direct thermal insolation, which supports the cryogenic vacuum chamber with the low-noise amplifiers.

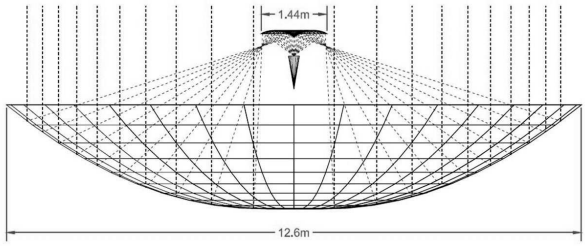

Fig. 2 The ring focus design.

4 Structure optimization

As the TWIN radio telescopes are especially designed for geodetic applications it is essential to achieve extremely low deviations in path length between main reflector, phase center of the feed horn and axis intersection of the telescope (a path length error of 0.3 mm was specified!). Elaborate simulations using the Finite Element Method (FEM) were performed by the construction company Vertex Antennentechnik GmbH in Duisburg, Germany to achieve a very torsion-resistant and solid supporting structure. All components from the main reflector to the concrete tower were optimized for occurring load cases (wind, gravitational effects caused by operating weight, thermal insolation, etc.) to guarantee the required stability. The sub-reflector can be positioned with a hexapod for gravity corrections which optimizes the path length and beam efficiency up to 40 GHz.

5 Microwave receiving and acquisition systems

The VLBI2010 concept suggests a broadband receiving system with a total bandwidth of 2 - 14 GHz, with the option to integrate the Ka-band (28 - 36 GHz). To realize these ideas new receiving systems have to be developed, supported by a homogeneous illumination of the main reflector. Helpful is also a stable phase center over the different frequencies and a system noise temperature below 50 K. Two possible feeds are promising to be used within the TWIN telescopes: a tri-band corrugated horn and the Elevenfeed (the upcoming Caltech feed design based on the original Lindgreen feed might also be a possible solution in the future (Akgiray, 2010), which should be investigated, but is not commercially available yet)

BKG has commissioned a tri-band feed horn (see 3 on the left side) that is able to work in the two geodetic frequency bands (S and X band), and also in the Ka band (Göldi, 2009). Therefore it will be possible to participate in all standard VLBI and also in deep space network observations. It also opens a substantial contribution to the improvement of the ICRF in the Ka band.

The Elevenfeed (see 3 on the right side) of Prof. Kildal (Chalmers University, Sweden) presently offers the best preconditions for the reception of a continuous frequency range of 2 to 14 GHz (Kildal and Yang, 2009). Extensive simulations show

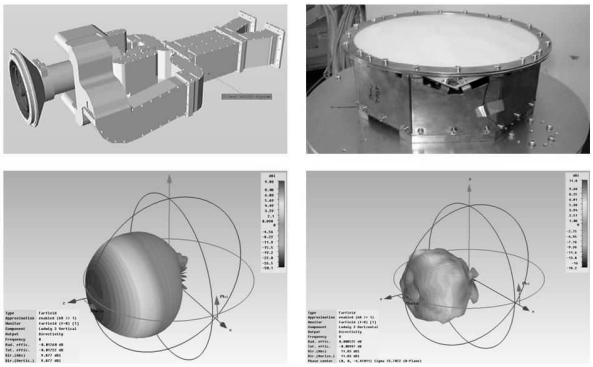

Fig. 3 The proposed feed horns: a tri-band coaxial feed and the Elevenfeed.

good performance of the feed up to ca. 10 GHz. From 10 - 14 GHz the performance is slightly lower but also suitable. The ohmic matching of the copper lines and the differential outputs pose some problems, where the solutions are on a good way. Cryogenic cooling as well as several special low noise amplifiers are necessary. Because of the broadband receiving, which covers approximately three octaves, two frequency converters are required. It is also essential to care for reduced system temperatures. The whole receiving system for the first antenna is shown in fig. 4.

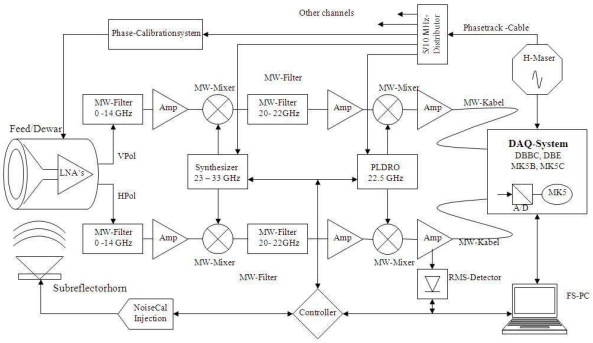

Fig. 4 The whole receiving system.

The microwave converter is designed for four 1 GHz wide frequency bands, which can be recorded using digital data recording systems with a better quantization of the signals and higher sampling and data rates of 2 Gbit/sec and higher with 2, 4 and 8 bit quantization. Currently the Digital Baseband Converter (DBBC) from HatLab s.r.l., a spin-off company of the Istituto Nazionale di Astrofisica (INAF), is forced. But also the compact Japanese system ADS3000+ from the National Institute of Information and Communications Technology (NICT) in Kashima (Takeuchi et. al., 2009) is under acquisition request for a future usage.

6 Control and operations

Both telescopes have been designed for continuous operations over 24 hours 7 days per week. Therefore special attention was turned to the control concept and the servo system. All components were designed for high availability, precise tracking and 1000 source observations per day. Continuous geodetic time series with higher accuracy can be generated following this strategy. Especially the increased number of sources and efficient observations within optimized sessions might improve the tropospheric corrections. According to this new observation strategies must be developed where the telescopes can operate parallel on different sources, additive on the same sources or in single telescope mode. It is also possible to maintain the non-operative telescope while the other is working.

Other new techniques will allow to increase the e-VLBI sessions and to run the observations with remote control or completely unattended. The new operational building is designed to allow such new control modes. It offers possibilities for local fringe test and zero baseline correlators as well as the connectivity and control room to run different sites from there. This is very important for the operations of the telescopes at the Transportable Integrated Geodetic Observatory (TIGO) in Concepción, Chile and at the German Antarctic Receiving Station (GARS) O'Higgins, which are operated by personnel stuff of Wettzell. To realize such remote control scenarios the e-RemoteCtrl software will be used, which is developed by a team of the observatory (Neidhardt, 2009).

7 Conclusions and outlook

Fig. 5 The new skyline of the Geodetic Observatory Wettzell: in the background are the new TWIN telescopes.

The described setup is the first complete and rigorous realization of the visions described in the VLBI2010 proposal (Niell et. al., 2004). Currently the telescopes are in the final construction phase and have already changed the skyline at Wettzell sig-

nificantly (see fig. 5). All of the high frequency components are commissioned and are under construction now. The digital broad band acquisition system is under test. The new antennas will be tested for operations end of the year 2011 and beginning 2012. Colocated with the existing 20m radio telescope, which can be used for dedicated research and development sessions after completion of the TWIN, and with the other instruments for space geodesy at Wettzell the new project is a pathfinder technology for the new proposed stations within the Global Geodetic Observing System (GGOS).

References

A. Akgiray, S. Weinreb. Progress Report: SKA LNA's and Feeds. http://www2.skatelescope.org/indico/getFile.py/access?contribId=16&sessionId=10&resId=0&materialId=0&confId=3, 2010 (Download 2011-05-29).

W. Göldi. Evaluation of Suitable Feed Systems. Presentation at the IVS VLBI 2010 Workshop on Future Radio Frequencies and Feeds, http://www.fs.wettzell.de/veranstaltungen/vlbi/frff2009/Part3/10-Goeldi_Workshop21.pdf, 2009 (Download 2011-05-29).

H. Hase, R. Dassing, T. Klügel, G. Kronschnabl, A. Neidhardt, P. Lauber, R. Kilger, K. Pausch. Twin Telescope Wettzell (TTW) - A VLBI2010 project. Presentation at the IVS VLBI 2010 Workshop on Future Radio Frequencies and Feeds, http://www.fs.wettzell.de/veranstaltungen/vlbi/frff2009/Part8/ttwvlbi2010e.pdf, 2009 (Download 2011-05-29).

P.-S. Kildal. Characterization of Feeds for Radio Telescopes. Presentation at the IVS VLBI 2010 Workshop on Future Radio Frequencies and Feeds, http://www.fs.wettzell.de/veranstaltungen/vlbi/frff2009/Part3/00-Tutorial-Wettzel-Kildal-090317cr.pdf, 2009 (Download 2011-05-29).

A. Neidhardt, M. Ettl, C. Plötz, M. Mühlbauer, R. Dassing, H. Hase, S. Sobarzo, C. Herrera, W. Alef, H. Rottmann. e-control: new concepts for remote control of VLBI-telescopes and first experiences at Wettzell. The 8th International e-VLBI Workshop, EXPReS09, PoS(EXPReS09)038, 2009 (Download 2011-05-29).

A. Niell, et. al.. IVS Memorandum 2006-008v01. "VLBI2010: Current and Future Requirements for Geodetic VLBI Systems". http://ivscc.gsfc.nasa.gov/publications/memos/index.html, Sept. 2004 (Download 2011-05-29).

H. Takeuchi, M. Kimura, T. Kondo, Y. Koyama. Current Status of Developments of Digital Backend Systems at NICT Kashima. Presentation at the IVS VLBI 2010 Workshop on Future Radio Frequencies and Feeds, http://www.fs.wettzell.de/veranstaltungen/vlbi/frff2009/DBE_DBBC/V2C_DBE_correlation_Meeting_Ishii.pdf, 2009 (Download 2011-05-29).

Sensitivity evaluation of two VLBI2010 candidate feeds

C. Beaudoin, B. Whittier

Abstract VLBI2010 ushers in a new generation of geodetic VLBI observing systems possessing far more bandwidth than their predecessors. As such, MIT Haystack Observatory has been actively involved in the evaluation of broadband microwave feeds for the new Patriot Antenna Systems Inc. 12m antenna installed at the Goddard Geophysical Astronomical Observatory in Greenbelt MD, USA. Currently, two antennas proposed as feeds that meet the demanding requirements for VLBI2010 now have hardware realizations. The first antenna is the cryogenic Eleven design which was developed at Chalmers University of Technology by Per-Simon Kildal and Jian Yang. The second candidate is the QuadRidge Feed Horn(QRFH) developed by Sandy Weinreb and Ahmed Akgiray at the California Institute of Technology and was introduced in December 2010. In this contribution, the up-to-date development efforts undertaken at the MIT Haystack Observatory are described and sensitivity expectations are outlined.

Keywords VLBI2010, Sensitivity, Feeds

1 Cryostat construction and considerations

The Patriot 12m antenna system incorporates a shaped-Cassegrain optical design as opposed to a traditional system incorporating parabolic primary and hyperbolic secondary reflectors. Due to the shaped nature of the antenna optics, a 24° shadow is cast by the subreflector in order to minimize losses incurred by blockage of the feed as shown in Fig. 1. Furthermore, since the Patriot 12m optics were designed specifically for X and Ka bands, an approximately-monotonic, frequency-dependent contraction of the shadow angle is expected below X-band due to wavefront diffraction. Given this constraint of the antenna system, emphasis was placed on the construction of a compact cryostat as described in Beaudoin et al. (2010). In short, it is not possible to avoid optical blockage of the cryostat with the aforementioned shadow angle; however, minimizing the interference is in the best interest of maximizing the sensitivity of the antenna. Photos of the new broadband cryostat developed for the Patriot 12m antenna are shown in Fig. 2 with the cryostat design described in Imbriale et. al. (2007).

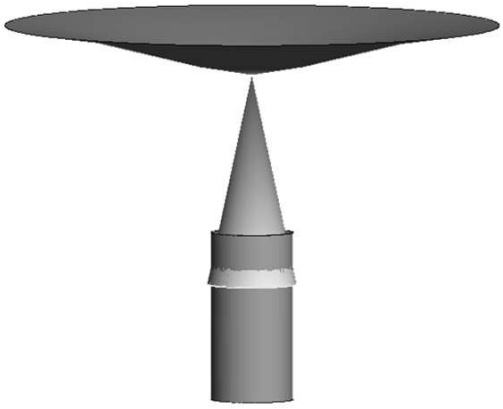

Fig. 1 Graphic displaying the shadow projected by the subreflector incorporated by the Patriot 12m antenna. In this figure, a 24° cone with apex at the vertex of the subreflector represents the shadow region, outside of which the radio telescope system is sensitive to signals reflected by the primary reflector. Interference of this cone with the feed results in blockage losses which limit the sensitivity of the radio telescope.

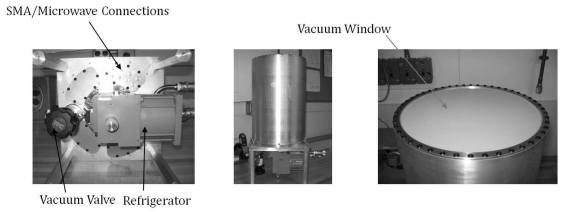

Fig. 2 Photos of the new broadband cryostat developed for the Patriot 12m antenna. The outer diameter of the cryostat is 280mm and the cylindrical length is 420mm.

Christopher Beaudoin, Bruce Whittier MIT Haystack Observatory, Westford Massachusetts, USA, 01886

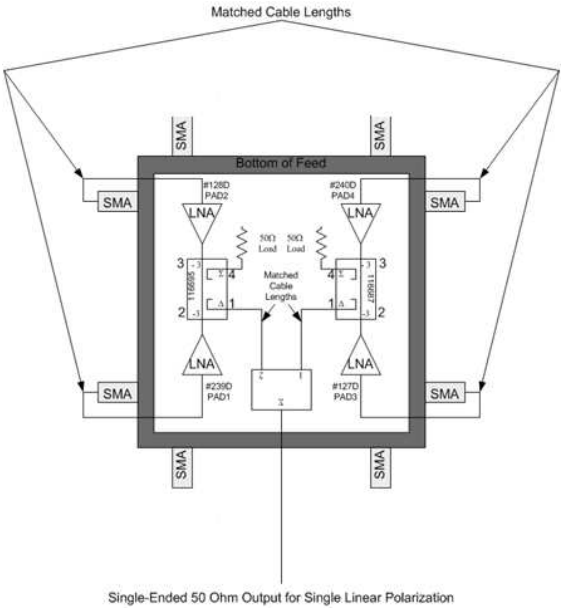

Fig. 3 Schematic representation of the balanced combiner network currently required to realize the cryogenic 2-13 GHz Eleven antenna as a radio telescope feed.

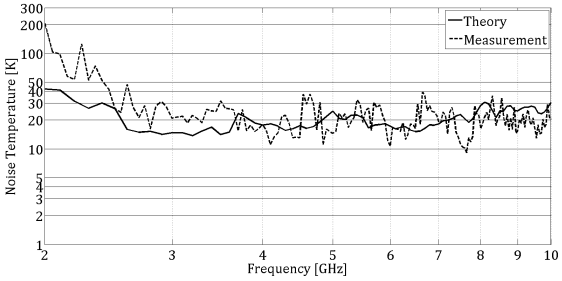

Fig. 4 Plot of measured and computed noise temperature results obtained from a frontend based on the cryogenic 2-13 GHz Eleven antenna and the CRYO1-12 LNA. The differences below 3.5 GHz are believed to be a result of the unmodeled cryostat in the computations as well as external radio frequency interference in the measurements.

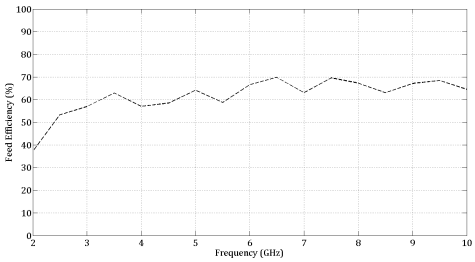

Fig. 5 Aperture efficiencies calculated for the Patriot 12m antenna under illumination by the Eleven antenna pattern described in Kildal and Yang (2009)

2 Aperture and noise performance of the candidate feeds

The sensitivity of a radio telescope receiver is determined by the effective collecting area of the telescope and the noise temperature of the frontend. As described in Petrachenko et. al. (2009), the VLBI2010 sensitivity goals for a 12 meter radio telescope are 50% collecting area efficiency and 50 Kelvin frontend noise temperature. These attributes have been evaluated for frontends based on the Eleven antenna and the QRFH antenna.

2.1 Eleven antenna

In January 2010, MIT Haystack observatory conducted Y factor measurements to assess the noise performance of a radio telescope frontend based on the the Eleven antenna and the Caltech CRYO1-12 LNA. Since the Eleven is a balanced antenna design, a balanced combiner network is necessary for each polarization to realize the operation of this antenna as a radio telescope feed. The combiner network shown in shown in Fig. 3 was incorporated and Y-factor measurements were conducted from which the frontend noise temperature was estimated. Fig. 4 displays a plot of the noise temperature comparing the quantities estimated from the Y-factor measurements with the theoretical expectation calculated as described in Yang et. al. (2011). The agreement is excellent from 3.5-10 GHz, however it falters below 3.5 GHz. The disagreement below 3.5 GHz is believed to be a result of strong RFI in S-band as well as the influence of the cryostat, which was not modeled in the expectation as explained in Yang et. al. (2011).

Aperture(feed) efficiency expectations were computed (see Kildal, 1985) for the Patriot 12m antenna under illumination by the Eleven feed pattern. The aperture efficiency results shown in Fig. 5 were calculated utilizing the feed patterns described in Kildal and Yang (2009). It is important to note that the calculations performed to obtain the efficiencies reported in Fig. 5 do not model blockages imposed by the subreflector and supporting struts. Hence, the efficiencies shown in Fig. 5 are regarded as best case. Not considering the physical antenna blockages, the results shown in Fig. 4 and Fig. 5 suggest that a frontend based on the Eleven antenna is well-suited to meet the VLBI2010 sensitivity requirements outlined in section 2 .

2.2 Quadridge Feed Horn antenna

In May 2011, Y-factor measurements were conducted on a frontend composed of the QRFH and CRYO1-12 LNAs. Since the QRFH is an unbalanced design with one receive port per polarization, only two LNAs are required to realize this antenna as a dual-linearly polarized radio telescope feed. The noise temperature estimates calculated from the Y-factor measurements are shown in Fig. 6.

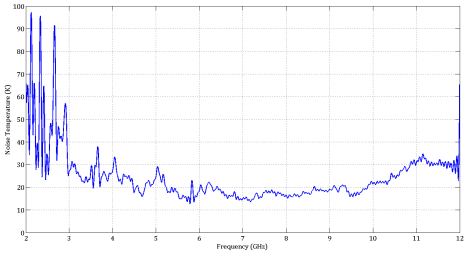

Fig. 6 Plot of noise temperature results obtained from Y-factor measurements of a frontend based on the QRFH antenna and the CRYO1-12 LNA on the Patriot 12m antenna. Evidence of radio frequency interference is also observed in this plot below 3 GHz.

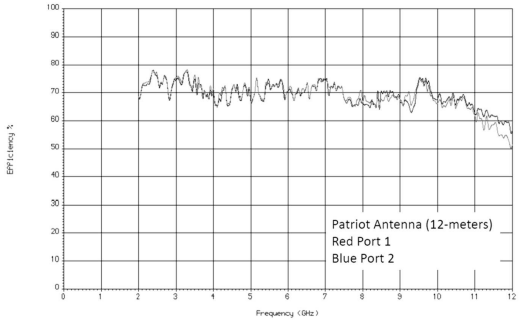

Fig. 7 Aperture efficiencies calculated for the Patriot 12m antenna under illumination by the measured QRFH antenna patterns. Reproduction of plot in Akgiray and Weinreb (2011)

Expected aperture efficiencies were also calculated for the Patriot 12m antenna under illumination by the QRFH antenna patterns. This computation is reported in Akgiray and Weinreb (2011) and the results are duplicated in Fig. 7. Similarly to the aperture efficiencies in 2.1, the aperture fields from which the Patriot 12m efficiencies were calculated under QRFH illumination did not model physical blockages by the subreflector and struts. Again, ignoring such physical blockages, it is clear from Fig. 6 and Fig. 7 that a frontend based on the QRFH antenna is also well-suited to meet the sensitivity requirements set forth by VLBI2010.

3 Conclusions

It has been shown that a frontend receiver based on either the Eleven antenna or the QRFH antenna is expected to meet the sensitivity goals for VLBI2010. Since the sensitivities expected from a frontend based on either feed are comparable, the selection of feed for the Patriot 12m antenna will likely be based on other aspects of the VLBI2010 receiver requirement, namely, phase and noise calibration injection as well as frontend simplicity. Since the QRFH requires only two LNAs for operation, it can easily incorporate stripline couplers in the receiver chain to inject pre-LNA phase and noise calibration signals into the receiver. It is important to realize that this method of injection will increase the frontend noise temperature relative to that shown in 6. At cryogenic temperature (i.e. 25K), however the increase is expected to be 5K but this will need to be demonstrated.

Phase and noise calibration injection via stripline coupler is not easily accommodated by a receiver frontend based on the Eleven antenna because of the matching requirements imposed by the balanced combiner network. Because of this, the most feasible option for pre-LNA phase and noise calibration signal injection is to radiate these signals into the frontend. Noise calibration injection by this technique is thought to be quite feasible. However, the experience at Haystack has shown that great care must be taken if the phase calibration signal is radiated into the frontend. The concern is raised because of the extremely weak phase calibration signal levels in question (approx. -180 dBm) as well as the possibility for multipath reflections which must be stable with antenna pointing and remain at a level of 50 dB below the direct-coupled signal in order to accurately phase calibrate the receiver chain.

References

A. Akgiray and S. Weinreb. "Wideband Near-Constant Beamwidth Flared Quad-Ridge Horn Feed for Reflector Antennas in Radio Astronomy." Presented at *URSI National Radio Science Meeting*, Jan. 5-8 2011, Boulder, CO, USA.

C. Beaudoin, P.-S. Kildal, J. Yang, and M. Pantaleev. "Development of a Compact Eleven Feed Cryostat for the Patriot 12m Antenna System." *International VLBI Service for Geodesy and Astrometry 2010 General Meeting Proceedings* Feb. 7-13, 2010 Hobart, Tasmania, Australia, volume NASA/CP-2010-215864, Hanover, MD: NASA Center for AeroSpace Information, p. 420-424, December 2010.

W.A. Imbriale, S. Weinreb, and H. Mani. "Design of a Wideband Radio Telescope." In J.H. Yuen Editor in Chief *The Interplanetary Network Progress Report*, volume 42-168, Pasadena, CA, NASA JPL California Institute of Technology, Feb. 2007.

P.-S. Kildal. "Factorization of the feed efficiency of paraboloids and Cassegrain antennas" *IEEE Transactions on Antennas and Propagation*, volume 33, no. 8, pp.903-908, August 1985.

P.-S. Kildal and J. Yang. *Report with Measurements of a coolable 2-14 GHz Eleven feed for VLBI 2010 delivered to Vertex*, June 2009.

B. Petrachenko et. al. "Design Aspects of the VLBI2010 System." *Progress Report of the IVS VLBI2010 Committee*, volume NASA/TM-2009-214180, Hanover, MD: NASA Center for AeroSpace Information, pg. 10 and 27-28, June 2009.

J. Yang, M. Pantaleev, P.-S. Kildal, B. Klein, Y. Karandikar, L. Helldner, N. Wadefalk, and C. Beaudoin. "Cryogenic 2-13 GHz Eleven feed for reflector antennas in future wideband radio telescopes" *IEEE Trans. on Antennas Propag. Special Issue on Antennas for Next Generation Radio Telescopes*, volume 59, no. 3, March 2011.

Assessing the Accuracy of Geodetic Measurements for the VLBI2010 Observing Network

D. MacMillan

Abstract We investigate the expected accuracy of geodetic estimates made by the next generation VLBI2010 network. To do this we simulated the effect of several known input contributions including troposphere turbulence, troposphere mapping function error, antenna deformation, and site pressure error. These contributions propagate to estimates of station coordinates. By comparing estimated values of parameters with known input values, we can evaluate biases that result from mismodeling.

Keywords VLBI2010, Reference frames

1 Introduction

In previous work, we have investigated the expected precision of the VLBI2010 observing network (MacMillan, 2006). In this studies, we looked at the effects of troposphere, clock, and measurement noise by performing Monte Carlo simulations. Here we try to answer the question: What is the level of systematic error for VLBI2010? One of the goals is to generate an error budget. Here, we consider the following errors: 1) troposphere turbulence, 2) clock error, 3) observation noise, 4) hydrostatic troposphere mapping function error, 5) antenna gravitational deformation, and 6) site pressure error.

2 Simulation description

For these simulations, we used the same 16-station network shown in Figure 1 that was used by the VLBI2010 working group. The observing schedule was a uniform sky schedule with each antenna observing at 60 observations/hour (T. Searle and B. Petrachenko, personal communication). The concept of the uniform sky schedule is that a series of pairs of approximately diametrically opposed quasars is observed during an observing session. For each pair, antennas on one half of Earth observe one quasar and the remaining antennas on the other side of the Earth observe the other quasar. The scheduling software chooses a sequence of source pairs to maximize the uniformity of the sky distribution of sources at each of the antennas. This type of schedule can work because the antennas in the network were assumed to slew with the same speed. For current networks with mixed types of antennas, this strategy does not work ideally. The 60 observations/hour schedule corresponds to an antenna with a slew rate of 5 deg/sec in azimuth and 1.2 deg/sec in elevation.

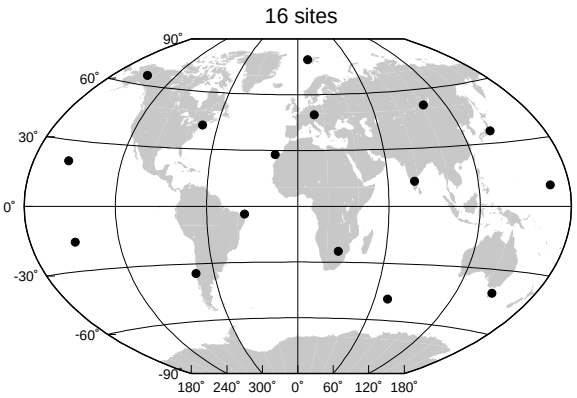

Fig. 1 Global 16-site simulation network.

Clock delays for each station are modeled as a random walk plus an integrated random walk corresponding to an Allan variance of $1\text{x}10^{-14}$ at 50 minutes. A white noise contribution corresponding to the observation uncertainty is added. The wet delay error is based on Kolmogorov turbulence delay modeling. The term τ_{si} refers to systematic errors that are studied in simulations. The observation error model is:

$$O-C = [m_{wet}(el_2)\tau_{wz2} + clk_2 + \tau_{s2}] - [m_{wet}(el_2)\tau_{wz1} + clk_1 + \tau_{s1}] + \sigma_{obs}$$

3 Modeling Results

In the following sections, we discuss the effect of each error source separately on the topocentric site position estimates. We

D. MacMillan, NVI, Inc.,NASA Goddard Space Flight Center, Greenbelt,MD, 20771 USA

summarize the results at the end in the error budget shown in Table 1.

3.1 Turbulence

We derived a latitude and site-height dependent model for the troposphere refractive index structure constant C_n, where we have averaged over the seasonal variation. We started with the C_n and heights computed by T. Nilsson (personal communication) from a global distribution of high resolution radiosonde site data. The C_n increase towards the equator corresponding to increased troposphere water vapor content. The delay model is based on the Treuhaft-Lanyi Kolmogorov turbulence model. To test the model we ran simulations with the two-week series of CONT05 data. Baseline length repeatability scatter from the simulation runs is reasonably close to observed scatter, overestimating the observed scatter by a factor of 1.2 ± 0.4.

The main systematic effect shown in Figure 2 from the turbulence error is the increase in vertical scatter from about 1 mm at high latitude sites like Ny Alesund to 3 mm near the equator. There is some variability due to site height, for example, scatter is reduced for sites with large heights - Kokee (1177 m), HartRao (1435 m), and BAN2 (835 m). The horizontal scatter is 0.5-1.0 mm and is nearly independent of latitude. Since turbulence is a noise process there is essentially no bias produced in the geodetic estimates.

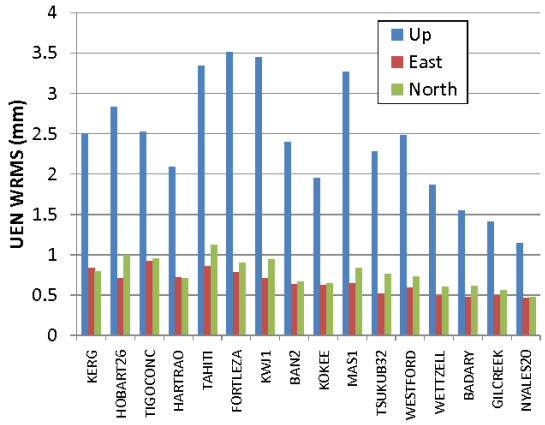

Fig. 2 Site position (UEN) scatter due to tropospheric turbulence, where sites are ordered by increasing latitude

3.2 Clock Error

We modeled the effect of clock error characterized it by an Allan variance of 1×10^{-14} at 50 minutes. The resulting site vertical scatter is 0.5-0.8 mm and horizontal scatter is only 0.2 mm. There is minimal latitude dependence. There is essentially no resulting bias. This level of clock variance is fairly conservative in the sense of what we expect to have for the VLBI2010 system.

3.3 Observation Error

The nominal precision of the VLBI2010 observable is 4 psec. Modeling this as a white noise process in a simulation yields a vertical precision of only 0.15 mm and horizontal precision of 0.05 mm. The simulation is linear in the sense that if we have a 12 psec observable, the site position scatter is tripled.

3.4 Hydrostatic Mapping Function

Currently, the best available mapping functions are the VMF1, which are based on one-dimensional raytracing of ECMWF weather model profiles (Böhm et al., 2006a). VMF1 assumes that the troposphere about a site is azimuthally symmetric. Comparisons have been made between VMF1 and one-dimensional raytracing of radiosonde profile data. Niell (2006) computed the WRMS delay error of the hydrostatic VMF1 at a 5 deg elevation angle for a globally-distributed set of radiosonde data sites. We simulated this error as an error in the a-coefficient of the continued fraction form of the mapping function. The error is linear in the derivative of the mapping function with respect to the a-coefficient. Similarly, we simulated the bias error of the mapping function using bias errors from radiosonde delay comparisons from Böhm et al. (2006b). The site vertical scatter increases from 0.5 mm near the equator to 2 mm at high latitude in Figure 3. It is seen in Figure 4 that vertical bias error has a magnitude as large as 0.8 mm at high latitude and is positive in the northern hemisphere and negative in the southern hemisphere. There is also a systematic bias error of the North component of site position. This is due to the no-net-translation constraint applied in the solution and the fact that there are more northern hemisphere sites for the 16-site network. The problem is difficult to avoid because the land mass in the southern hemisphere is so much less than in the northern hemisphere.

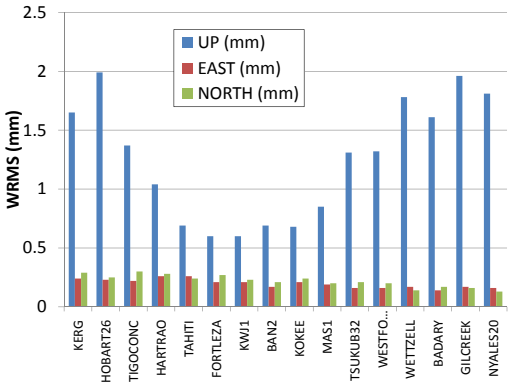

Fig. 3 Site position (UEN) scatter due to VMF1 mapping function error, where sites are ordered by latitude.

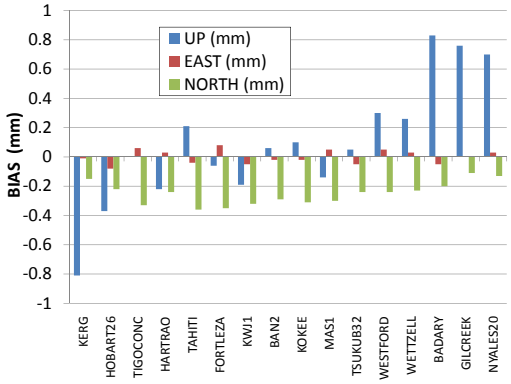

Fig. 4 Site position (UEN) bias due to VMF1 mapping function bias.

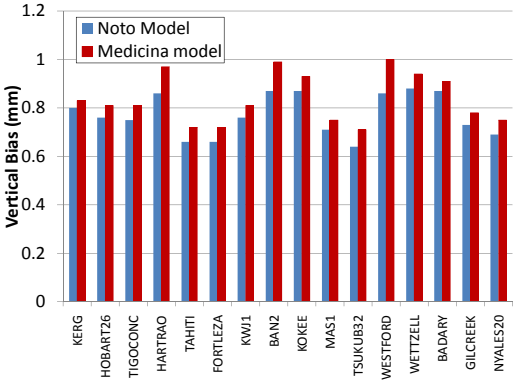

Fig. 6 Site vertical bias error due to gravitational deformation.

3.5 Site Pressure Data

It is essential that pressure be estimated accurately at each site. To assure this, 1) pressure sensor calibration must be maintained, 2) pressure data cannot be missing, and 3) one must account for sensor height relative to the reference point of the VLBI antenna. To quantify the effect of pressure error, we simulated the effect of a 10 mbar pressure error. Figure 5 shows that this error biases vertical estimates by 0.15-0.20 mm/mbar for a 5 deg minimum elevation cutoff. The error decreases by a factor of about 2 between a 5 and 10 deg cutoff.

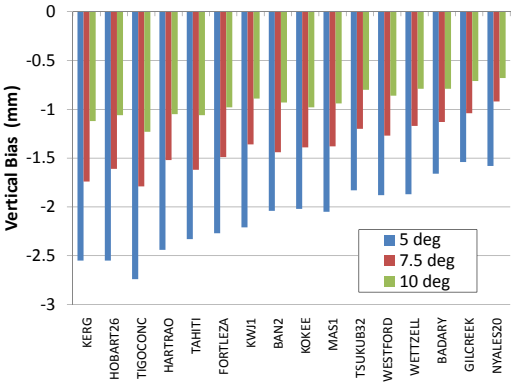

Fig. 5 Site position (UEN) bias due bias error site pressure of 10 mbar.

3.6 Antenna Gravitational Deformation

Gravitational deformation is an important effect that until recently has not been included in VLBI analysis. Sarti and Abondanza (Sarti et al., 2009) have measured the deformation as function of elevation of the 32-meter antennas at Noto and Medicina using a laser scanner to determine the focal point variation, terrestrial survey to measure the receiver position variation, and finite element modeling to determine the vertex position variation. They used a model for the signal path dependence on elevation caused by deformation based on the work of Clark and Thomsen (1988). The model is linear in the variations of focal length, receiver position, and vertex position. The effect for Noto is less because of improvements made to its surface. The models for these antennas were scaled down from 32 m to the 12 m nominal diameter of VLBI2010 antennas, assuming that the effect is proportional to the area of the antenna. Simulation results in Figure 6 show that the deformation causes a station vertical bias of 0.7-1.0 mm.

Table 1 Site Vertical Position Error Budget

Parameter	Bias (mm)	WRMS (mm)
Turbulence	< 0.5	1-3
Hydrostatic mapping	0.5-1.5	0.5-2.0
Clock error	< 0.2	0.6
Gravity deform	0.6-1.0	-
Obs noise (4 ps)	< 0.1	< 0.15
Thermal (mm/C)	0.07	-
Pressure (mm/mb)	0.15-0.25	-
Source structure	?	?

References

J. Böhm, B. Werl, H. Schuh, Troposphere mapping functions for GPS and VLBI from ECMWF operational analysis data, J Geophys Res, vol. 111, B02406, doi:10.1029/2005JB003629, 2006.

J. Böhm, A. Niell, P. Tregoning, and H. Schuh, Global Mapping Function (GMF): a new empirical mapping function based on numerical weather model data, Geophys. Res. Lett., 33, 2006.

T.A. Clark, P. Thomsen, Deformations in VLBI antennas, Tech. report 100696, NASA, Greenbelt, MD, 1988.

D. MacMillan, Simulation analysis of the geodetic performance of networks of VLBI2010 stations, Proc. IVS 2008 General Meeting, 416-420, 2008.

A. Niell, Interaction of atmospheric modeling and VLBI analysis strategy, Proc. IVS 2006 General Meeting, 252-256, 2006.

P. Sarti, L. Vittuari, and C. Abbondanza, Gravity dependent signal path variation in a large VLBI telescope modelled with a combination of surveying methods, J. Geod., 83(11), 1115-1126, 2009.

The Future Global VLBI2010 Network of the IVS

Hayo Hase, Dirk Behrend, Chopo Ma, William Petrachenko, Harald Schuh, Alan Whitney

Abstract The VLBI2010 concept was developed by the International VLBI Service for Geodesy and Astrometry (IVS) in order to create the next generation VLBI system needed to meet the goals of the Global Geodetic Observing System (GGOS) of the International Association of Geodesy (IAG). Global measurement goals of 1mm position error and 0.1mm/year site velocity error require new radio telescope designs, new VLBI receiving and recording systems, new concepts for data transmission and correlation, as well as updated software for scheduling, data analysis, and archiving. In December 2010, the IVS VLBI2010 Project Executive Group (V2PEG) conducted a survey among existing IVS network stations to measure awareness of VLBI2010 and to learn about modernization plans towards VLBI2010; the results of this survey indicate that most of the IVS network stations are already planning the transition to VLBI2010 capabilities. The survey indicated that up to 20 new radio telescopes at 17 sites with VLBI2010 compliance could become operational by 2017; a sufficient number of VLBI2010-compatible radio telescopes should be available by 2014-15 to support initial VLBI2010 operations. The survey also indicated that a number of network stations need technical consultation about VLBI2010, as well as some needing letters of support to be successful in obtaining the necessary support and funding.

Keywords VLBI2010, IVS, V2PEG, radio telescope, VLBI network, GGOS

Hayo Hase
Bundesamt für Kartographie und Geodäsie, Geodätisches Observatorium Wettzell, Sackenrieder Str. 25, 93444 Bad Kötzting, Germany
Dirk Behrend
NVI, Inc./GSFC, Greenbelt, MD, U.S.A.
Chopo Ma
NASA GSFC, Greenbelt, MD, U.S.A.
William Petrachenko
NRCan, Penticton, BC, Canada
Harald Schuh
TU Wien, Wien, Austria
Alan Whitney
MIT Haystack Observatory, Westford, MA, U.S.A

1 Introduction

The Directing Board (DB) of the International VLBI Service for Geodesy and Astrometry (IVS) established the VLBI2010 Project Executive Group (V2PEG) in early 2009 to provide strategic leadership to the VLBI2010 project and guide the transition from the VLBI2010 development phase to the VLBI2010 implementation phase. V2PEG is also the primary point of contact for VLBI2010-related questions from institutions that are interested either to upgrade existing VLBI operations to VLBI2010 compatibility or to build new compatible systems. The V2PEG has also been involved at different levels to help expedite administrative processes concerning the setup of VLBI2010 radio telescope projects, including the proof-of-concept project.

In 2010, V2PEG conducted a survey among existing IVS network stations in order to:

- gather information about individual VLBI2010 plans,
- trigger VLBI2010 discussion at the network station level,
- solicit input on what the V2PEG can do to provide the best support to individual VLBI2010 projects.

The survey addressed 31 IVS network stations, all of which replied. Subsequently, the survey results were re-distributed back to the IVS-network stations in January 2011, which are also available at the IVS web site (Hase et al., 2011).

2 VLBI2010

In the first decade of this millennium the IVS established two working groups to define the outline of VLBI2010. Working Group 2 defined “Product Specifications and Observing Programs” that describes the VLBI2010 measurement goals and proposed observing programs. The Working Group 2 report was completed in 2002 (Schuh et al., 2002), describing the future demands of the service products. Several products, such as station coordinates, episodic events, Earth rotation velocity, rotational pole position, nutational parameters, as well as geophysical properties of the ionosphere and troposphere, demand continuous seven days per week observation. The follow-up IVS Working Group 3 “VLBI 2010” was created in September 2003.

It examined current and future requirements for VLBI geodetic systems, including all components from antenna to analysis, and published a report with recommendations for a new generation of systems. The final report was presented in 2005 (Niell et al., 2005). The main characteristics of the future VLBI2010 system can be identified as follows:

- continuous observations in 30s slew-track cycles,
- fast radio telescopes of $\geq$ 12m reflector class with kinematic parameters of either a single 12-m diameter antenna with very high slew rates, e.g. 12 deg/s in azimuth, or a pair of 12-m diameter antennas, each with more moderate slew rates, e.g. 5 deg/s in azimuth (Petrachenko et al., 2009),
- wideband feed, 2-14 GHz (later 2-18 GHz),
- digital baseband converter,
- high-data-rate sampling data acquisition, ≥ 8 *Gbps*,
- broadband connectivity for e-transfer and e-VLBI,
- distributed remote controlled continuous operation of the VLBI network,
- software correlator,
- automated production process including analysis.

3 Global Geodetic Observing System

The International Association of Geodesy (IAG), as a member of the International Union of Geodesy and Geophysics (IUGG), contributes with the Global Geodetic Observing System (GGOS) to the Global Earth Observing System of Systems (GEOSS). GEOSS is an outcome of the Group on Earth Observation (GEO) which is composed of 86 nations plus the European Commission and 61 participating organizations (as of May 2011). The envisaged goals of GGOS are:

- 1mm position accuracy, 0.1 mm/year velocity accuracy,
- continuous observations for time series of station positions and Earth orientation parameters,
- turnaround time to initial geodetic products of less than 24 hours.

The realization of GGOS calls on the IVS community to improve its performance to VLBI2010 standards.

4 IVS Network Station Survey

The survey consisted of six questions (see detailed questions in the analysis report Hase et al., 2011):

1. Specify plan to upgrade your site to full VLBI2010 capability.
2. Do you plan to acquire a new radio telescope that fully meets the VLBI2010 recommendations?
3. Do you plan to continue operating your existing legacy radio telescope in the future?
4. What is the best estimate of the year in which your VLBI2010 capability will become operational?
5. At what stage are you in the planning process?
6. What support do you need from the IVS?

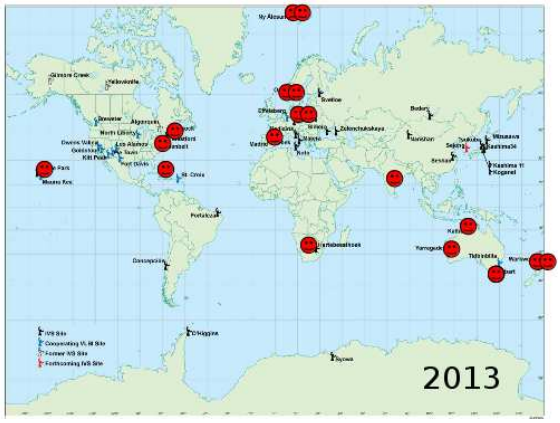

Fig. 1 Prediction for 2013: Approximately 13 stations will be available, allowing significant, but not full-time, VLBI2010 observations.

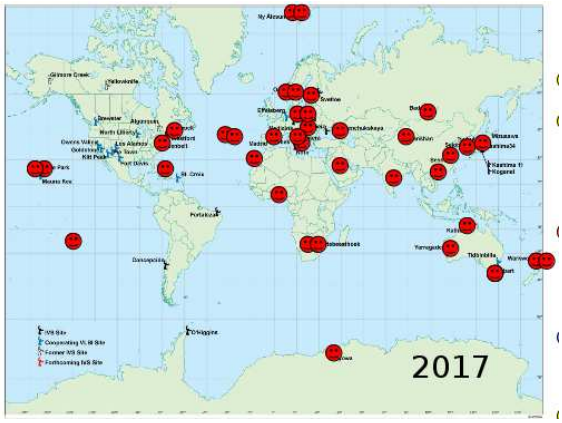

Fig. 2 Prediction for VLBI2010 observations in 2017: Approximately 20 stations will be available for full-time observations. Additional sites in Tahiti, Nigeria, Saudi-Arabia and India may join the IVS network if funding is approved.

The answers received were, of course, based on best estimates of the availability of resources to build new systems. However, the average of optimistic and pessimistic estimates gives a first clue to the future development of the VLBI2010 network. Summarizing the results:

- By 2013, a sufficient number of VLBI2010 compatible radio telescopes will be available for significant, but not full-time, VLBI2010 operations (Figure 1).
- By 2017, approximately 20 new radio telescopes at 17 sites operated by IVS network station institutions will be available for full-time VLBI2010 observations (Figure 2). Additional new stations may also join if approved and constructed.

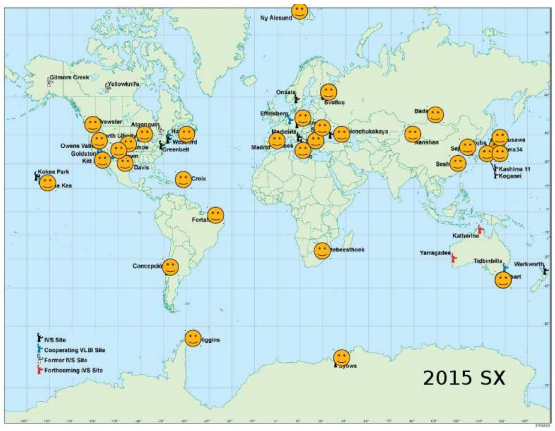

Fig. 3 Prediction for S/X observations in 2015: IVS will still utilize existing global S/X network stations for some time to support data continuity, astrometry and space applications.

- Even in 2017, the American/Pacific region will still lack presence of VLBI2010 network stations, though a 10-station NASA network covering some of this area may eventually be built.
- Through at least 2015, observations by a large number of legacy S/X-band telescopes will still be supported for data continuity, astrometry and space applications (Figure 3).
- Many network stations need technical consultation about VLBI2010, as well as support letters to be successful with the administration and funding level.

Table 1 shows detailed IVS station-by-station projections through 2017 according to survey results. The stations marked with an asterisk (*) are planning very fast radio telescopes that are compliant with the proposed VLBI2010 slewing rate and observation mode. Stations marked with two asterisks (**) will follow the twin telescope concept, which consists of two VLBI2010 radio telescopes at one location. Stations marked with a plus (+) will be VLBI2010 compliant except that only a single antenna with a $\sim$5 deg/sec azimuth slew rate is currently planned. Legacy stations upgrading to VLBI2010 receivers and data systems are unmarked. Stations marked with a minus (-) will continue to operate with S/X-band only. The indicated year is an estimate for operational capability for the IVS.

5 Conclusions

A highly capable VLBI2010 network will be implemented within this decade; new broadband 2-14GHz observation modes will come into regular operation from 2014/2015 onwards with full operation by about 2017. The current S/X operation mode will be maintained in parallel at a number of legacy stations for data continuity, astrometry and space applications.

Table 1 Details of the projected schedule of VLBI2010-station construction through 2017 (see text for details)

network station	country	year	project name
Hobart+	Australia	2010	AuScope
Warkworth+	New Zealand	2010	
Yarragadee+	Australia	2011	AuScope
Katherine+	Australia	2011	AuScope
Wettzell**	Germany	2011	TTW
Westford+	U.S.A.	2011	POC
Greenbelt+	U.S.A.	2011	POC
Kashima34	Japan	2013	
Koganei11	Japan	2013	
Yebes*	Spain	2013	RAEGE
Onsala**	Sweden	2013	
Badary*	Russia	2014	
Zelenchukskaya+	Russia	2014	
Matera*	Italy	2014	
Santa Maria*	Portugal	2014	RAEGE
Fortaleza	Brazil	2014	
Kokee Park*	U.S.A.	2014	
Sejong22	Korea	2015	
Gran Canaria*	Spain	2015	RAEGE
Hartebeesthoek*	South Africa	2015	
Tsukuba32	Japan	2016	
Tsukuba*	Japan	2016	
Sheshan*	China	2016	
Hainan*	China	2016	
Flores*	Portugal	2016	RAEGE
Ny Ålesund**	Norway	2017	
Arecibo+	Puerto Rico	2017?	
VERA-	Japan	n.a.	
Simeiz	Ukraine	n.a.	
Svetloe	Russia	n.a.	
Medicina	Italy	n.a.	
Noto	Italy	n.a.	
Syowa	Antarctica	n.a.	
O'Higgins	Antarctica	n.a.	
TIGO	Chile	n.a.	
VLBA-	U.S.A.	n.a.	

References

H. Hase, D. Behrend, C. Ma, W. Petrachenko, H. Schuh, A. Whitney "Network Station Survey 2010, Analysis", *2011,* `http://ivscc.gsfc.nasa.gov/technology/vlbi2010-docs/ns-survey2010.pdf`

H. Schuh, P. Charlot, H. Hase, E. Himwich, K. Kingham, C. Klatt, C. Ma, Z. Malkin, A. Niell, A. Nothnagel, W. Schlüter, K. Takashima, N. Vandenberg, "IVS Working Group 2 for Product Specification and Observing Programs, Final Report", *2002,* `http://ivscc.gsfc.nasa.gov/about/wg/wg2/`

IVS_WG2_report_130202-letter.pdf

A. Niell, A. Whitney, B. Petrachenko, W. Schlüter, N. Vandenberg, H. Hase, Y. Koyama, C. Ma, H. Schuh, G. Tuccari, "VLBI2010 - A Vision for Geodetic VLBI, Current and Future Requirements for Geodetic VLBI Systems", *2005*, http://ivscc.gsfc.nasa.gov/about/wg/wg3/IVS_WG3_report_050916.pdf

B. Petrachenko (chair), A. Niell, D. Behrend, B. Corey, J. Böhm, P. Charlot, A. Collioud, J. Gipson, R. Haas, T. Hobiger, Y. Koyama, D. MacMillan, Z. Malkin, T. Nilsson, A. Pany, G. Tuccari, A. Whitney, J. Wresnik, "Design Aspects of the VLBI2010 System: Progress Report of the IVS VLBI2010 Committee", *2009, Document NASA/TM-2009-214180*, ftp://ivscc.gsfc.nasa.gov/pub/misc/V2C/TM-2009-214180.pdf

EOP determination from observations of Russian VLBI-network "Quasar"

A. Finkelstein, A. Salnikov, A. Ipatov, S. Smolentsev, I. Surkis, I. Gayazov, I. Rahimov, A. Dyakov, R. Sergeev, E. Skurikhina, S. Kurdubov

Abstract Regular determinations of Earth orientation parameters are performed by the Russian "Quasar" VLBI network since August 2006. The observations are carried out weekly in the framework of two national programs: 24-hour sessions for determination of all EOP from observations on the "Quasar" network (Ru-E program) and 1-hour sessions for UT1 determination at "Zelenchukskaya" – "Badary" baseline (Ru-U program) using e-VLBI Transfer. For Ru-E sessions with the Mark 5B recording system RMS values of EOP deviations from the IERS EOP 08 C04 series are 0.95 mas for Pole position, 35 μs for UT1-UTC, and 0.40 mas for Celestial Pole position. RMS of UT1 deviations for Ru-U sessions is 60 μs.

Keywords EOP, VLBI observations, "Quasar" network

1 Introduction

"Quasar" VLBI network was founded for a wide range of coordinate and time determination tasks (Finkelstein, 2001; Finkelstein et al., 2004). The Network "Quasar" consists of three radio astronomical observatories (see Fig. 1): "Svetloe" (Leningradsky region) (Smolentsev and Rahimov, 2004), "Zelenchukskaya" (Republic Karachaevo-Cherkessia) (Smolentsev and Dyakov, 2006) and "Badary" (Republic Buryatia) (Smolentsev and Sergeev, 2008) connected by digital communication channels with the Operating and Data Processing Center (Surkis et al., 2007) and the Analysis Center (Skurikhina, 2010) located at the Institute of Applied Astronomy (IAA) in St. Petersburg.

All observatories of the "Quasar" network are equipped with 32-meter radio telescope (RT-32) and technical systems providing VLBI observations: low noise receivers, frequency and time keeping systems with H-masers, technical service systems, which are supported by the Technology Development Center (Ipatov et al., 2007). Recording terminals at the observatories differ in some details: "Svetloe" has DAS Mark IV, Mark 5A, Mark 5B recording terminals, "Zelenchukskaya" has DAS VLBA4, Mark 5A, Mark 5B recording terminals, "Badary" has DAS-R1000 developed in IAA (Fedotov, 2007) and Mark 5B recorder. By the end of 2011 all observatories will be equipped with new digital DAS R11002M (Fedotov et al., 2010).

More detailed description of "Quasar" complex components given in (Finkelstein et al., 2008), the state of art and future plans given in (Finkelstein et al., 2010).

Regular determinations of the Earth orientation parameters from domestic observational programs have been put into practice since August 2006 (Finkelstein et al., 2008). Current results of the analysis of these observations are presented.

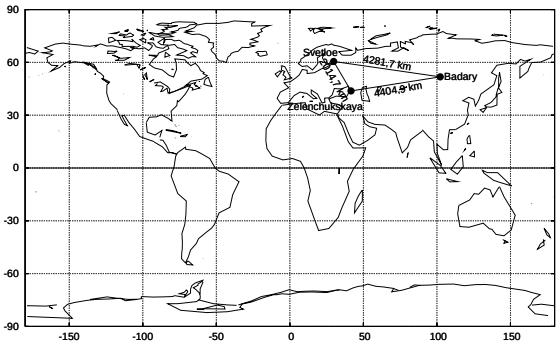

Fig. 1 "Quasar" network

2 Russian Domestic Programs of VLBI Observations

VLBI observations at the "Quasar" network for EOP monitoring are carried out in the framework of two domestic programs: Ru-E and Ru-U.

A.Finkelstein, A.Salnikov, A.Ipatov, S. Smolentsev, I.Surkis, I. Gayazov, I.Rahimov, A.Dyakov, R.Sergeev, E. Skurikhina, S.Kurdubov
Institute of Applied Astronomy of RAS, 10, Kutuzova emb., 191187 Saint Petersburg, Russia

The purpose of the Ru-E program is to provide EOP results on regular basis from 24-hours sessions on three-station network: "Svetloe" – "Zelenchukskaya" – "Badary".

The purpose of the Ru-U program is to provide UT1-UTC results on regular basis from Intensive sessions on one base "Badary" – "Zelenchukskaya" (or "Badary" – "Svetloe").

Statistics of "Quasar" domestic observational programs is shown in Tab. 1. Planned numbers of sessions in 2011 are indicated in brackets.

Year	Ru-U			Ru-E		
	Sv	Zc	Bd	Sv	Zc	Bd
2006		6	6	9	9	9
2007	10	12	17	9	9	9
2008	18	15	18	14	14	14
2009	13	26	30	23	23	23
2010	3	50	50	20	20	20
2011	6	23(50)	28(50)	16(50)	16(50)	16(50)

Table 1 Number of observations under Ru-E and Ru-U programs

All operations within the framework of the "Quasar" network are are performed as alike as in IVS. Sessions are scheduled by the Technical Consulate once for a year and are approved every month. Operating Center prepares the file with the schedule of observations session. Observations are carried out at S and X band.

Observational data from 1-hour Ru-U sessions are transmitted to the IAA correlator using e-VLBI data transfer. Data of 24-hour sessions are shipped to the correlator on disk modules. Results of correlation in NGS-format are sent to the Analysis Center, where EOP are calculated.

The main steps in progress of "Quasar" network observations are the following:

- January-July 2006: Test VLBI observations on X-band, August 2006: Start of regular observations (24-hour Ru-E sessions and 8-hour Ru-U sessions) twice a month with S2 recording system. One-base "MicroParsec" correlator were used for data processing. Typical Ru-E session contained about 265 scans of nearly 28 geodetic sources and typical Ru-U session – about 80 scans of 16 sources with flux 0.86–10.83 J.
- August 2008: Test Ru-U sessions of 1-2 hours duration using the Mark 5B recording system with correlation on the new IAA correlator ARC in one-base mode. November 2008: first experimental Ru-E session using the Mark 5B recording system and comparing the results of new IAA correlator ARC with the Bonn correlator data.
- February 2009: Start of weekly Ru-U and Ru-E sessions in experimental mode using the Mark 5B recording system. Duration of Ru-U sessions were reduced to 2 hours. New 6-station ARC correlator (Surkis et al., 2010) was used in test mode. The set of sources was extended up to 63 sources with flux more than 0.5 J for Ru-E sessions and up to 159 sources with flux from 0.25 J. Scan numbers are about 360 and 20 for Ru-E and Ru-U sessions correspondingly.
- April 2009: First successful e-VLBI experiment (Finkelstein et al., 2010). Regular e-VLBI data transfer for 1-hour Ru-U sessions started since September 2009 (Finkelstein et al., 2010). Weekly Ru-E and Ru-U sessions on regular base since July 2010. accounting the ionospheric delay from GPS TEC data.

3 The results of EOP Determination

For secondary data treatment of Domestic "Quasar" sessions QUASAR (Kurdubov, 2007) and OCCAM/GROSS (Malkin, 2005) program packages are used. All reduction models correspond to IERS Conventions (2003) (McCarthy and Petit, 2004). Celestial coordinate system is fixed by ICRF2 catalog (Fey, Gordon and Jacobs, 2009). Earth coordinate system is fixed by catalog ITRF2008 of station positions and velocities. Position and velocity of the Badary station were specified from both IVS and Domestic observations (Gayazov and Skurikhina, 2011).

The secondary data processing is implemented with delays 6 hour for Ru-U sessions and about 10 days for Ru-E sessions. When VMF1 (Boehm et al., 2006) data are unavailable the Niell mapping function (Niell, 1996) for accounting tropospheric path delay are used. Similarly instead of 3-D atmospheric loading data (Petrov and Boy, 2004) the regression model is applied. When these data become available the EOP time series are recalculated. The tropospheric gradients are not estimated in processing the "Quasar" observations.

As only the NGS file of Ru-U session appears at server after correlation the secondary data processing is performed automatically using the QUASAR program and special utilities.

The accuracy of EOP estimations from Ru-E and Ru-U sessions are presented in Tab. 2 for the period since August 2006. In Tab. 3 the results obtained with the Mark 5B recorders are given separately.

Differences of EOP with time series IERS EOP 08 C04 are presented in Fig. 2 – 8.

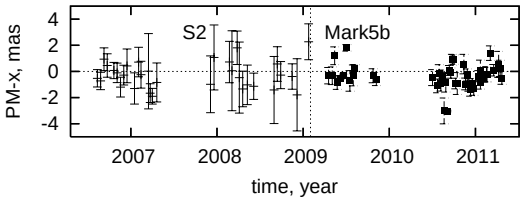

Fig. 2 Xpol: differences between IAA estimations and IERS EOP 08 C04

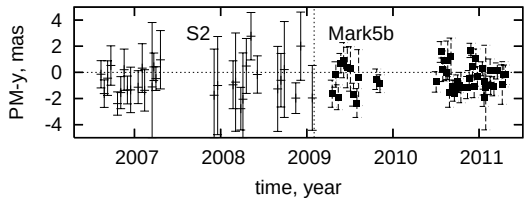

Fig. 3 Ypol: differences between IAA estimations and IERS EOP 08 C04

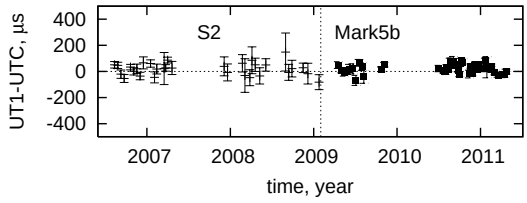

Fig. 4 UT1-UTC: differences between IAA estimations and IERS EOP 08 C04

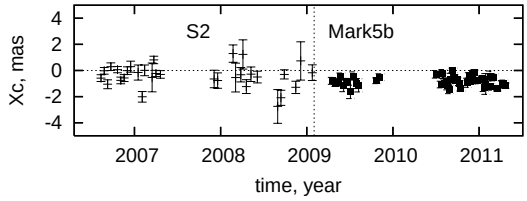

Fig. 5 Xc: differences between IAA estimations and IERS EOP 08 C04

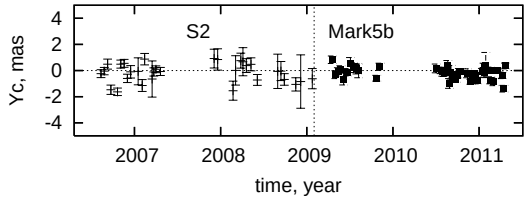

Fig. 6 Yc: differences between IAA estimations and IERS EOP 08 C04

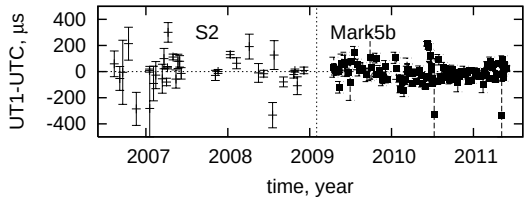

Fig. 7 UT1-UTC (Intensive) differences between IAA estimations and IERS EOP 08 C04

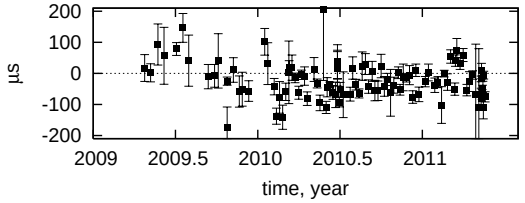

Fig. 8 UT1-UTC e-VLBI, differences between IAA estimations and IERS EOP 08 C04

EOP	N_{sess}	Bias	RMS
X_p, mas	77	-0.36	0.96
Y_p, mas	77	-0.50	1.13
UT1-UTC,μs	77	21	42
X_c,mas	77	-0.60	0.65
Y_c, mas	77	-0.20	0.57
UT1-UTC Int., μs	142	6	86

Table 2 Statistics of differences [IAA – IERS EOP 08 C04]

EOP	N_{sess}	Bias	RMS
X_p, mas	44	-0.38	0.91
Y_p, mas	44	-0.41	0.99
UT1-UTC,μs	44	23	35
X_c,mas	44	-0.82	0.37
Y_c, mas	44	-0.19	0.43
UT1-UTC Int., μs	104	-14	60

Table 3 Statistics of differences [IAA – IERS EOP 08 C04] for Mark 5B sessions

4 Summary

Observations on the ”Quasar” VLBI network are carried out on regular base weekly with correlation on the 6-station IAA correlator ARC. Data of 1-hour Ru-U sessions are transferred to the correlator in e-VLBI mode. Installation of Mark 5B recording system has led to noticeable improvement of the EOP results accuracy, particularly for UT1.

References

J. Boehm, B. Werl, H. Schuh. Troposphere mapping functions for GPS and very long baseline interferometry from European Centre for Medium-Range Weather Forecasts operational analysis data. In D. Behrend, K. D. Baver, editors, *Journal of Geophysical Research, Vol. 111*, 2006. doi: 10.1029/2005JB003629.

L. Fedotov VLBI Terminal in Badary Observatory. In J. Böhm, A. Pany, and H. Schuh, editors, *Proceedings of the 18th Workshop Meeting on European VLBI for Geodesy and Astrometry*, volume 79 of *Geowissenschaftliche Mitteilun-*

gen, Schriftenreihe Vermessung und Geoinformation der TU Wien, pages 222–224. TU Wien, 2007.

L. Fedotov, E. Nosov, S. Grenkov, D. Marshalov. The Digital Data Acquisition System for the Russian VLBI Network of New Generation. In D. Behrend, K. D. Baver, editors, *6th IVS General Meeting Proc.*, pages 400-404. NASA/CP-2004-212255, 2010.

A. Fey, D. Gordon, Ch. Jacobs. The Second Realization of the International Celestial Reference Frame by Very Long Baseline Interferometry, Presented on behalf of the IERS / IVS Working Group. Alan Fey, David Gordon, and Christopher S. Jacobs (eds.). *IERS Technical Note, No. 35*, Frankfurt am Main, Germany: Verlag des Bundesamts für Kartographie und Geodäsie, 2009. 204 pp., ISBN 3-89888-918-6.

A. Finkelstein. Radiointerferometric Network "Quasar". *Science in Russia, No. 5*, pages 20–26, 2001.

A. Finkelstein, A. Ipatov, S. Smolentsev. Radio Astronomy Observatories Svetloe, Zelenchukskaya and Badary of VLBI Network "Quasar". In R. Vandenberg, K. D. Baver, editors, *IVS 2004 General Meeting Proc.*, pages 161–165. NASA/CP-2004-212255, 2004.

A. Finkelstein, A. Ipatov, S. Smolentsev. The Network "Quasar": 2008–2011. In A. Finkelstein and D. Behrend editors,*"Measuring the future", Proc. of the Fifth IVS General Meeting*, pages 39-46. St. Petersburg, "Nauka", 2008.

A. Finkelstein, E. Skurikhina, I. Surkis, A. Ipatov, I.Rahimov, S. Smolentsev. "Quasar" National Programs of EOP Determinations. In A. Finkelstein and D. Behrend editors, *"Measuring the future", Proc. of the Fifth IVS General Meeting*, pages 319-323. St. Petersburg, "Nauka", 2008.

A. Finkelstein, A. Salnikov, A. Ipatov, M. Kaidanovsky, I. Bezrukov, A. Mikhailov, I. Surkis, E. Skurikhina. E-VLBI Technology in VLBI Network "Quasar". *8th International e-VLBI Workshop Proc.* PoS(EXPReS09) 098, 2009.

A. Finkelstein, A. Ipatov, S. Smolentsev, V. Mardyshkin, L. Fedotov, I. Surkis, D. Ivanov, I. Gayazov. The New Generation Russian VLBI Network. In D. Behrend, K. D. Baver, editors, *6th IVS General Meeting Proc.*, pages 161–165. NASA/CP-2004-212255, 2010.

A. Finkelstein, A. Ipatov, M. Kaidanovsky, I. Bezrukov, A. Mikhailov, A. Salnikov, I. Surkis, E. Skurikhina. The "Quasar" Network Observations in e-VLBI Mode Within the Russian Domestic VLBI Programs. In D. Behrend, K. D. Baver, editors, *6th IVS General Meeting Proc.*, pages 148–152. NASA/CP-2004-212255, 2010.

I. Gayazov, E. Skurikhina. Improved velocities of the "Quasar" network stations. *This volume*, 2011.

L. Fedotov, D. Ivanov, A. Ipatov, I. Ipatova, A. Lavrov, M. Kosobokov, A. Mikhailov. Institute of Applied Astronomy Technology Development Center. In D. Behrend and K. Baver, editors, *International VLBI Service for Geodesy and Astrometry 2006 Annual Report*, pages 255 – 258, NASA/TP-2007-214151, 2007.

S. Kurdubov. Quasar software in IAA EOP service: Global Solution and Daily SINEX. In J. Böhm, A. Pany, and H. Schuh, editors, *Proceedings of the 18th Workshop Meeting on European VLBI for Geodesy and Astrometry*, volume 79 of *Geowissenschaftliche Mitteilungen, Schriftenreihe Vermessung und Geoinformation der TU Wien*, pages 79–82. TU Wien, 2007.

S. Kurdubov, E. Skurikhina. Antenna Axis Offset Estimation from VLBI. In D. Behrend, K. D. Baver, editors, *6th IVS General Meeting Proc.*, pages 247-250. NASA/CP-2004-212255, 2010.

Z. Malkin, E. Skurikhina. OCCAM/GROSS software for VLBI data processing for IAA EOP Service. *Communications of IAA, Num. 93*, 1996 (in Russian).

D. D.McCarthy and G. Petit. *IERS Conventions (2003)*. IERS Conventions (2003). Dennis D. McCarthy and Gérard Petit (eds.), International Earth Rotation and Reference Systems Service (IERS). *IERS Technical Note, No. 32*, Frankfurt am Main, Germany: Verlag des Bundesamtes für Kartographie und Geodäsie, ISBN 3-89888-884-3, 2004, 127 pp., 2004.

A. Melnikov, J. Gipson. Running SKED under Linux. In *Proceedings of the 17th Working Meeting on European VLBI for Geodesy and Astrometry*. INAF, Noto, Italy, pages 131–132, 2005.

A. Niell. Global mapping functions for the atmosphere delay at radio wavelengths. emphJournal of Geophysical Research, Vol. 111, Num. B2, pages 3227-3246, 1996.

L. Petrov and J.-P. Boy. Study of the atmospheric pressure loading signal in very long baseline interferometry observations. *Journal of Geophysical Research (Solid Earth)*, 109:3405–+, Mar. 2004. doi: 10.1029/2003JB002500.

E. Skurikhina, S. Kurdubov, V. Gubanov. IAA VLBI Analysis Center Report 2009. In D. Behrend and K. Baver, editors, *International VLBI Service for Geodesy and Astrometry 2009 Annual Report*, pages 239–242. NASA/TP-2010-215860, 2010.

S. Smolentsev, I. Rahimov. Svetloe Radio Astronomical Observatory. In D. Behrend and K. Baver, editors, *International VLBI Service for Geodesy and Astrometry 2003 Annual Report*, pages 87–89. NASA/TP-2004-212254, 2004.

S. Smolentsev, A. Dyakov. Zelenchukskaya Radio Astronomical Observatory. In D. Behrend and K. Baver, editors, *International VLBI Service for Geodesy and Astrometry 2005 Annual Report*, pages 154–157. NASA/TP-2006-214136, 2006.

S. Smolentsev, R. Sergeev. Badary Radio Astronomical Observator. In D. Behrend and K. Baver, editors, *International VLBI Service for Geodesy and Astrometry 2007 Annual Report*, pages 33–36. NASA/TP-2008-214162, 2008.

I. Surkis, A. Bogdanov, A. Melnikov, V. Shantyr, V. Zimovsky. IAA Correlator Center. In D. Behrend and K. Baver, editors, *International VLBI Service for Geodesy and Astrometry 2006 Annual Report*, pages 143–146, NASA/TP-2007-214151, 2007.

I. Surkis, A. Melnikov, V. Shantyr, V. Zimovsky. The IAA RAS Correlator First Results. In D. Behrend, K. D. Baver, editors, *6th IVS General Meeting Proc.*, pages 167-170. NASA/CP-2004-212255, 2010.

Current Status of Development of New VLBI Data Analysis Software

S. Bolotin, J. Gipson, D. Gordon and D. MacMillan

Abstract At the 2010 IVS GM in Hobart we proposed a design for our next generation VLBI data analysis software. In this paper we review the current status of this software and plans for future development. We also demonstrate the current capabilities of the software.

Keywords VLBI, data analysis, software

1 Introduction

Due to the increased number of VLBI observations and participated stations, implementation of new VLBI2010 technology will require a sophisticated approach to data analysis. The current CALC/SOLVE system for VLBI data preparation and analysis should be replaced with more flexible, power and user friendly software.

The first step in this direction was made in 2007 when the IVS Working Group on VLBI data structures (IVS WG4) was established. The results of the work of the IVS WG4 made it possible to start work on developing the new VLBI data analysis software. In August of 2009 the VLBI group at the NASA GSFC started this development.

The core requirements of the software and its general design and architecture overview were presented at the IVS General Meeting at Hobart (Tasmania) in February, 2010 (Bolotin et al., 2010). After discussion of the software design at the meeting, the whole architecture was reviewed and slight modifications were made. In March, 2010 the first lines of the source code were written.

The first executable that will replace a part of the current CALC/SOLVE system will be νSolve, an interactive part of the SOLVE system that is currently used in preliminary data analysis.

Sergei Bolotin, John Gipson, David Gordon and Daniel MacMillan
NVI, Inc./ NASA Goddard Space Flight Center, 8800 Greenbelt Road, Greenbelt, Maryland 20771, USA

In this article we will cover the current status of the software development process. Section 2 describes tools that are used in the development process. In Section 3 we provide an overview of the modular design of the software. The current functionality is described in Section 4. In Section 6 we outline our plans for the future.

2 Software development environment

The software is written in the *C++* programming language. It uses the *Qt* library for high level data abstraction, the system's *libc* library for low level system functions and the *libm* library for standard mathematical procedures.

The new VLBI data analysis software will be distributed as source codes. To make the software distribution portable we use the *autoconf*, *automake* and *libtool* packages. These packages are parts of *GNU Build System*. With this we can create a highly portable software distribution, adjust the distribution to local needs, and minimize end-user effort to compile the package.

As a text editor we chose the *Geany* software. It has the following advantages. *Geany* possesses basic integrated development environment (IDE) features: syntax highlighting, code folding, symbol name auto-completion, code navigation and build system. It depends on only a few external packages and is independent of distributives. It is also small, lightweight and fast. *Geany* is known to run under Linux, FreeBSD, NetBSD, OpenBSD, MacOS X, AIX v5.3, Solaris Express and Windows operating systems.

We are also using *Doxygen* software to generate a reference documentation from source tree. *Doxygen* is a documentation system for *C*, *C++* and many other programming languages. It can automatically generate reference documentation in different formats: HTML, man pages, LaTex, RTF, PDF, etc. The documentation is generated directly from the source code, which makes it consistent with the current source tree.

Currently, the VLBI data analysis software consists of two parts:

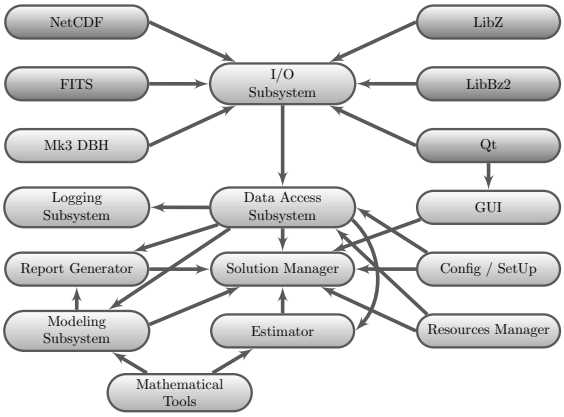

Fig. 1 Modular design of the new VLBI data analysis software

1. *Space Geodesy Library*, a library where data structures and algorithms are implemented (about 90% of total source code);
2. an executable *vSolve* – a driver that calls the library and organizes work with an end-user (about 10% of total source code).

3 Modules

To be stable and flexible, our system has a modular design. A module is a logical block of code that is loosely tied with other parts of the software.

The general modular structure of the software is presented on Fig. 1. Each arrow on the figure represents a dependency that provides information (data types, function calls, constants). Only the main dependencies are shown on the figure.

Several modules in the figure (*FITS*, *NetCDF*, *LibZ*, *LibBz2* and *Qt*) represent external libraries.

The sizes of the modules could vary. There are small blocks, like *Logging system* with a few hundred lines of source code and commentaries, and large modules, such as *Modeling Subsystem* with tens of thousands of source code lines. Not all modules currently are completed, and some modules will be realized later. Now, we will give an an overview of currently implemented modules.

Logging subsystem is a small module that implements the system logging functionality. The *Logging subsystem* is capable of receiving a message from other parts of the software, filter it by a level and a facility, display the filtered messages to a user and save it in a log file. This module is used by all other modules of the software.

A module that describes the mathematical data structures and related functions is *Mathematical Tools*. Currently it contains realizations of the following mathematical concepts: *Vector* and *Matrix*, the general classes of linear algebra, specialized objects (like *Symmetric Matrix* or *Upper Triangular Matrix*, to optimize calculations), and classes that describe coordinate transformations in 3-Dimensional space, like *Vector3D* and *Matrix3D*.

Geodetic data structures, their relationships and relevant procedures are implemented in the module *Modeling Subsystem*. The main purpose of this module is computation of theoretical values of observables (time delay and delay rate) and their corresponded partial derivatives. The module implements the following abstractions: *Epoch* of observation and *time interval*, identities and attributes of various objects (*radio sources*, *stations* and *baselines*), VLBI *observations* and auxiliary data. It calculates ionospheric corrections, zenith delay and mapping functions, and provides models for clock breaks. This module uses data structures and algorithms from *Mathematical Tools*.

The module *Estimator* is responsible for performing Least Squares Estimation. The core of this module is a class called *Estimator* that solves systems of equations and obtains estimated parameters. Also the module provides an interface to other parts of the software to communicate with the *Estimator*, feeding it data and retrieving solutions. That is made possible with the classes *Partial* and *Parameter*. The current realization implements estimation of unbiased, session-wide parameters. Later we will add global and stochastic parameters.

The module *I/O Subsystem* provides operations of input/output and supports various data formats. The module communicates with other modules which implement a particular format for data representation and provides a unified I/O interface to other parts of the software. Currently, only Mk3 database handling is implemented, which is realized in the module *Mk3 DBH*. This module allows one to read the content of a Mark-III DBH file into a temporary place in computer memory, get access to data and modify them, change format (add or delete a particular LCODE) and write modified data into a file in the Mark-III DBH format.

The module *Config/Setup* is a small module that describes models, system configuration and the parameter set up that should be applied in the analysis.

The module *Solution Manager* controls solution production. Depending on the configuration of the solution, it checks the available (O-C) and partials and, if necessary, calls proper procedures from the *Modeling Subsystem* to evaluate them. It asks the *Estimator* to create the solution and *Report Generator* to prepare the end user output. Finally, it provides obtained results to an end user. This module could be considered as a core of the software – it uses almost all other modules and realizes communication between different parts of the software.

The Graphical User Interface is implemented in *GUI* module. The module interacts with a user to visualize observations, solutions and auxiliary data. One part of the *GUI* module, the *Plotting Subsystem*, allows it to browse a wide spectrum of data. Also, it allows a user to modify the data. The *Plotting Subsystem* is universal and can be used in various applications. This module uses widgets from the *Qt* library.

4 Current Functionality

Currently, the software development process is in the intermediate stage and not all functions are realized. The following abilities are realized.

- *v*Solve can read VLBI observations in Mk3 DBH format, modify data and save modified information into a file on the disk. It assumes that the observations are multiband and automatically loads all bands of closest version number (if the files are available). There is no limitation on the number of bands.
- It can display various values that are stored in the files, evaluated on the fly or estimated in data analysis. Using the *Plotting Subsystem* a user can eliminate outliers, resolve ambiguities and edit clock break parameters interactively.
- The *v*Solve software has ability to compute ionospheric corrections from dual channel observations.
- The software is able to estimate the parameters of clock functions, zenith delays, stations positions and source coordinates. Also, it applies No-Net-Translate and No-Net-Rotation constraints specified by the user to stations and sources while estimating their coordinates.
- Automatic ambiguity resolution is implemented in the *v*Solve. It assumes that ambiguity spacing could vary from baseline to baseline.
- It can detect and take into account clock breaks. There are two approaches to dealing with clock breaks, manual and automatic.

5 Plans for Future

We expect that the first public release of *v*Solve will be made in the middle of 2011. To make it available, the following procedures need to be implemented in the software: 1) linear piecewise and stochastic estimation of parameters; 2) data reweighting; and 3) interaction with current CALC/SOLVE data structures.

References

S. Bolotin, J. M. Gipson and D. MacMillan. *Development of a New VLBI Data Analysis Software*. In D. Behrend, and K.D. Baver, editors, *IVS 2010 General Meeting Proceedings*, NASA CP 2010-215864, NASA GSFC, Maryland, pages 197–201. 2010.

VLBI analysis with c5++ - status quo and outlook

T. Hobiger, M. Sekido, T. Otsubo, T. Gotoh, T. Kubooka, H. Takiguchi, H. Takeuchi

Abstract Otsubo and Gotoh (2002) have developed an analysis software package based on Java named concerto version 4 (c4) which enabled the user to consistently process SLR, GPS and other satellite tracking data. Driven by the need to update the software and replace the existing Java code, VLBI was added as an additional module to this analysis package and renamed c5++. The software provides state-of-the-art modules for a variety of geodetic, mathematical and geophysical tasks that can be combined to a stand-alone VLBI application. Although many of these modules can be used for any of the space geodetic techniques, a couple of technique specific solutions (like relativity, antenna deformation, etc.) had to be coded exclusively for VLBI. It is outlined how the automated analysis procedure of the real-time UT1 experiments has been realized with c5++. Other fields of applications for this software will be shown as well.

Keywords Analysis software, UT1, Earth Rotation, Automation, Ambiguity Resolution

1 Introduction

An analysis software package based on Java and named concerto version 4 (c4, Otsubo and Gotoh, 2002) enabled the user to consistently process SLR, GPS and other satellite tracking data. The next version of this program package will also include VLBI as additional space-geodetic technique. As the software is currently being redesigned and completely re-written in C++, the requirements for VLBI data analysis could be taken into account. Moreover, combination of space-geodetic techniques was considered during the design phase.

Thomas Hobiger, Mamoru Sekido, Tadahiro Gotoh, Toshihiro Kubooka, and Hiroshi Takiguchi
National Institute of Information and Communications Technology, Tokyo, Japan

Toshimichi Otsubo
Hitotsubashi University, Tokyo, Japan

Hiroshi Takeuchi
Institute of Space and Astronautical Science / Japan Aerospace Exploration Agency, Sagamihara, Japan

2 Space-geodesy with c5++

Basically, c5++ provides the framework (figure 1) under which space-geodetic applications can be built. Thus, stand-alone technique specific applications can be developed or multi-technique solutions can be realized. Thereby consistent geophysical and

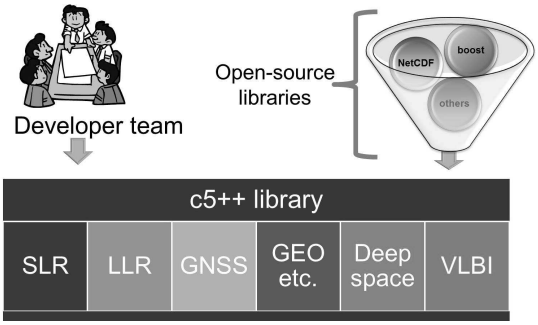

Fig. 1 Building space-geodetic analysis software for SLR, GNSS,VLBI or other applications by interfacing the c5++ libraries.

geodetic models, based on the IERS Conventions 2003, are applied to each technique, which enables the combination either on the observation level or on the normal-equation level. External libraries, which are available as open source packages, are utilized for data input/output as well as vector and matrix operations. c5++ has been successfully compiled and tested under Windows, Linux and Mac OS using 32-bit and 64-bit environments. Modules are commented within the code and information is extracted via Doxygen, which outputs on-line the documentation (in HTML) and/or an off-line reference manual.

2.1 VLBI with c5++

Based on the main classes of c5++ a dedicated VLBI analysis chain can be implemented with minimal efforts. Thereby, modules can be attached like building blocks and even dedicated/specialized VLBI software solutions can be realized, without in-depth knowledge of the specific classes. In order to fulfill the requirements of different applications the following observation formats are supported within c5++

- NGS
- NetCDF
- MK3
- Raw correlator (K5 format)

A Gauss-Markov type least-squares adjustment model has been implemented to estimate target and nuisance parameters from the observables. Moreover, as raw-correlator format can be interfaced directly an option for automated ambiguity resolution was implemented that enables unattended operation of low latency sessions as described in the next section.

2.2 Automated UT1 processing

Beside multi-baseline sessions, regular single baseline VLBI experiments are scheduled in order to provide estimates of UT1 for the international space community. As shown by Sekido et al. (2008) and Matsuzaka et al. (2008), the latency of these Intensive experiments could be improved tremendously and results could be made available within less than an hour if e-VLBI and automated processing routines were applied. If the whole processing pipeline works well, results can be obtained even within minutes after the last scan has been recorded, which is highly appreciated by the users community as discussed in Luzum and Nothnagel (2010). Based on the experience gained over the last two years, the automated processing chain has been improved and the analysis software used until now could be replaced by c5++. Since the correlator output format can be read directly with c5++, no intermediate interface is necessary. Moreover, ambiguity resolution and ionosphere correction can be done within the framework of c5++. Not only the target parameter, i.e. UT1, will be estimated with c5++ but also databases for the VLBI community can be created with that software. Figure 2 summarizes the data flow of the automated UT1 VLBI processing as implemented with c5++. It is also possible to input a-priori delay models to the correlator in order to achieve highest possible consistency between all the data processing stages. First tests with c5++ were carried out in the middle of 2010 and since then the Geospatial Information Authority of Japan (GSI) has been using c5++ for routine operation of the Intensive and Ultra-Rapid sessions. Results are currently submitted to the IERS to check their consistency in order to be included for UT1 predictions. A long-term comparison of INT2 based on automatically processed UT1 estimates w.r.t. results from CALC/SOLVE (Baver, 2010) has been summarized by Hobiger et al. (2010).

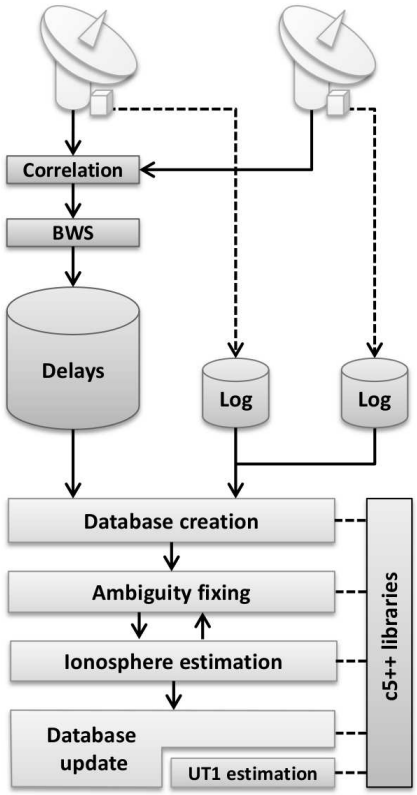

Fig. 2 Data flow in automated VLBI processing (abbreviations: band width synthesis (BWS), station log information (Log); after Hobiger et al., 2010).

2.3 Ambiguity resolution

Due to the fact that current geodetic VLBI systems do not observe broadband delays, but rather sample the covered observing band by several narrow channels, the obtained delays contain an unknown number of integer ambiguities. Thereby, the ambiguity spacing is equal to the reciprocal of the unit spacing of all channels belonging to one observing band. Ambiguity estimation in VLBI is an iterative process that involves the computation of a simplified geodetic solution, shifting of the ambiguities according to the residuals obtained and an update of the resulting ionosphere correction, which depends on the selection of the X/S band ambiguities. Usually, the ambiguities are assigned to the ionosphere free linear combination, which has the drawback that the ambiguity spacing becomes a non-integer number. The c5++ implementation of the ambiguity estimation algorithm does not follow this procedure, but introduces X- and S- band delays as independent observations. Thus, the integer nature of the ambiguities does not change, but the ambiguity shifting based on the residual must be split according to the spacing of each band. Shifting the ambiguities and simplified geodetic adjustment is iterated as long as the residuals do no exceed the corresponding ambiguity spacings. This approach will work properly only

if the ionosphere delay does not exceed the ambiguity spacing defined by the X/S band set-up. Figure 3 shows an example of a successful ambiguity resolution based on INT2 data.

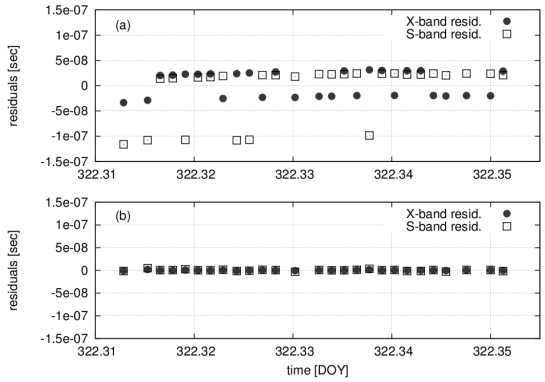

Fig. 3 Residuals after first (a) and sixth (b) iteration of the ambiguity resolution algorithm for an INT2 experiment in 2007. All residuals in the sixth, i.e. last iteration (figure (b) are much smaller than the corresponding ambiguity spacing (i.e. 50 ns at X-band and 125 ns at S-band) and thus it can be assumed that all ambiguities are detected properly (after Hobiger et al., 2010).

2.4 Software validation

To make sure that all modules of c5++ are properly debugged and consistent with state-of-the-art geophysical models, an effort was made to validate the software against other VLBI packages. Therefore c5++ derived results were submitted to the "Delay and Partial Derivatives Comparison Campaign" (DeDeCC, Plank et al., 2010) in order to determine how the theoretical models of this software package differ from those of other analysis packages. DeDeCC requires the contributors to submit their theoretical delays for a single baseline, i.e. Westford - Wettzell, using a given observing schedule and Earth rotation parameters. The obtained differences (see figure 4) are well within one picosecond (or 0.3 mm) which is much below the measurement accuracy of existing and planned VLBI systems. Thus, based on this external validation, it can be concluded that c5++ is able to provide theoretical VLBI delays with up-to-date geophysical models which are consistent with other analysis packages. Following this evaluation, UT1 estimation was implemented in c5++ knowing that no significant model biases from the software can propagate into the estimates.

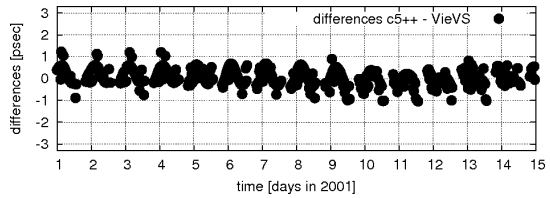

Fig. 4 Differences of total theoretical delay for the baseline Westford-Wettzell between c5++ and VieVS as obtained within DeDeCC (after Hobiger et al., 2010).

3 Outlook

The upcoming changes of c5++ will affect (geo)physical and mathematical models as well as increase the number of supported space-geodetic techniques.

3.1 Model updates

New and updated models belonging to the IERS Conventions 2010 have been implemented and are currently being tested for consistency purposes. Once the technique specific analysis coordinator has decided to switch over to this implementation, c5++ should be ready to support the new conventions. Moreover, novel (geo)physical models are being developed and tested under the framework of c5++. In addition work has been done to implement a Kalman filter as an optional estimation method beside the currently supported least-squares adjustment. Since several of the models, especially those related to orbit modeling, can become computational intensive it will be necessary to make use of parallel computing to overcome this drawback.

3.2 Adding space geodetic techniques and other applications to c5++

Currently SLR and VLBI are being supported by c5++. GNSS is expected to be included as a third space-geodetic technique within this year, i.e. 2011. Since all space-geodetic techniques can utilize the same physical and geophysical models from c5++, consistent combination across the techniques will be realized. Thereby, results can be either combined on the normal-equation level or on the observation level, in accordance with the goals of the Global Geodetic Observing System (GGOS). Moreover, novel applications like space-craft tracking are being developed, whereas orbit calculations based on multi-technique observations (GNSS, SLR and VLBI) are expected to provide an utmost accurate 3D trajectory of the satellite.
Moreover, as NICT is carrying out a feasibility study to utilize VLBI for time and frequency transfer purposes the software will be extended to support this application as well.

Acknowledgments

The Geospatial Information Authority of Japan (GSI) is acknowledged for carrying out the INT2 and ultra-rapid sessions and providing observational data. The authors are very grateful to Ms. Lucia Plank for enabling us to validate our software within the IVS software comparison campaign, as well as the IERS and the IVS are thanked for providing products and data.

References

K. Baver Mark V VLBI analysis software Calc/Solve *http://gemini.gsfc.nasa.gov/solve/*, 2010.

T. Hobiger, T. Otsubo, M. Sekido, T. Gotoh, T. Kubooka, and H. Takiguchi Fully automated VLBI analysis with c5++ for ultra-rapid determination of UT1 *Earth Planets Space*, 62(12), 933-937, 2010. doi: 10.5047/eps.2010.11.008

B. Luzum and A. Nothnagel Improved UT1 predictions through low-latency VLBI observations *Journal of Geodesy*, 84(6), 399–402, 2010. doi: 10.1007/s00190-010-0372-8

S. Matsuzaka, H. Shigematsu, S. Kurihara, M. Machida, K. Kokado, and D. Tanimoto Ultra Rapid UT1 Experiments with e-VLBI *Proceedings of the 5th IVS General Meeting*, 68–71, 2008.

T. Otsubo and T. Gotoh. SLR-based TRF Contributing to the ITRF2000 project *IVS 2002 General Meeting Proceedings*, 300–303, 2002.

L. Plank, J. Böhm and H. Schuh Comparison Campaign of VLBI Data Analysis Software - First Results *Proceedings of the 6th IVS General Meeting*, in print, 2010.

M. Sekido, H. Takiguchi, Y. Koyama, T. Kondo, R. Haas, J. Wagner, J. Ritakari, S. Kurihara, and K. Kokado Ultra-rapid UT1 measurement by e-VLBI *Earth Planets Space*, 60, 865–870, 2008.

Status and future plans for the Vienna VLBI Software VieVS

T. Nilsson, J. Böhm, S. Böhm, M. Madzak, V. Nafisi, L. Plank, H. Spicakova, J. Sun, C. Tierno Ros, H. Schuh

Abstract The Vienna VLBI Software (VieVS) is a new geodetic Very Long Baseline Interferometry (VLBI) data analysis software which has been developed at the Institute of Geodesy and Geophysics, Vienna University of Technology, since 2008. This paper presents the software, its latest developments, and the planned future developments. A few results obtained with VieVS are also presented, as well as a brief description of how the software can be used for automated VLBI data analysis.

Keywords VLBI, geodetic software, Matlab

1 VieVS overview

In order to be able to cope with the future requirements of Very Long Baseline Interferometry (VLBI) data analysis, the VLBI group at the Institute of Geodesy and Geophysics (IGG), Vienna University of Technology, began to develop a new VLBI data analysis software, called VieVS (Vienna VLBI Software) (Böhm et al., 2011), in 2008. The software has now reached a mature state and it has an increasing number of users around the world. VieVS is written completely in Matlab. This has the advantage that it works on all operating systems which are able to run Matlab (Windows, Linux, Mac OS). Furthermore, it is easy to use and the source code can easily be modified if needed. VieVS needs Matlab versions 7.6 (R2008a) or later. A Graphical User Interface (GUI) for VieVS has been developed which makes the software easy to use even for people who are not VLBI experts.

A flowchart of the different parts of VieVS is shown in Fig. 1. The main parts of VieVS are:

VIE_INIT In this part the VLBI observations are read in. Presently the software can read data in NGS-format. In the future it will also support the new VLBI data format proposed by IVS Working Group 4 (Gipson, 2010), once the definition of the format is completed.

VIE_MOD Here the theoretical delays are calculated, as well as the partial derivatives of the delays w.r.t. the unknown parameters (station coordinates, zenith wet delays, Earth Orientation Parameters (EOP), etc.). These calculations are done following the IERS Conventions (Petit and Luzum, 2010) and the IVS Analysis Conventions such as the thermal expansion of radio telescopes (Nothnagel, 2009).

VIE_LSM The unknown parameters are estimated using the classical least-squares method. All parameters are estimated as piecewise linear offsets at integer hours. For more details on the estimation procedure, see Teke et al. (2009) and Teke (2011). The results (and the normal equation matrices) can be saved as Matlab structure arrays, as well as in SINEX format and other text formats. The following parameters can be estimated in the analysis of a single session: station clocks, zenith tropospheric delays, horizontal tropospheric gradients, EOP, station coordinates, and the coordinates of selected radio sources.

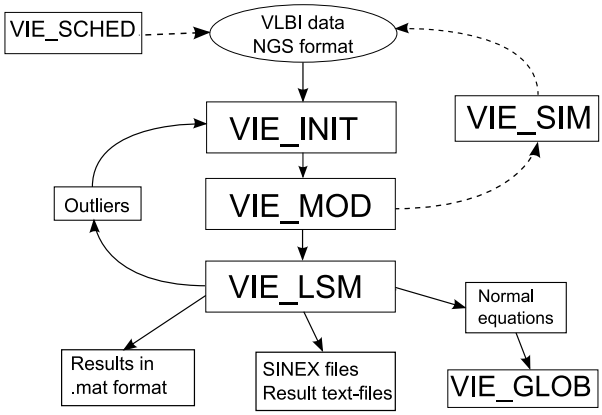

Fig. 1 Structure of VieVS.

Apart from these main parts, there are three additional modules connected to VieVS:

VIE_SCHED A scheduling software. For more details, see Sun et al. (2011).

T. Nilsson, J. Böhm, S. Böhm, M. Madzak, V. Nafisi, L. Plank, H. Spicakova, J. Sun, C. Tierno Ros, and H. Schuh
Institute of Geodesy and Geophysics, E128/1, Vienna University of Technology, Gußhausstraße 27-29, A-1040 Vienna, Austria
tobias.nilsson@tuwien.ac.at

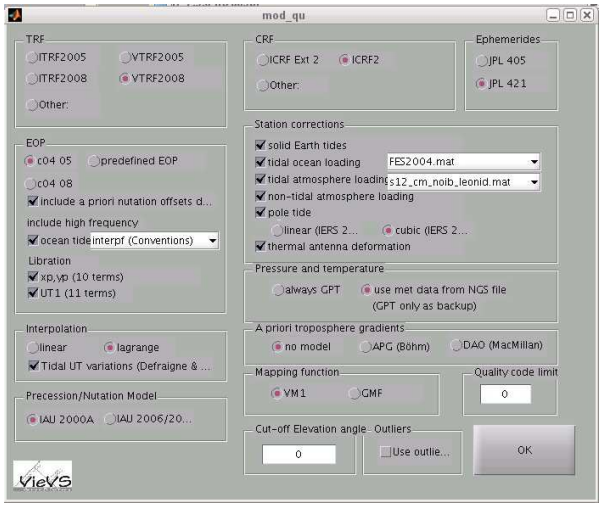

Fig. 2 Part of the VieVS Graphical User Interface. This part is for selecting the models to be used in VIE_INIT and VIE_MOD.

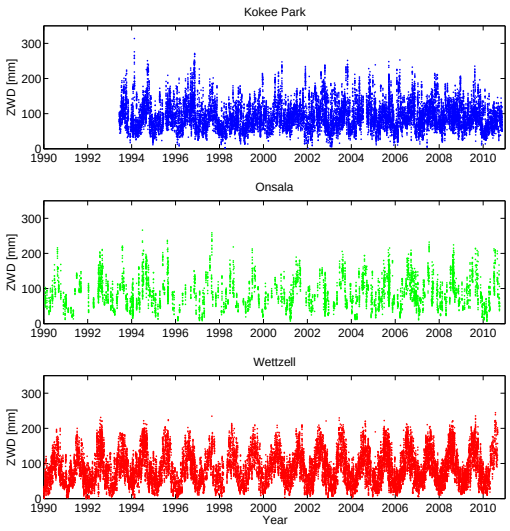

Fig. 3 Time series of zenith wet delays 1990–2010 estimated by VieVS for three VLBI stations.

VIE_SIM Simulation tool that can be used to create simulated VLBI observations. The simulated delays will be the theoretical delays as calculated by VIE_MOD plus simulated errors due to the wet troposphere (simulated using the method presented by Nilsson and Haas (2010)), clocks (simulated as a sum of a random walk process and an integrated random walk process), and observation noise (simulated as white noise). The simulated delays are saved as an ordinary VLBI observation file in NGS format. It can then be analysed by VieVS or by any other VLBI analysis software.

VIE_GLOB Global solution combining the normal equations of several single sessions in order to estimate e.g. a Terrestial Reference Frame (TRF) and/or a Celestial Reference Frame (CRF). For more details, see Spicakova et al. (2011).

The setup of the parameterisation and models to be used in the different parts of VieVS can easily be done using the VieVS GUI, VIE_SETUP. A part of the GUI is shown in Fig. 2.

Tests have been performed to see if VieVS is working on the free Matlab counterpart GNU Octave (`http://www.octave.org/`). The main problem with running VieVS under Octave is that the GUI is not working since Octave currently does not have any GUI support. It is in principle possible to run VieVS without the GUI, although the setup of the processing is then more complicated. Except from the GUI, the tests showed that it is possible to run VieVS on Octave. However, VieVS is slower under Octave than under Matlab. As an example, analysing the session R1412 with Matlab takes about 47 s using standard setup on a 3 GHz dual core, 32 bit, Linux PC. Analysing the same session with Octave using the same computer and setup takes about 7 minutes. The results obtained with the two softwares are in principle identical; there are some minor differences ($<10^{-6}$ cm) likely to be of numerical causes.

2 Results obtained with VieVS

In this section two examples of results obtained with VieVS are presented.

Figure 3 shows time series of zenith wet delays (ZWD) for three VLBI stations: Kokee Park, Onsala, and Wettzell. These time series were obtained by analysing all 24 hour VLBI sessions from the time period 1990 to 2010 with VieVS. Long series of ZWD are interesting e.g. for climate studies because the ZWD is approximately proportional to the integrated water vapour content above the stations, and water vapour is an important greenhouse gas which is closely related to temperature. Calculating linear trends in the ZWD from these time series we find -0.9 mm/decade for Kokee Park, 3.8 mm/decade for Onsala, and 5.0 mm/decade for Wettzell.

VieVS has been used to estimate the displacements of the VLBI station Tsukuba caused by the magnitude 9.0 Earthquake on March 11, 2011. Figure 4 shows the time series of the estimated position of Tsukuba in the period February to May, 2011. As comparison the position of the GPS station in Tsukuba, TSKB, is plotted; this time series was obtained from the IGS (International GNSS Service) weekly solution (Dow et al., 2009). The main displacement (70 cm) is towards the East direction. There are also small movements in the North (1 cm) and vertical (-8 cm) directions. There is a good agreement with the GPS results.

3 Automated data analysis

At IGG an automated data analysis of new VLBI sessions with VieVS has been set up. Every night the VieVS server at IGG

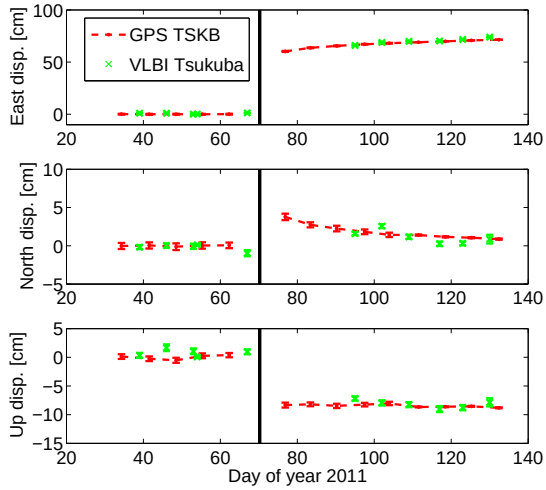

Fig. 4 The displacement of Tsukuba by the Earthquake on March 11, 2011, estimated by VLBI and by GPS. Black line denotes the epoch of the Earthquake.

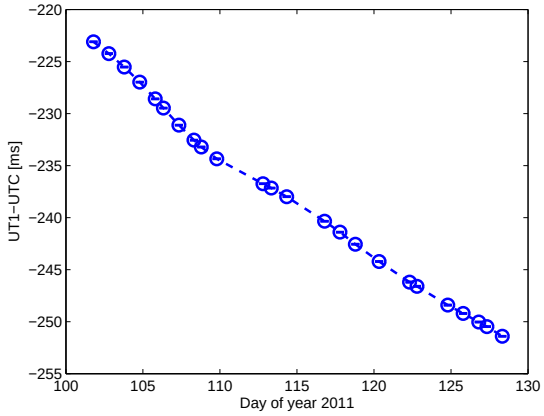

Fig. 5 UT1-UTC estimated from the automated analysis of the Intensives in the period 11 April–8 May, 2011.

checks if there are any new VLBI data files available at the IVS server, and if so these are downloaded. Also other files needed for VLBI data analysis are automatically downloaded, such as a priori EOP (IERS C04 and IERS Bulletin A), Vienna mapping functions (Boehm et al., 2006), and atmospheric loading corrections (Petrov and Boy, 2004). The data are then automatically analysed.

For 24 hour sessions only a simple analysis is made where clocks and tropospheric parameters are estimated while the station and source coordinates as well as the EOP are fixed to their a priori values. The main purpose of this analysis is to detect outliers. After the analysis is finished, a basic report is compiled and sent to a responsible analyst in the VLBI group at IGG. This analyst should then determine if the session is good or if there are any problems that need to be fixed, e.g. clock breaks.

For the 1 hour Intensives a normal data processing is performed in order to estimate Universal Time (DUT1=UT1-UTC). The estimated DUT1 values are saved in a file, and a plot of DUT1 for the last month is produced and put on the VieVS website (`http://vievs.hg.tuwien.ac.at`). An example is shown in Fig. 5.

4 Planned future developments

The major planned future developments of VieVS include:

Group delay ambiguity resolution: Currently VieVS has not the possibility to resolve the group delay ambiguities, however this feature will be added. Then we will get the results from new sessions faster since there is normally a delay of up to one day between the release of the first version of the VLBI database from the correlator until a version of the database with ambiguities resolved is available. A long-term aim is to be able to solve for phase delay ambiguities, which will be needed for VLBI2010 (Petrachenko et al., 2009) data analysis.

Ionospheric corrections: In addition to ambiguity resolution we will also cover other earlier steps in the VLBI analysis chain, like the calculation of ionospheric corrections. Furthermore, we will add the possibility to use ionospheric delays from external sources, e.g. calculated from GNSS ionospheric TEC (Total Electron Content) maps (Tierno Ros et al., 2011).

External tropospheric delays: The possibility of using external tropospheric delays in VieVS is currently being implemented. These could for example be observed by external instruments such as water vapour radiometers, or obtained by ray-tracing through numerical weather prediction models.

Spacecraft tracking: We will add the possibility to analyse VLBI observations of artificial satellites and space probes. For further details about this work, see Plank et al. (2011).

Kalman filter solution: As an alternative to the classical least-squares solution, a Kalman filter solution will be implemented. Some parameters, like the clocks and the tropospheric delays, have stochastic variations which cannot be completely described by piece-wise linear functions. In a Kalman filter it is possible to model the variations in these parameters better. Furthermore, a Kalman filter is ideal for real-time data analysis.

5 Concluding remarks

VieVS is freely available to registered users. For more information on the software and how to obtain it, see the VieVS website: `http://vievs.hg.tuwien.ac.at`.

Acknowledgements We would like to thank the International VLBI Service for Geodesy and Astrometry (IVS) (Schlüter and Behrend, 2007) for providing the VLBI data. Tobias Nilsson is grateful to the Deutsche Forschungsgemeinschaft (DFG) for supporting his work (project SCHU 1103/3-2), Hana Spicaova to Mondi Austria Privatstiftung for financal support during her PhD study, and Vahab Nafisi, Jing Sun, and Claudia Tierno Ros to the Austrian Science Fund (FWF) for financing their projects (P20902, P21049, and P22203, respectively).

References

J. Böhm, B. Werl, and H. Schuh (2006), Troposphere mapping functions for gps and very long baseline interferometry from European centre for medium-range weather forecasts operational analysis data, *J. Geophys. Res.*, *111*, B02,406, doi: 10.1029/2005JB003629.

J. Böhm, S. Böhm, T. Nilsson, A. Pany, L. Plank, H. Spicakova, K. Teke, and H. Schuh (2011), The new Vienna VLBI software, in *IAG Scientific Assembly 2009*, edited by S. Kenyon, M. C. Pacino, and U. Marti, no. 136 in International Association of Geodesy Symposia, Springer, Buenos Aires, Argentina, in press.

J. M. Dow, R. E. Neilan, and C. Rizos (2009), The international GNSS service in a changing landscape of global navigation satellite systems, *J. Geodesy*, *83*, 191–198, doi: 10.1007/s00190-008-0300-3.

J. Gipson, (2010), IVS working group 4: VLBI data structures, in *Proceedings of IVS 2010 General Meeting: VLBI2010: From Vision to Reality*, edited by D. Behrend and K. D. Baver, NASA/CP-2010-215864, pp. 187–191.

T. Nilsson, and R. Haas (2010), Impact of atmospheric turbulence on geodetic very long baseline interferometry, *J. Geophys. Res.*, *115*, B03,407, doi:10.1029/2009JB006579.

A. Nothnagel, (2009), Conventions on thermal expansion modelling of radio telescopes for geodetic and astrometric VLBI, *J. Geodesy*, *83*, 787–792, doi:10.1007/s00190-008-0284-z.

G. Petit, and B. Luzum (Eds.) (2010), *IERS Conventions (2010)*, IERS Technical Note 36, Verlag des Bundesamts für Kartographie und Geodäsie, Frankfurt am Main, Germany.

B. Petrachenko, A. Niell, D. Behrend, B. Corey, J. Böhm, P. Charlot, A. Collioud, J. Gipson, R. Haas, T. Hobiger, Y. Koyama, D. MacMillan, Z. Malkin, T. Nilsson, A. Pany, G. Tuccari, A. Whitney, and J. Wresnik (2009), Design aspects of the VLBI2010 system, in *International VLBI Service for Geodesy and Astrometry 2008 Annual Report*, edited by D. Behrend and K. Baver, NASA/TP-2009-214183, NASA Technical Publications.

L. Petrov, and J.-P. Boy (2004), Study of the atmospheric pressure loading signal in VLBI observations, *J. Geophys. Res.*, *109*, B03,405, doi:10.1029/2003JB002500.

L. Plank, J. Böhm, and H. Schuh (2011), First steps of processing VLBI data of space probes with VieVS, in *Proceedings 20th European VLBI for Geodesy and Astrometry (EVGA) Working Meeting*, Bonn, Germany, this issue.

W. Schlüter, and D. Behrend (2007), The International VLBI Service for Geodesy and Astrometry (IVS): current capabilities and future prospects, *J. Geodesy*, *81*(6-8), 379–387, doi:10.1007/s00190-006-0131-z.

H. Spicakova, L. Plank, T. Nilsson, J. Böhm, and H. Schuh (2011), Terrestrial reference frame solution with the Vienna VLBI software VieVS and implication of tropospheric gradient estimation, in *Proceedings 20th European VLBI for Geodesy and Astrometry (EVGA) Working Meeting*, Bonn, Germany, this issue.

J. Sun, A. Pany, T. Nilsson, J. Böhm, and H. Schuh (2011), Status and future plans for the VieVS scheduling package, in *Proceedings 20th European VLBI for Geodesy and Astrometry (EVGA) Working Meeting*, Bonn, Germany, this issue.

K. Teke, (2011), Sub-daily parameter estimation in VLBI data analysis, Ph.D. thesis, Vienna University of Technology, Vienna, Austria.

K. Teke, J. Boehm, H. Spicakova, A. Pany, L. Plank, H. Schuh, and E. Tanir (2009), Piecewise linear offsets for VLBI parameter estimation, in *Proceedings 19th European VLBI for Geodesy and Astrometry (EVGA) Working Meeting*, pp. 63–67, Bordeaux, France.

C. Tierno Ros, J. Böhm, and H. Schuh (2011), Use of GNSS-derived TEC maps for VLBI observations, in *Proceedings 20th European VLBI for Geodesy and Astrometry (EVGA) Working Meeting*, Bonn, Germany, this issue.

Evaluation of Combined Sub-daily UT1 Estimates from GPS and VLBI Observations

T. Artz, A. Nothnagel, P. Steigenberger and S. Tesmer

Abstract Hourly estimates of UT1 were determined in a combination procedure of Very Long Baseline Interferometry (VLBI) and Global Positioning System (GPS) observations based on homogeneous normal equation (NEQ) systems. The combination sustains the strengths of both techniques with the short period variations mainly originating from the GPS observations while VLBI delivers the long term information. It is shown that the resulting hourly resolved UT1 time series is improved by the combination. Furthermore, the impact of different VLBI session types is evaluated by UT1 and length of day (LOD) comparisons. The noise of the combined UT1 results decreases the more VLBI sessions are used, in contrast, the LOD consistency with geophysical fluids slightly degrades. Finally, an empirical model for sub-daily variations of the Earth Rotation Parameters was determined based on transformations of the given NEQ systems. Using this model for the estimation of the time series clearly reduces the remaining sub-daily UT1 variations.

Keywords UT1, Combination, VLBI, GPS

1 Introduction

Measurements of the Earth orientation parameters (EOPs) are usually done by employing space geodetic techniques such as the Global Positioning System (GPS) or Very Long Baseline Interferometry (VLBI). However, each technique has its own strengths and weaknesses in measuring the EOPs. For instance, VLBI is the only technique which is able to determine all components of the Earth's orientation simultaneously. However, the VLBI-derived polar motion (PM) does not have the accuracy which can be provided by GPS observations, because VLBI uses smaller observing networks and a much smaller number of observations. When using GPS measurements, only the time derivatives of UT1 can be determined unambiguously as a consequence of the one to one correlation between the satellite orbits and UT1 (Rothacher et al., 1999). Thus, estimating UT1 from GPS observations leads to random offsets and drifts w.r.t. VLBI-derived parameters during a time span of five years. To overcome these peculiarities, combination efforts have been undertaken.

So far, the combination had been predominantely used for EOPs with a daily resolution. Concerning the combination of sub-daily resolved EOPs, Thaller et al. (2007) performed a robust combination of GPS and VLBI normal equation (NEQ) systems for the time span of the Continuous VLBI Campaign 2002. In addition, Steigenberger (2009) described the effect of combining two empirical tidal EOP models based on GPS and VLBI EOP time series.

Within this paper, a combination approach was applied which is similar to the one performed by Thaller et al. (2007). The goal of this combination was to determine improved sub-daily UT1 variations. On the one hand, combined long term UT1 time series with an hourly resolution were derived. On the other hand, a combined empirical EOP model containing tidal components with diurnal and semi-diurnal terms was estimated. The data used in this paper were GPS and VLBI NEQ systems taken from the project GGOS-D (Rothacher et al., 2010). One of the aims of GGOS-D was the homogeneous modeling and parameterization among the different techniques leading to highly homogeneous and consistent contributions of the different techniques in the form of NEQ systems. Thus, an outstanding basis for combination efforts is given.

2 Solution Procedure

From GGOS-D, NEQ systems are available for the time-span 1994.0 – 2007.0 for both techniques. These NEQ systems contain the observations of one day in the case of GPS and one session for VLBI. For these NEQ systems, special technique-specific analysis options were applied:

Thomas Artz, Axel Nothnagel and Sarah Tesmer
Rheinische Friedrich-Wilhelms Universität Bonn, IGG, Nußallee 17, D-53115 Bonn, Germany

Peter Steigenberger
Technische Universität München, IAPG, D-80333 München, Arcisstraße 21, Germany

- for VLBI, weak stabilizing constraints were imposed on parameters set-up as continuous piece-wise linear functions (CPWLF)
- for GPS, the geocenter was fixed to zero and standard constraints were applied for the satellite orbits (e.g., Steigenberger 2009)

Furthermore, the a priori station positions were transformed and fixed to ITRF2008 (Altamimi et al., 2011). Likewise, the positions of the radio sources were fixed to their ICRF2 (IERS, 2009) positions. Unstable sources, for which the assumption of being representable by a constant position over time did not hold, were estimated session-wise. The PM and UT1 parameters were parameterized by CPWLF with epochs exactly at full hours. Except for the EOPs, all remaining parameters were treated independently for each technique as well as for each day or session.

For the combination, first, two-weekly NEQ systems were built for GPS and VLBI independently. Parameters that were present in the two NEQ systems were stacked to one single parameter. For both two-week NEQ systems (GPS and VLBI), the nutation representation was transformed to one offset and one rate for the respective 14 days as it can be assumed that nutation corrections change significantly only over a longer period of time. Finally, these two NEQ systems were added to form a combined one. To account for a different variance level that might be present due to the discordance in the number of observations, the NEQ systems were scaled to have identical traces:

$$\mathbf{N}_{\mathrm{COMBI}} = \frac{tr(\mathbf{N}_{\mathrm{GPS}})+tr(\mathbf{N}_{\mathrm{VLBI}})}{4\cdot tr(\mathbf{N}_{\mathrm{GPS}})}\mathbf{N}_{\mathrm{GPS}} + \frac{tr(\mathbf{N}_{\mathrm{GPS}})+tr(\mathbf{N}_{\mathrm{VLBI}})}{4\cdot tr(\mathbf{N}_{\mathrm{VLBI}})}\mathbf{N}_{\mathrm{VLBI}} \quad (1)$$

Here, $\mathbf{N}_{\mathrm{GPS}}$ represents a GPS NEQ matrix and $\mathbf{N}_{\mathrm{VLBI}}$ as well as $\mathbf{N}_{\mathrm{COMBI}}$ denote the VLBI and combined NEQ matrices, respectively. The same scaling was done for the right hand side of the NEQ system.

In Sec. 5, an combined empirical sub-daily EOP model is used. This model was estimated from the same set of NEQ systems, applying the same combination procedure as for the time series solution. For this purpose, the combined two-week NEQ systems were transformed to the model representation as described by Artz et al. (2011b). For the UT1 part of the model (u_j^c and u_j^s), the functional dependence between the old and the new parameters is:

$$UT1(t) = \sum_{j=1}^{n} u_j^c \cos\psi_j(t) + u_j^s \sin\psi_j(t) \quad (2)$$

In this equation, t denotes the epoch of every originally parameterized hourly UT1 and n is the number of tidal terms in the model. The symbols ψ_j are the corresponding angular arguments for any j^{th} tide. The new NEQ system can be derived by

$$\widetilde{\mathbf{N}} = \mathbf{B}^T\cdot\mathbf{N}\cdot\mathbf{B}, \qquad \widetilde{\mathbf{n}} = \mathbf{B}^T\cdot\mathbf{n} \quad (3)$$

where the matrix $\mathbf{B}$ consists of the partial derivatives of the EOPs w.r.t. the new parameters.

All combined (and optionally transformed) two-week NEQ systems were then added to a global NEQ system for the entire time-span. Solving this NEQ system leads to the simultaneous estimation of nutation corrections linear over two-week intervals and a time series of hourly resolved PM and UT1 or a tidal sub-daily EOP model.

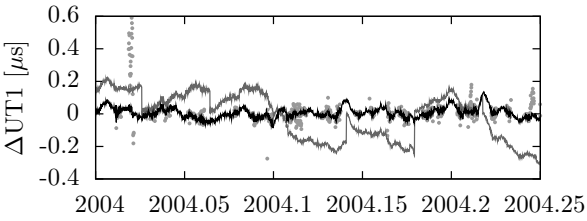

Fig. 1 Excerpt of the UT1 differences to IERS 05C04 for the individual solutions (light gray dots: VLBI, dark gray: GPS) and the combined solution (black).

Within this investigation, only the combined UT1 time series is analyzed. Furthermore, this time series was generated only for the time span 2002.0 – 2007.0 to allow a meaningful analysis of the impact of different VLBI observing types especially of the rapid turnaround R1 and R4 sessions (Schlüter and Behrend, 2007) that started in 2002. However, the sub-daily model presented in Sec. 5 was estimated from the entire time span (1994.0 – 2007.0).

3 UT1 Comparisons

As described above, several combined UT1 time series were estimated for a time span of five years. These solutions differ in the VLBI-contribution where all possible VLBI session types, only R1 and R4 sessions, or the one hour long Intensive sessions were used. Furthermore, technique independent time series were estimated. In Fig. 1, three time series with a duration of twelve weeks are displayed. For the UT1 comparisons, the GPS solution was fixed to the a priori values at the beginning of each two-week interval to overcome the random walk behavior of the GPS-only solution. However, this leads to jumps at the boundaries of the fortnightly time spans. In Fig. 1 it can clearly be seen that the absolute information of the combined time series is defined by VLBI while GPS delivers the relative one.

In Tab. 1 the root mean squared (RMS) differences of the UT1 estimates to the IERS 05C04 series (Bizouard and Gambis, 2009) are listed. IERS 05C04 is a combined EOP series with a daily resolution, which was linearly interpolated. A better agreement to this series implies a higher quality of the derived time series, as the roughness of the hourly estimates is reduced. Obviously, a significant reduction of the noise within the time series is achieved by the combination procedure. The combined series is less noisy the more VLBI sessions are used, however, using only VLBI Intensive sessions for the combination already leads to an improved UT1 series.

Individual		Combination					
GPS	VLBI	all	24h	R1&R4	R1	R4	Int.
106	54	33	34	34	44	40	43

Table 1 RMS differences [μs] between to the IERS 05C04 series. Several combined solutions were performed, with: all VLBI sessions, only 24 h VLBI sessions or R1, R4 or Intensives alone.

GPS		COMB				
uncnstr.	cnstr.	all	24h	R1	R4	Int.
56	83	59	58	56	58	73

Table 2 RMS residuals [μs] of the adjusted LOD - (AAM + OAM) differences.

4 Length of Day Comparisons

The time derivative of UT1 is called length of day (LOD). Due to the differential characteristic, LOD can be determined from GPS observations without hypothesis as well. Thus, LOD time series were generated from the UT1 time series analyzed in Sec. 3, to evaluate the consistency with oceanic and atmospheric angular momentum (OAM, AAM) series. In contrast to the UT1 comparisons presented, this represents an independent validation of the hourly resolved time series. The AAM values were taken from the NCEP Reanalysis[1] (Salstein and Rosen, 1997), where the inverted barometer assumption was applied, and the OAM values were taken from the ECCO_kf066b_6hr model[2] (Gross, 2009).

For generating the LOD time series, the UT1 time series was first reduced by zonal tides. For this purpose, the elastic body and equilibrium ocean tide model of Yoder et al. (1981), the in-phase and out-of-phase components of the Wahr and Bergen (1986) inelastic body tide model and the dynamic ocean tide model "A" of Kantha et al. (1998) were used. From these time series, the LOD time series was derived by subtracting two subsequent reduced UT1 values and dividing this difference with the time difference of 1/24 d. For the comparison with the AAM and OAM data, the LOD time series was smoothed to a temporal resolution of 6 h by calculating the mean values of the corresponding 12 h intervals around a specific epoch.

For this comparisons, the time series LOD - (AAM + OAM) was built and a quadratic polynomial as well as an annual, and a semi-annual signal were fitted. The RMS residuals for two GPS-only solutions and several combination approaches are listed in Tab. 2. The VLBI RMS residuals are not shown as a consequence of the non-continuity of the VLBI-only time series. One GPS-only solution was estimated without any UT1 constraints, thus, this series is not usable for UT1 analysis. The second series is the GPS-only series which was analyzed as described in Sec. 3, where every 14th day one offset was fixed to the IERS 05C04 series. This series represents more reliable UT1 results, but, the derived LOD series possesses jumps. This can clearly be seen in the RMS differences, which are largest for the constrained GPS-only series. In contrast, the unconstrained GPS-only series shows the best agreement with the AAM/OAM series. When only R1 sessions are used in the combination, the agreement to AAM/OAM is equal to using GPS-only. Adding other VLBI session types leads to a small degradation of at most 5% when using all VLBI data. However, this reduced consistency to the geophysical data is not supposed to be forced by the amount of used VLBI data rather than to be sticked to the VLBI observing networks. When using only VLBI Intensive sessions for the combination, the RMS residuals get worse. However, the agreement between this type of combination and the AAM/OAM series is still better compared with the constrained GPS-only solution. For all types of combined solutions it is remarkable, that the noise of the UT1 time series is improved (see Sec. 3) while the agreement with AAM/OAM time series is only slightly reduced, at least if 24 h VLBI sessions are used.

5 Impact of an empirical sub-daily EOP model

As described in Sec. 2, an empirical sub-daily EOP model can be estimated as well from the same set of NEQ systems. A comprehensive analysis of the determined combined model can be found in Artz et al. (2011a). This combined model generally appears as a weighted mean of the individual models, where the impact of GPS is higher than the VLBI one. The main fact concerning the combined sub-daily EOP model is an improved agreement with the IERS2003 model (Tab. 8.2 and 8.3 of McCarthy and Petit 2004) compared to technique specific models. However, a partial degradation is present due to GPS-specific errors which lead, e.g., to bad Sun-synchronous terms.

Here, this model was used as a priori model to investigate the impact on the time series of hourly resolved UT1. As presented in the previous sections, UT1 and LOD comparisons were performed to demonstrate the impact of the new sub-daily EOP model. For this combination, all VLBI sessions were used. The overall impact of the new model is small, as the RMS differences are improved by less than 0.5% for LOD and UT1. The reason can be seen in the fact that the remaining variations with periods above one day are significantly larger than those with one day and below. Thus, the RMS difference is not significantly changed if the consistency of the daily and sub-daily part of the time series is improved. This improvement is, nevertheless, visible in the frequency domain. The residual UT1 amplitude spectrum of a least squares B-spline fit to the UT1 time series is shown in Fig. 5. The reduction of diurnal and semi-diurnal variations due to the use of the combined empirical sub-daily EOP model demonstrates the higher consistency. A comparable improvement can be seen for the diurnal periods of the LOD amplitude spectrum (not shown here). For the semi-diurnal part almost no change is visible as

[1] ftp.aer.com/pub/anon_collaborations/sba/aamf.ncep.reanalysis.1948.2009

[2] ftp://euler.jpl.nasa.gov/sbo/oam_global/ECCO_kf066b_6hr.chi

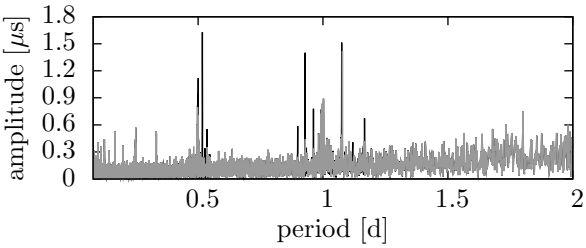

Fig. 2 UT1 amplitude spectrum where the IERS2003 (black) and the empirical combined (gray) sub-daily EOP model were used.

the 6 h spacing of the LOD time series does not provide reliable results of the 12 h period range.

6 Conclusions

Within this investigation, a combination procedure of GPS and VLBI observations was applied on the NEQ-level to estimate sub-daily UT1 parameters. It is shown, that this combination procedure crosswise compensates the geometric instabilities of both techniques. Thus, relative variations were primarily defined by the GPS observations while the VLBI observations defined the absolute information.

Compared to the interpolated IERS 05C04 series, hourly resolved UT1 was significantly improved. Furthermore, the noise of this time series decreased the more VLBI sessions were used within the combination. The worst combined result is based only on Intensive sessions, however, the RMS differences of this solution are still better compared to the VLBI-only solution.

In comparison to an OAM/AAM time series, even the GPS-only LOD solution showed a good consistency due to the high relative precision of GPS. By adding VLBI observations in the combination procedure, no improvement could be achieved. In contrast, a minute degradation of the consistency to the geophysical fluids occurred when all VLBI sessions were used. The reason can be seen in the network geometries and, thus, in a worse sensitivity of the VLBI observations to the determination of LOD.

Finally, a combined sub-daily EOP model was estimated from the same set of NEQ systems. This model represents an improvement in comparison to the technique independent solutions. Using this model for the generation of hourly resolved UT1 time series, decreased harmonic variations in the diurnal and semi-diurnal band significantly.

Acknowledgements This work has partially been funded by the Geotechnologien Progamm of the German Bundesministerium für Forschung und Technologien (FKZ03F0425D). Furthermore, we want to thank the Department of Theoretical Geodesy of the IGG-Bonn for providing computation capabilities.

References

Z. Altamimi, X. Collilieux, and L. Métivier. ITRF2008: an improved solution of the international terrestrial reference frame. *J Geod*, 2011. doi: 10.1007/s00190-011-0444-4. online first.

T. Artz, L. Bernhard, A. Nothnagel, P. Steigenberger, and S. Tesmer. A Rigorously Combined Sub-daily Earth Rotation Model from GPS and VLBI Observations. submitted to *J Geod* in February 2011, 2011a.

T. Artz, S. Böckmann, and A. Nothnagel. Assessment of Periodic Sub-diurnal Earth Orientation Parameter Variations at Tidal Frequencies via Transformation of VLBI Normal Equation Systems. *J Geod*, 2011b. doi: 10.1007/s00190-011-0457-z. online first.

C. Bizouard and D. Gambis. The combined solution C04 for Earth orientation parameters consistent with International Terrestrial Reference Frame 2005. In H. Drewes (ed.), *Geodetic Reference Frames, International Association of Geodesy Symposia*, Vol. 134, 265 – 270. Springer Berlin Heidelberg, 2009. doi: 10.1007/978-3-642-00860-3_41.

A. Fey, D. Gordon, and C. S. Jacobs. The second realization of the international celestial reference frame by very long baseline interferometry. IERS Technical Note 35, Verlag des Bundesamtes für Kartographie und Geodäsie, Frankfurt am Main, 2009.

R. Gross. An improved empirical model for the effect of long-period ocean tides on polar motion. *J Geod*, 83(7):635 – 644, 2009. doi: 10.1007/s00190-008-0277-y.

L. H. Kantha, J. S. Stewart, and S. D. Desai. Long-period lunar fortnightly and monthly ocean tides. *J Geophys Res*, 103 (C6):12639 – 12648, 1998. doi: 10.1029/98JC00888.

D. McCarthy and G. Petit. IERS Conventions 2003. IERS Technical Note 32, Verlag des Bundesamtes für Kartographie und Geodäsie, Frankfurt am Main, 2004.

M. Rothacher, G. Beutler, T. A. Herring, and R. Weber. Estimation of nutation using the Global Positioning System. *J Geophys Res*, 104(B3):4835 – 4860, 1999. doi: 10.1029/1998JB900078.

M. Rothacher, H. Drewes, A. Nothnagel, and B. Richter. Integration of Space Geodetic Techniques as a Basis for the Global Geodetic-Geophysical Observing System (GGOS-D): An Overview. In F. Flechtner, T. Gruber, A. Güntner, M. Mandea, M. Rothacher, T. Schöne, and J. Wickert (eds.), *System Earth via Geodetic-Geophysical Space Techniques*, 529 – 537. Springer Berlin Heidelberg, 2010. doi: 10.1007/978-3-642-10228-8_43.

D. Salstein and D. Rosen. Global momentum and energy signals from reanalysis systems. In *7th Conference on Climate Variations, 02 – 07 February 1997, Long Beach*, 344 – 348. American Met. Soc., Boston, Massachusetts, 1997.

W. Schlüter and D. Behrend. The International VLBI Service for Geodesy and Astrometry (IVS): current capabilities and future prospects. *J Geod*, 81(6):379 – 387, 2007. doi: 10.1007/s00190-006-0131-z.

P. Steigenberger. *Reprocessing of a global GPS network*. PhD thesis, Technische Universität München, 2009. Deutsche

Geodätische Kommission Bayer. Akad. Wiss. München, Reihe C, Vol. 640.

D. Thaller, M. Krügel, M. Rothacher, V. Tesmer, R. Schmid, and D. Angermann. Combined Earth orientation parameters based on homogeneous and continuous VLBI and GPS data. *J Geod*, 81(6–8):529 – 541, 2007. doi: 10.1007/s00190-006-0115-z.

J. Wahr and Z. Bergen. The effects of mantle and anelasticity on nutations, earth tides, and tidal variations in rotation rate. *Geophys J*, 87(2):633 – 668, 1986. doi: 10.1111/j.1365-246X.1986.tb06642.x.

C. F. Yoder, J. G. Williams, and M. E. Parke. Tidal variations of earth rotation. *J Geophys Res*, 86(B2):881 – 891, 1981. doi: 10.1029/JB086iB02p00881.

VLBI Analysis at BKG

G. Engelhardt, V. Thorandt, D. Ullrich

Abstract The VLBI group of the Federal Agency for Cartography and Geodesy (BKG) in Leipzig is part of the jointly operated IVS Analysis Center of BKG and the Institute for Geodesy and Geoinformation of the University of Bonn (IGGB). BKG is responsible for regular submissions of time series of Earth Orientation Parameters (EOP) and tropospheric parameters, the generation of daily SINEX (Solution INdependent EXchange format) files for 24-hours sessions and Intensive VLBI sessions, quarterly updated solutions to produce terrestrial and celestial reference frame realizations (TRF, CRF), and generating Intensive schedules (mainly Tsukuba-Wettzell). The data processing steps are explained and also some problems in the procedure of data analysis are pointed out.

Keywords VLBI, Data Analysis

1 General Information on Data Analysis

At BKG the latest version of the data analysis software system Calc/Solve, release 2010.05.21 (GSFC, 2010), has been used for VLBI data processing. It is running on a Linux operating system.

As in the previous releases the Vienna Mapping Function (VMF1) has been implemented in a separate Solve version. This modified version is used for all work of data analysis. The VMF1 data are downloaded daily from the server of the Technical University Vienna.

Additionally an independent technological software environment for the Calc/Solve software is available for linking up the Data Center management with the pre- and post-interactive part of the EOP series production and to monitor all Analysis and Data Center activities.

Gerald Engelhardt, Volkmar Thorandt, Dieter Ullrich
Bundesamt für Kartographie und Geodäsie (BKG), Karl-Rothe-Str. 10-14, D-04105 Leipzig, Germany

2 Processing of Correlator Output

One important task in data analysis at BKG is the generation of calibrated databases for the sessions correlated at the MPIfR/BKG Mark 5 Astro/Geo Correlator at Bonn (e.g. EURO, OHIG, T2) and submitting them to the IVS Data Centers.

3 Scheduling

BKG is responsible for scheduling the INT2 Intensive sessions, which are observed on the baselines TSUKUBA-WETTZELL, KASHIMA-WETTZELL, KASHIMA-WESTFORD, TSUKUBA-WESTFORD by using the program system SKED [1] developed by John Gipson (NVI, Inc/NASA Goddard Spaceflight Center).

4 IVS EOP Time Series bkg00013

The solution for generating the EOP series is based on a global solution mode with common estimation of all parameter types. The EOP are one part of the arc-parameters, i.e. estimations for each experiment session. The global parameter adjustments refer to the entire data set, e.g. station positions and velocities or source positions.

Each new VLBI session issued from correlator as database version 1 is processed and after that a new global solution with 24-hours sessions since 1984 is computed. Then the EOP time series bkg00013 is extracted.

Some topics of solution bkg00013 are:

- number of sessions more than 4100,
- datum definition is realized by applying no-net-rotation and no-net-translation conditions for 26 selected station positions and velocities with respect to VTRF2008a and no-net-rotation condition for 295 defining sources with respect to ICRF2 (Ma et al., 2009),

[1] ftp://gemini.gsfc.nasa.gov/pub/sked

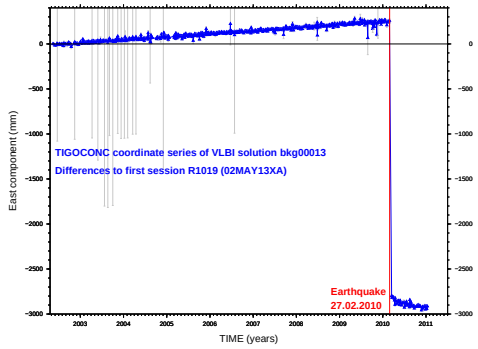

Fig. 1 Station position time series of TIGOCONC (Chile) in east component

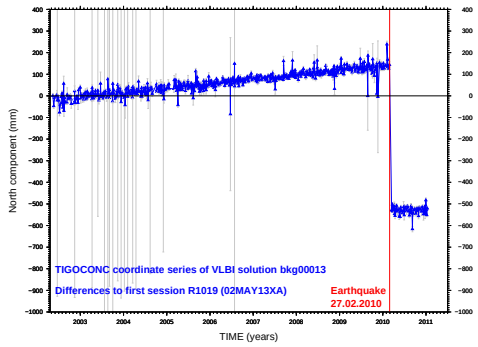

Fig. 2 Station position time series of TIGOCONC (Chile) in north component

- global parameter types station coordinates and velocities, radio source positions,
- local parameter types in each session, e.g. EOP, tropospheric parameters (zenith wet delays at 1 hour intervals), local station coordinates for AIRA (Japan), CHICHI10 (Japan), CTVASTJ (Canada), DSS13 (USA), HOBART12 (Australia), PT-REYES (USA), SEST (Chile), SINTOTU3 (Japan), TIGOCONC (Chile), WIDE85-3 (USA), VERAISGK (Japan), VERAMZSW (Japan), and YEBES40M (Spain).

Because of a big earthquake in the region of the VLBI station TIGOCONC in Chile with station displacements of about 3 meters the modeling of this station was changed from globally estimated station coordinates to locally estimated coordinates in all respective sessions. The time series of the station coordinates can be seen in Figures 1, 4, and 3. You can see big offsets in north and east component but also different rates after the earthquake.

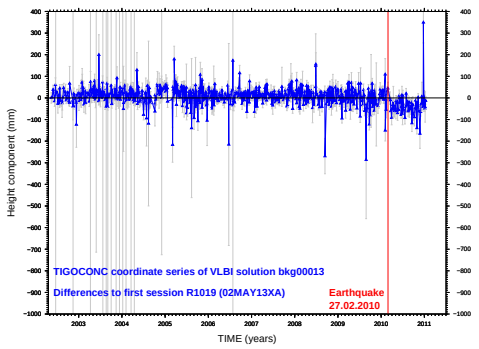

Fig. 3 Station position time series of TIGOCONC (Chile) in height component

5 IVS UT1 Time Series bkgint09

The UT1-UTC Intensive time series is based on independent session solutions. The Intensive sessions include mainly observations of the baselines KOKEE-WETTZELL or TSUKUBA-WETTZELL, but also of the networks KOKEE-SVETLOE-WETTZELL and NYALES20-TSUKUBA-WETTZELL. Series bkgint09 is generated with fixed TRF (VTRF2008a) and fixed ICRF2. The estimated parameter types are only UT1-TAI, station clock, and zenith troposphere. The UT1 Intensive sessions are processed from 1999.01.01 on.

6 Quarterly Updated TRF and CRF Solutions for Submission to IVS

Every year quarterly updated solutions for the IVS products TRF and CRF are computed. There are no differences in the solution strategy compared to the continuously computed EOP time series bkg00013. The results of the radio source positions are submitted to IVS in IERS format. The TRF solution is available in SINEX format, version 2.1 and includes station coordinates, velocities (Figures 4 and 5), and radio source coordinates together with the covariance matrix, information about constraints, and the decomposed normal matrix and vector.

7 Tropospheric Parameters

The VLBI group of BKG continues regular submissions of long time series of tropospheric parameters to the IVS (wet and total zenith delays, horizontal gradients) for all available VLBI sessions since 1984. The tropospheric parameters are extracted from the standard global solution for the EOP time series bkg00013 and transformed into SINEX format.

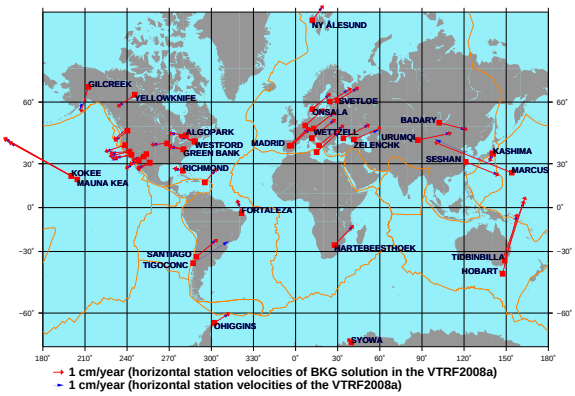

Fig. 4 Horizontal station velocities derived from VLBI data 1984.0 to 2010.9

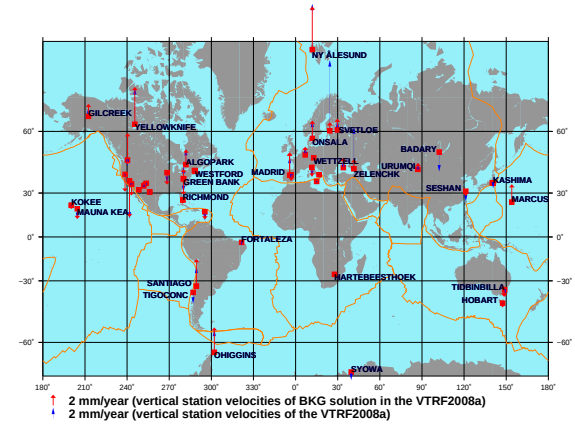

Fig. 5 Vertical station velocities derived from VLBI data 1984.0 to 2010.9

8 Daily SINEX Files

In addition to the global solutions daily SINEX files for all available 24-hours sessions as base solutions for the IVS time series of baseline lengths and for combination techniques are submitted. Independent session solutions are computed for the parameter types station coordinates, radio source coordinates, and EOP including the X,Y-nutation parameters. The a priori datum for TRF is defined by the VTRF2008a, and ICRF2 is used for the a priori CRF information.

9 SINEX Files for Intensive Sessions

IVS SINEX files for Intensive sessions are created and submitted to IVS. The parameter types are station coordinates, pole coordinates and their rates, and UT1-TAI with rate. Only the normal equations stored in the SINEX files are important for further combination with other space geodetic techniques.

10 Problems with Logfile Formats

Before running the extracting program XLOG for calibration data different errors in the logfiles have to be fixed. Some logfile errors are:

- wrong filename of the logfile (i.e. euro87ro.log instead of euro876a.log),
- wrong station name in the header (i.e. NyAlesun instead of NYALES20),
- superfluous header records,
- records outside of observation time span,
- implausible meteorological data,
- empty records,
- wrong time fields,
- format error in meteorological data field,
- wrong cable sign.

11 Outlook

If no or unrealistic meteorological data are available in a logfile of a station presently standard values for the meteorological data are used. In future more realistic values included in the VMF1 data files for 0, 6, 12, and 18 UT should be used. Furthermore the a priori EOP values will be included in the solution file for Intensive sessions.

References

GSFC, NASA (2010): Release of Mark 5 VLBI Analysis Software Calc/Solve from May 21, 2010 (Web reference: http://gemini.gsfc.nasa.gov/solve).

Chopo Ma et al (2009): IERS Technical Note No. 35: The Second Realization of the International Celestial Reference Frame by Very Long Baseline Interferometry; Presented on behalf of the IERS/IVS Working Group, edited by Alan L. Fey, David Gordon, Christopher S. Jacobs.

Radio frequency interference at QUASAR Network Observatories

Gennadii Ilin

Keywords Radio frequency interference

QUASAR radio telescopes RT-32 are equipped with high sensitive cryogenic receivers. Main frequency parameters of the receivers are presented in table 1 (Finkelstein et al., 2008).

Wavelength, cm	Frequency band	Bandwidth, GHz	LO freq. GHz	IF Bandwidth, MHz
18–21	L	1.38–1.72	1.26	130–470
13	S	2.15–2.50	2.02	130–480
6	C	4.60–5.10	4.50	100–600
3.5	X	8.18–9.08	8.08	100–1000
1.35	K	22.02–22.52	21.92	100-600

Table 1 Main parameters of the QUASAR receivers

RFI is one of the factors reducing sensitivity of the radio telescopes.

It is well known, that all RFI affected on sensitivity of radio telescope can be divided by origin into two types: external and internal origin. The structure of most powerful RFI presented on Fig. 1.

Most of external RFI's are closely connected with human activities around the place of the QUASAR network observatories location. QUASAR radio telescopes were built in places remote from major settlements, but now this situation changed, and resulted in increasing RFI level especially in L and S-band.

For example, Svetloe observatory radio telescope was built in a valley, about 100 km far from St. Petersburg, surrounded by hills, served as additional shield against RFI. Now these hills serve as a popular ski resorts. As a result we have powerful source of RFI from mobile phone base station transmitters installed near (2.5 km away) radio telescope as infrastructure element of the resort.

The same mobile service recently appeared near the radio telescope of Badary and Zelenchukskaya observatory.

Practically RFI level in S- band is determined by radiation of the mobile phone base stations built near QUASAR observatories (look at frequency parameters of mobile communication links presented in Tab.2 and receiver parameters in Tab. 1). Signals of these communication links can affect on IF directly (GSM-900) or generate RFI in L-band (GSM-1800) and S-band (UMTS) at the LNA's inputs.

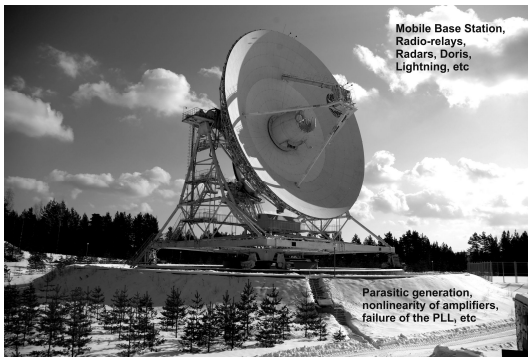

Fig. 1 Structure of RFI: external and internal origin

Transmission(up-down)	GSM-900	GSM-1800	UMTS
From HS to BS, MHz	890–915	1710–1785	1885–2025
From BS to HS, Hz	935–960	1805–1880	2110–2200

Table 2 Frequency parameters of mobile communications used in Russian Federation: GSM 900/1800, UMTS, (BS — Base Station, HS — handsets)

For estimation of RFI parameters, receiver intermediate frequency (IF) signals are controlled to measure RFI spectral characteristics: frequency, bandwidth, level (Fig. 2). Spectrum analyzer GSP 827 is used for this purpose. Spectral measurements of the receivers IF all QUASAR network observatories. Spectrograms obtained from these measurements fill RFI database.

Using this technique we can register only relatively strong, stationary narrow band RFI.

Radio telescope also detects the presence of impulses of various origins, which do not plot on the spectrograms. Different types of narrow band RFI registered at QUASAR network observatories listed in Tab. 3–5.

All problems concerned electromagnetic compatibility (EMC) of radio equipment are regulated by the State Radio Fre-

Gennadii Ilin
Institute of Applied Astronomy of RAS, 10, Kutuzova emb., 191187 Saint Petersburg, Russia

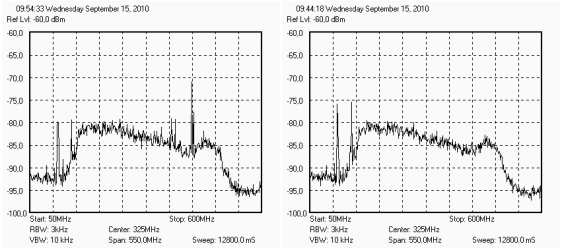

Fig. 2 Svetloe RT-32 reflector direction: $Az = 250°$, $El = 20°$, on the resort — left and in opposite direction — right. Main RFI: $f_1 = 114.9$ MHz, $U = -80.1$ dBm; $f_2 = 147.9$ MHz, $U = -80.9$ dBm; $f_3 = 433.9$ MHz $U = -72.7$ dBm

RFI	Source	Input frequency, MHz	Level, over system noise, dBm	Notes
L-band	Radionavigati-onal satellite (GLONASS L1, GPS L1)	1598.0625–1608.75 1575.42	25–30	Maximum value
	DORIS	401.25	10	
	MOBILE SATELLITE (S–E)	1525–1560	5–7	
S-band	Mobile (UMTS)	2134–2139	15	Observed in three azimuths
C-band	DORIS	401.25	10	
X-band	Clear			

Table 3 RFI type and some characteristics. Badary observatory

quency Center and its local territory departments. Most intensive EMC regulation process concerned mobile operators. Otherwise S-band can't be used for VLBI observations, as it follows from Fig. 3 — intermodulation products bring down the entire S-band receiver.

Fig. 2 demonstrates "compatible" UMTS BS signals (in low frequency part of spectrograms). Additional High Pass filter was used at the output of the LNA to attenuate UMTS signal. At the left plot MW — oven signal (f3) can be seen. Intermods are produced UMTS BS (RT-32 reflector is directed to BS).

For more accurate estimation of RFI affect on VLBI observations, spectrograms obtained by IAA correlator can be used (Surkis et al., 2008). This technique was applied to estimate IF spectrum distortion caused by DORIS signal for the S and X-band receivers. DORIS 401.25 MHz signal penetrate directly in to the IF band of all receiver, probably via the long cable wrap. Significantly attenuated DORIS signals do not overload amplifiers and can be registered in IF band with the help of low resolution GSP 827 spectrum analyzer (Il'in et al., 2010). For the experiment with correlator 16 MHz video convertors were tuned on frequency 401.25 MHz.

Result of the data processing presented on Fig. 4: components of DORIS 401.25 MHz signal spectrum filled practically all 16MHz band of the video convertor. Thus we can conclude that DORIS transmitter has to be torn-off if 401 MHz signal is within bandwidth of signal registered, as it take place in some EVN observation sessions. Another possibility is to filter 401 MHz signal in some way or protect IF equipment from this signal.

Otherwise, in standard IVS sessions this low frequency signal doesn't impact on observations because this signal is

RFI	Source	Input frequency, MHz	Level, over system noise, dBm	Notes
L-band	Radionavigati-onal satellite (GLONASS L1, GPS L1)	1598.0625–1608.75 1575.42	25–30	Maximum value
	Fixed service	1532	25	Azimuth depended
S-band	Mobile (UMTS)	2134–2139	1–5	high-pass filter added
	Fixed service, MW oven	2400–2500	15	Direction on resort, 2 km distance
C-band	Spurious harmonics PLL	4800, 4900	30	Will be removed after PLL upgrade
X-band	Clear			

Table 4 Svetloe observatory

RFI	Source	Input frequency, MHz	Level, over system noise, dBm	Notes
L-band	Radionavigati-onal satellite (GLONASS L1, GPS L1)	1598.0625–1608.75 1575.42	25–30	Maximum value
	Fixed service	1532	25	Azimuth depended
S-band	Mobile (UMTS)	2134-2139	20	Maximum value, no intermods
	Fixed service	2400-2500	10	
C-band	Spurious PLL harmonics	4800, 5100		Will be removed after PLL upgrade
X-band	L-Clear, R:Spurious PLL harmonics			Will be removed after PLL upgrade
K-band	Clear			

Table 5 Zelenchukskaya observatory

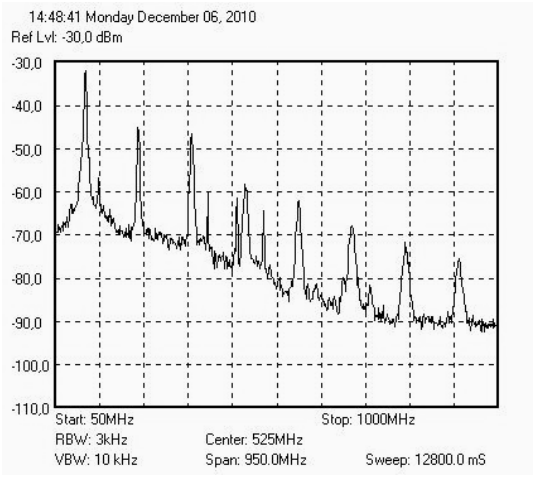

Fig. 3 Spectrogram of Svetloe S-band receiver IF signal

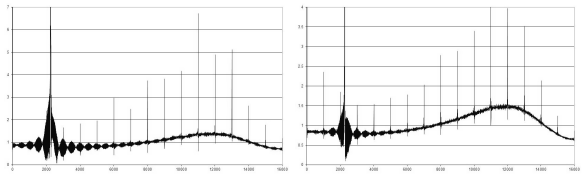

Fig. 4 Spectrum of DORIS 401.25 MHz (Badary observatory) and phase calibration signal generator on measured at 16 MHz bandwidth video convertor with frequency resolution 2 KHz. S-band receiver — left and X-band — right. Signal processed by IAA correlator

out of video convertors band. DORIS high frequency signal (2036 MHz) must be carefully filtered too when a wide-band receiver is used (Il'in et al., 2010).

RFI and QUASAR network in the future

Now we can conclude that S-band receiver in QUASAR observatories substantially affected by RFI at the 2.15 GHz frequency range.

At the end of 2010 Russian mobile operators announced intentions to obtain frequency range 2.5–2.7 GHz for wide band communication service. This can create problems for VLBI2010 operating in low frequency range in the future. RFI — free frequency range will be narrower than expected or low frequency end of this range will be moved to 3 GHz.

The impact of RFI on VLBI2010 discussed in many papers (Ambrosini, 2009; Tuccari, 2009; Petrachenko, 2010) and it is not the end. Problems are more complicated than it can be seen at first sight. One of them — how to combine demands of the receiver low noise, wide frequency range and it high dynamic range to ensure high linearity amplification of the signals and RFI received. Receiver design concept suggested in (Finkelstein et al., 2010) looks more preferable, because of using several relatively narrow band amplifiers operating in RFI low level region. (On the other hand, such a solution provides limited possibilities for changing or tuning the frequency range of the receivers).

For the beginning, it is necessary to determine RFI free bands taking into account very specific situation in observatories and RFI dynamic for a long period interval. These measurements planned to begin at the near future.

References

R. Ambrosini, A spectral management view about VLBI2010: the CRAF experience, From: VLBI2010 Workshop on Future Radio Frequencies and Feeds (FRFF). Wettzell, Germany, March 18–21, 2009.

A. Finkelstein, A. Ipatov, S. Smolentsev, The Network "Quasar": 2008–2011, Proc. 5th IVS General Meeting, p. 39–46, 2008.

A. Finkelstein et al., The New Generation Russian VLBI Network. IVS 2010 General Meeting Proceedings, p. 106–110.

G. Il'in et al.: About the Compatibility of DORIS and VLBI Observations. IVS 2010 General Meeting Proceedings, p. 180–183.

B. Petrachenko, The Impact of Radio Frequency Interference (RFI) on VLBI2010, IVS 2010 General Meeting. Proceedings, p. 434–438.

I. Surkis, V. Zimovsky, A. Melnikov, V. Shantyr, A. Fateev, A. Bogdanov, The IAA RAS 6-station VLBI Correlator. In: Measuring The Future, Proceedings of the Fifth General Meeting of the International VLBI Service for Geodesy and Astrometry. Saint Petersburg, p. 124–128. Nauka, 2008.

G. Tuccari, Interference at a VLBI station: Analysis and mitigation. http://www.fs.wettzell.de/veranstaltungen/vlbi/frff2009/Part6/Interference%20at%20a%20VLBI%20Station.pdf

VLBI mapping of the globular cluster M15 - A pulsar proper motion analysis

F. Kirsten, W. H. T. Vlemmings, M. Kramer, P. Freire, H. J. v. Langevelde

Abstract Here we present preliminary results of our on-going multi epoch global VLBI-campaign observing the globular cluster M15. The aim of the project is to measure the proper motion of the known pulsars in M15, and we search for so far undetected compact radio sources. The observations also offer the potential to provide further observational evidence for the existence of the central intermediate mass black hole (IMBH). The observations are conducted at a central frequency of 1.6 GHz with the longest baselines spanning 7500 km. From the first three of a total of six observation epochs we measure the proper motion of the strongest millisecond pulsars 15A and 15C and of the low mass X-ray binary (LMXB) AC211 to be $\mu_\alpha^{15A} = -2.88 \pm 0.04$ mas/yr, $\mu_\delta^{15A} = -2.1 \pm 0.2$ mas/yr; $\mu_\alpha^{15C} = -2.74 \pm 0.15$ mas/yr, $\mu_\delta^{15C} = -26 \pm 20$ mas/yr; and $\mu_\alpha^{AC211} = -3.90 \pm 0.06$, $\mu_\delta^{AC211} = 4.1 \pm 1.1$ mas/yr, respectively. The positions and directions of motion of the pulsars agree with the ones as extrapolated from the values determined by Jacoby et al. (2006) within 1σ. At our noise level of about $3-7$ μJy we have found no evidence of a central IMBH at 1.6 GHz.

Keywords Pulsars, Astrometry, VLBI

1 Introduction

The globular cluster M15 (NGC 7078) is a massive cluster at a distance of 10.3 ± 0.4 kpc. Its radial stellar density profile shows a steep cusp towards the central arcsecond possibly indicating an advanced stage of core collapse. Dynamical models based on line-of-sight velocities and proper motions infer a mass of 3400 solar masses within the central 1 arcsecond ($\sim$ 10 000 AU). The nature of this mass concentration is unknown, but it may be composed of neutron stars (Baumgardt et al., 2003) or an intermediate-mass black hole (Gerssen et al., 2002). M15 is host to at least eight millisecond pulsars (MSPs, Sun et al., 2002, estimate that M15 could host up to about 300 pulsars) and two bright low mass X-ray binaries (LMXRBs). The proximity of the majority of the pulsars to the cluster center makes M15 a promising target to study cluster dynamics. The most common way to study pulsar motion is through pulse timing. For millisecond (recycled) pulsars (MSPs) that have stable enough rotation periods of a few milliseconds this technique reaches submilliarcsecond accuracy by measuring the pulse time of arrival (TOA). When modeling the observed TOAs a large number of parameters need to be considered which sometimes are covariant with the proper motion. Very long baseline interferometry (VLBI) measurements, however, provide a model-independent, direct observation of pulsar motion and, thereby, can lift the degeneracy between, e.g., the orbital motion of a pulsar in a binary system and its overall motion on the sky. Thus, in the case of M15 our data contributes to the timing solution for the double neutron star system 15C. Furthermore, high sensitivity VLBI campaigns with a large field-of-view (FOV) have the potential to find compact radio sources that were missed by previous FFT-based pulsar searches because of tight orbits, eclipses or shrouding by dense clouds caused by the stellar wind of the companion star.

In the following I will describe our observing strategy and the data reduction process. Afterwards, I will elaborate on our preliminary results and the problems we encountered.

2 Observations and data reduction

The three observations presented here were conducted on 11 November 2009, 7 March 2010, and 5 June 2010. These three and all following observations are correlated at the EVN-MkIV correlator at JIVE (Schilizzi et al., 2001). The telescopes included are Jodrell Bank, Onsala, Westerbork, Effelsberg, Noto, Medicina, Toruń, the GBT, and Arecibo. The choice of telescopes and of the central observing frequency of 1.6 GHz was driven by the need for high angular resolution and high sensi-

F. Kirsten and W.H.T. Vlemmings
Rheinische Friedrich-Wilhelms Universität Bonn, AIfA, Auf dem Hügel 71, D-53121 Bonn, Germany
M. Kramer and P. Freire
Max-Planck-Institut für Radioastronomie, Auf dem Hügel 69, D-53121 Bonn, Germany
H.J.v. Langevelde
Joint Institute for VLBI in Europe, Postbus 2, 7990 AA Dwingeloo, The Netherlands

Correlation center	RA (2000.0)	DEC (2000.0)
M15 (epoch 1 only)	21:29:58.3500	12:10:01.500
AC211	21:29:58.3120	12:10:02.679
15C	21:30:01.2034	12:10:38.160
S1	21:29:51.9025	12:10:17.132
VRTX1	21:29:56.3050	12:11:01.500
VRTX2	21:29:56.3050	12:09:11.500
VRTX3	21:30:02.4410	12:09:11.500

Table 1 Correlation centers throughout M15 used in all observation epochs after epoch one. The pointing center M15 which was also the correlation center in epoch 1 is also given

tivity at the same time. A higher frequency would result in an improved angular resolution but the steep spectrum of pulsars would render them undetectable. On the other hand, the pulsars would be more easy to detect at a lower frequency but only for the price of insufficient astrometric precision.

Using only one Westerbork antenna, the FOV is constrained by the Arecibo beam ($\sim$ 2.5 arcmin). The FOV is thus large enough to use the strong unclassified source S1 (Johnston et al., 1991) located about $94''$ to the west of the cluster center as in beam calibrator. In order to counteract time and bandwidth smearing degrading our sensitivity and astrometric precision towards the outer regions of the FOV we initially required an integration time of 0.25 seconds and a spectral resolution of 512 channels in each of the two polarizations and eight sub-bands of 16 MHz bandwidth. The size of the resulting dataset, however, proved to be unpractical such that observations after epoch 1 are still performed using only one pointing center but the data are correlated at six different correlations centers throughout M15 (Table 1). Therefore, the integration time and spectral resolution could be reduced to 0.5 seconds and 128 channels, respectively, resulting in six different overlapping tiles with a FOV of ~ 0.75 arcmin each. The blazar 3C454.3 serves as bandpass calibrator and is observed twice for about 10 minutes during each observations, once at the beginning and once towards the end. The quasar J2139+1423, located 3.13 degrees away from the pointing center, is used as phase reference source and is observed in an alternating fashion for roughly 1.2 minutes after each 3.5 minute scan of M15. Altogether, the total integration time on M15 amounts to about 3.6 hours in all three epochs, 85 (56) minutes of which Arecibo is included in epoch 1 (epoch 3). The noise level in epochs 1 and 3 is $\sim\ 3\mu$Jy. The synthesized beam sizes (RA$\times$DEC) are 3.6×6.3 mas and 2.8×8.1 mas for epochs 1 and 3, respectively. Unfortunately, epoch 2 lacked the Arecibo telescope and suffered from RFI which is why the rms is $\sim 7\,\mu$Jy and the beam size is 2.4×26.2 mas.

All data is reduced, calibrated and imaged using the software package AIPS[1]. First flagging of band edges and off-source times as well as system temperature and gain curve corrections are provided by the EVN pipeline[2] and are applied as such. Parallactic angle corrections are applied with the task CLCOR. Afterwards we calculate first ionospheric corrections running TECOR on the TEC maps[3] published by the Center for Orbit Determination in Europe. Further flagging of RFI is performed manually on all three pointing centers before running BPASS on the data for 3C454.3 to obtain flat and continuous gain curves across the band for all antennas. We perform a manual fringe correction running FRINGE on 3C454.3 solving only for different delays in the electronics for each of the eight subbands and, thus, obtain a continuous phase curve across the eight subbands. Applying all solutions obtained at this stage we run FRINGE a second time on the phase calibrator, this time solving for phase delays and phase rates simultaneously. The resulting solutions are applied to the M15 data and any remaining bad visibilities are flagged manually after inspection. In order to eliminate any residual phase delays we take advantage of the aforementioned strong source S1 and use it for in-beam calibration. An initial model of the source obtained through imaging with the task IMAGR is used in the task CALIB solving first for phases only. The found solutions are applied in another IMAGR run producing a new (better) model of the source. With further improvement of the model (higher SNR) we also solve for the amplitude to compute a final solution table that is then combined with all previous ones into a master solution table.

The largest possible size of an image supported by IMAGR is 16k$\times$16k pixels. At our angular resolution we aim for a pixel scale of 1 mas/pixel which is why we have to divide our FOV into a total of 15×15 tiles. Therefore, before the actual imaging, we run UVFIX shifting the correlation center in right ascension and declination by multiples of 13 arcseconds to ensure a sufficient overlap of the individual tiles. However, we will investigate more optimal methods to maintain good astrometric precision. To speed up the imaging process we then average the data to 2 seconds integration time and 64 channels per IF.

3 Results

In all three epochs presented here, the high sensitivity of the data enabled us to detect two of the know MSPs, 15A and 15C, and the LMXB AC211 with SNR$\geq$ 5. We have thus detected the double neutron star system 15C using VLBI for the fist time. We note, however, that 15C seems to perform a rather erratic movement from epoch 1 to epoch 2 (Fig. 2) which is inconsistent with the global movement of the cluster itself (Johnston et al., 1991). In contrast, the apparent motion of 15A follows M15 as expected (Fig. 1). Therefore, we conclude that 15C's relative change in position from epoch 1 to epoch 2 might be an artifact caused by inaccuracies introduced when running UVFIX to shift the (u,v,w) coordinates out to large angular distances from the original correlation center. The fact that the correlation center in epoch 1 was ~ 0.94' away from the position of 15C whereas 15A is located within 1.5" of the core of M15 indicates that the positional accuracy is degraded when running UVFIX out to large angular distances in epoch 1 (Morgan et al., 2011). This notion

[1] `http://www.aips.nrao.edu/`

[2] `http://www.evlbi.org/pipeline/user\_expts.html`

[3] downloaded from `ftp://ftp.unibe.ch/aiub/CODE/`

Source	μ_α [mas/yr]	μ_δ [mas/yr]
15A	-2.88 ± 0.04	-2.1 ± 0.2
15C	-2.74 ± 0.15	-26 ± 20
AC211	-3.90 ± 0.06	4.1 ± 1.1

Table 2 Proper motion results from the first three observation epochs.

is supported by the fact that as of epoch 2 where one correlation center coincides with 15C's tabulated position (Table 1) the binary system follows the global motion of the cluster. Hence, we ignore the position of 15C in epoch 1 for the analysis. As a result, the proper motion for 15C carries a very large error. In the case of AC211 we observe a bipolar structure in epoch 3 (Fig. 3) which is still under investigation. For the proper motion results presented here we, thus, excluded epoch 3 from the analysis for AC211. The deduced proper motions of all three sources are summarized in Table 2 where μ_α and μ_δ denote proper motion in right ascension and declination, respectively.

4 Conclusions

We have shown that it is possible to determine pulsar proper motions in a globular cluster with high precision using global VLBI. However, we have encountered problems with failing telescopes and still need to investigate how to fix the positional inaccuracies in running UVFIX in order be able to use this data in the analysis. To meet all our goals we still need to wait for the remaining observations to be carried out and correlated.

References

H. Baumgardt, P. Hut, J. Makino, S. McMillan, & S. Portegies Zwart 2003, ApJL, 582, L21
J. Gerssen, R. P. van der Marel, K. Gebhardt, P. Guhathakurta, R. C. Peterson, & C. Pryor 2002, AJ, 124, 3270
B. A. Jacoby, P. B. Cameron, F. A. Jenet, S. B. Anderson, R. N. Murty, & S. R. Kulkarni 2006, ApJL, 644, L113
H. M. Johnston, S. R. Kulkarni, & W. M. Goss 1991, ApJ, 382, L89
J. S. Morgan, F. Mantovani, A. T. Deller, W. Brisken, W. Alef, E. Middelberg, M. Nanni, & S. J. Tingay 2011, A&A, 526, A140
R. T. Schilizzi et al. 2001, Experimental Astronomy, 12, 49
X.-H. Sun, J.-L. Han, & G.-J. Qiao 2002, ChJAA, 2, 133

5 Appendix

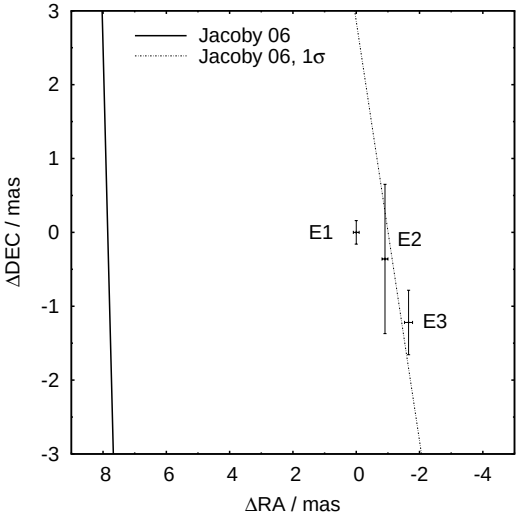

Fig. 1 Relative change in position for MSP 15A. The solid (dotted) lines indicate the position extrapolated with the proper motion (1σ error) as determined by Jacoby et al. (2006).

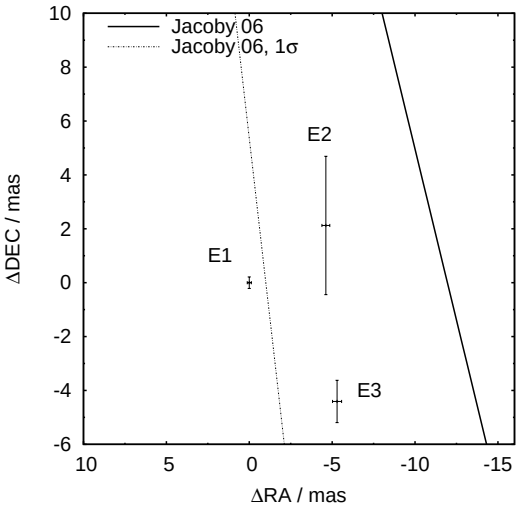

Fig. 2 Relative change in position for the double neutron star system 15C. The solid (dotted) lines indicate the position extrapolated with the proper motion (1σ error) as determined by Jacoby et al. (2006).

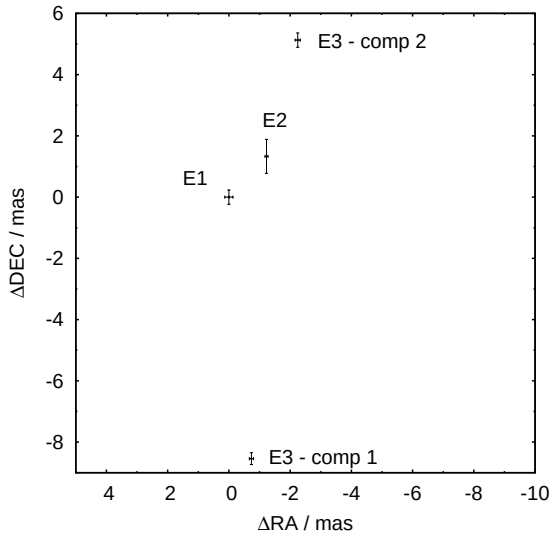

Fig. 3 Relative change in position for AC211. The bipolar structure observed in epoch 3 is still under investigation.

Estimation of Solar system acceleration from VLBI

Sergey Kurdubov

Abstract The estimation of Solar system acceleration from VLBI-observations was obtained. Obtained value compared with the results of other authors. Calculation was performed by the global adjustment of the VLBI data using QUASAR software. The estimated value of acceleration vector $a = (4.7 \pm 0.5) \cdot 10^{-10} m/s^2$ in direction $\alpha = 288 \pm 5$, $\delta = 0 \pm 5$ significantly differs from the theoretical one but comparable with the other results.

Keywords VLBI, solar system motion

1 Introduction

The phenomenon of secular aberration is not currently accounted in the reduction model of VLBI observations. Catalogues of extragalactic radio sources includes aberration bias due to movement of the solar system in the galaxy. However, as noted by many authors this effect can be estimated from continuous VLBI observations. The theoretical value of the acceleration is about $2 \cdot 10^{-10} m/s^2$ in the case of circular motion of the solar system in the Galaxy (Walter and Sovers, 2000; Kopeikin and Makarov, 2006). There are various options for the solution (Titov, 2010a):

1. The construction and subsequent analysis of the radio source positions time series (used in Popova, 2009).
2. Presentation of a systematic shift of the radio source positions in the form of expansions and estimation the parameters of these expansions in VLBI global solution (used in Titov, 2010a,b; Titov et al., 2010).
3. Addition of new parameter Solar System acceleration in VLBI observations model. (used in this paper)

Sergey Kurdubov
Institute of Applied Astronomy RAS, naberezhnaya Kutuzova 10, Saint-Petersbug, Russia

2 Data processing

We add new parameter Earth velocity in the LSC model and process VLBI observations with the QUASAR software (Gubanov et al., 2007). The 6,353,387 delays have been processed for the period August 1979 - October 2009. We use the following parameterization:

1. As the global parameters: coordinate and velocity of the stations (141 stations total, 14 with discontinuous), coordinates of radio sources (3009 sources total) and linear trend of the Earth velocity.
2. Arc parameters include: EOP, a linear trend of the wet tropospheric delay (WZD), tropospheric gradients, quadratic trends of clock offsets.
3. Stochastic (diurnal) parameters are: UT1-UTC, stochastic component of WZD and clock offset. Minimal constraints was used for fixing the frames: for the CRF no-net-rotation with respect to the 203 defining sources of ICRF-Ext.2 catalogue; for the TRF no-net-rotation and no-net-translation to the 11 stations from ITRF2005 catalogue.

3 Results

Velocity of the Earth was included in the global solution parameters set in the form of a linear trend. Offset component corresponds to the uncertainty of the zero point for the estimation of acceleration and depends on the CRF constraints of fixing the origin and distribution of observations. Rate of the velocity will be required acceleration. Two solutions were calculated in order to estimate the impact of radio source coordinate and the possible impact of conditions on the estimated acceleration.

1. With fixed source positions the following values of acceleration were obtained:

$$a_x = -1.9 \pm 0.2 \cdot 10^{-10} m/s^2,$$
$$a_y = -4.2 \pm 0.2 \cdot 10^{-10} m/s^2,$$
$$a_z = -0.2 \pm 0.4 \cdot 10^{-10} m/s^2.$$

2. With estimation of source positions the following values of acceleration were obtained:

$$a_x = -1.5 \pm 0.2 \cdot 10^{-10} m/s^2,$$

$$a_y = -4.4 \pm 0.2 \cdot 10^{-10} m/s^2,$$

$$a_z = -0.1 \pm 0.4 \cdot 10^{-10} m/s^2.$$

One can see the errors of radio source positions had little effect on estimated acceleration. In what follows we shall consider the estimate obtained with the coordinates. After transformation to the equatorial coordinates it corresponds to absolute acceleration $a = (4.7 \pm 0.5) \cdot 10^{-10} m/s^2$ and direction to the point $\alpha = 288 \pm 5$, $\delta = 0 \pm 5$.

4 Discussion

Obtained value $4.7 m/s^2$ significantly differs from the theoretical result for the circular motion of the Sun in the Galaxy. It is partly consistent with results obtained by the first method and presented in Titov (2010a,b) (13.1 microseconds of arc per year, which corresponds to about $6 \cdot 10^{-10} m/s^2$) and new result presented in [7] (5.8 ± 1.4 microseconds of arc per year (about $3 \cdot 10^{-10} m/s^2$) directed towards $\alpha = 266 \pm 8$, $\delta = -18 \pm 18$). The time series of source positions obtained by different analysis centers were used in Popova (2009) to estimate the acceleration and results are significantly different for different series, which may indicate that the time-series analysis is not suitable to solve the problem, because in each session, the coordinates of the radio source can be obtained only on a set of others, participated in the session and thus the effects of global displacements may be lost.

References

V. S. Gubanov, S. L. Kurdubov, I. F. Surkis, New version of QUASAR software for VLBI data processing, IAA RAS Transactions, Issue 16, Saint-Petersburg, 2007, 61-82.(in Russian)

S. M. Kopeikin, V. V. Makarov, Astrometric Effects of Secular Aberration, AJ, 131:1471-1478, 2006

E. A. Popova, Investigations of systematic variations of radio sources by positions time series, Izvestiya GAO, 219, Issue.4,2009. pp 273-279 (in Russian)

O. Titov, Secular Aberration Drift and IAU Definition of ICRS, MNRAS Letter, 407, L46, 2010.

O. Titov, VLBI 2010: from vision to reality in General IVS Meeting, Hobart 8 February 2010

O. Titov, S. B. Lambert, A.-M. Gontier, VLBI measurement of the secular aberration drift, eprint arXiv:1009.3698 2010

H. G. Walter , O. J. Sovers, Astrometry of Fundamental Catalogues: the Evolution from Optical to Radio Reference Frames, Springer-Verglas, Berlin, 2000

Use of GNSS-derived TEC maps for VLBI observations

C. Tierno Ros, J. Böhm, H. Schuh

Abstract The ionospheric delay makes up a large fraction of observed VLBI group delays; it depends on the total number of free electrons (TEC) along the ray path. Usually, a correction can be applied by making simultaneous observations in both S- and X-band. However, this is not always possible. For such cases, the alternative of calculating the ionospheric correction from Global Navigation Satellite Systems (GNSS) TEC maps is studied. A comparison of the ionospheric correction obtained from dual-band VLBI observations and from GNSS TEC maps is shown and first results of ionospheric corrections derived from GNSS applied to VLBI are presented.

Keywords Ionosphere, GNSS-derived TEC map, VLBI

1 Introduction

The ionosphere is a portion of the upper atmosphere; it is extended from about 60 km to 2000 km and has the characteristics that the particles there can be easily ionized by solar radiation resulting in a positive ion and a free electron. The structure of the ionosphere and its peak electron density vary strongly with time, geographic location, and certain solar and geomagnetic disturbances. The ionosphere is divided in four regions (D, E, F1 and F2) with different daytime characteristics like extent and electron density. The main concentration of electrons is from 300 to 400 km height (F2 layer). The D and F1 regions vanish at night and the E region becomes much weaker. The F2 region persists though at a reduced intensity. Radio signals travelling through the ionosphere suffer a delay caused by the number of free electrons within the ray path (Slant Total Electron Content, STEC). This effect is called ionosphere refraction and has to be considered when determining the propagation velocity of signals of all space geodetic techniques operating in microwave band (Alizadeh et al., 2011). The ionospheric delay is directly corrected from VLBI geodetic measurements by observing at two frequency bands, usually S-band (2.3 GHz) and X-band (8.4 GHz), and using the relationship that propagation delays in the ionosphere are - to the first order - proportional to the inverse square of the wave frequency (Kondo, 1991).

Global Navigation Satellite Systems (GNSS) total electron content (TEC) maps are representing the TEC values over the whole globe determined from GNSS observations. The ionosphere is treated in these maps as a thin spherical shell at a specified height (usually 400 or 450 km). Such maps exist since 1998 and have a latitude/longitude resolution of 2.5/5.0 degrees as can be seen in Figure 1 which gives an example of the ionosphere map provided by one analysis center (Center for Orbit Determination in Europe, CODE) of the International GNSS Service (IGS). Each daily file includes 13 ionosphere maps, starting from 0:00 to 24:00 hours, thus each map covers a 2 hours period (Gordon, 2010). The routine generation of these Global Ionosphere Maps (GIMs) is currently done at four analysis centers of the IGS, more details about the different techniques they use can be found in Schaer (1999); Feltens (1998); Mannucci et al. (1998) and Hernández-Pajares et al. (1999). The analysis centers transmit their products to the IGS Ionosphere Product Coordinator, who produces a weighted combined product (Hernández-Pajares et al., 2009). The accuracy of the maps is between 2 to 8 TECU (http://igscb.jpl.nasa.gov/components/prods.html).

2 Procedure followed

In this work, ionospheric delay corrections have been computed from CODE GIMs (they are the only ones including data from GLONASS, (they are the only ones including data from GLONASS, Hernández-Pajares et al., 2009) for CONT05, a two-week campaign of continuous VLBI sessions with 11 stations (Fig. 2) taking part that took place from 12th to 27th September, 2005. The procedure followed to calculate the ionospheric delay corrections has been:

1. Calculation of azimuth and elevation from antenna to quasar for all observations in the VLBI observation file (in NGS format).

Claudia Tierno Ros, Johannes Böhm, Harald Schuh
Institute of Geodesy and Geophysics, Vienna University of Technology, Gußhausstraße 27-29, 1040 Wien, Austria.
claudia.ros@tuwien.ac.at

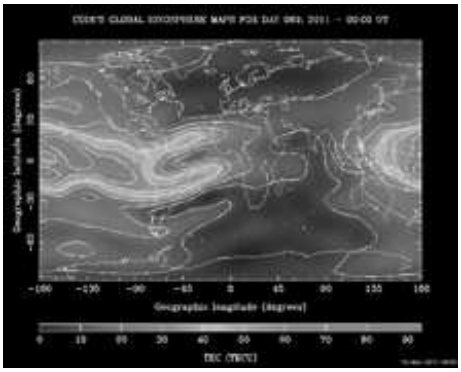

Fig. 1 Example of CODE GNSS TEC maps, 00:00 UT for day 089, 2011. Source: CODE Homepage http://aiuws.unibe.ch/ionosphere/

Fig. 2 Stations involved in the CONT05 campaign. Source: IVS Homepage http://ivscc.gsfc.nasa.gov/

2. Calculation of latitude and longitude of the Ionospheric Pierce Point (IPP, intersection between ionospheric layer and ray path).
3. Interpolation of VTEC value for the IPP from GIM.
4. Calculation of Slant TEC (STEC) values with help of a mapping function (eq. 1).

$$M(zd) = \frac{1}{\sqrt{1 - [\frac{Re}{Re+h} * sin(zd)]^2}} \tag{1}$$

$$STEC = VTEC * M(zd) \tag{2}$$

M(zd)... mapping function
zd... zenith distance
Re... radius of the Earth
h... height of the ionospheric layer

3 Evaluation of results before adjustment with VieVS[1]

In figure 3 we can see plots of both corrections (VLBI and GNSS) which obviously contain an offset. It is due to different signal paths of the X- and S-band systems at the radio telescopes (Gordon, 2010). However, this offset is not affecting the adjustment with VieVS, since it is a constant value for each station which is included in the clock offset parameters estimated for each VLBI station. Optimally, interpolation lines of VLBI ionosphere delay correction vs. GNSS ionosphere delay corrections (Fig. 4) should have slopes of 1.0 (Gordon, 2010). For CONT05, from 592 analysed baselines 86% have slopes from 0.8 to 1.2. Slopes outside these values are mostly due to the fact that there are only few observations of the baseline.

4 Evaluation of results after adjustment with VieVS

The CONT05 sessions have been adjusted with VieVS using NNR/NNT conditions for the station coordinates. Three versions of this adjustment have been carried out:

1. Using the VLBI ionosphere delay correction, included in NGS file.
2. Using the GNSS ionosphere delay correction, calculated from GIM.
3. Setting the correction to 0, in order to have a second reference value for the evaluation of the GNSS correction.

In the following two adjustment solutions will be compared:

1. First solution: it is meant to remove large clock offsets, rates, and quadratic terms for numerical reasons. Together with the clocks, also constant zenith delays per station are estimated but these troposphere delays are not removed from the observations. This solution is important because the possible mistakes done in the ionospheric correction will not be by mistake included in any other error.
2. Second solution: it estimates and removes clock parameters every 60 minutes, constant zenith wet delays every 30 minutes and north and east gradients every 6 hours.

Figures 5 and 6 show the χ^2 (equation 3) of both solutions for each session. χ^2 is a statistical test about the goodness of the fit between the observed and the expected data. The smaller the value of χ^2 is, the better the fit is.

$$\chi^2 = \frac{v^T P v}{n-u} \tag{3}$$

v...corrections
P...weights

[1] VieVS is the Vienna VLBI data analysis software that has been developed at the Institute of Geodesy and Geophysics, Vienna University of Technology, since 2008 (Nilsson et al., 2011)

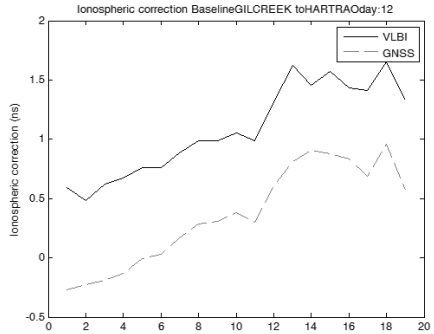

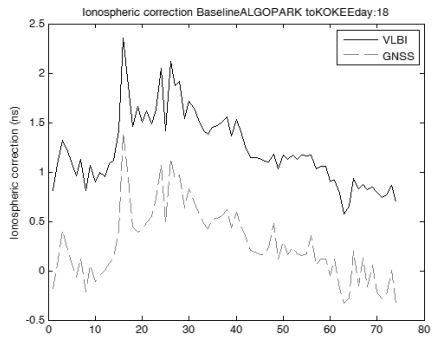

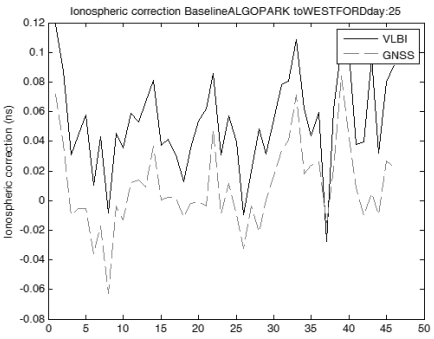

Fig. 3 VLBI and GNSS ionospheric delay corrections (nanosec).

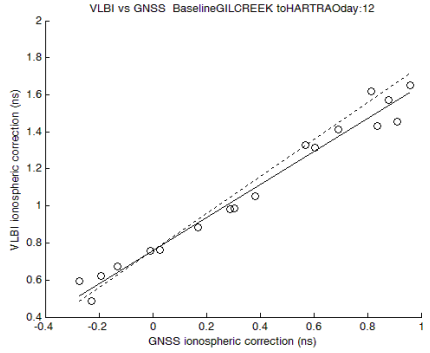

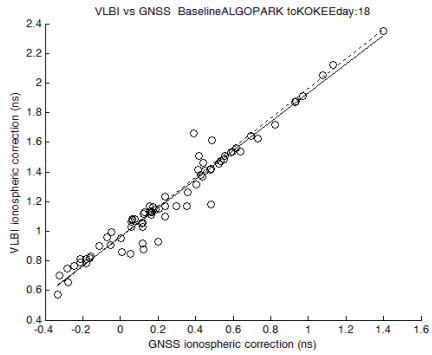

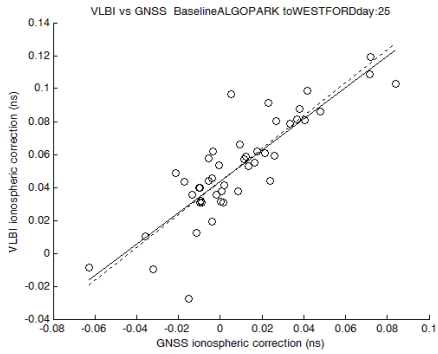

Fig. 4 VLBI (y-axis) vs GNSS (x-axis) ionospheric delay corrections (nanosec). The continuous line is obtained by interpolation between both corrections and the dashed line has a slope of 1.0 for reference.

n...number of observations
u...number of unknown parameters

Figure 7 shows the exponential trendline of the baseline repeatability. In all three cases the GNSS correction has provided better results than the 0 correction and worse results than the VLBI correction, as expected.

5 Conclusions

There are some differences between VLBI and GNSS ionosphere values (interpolation lines of VLBI ionosphere delay correction vs. GNSS ionosphere delay correction should have slopes of 1.0 (Gordon, 2010) but usually they take values from 0.8 to 1.2). This is due to the fact that the X/S ionosphere values are instantaneous direct measurements while the GNSS ionosphere values suffer from low spatial and temporal resolution (Gordon, 2010). However, the application of GNSS-derived TEC maps on VLBI observations provides a good approximation to the original VLBI ionosphere values and could be used in case of lack of VLBI ionosphere values or when the measurements are done on single frequency.

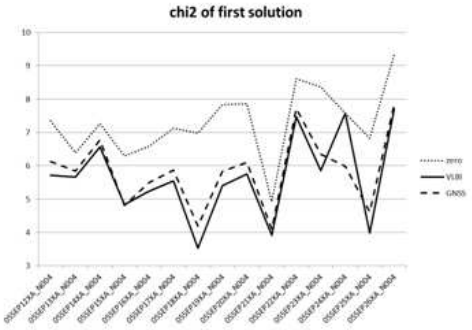

Fig. 5 χ^2 of 1st solution (see text) for CONT05 sessions with different types of ionospheric delay correction.

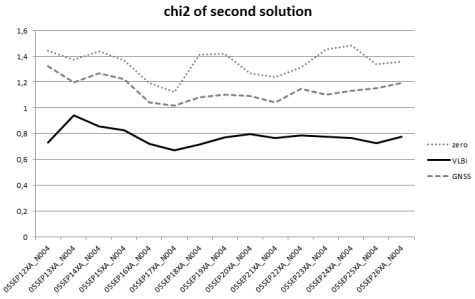

Fig. 6 χ^2 of 2nd solution (see text) for CONT05 sessions with different types of ionospheric delay correction.

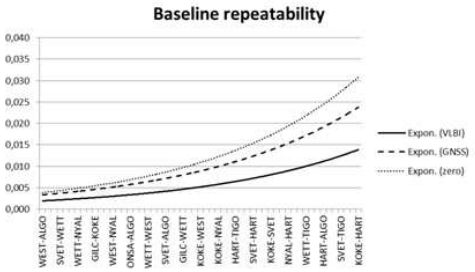

Fig. 7 Baseline repeatability (in meters) for CONT05 sessions with different types of ionospheric delay correction.

Acknowledgements The authors would like to thank the Austrian Science Fund (FWF) for supporting this work (Project: P22203-N22). They would also like to thank the International VLBI Service for Geodesy and Astrometry (IVS) and in particular all stations which contributed to CONT05, as well as the Center for Orbit Determination in Europe (CODE).

References

M. M. Alizadeh, H. Schuh, S. Todorova, M. Schmidt. Global Ionosphere Maps of VTEC from GNSS, Satellite Altimetry, and Formosat-3/Cosmic Data. *Journal of Geodesy*, doi: 10.1007/s00190-011-0449-z , 2011.

J. Feltens. Chapman Profile Approach for 3-d Global TEC Representation. *Proceedings of the 1998 IGS Analysis Centers Workshop, ESOC, Darmstadt, Germany, pages 285-297,* 1998.

D. Gordon. Use of GPS TEC Maps for Calibrating Single Band VLBI Sessions. *IVS 2010 General Meeting Proceedings, pages 242-246,* 2010.

M. Hernández-Pajares, J. M. Juan, J. Sanz. New approaches in global ionospheric determination using ground GPS data. *Journal of Atmospheric and Solar Terrestrial Physics, Volume 61, pages 1237-1247,* 1999.

M. Hernández-Pajares, J. M. Juan, J. Sanz, R. Orus, A. Garcia-Rigo, J. Feltens, A. Komjathy, S. C. Schaer, A. Krankowski. The IGS VTEC maps: a reliable source of ionospheric information since 1998. *Journal of Geodesy*, doi: 10.1007/s00190-008-0266-1, 2009.

T. Kondo. Application of VLBI data to measurements of ionospheric total electron content. *Journal of the Communications Research Laboratory, Volume 38, pages 613-622.* Communications Research Institute, Ministry of Posts and Telecommunications, Tokyo, Japan, 1991.

A. J. Mannucci, B. D. Wilson, D. N. Yuan, C. H. Ho, U. J. Lindqwister, T. F. Runge. A global mapping technique for GPS-derived ionospheric total electron content measurements. *Radio Science, Volume 33, pages 565-582,* 1998.

T. Nilsson, J. Böhm, S. Böhm, M. Madzak, V. Nafisi, L. Plank, H. Spicakova, J. Sun, C. Tierno Ros, H. Schuh. Status and future plans for the Vienna VLBI Software VieVS. *Proceedings 20th European VLBI for Geodesy and Astrometry (EVGA) Working Meeting, Bonn, Germany,* this issue, 2011.

S. Schaer. Mapping and Predicting the Earth's Ionosphere Using the Global Positioning System, PhD Dissertation, Astronomical Institute, University of Berne, Berne, Switzerland, 1999.

Terrestrial reference frame solution with the Vienna VLBI Software VieVS and implication of tropospheric gradient estimation

H. Spicakova, L. Plank, T. Nilsson, J. Böhm, H. Schuh

Abstract The Vienna VLBI Software (VieVS) has been developed at the Institute of Geodesy and Geophysics of TU Vienna since 2008. In this paper we present the determination of the Vienna Terrestrial Reference Frame (VieTRF10) with VieVS using all suitable VLBI sessions from 1984.0 to 2011.0, and we compare it to the IVS combined solution (VTRF2008). We focus on horizontal tropospheric gradients which influence the TRF determination and we show the effect of tropospheric gradients on station height and north-south components. The necessity of using absolute constraints when estimating tropospheric gradients in sessions before 1990 is visible from the coordinate time series.

Keywords VieVS, TRF, tropospheric gradients

1 Introduction

A Terrestrial Reference Frame (TRF) is a set of points (e.g. geodetic markers) on the Earth surface with precisely determined coordinates in a specific coordinate system. The International VLBI Service for Geodesy and Astrometry (IVS) provides a solution of the Terrestrial Reference Frame based on Very Long Baseline Interferometry (VLBI) observations. The recent realization (VTRF2008) is an IVS combined solution computed from normal equation systems (NEQs) provided by seven IVS analysis centers including data from 1979.7 to 2009.0 (Böckmann et al., 2010). We present in this paper a new TRF solution called VieTRF10 computed with the software VieVS (Böhm et al., 2011) and make comparisons with respect to VTRF2008.

We focus on the estimation of horizontal tropospheric gradients in the VLBI analysis. The extension of atmosphere above the equator is larger than in the polar regions. This atmospheric bulge is responsible for a systematic effect in the measured time delay mainly in north-south direction because the path of the radio wave through the atmosphere is larger if an antenna in the northern hemisphere observes in south direction than if it would observe towards north. We investigate the optimum parametrization for the gradient estimation in the VLBI analysis and how much station coordinates are affected if we would neglect this phenomenon.

Hana Spicakova, Lucia Plank, Tobias Nilsson, Johannes Böhm and Harald Schuh
Vienna University of Technology, Institute of Geodesy and Geophysics, Gußhausstraße 27-29, A-1040 Wien, Austria

2 VieTRF10

VieTRF10 is a terrestrial reference frame including 62 stations (see Fig. 1) estimated by a combination of datum-free NEQs of 3580 VLBI sessions from 1984.0 to 2011.0 produced by the Vienna VLBI Software VieVS. We included only sessions with more than two stations and if the a posteriori sigma of unit weight obtained from a single-session adjustment was less than two. In Table 1 selected modeling and parametrization options are summarized. With VieVS it is possible to create datum-free NEQs containing station coordinates, Earth orientation parameters (EOP), source coordinates, clock parameters, zenith wet delays (zwd), and tropospheric gradients. These are stored in an internal format for further use with a module vie_glob which allows stacking of the NEQs and estimating parameters from multiple VLBI sessions in a so-called global solution. For VieTRF10 we fixed the source coordinates to ICRF2 values (Fey et al., 2009). All Earth orientation parameters, together with clock parameters, zwd and tropospheric gradients were session-wise reduced from the NEQs. We also reduced session-wise coordinates of stations which participated in less than 10 sessions (mainly stations occupied with mobile antennas) which usually had observing time of less than three years, what is not sufficient to estimate reliable velocities. Exceptions were stations placed in a vicinity of another station with longer observation history, where the velocities were constrained to each other (Richmond - Miami20, Wettzell - Tigowtzl, Kashima - Kashima34, Hobart26 - Hobart12, and Yebes - Yebes40m). The resulting single-session NEQs containing positions and velocities were than stacked. The datum definition was done by applying no-net-translation and no-net-rotation conditions w.r.t. VTRF2008 on 22 stations with a long time history and good global distribution (i.e., Algopark, BR-VLBA, DSS45, FD-VLBA, Fortleza, HartRAO, Hobart26, Kashim34, Kashima, Kokee, LA-VLBA, Matera, MK-VLBA,

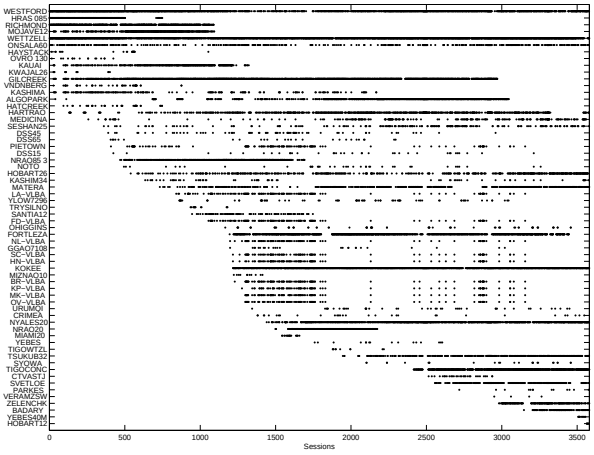

Fig. 1 Overview of participation of stations in VLBI sessions used for VieTRF10 determination.

NL-VLBA, NRAO85_3, NyAles20, Onsala60, Richmond, SC-VLBA, Seshan25, Westford, and Wettzell). Figure 2 shows the differences in vertical and horizontal components between VieTRF10 and VTRF2008 at epoch 2000.0 for 46 stations which participated in more than 30 sessions. Larger differences can be observed mainly at three stations. At Zelenchukskaya ((Zc), Russia) and Badary ((Bd), Russia) it is probably due to the fact, that these stations started their observations in 2006.0 and 2007.4, respectively, so that VTRF2008 includes only two years of data for Zelenchukskaya and a few months for Badary. For VieTRF10 the time span was longer by two years and we can assume, that the estimation of positions for these two stations is therefore more stable. The third station HRAS_085 ((Hr), Texas, USA) observed only in the early years within networks with poor geometry and stopped observations in 1990. In that time unusual apparent station motions of HRAS_085 were an often discussed open question which never could be answered. In terms of RMS the agreement between these TRFs is 6.8 mm for the height components and 7.0 mm for the horizontal differences over all 46 stations at epoch 2000.0. By excluding Hr, Zc, and Bd from the comparison the RMS decreases to 1.8 mm for height as well as horizontal components. Another comparison was done in terms of Helmert parameters for the transformation from VieTRF10 to VTRF2008 at epoch 2000.0. In Table 2 the results for two different sets of stations are listed. The first column shows the Helmert parameters for the transformation between stations used for datum definition. In the second column a network with all stations participating in more than 30 sessions (see Fig. 2), except stations Hr, Zc and Bd, is used. The differences between these two networks are very small and for both sets of stations we see a good agreement between VieTRF10 and VTRF2008 as the Helmert parameters are not significantly different from zero.

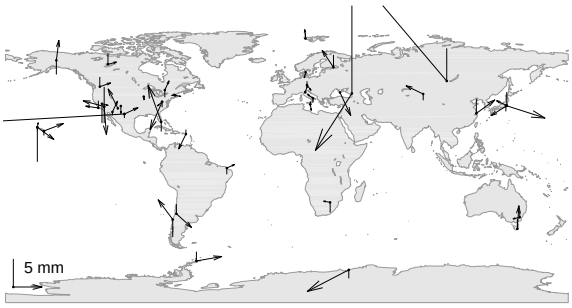

Fig. 2 Horizontal and vertical position differences at epoch 2000.0 between VieTRF10 and VTRF2008. Only differences for stations participating in more than 30 sessions are plotted.

Helmert parameters	22 datum stations	stations participated in >30 sessions (see Figure 2) except Hr, Zc, Bd
Tx [mm]	0.01 ± 0.44	0.23 ± 0.40
Ty [mm]	0.03 ± 0.44	-0.14 ± 0.39
Tz [mm]	-0.07 ± 0.42	-0.39 ± 0.38
Rx [mas]	-0.00 ± 0.02	-0.00 ± 0.01
Ry [mas]	-0.00 ± 0.02	0.03 ± 0.02
Rz [mas]	0.00 ± 0.02	-0.03 ± 0.01
Scale [mm]	0.15 ± 0.42	0.26 ± 0.38

Table 2 Helmert parameters for the transformation between VieTRF10 and VTRF2008 (VTRF2008-VieTRF10) at epoch 2000.0.

3 Horizontal Tropospheric Gradients

The azimuth-dependent part of the neutral atmosphere delay $\triangle L_{azim}$ measured by VLBI antennas can be expressed by:

$$\triangle L_{azim}(\alpha,\varepsilon) = m_g(\varepsilon) \times [G_n \cdot \cos(\alpha) + G_e \cdot \sin(\alpha)] \quad (1)$$

where ε is the elevation angle, α the azimuth angle, G_n and G_e the components of the horizontal gradient vector, and m_g is the gradient mapping function. To test the hypothesis that atmosphere asymmetry causes a systematic effect on the estimated station coordinates, we ran three test solutions (Tab. 3):

1. In the first solution we fixed the asymmetric part to zero and neglected the atmosphere gradients in the VLBI analysis.
2. The asymmetric part was a priori set to zero, and the components G_n and G_e of the horizontal gradient vector were estimated in the least-squares analysis with relative constraints (0.5 mm/6 h) to stabilize the NEQs.
3. The parametrization was identical to solution 2 with additional absolute constraints (0.5 mm) applied on G_n and G_e.

In Figure 3 session-wise estimated gradients at station Westford from 1984.0 till 2011.0 are plotted. Gradients from solu-

some modeling options	
TRF	VTRF2008 a priori
CRF	ICRF2 fixed
EOP	C04 05, IERS2003 (McCarthy and Petit, 2004)
precession/nutation model	IAU2000A
solid Earth tides	IERS2003
pole tides	linear model, IERS2003
ocean tidal loading	FES2004 (Lyard et al., 2006)
atmosphere loading	(Petrov and Boy, 2004)
a priori tropospheric gradients	DAO (MacMillan and Ma, 1997)
mapping functions	VMF1 (Böhm et al., 2006)
some options for parametrization	
clock parameters	60 min piece-wise linear (pwl) offsets (relative constraints: 42 ps) + rate + quadratic term
zenith wet delay	30 min pwl offsets (relative constraints: 35 ps)
tropospheric gradients	6 h pwl offsets (relative constraints: 0.5 mm + absolute constraints: 1 mm)
EOP	24 h pwl offsets (relative constraints: 0.0001 mas for polar motion and precession/nutation, and 0.0001 ms for UT1)

Table 1 Overview of selected modeling and parametrization options used for VLBI data processing for the estimation of the VieTRF10.

	estimation of gradients	relative constraints	absolute constraints
solution 1	no	-	-
solution 2	yes, 6-h offsets	0.5 mm	no
solution 3	yes, 6-h offsets	0.5 mm	0.5 mm

Table 3 Overview of the three solutions with different gradient handling.

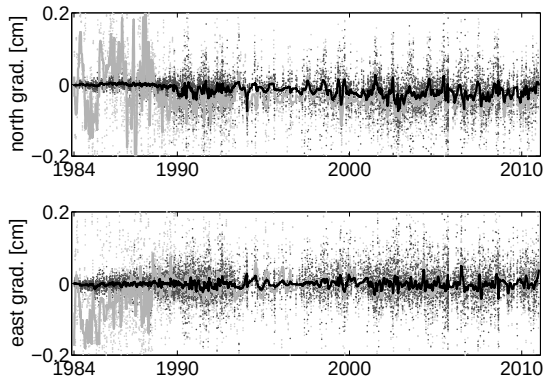

Fig. 3 Total session-wise estimated gradients at station Westford. In light grey gradients from solution 2 are plotted, in black from solution 3. Bold lines are smoothed values over 100 days.

tion 2 are plotted in light grey and from solution 3 in black. It can be seen, that before 1990 the determination of gradients without applying absolute constraints in the least-squares analysis is very unreliable. This is most probably due to the limited number of observations and the poor network geometry in

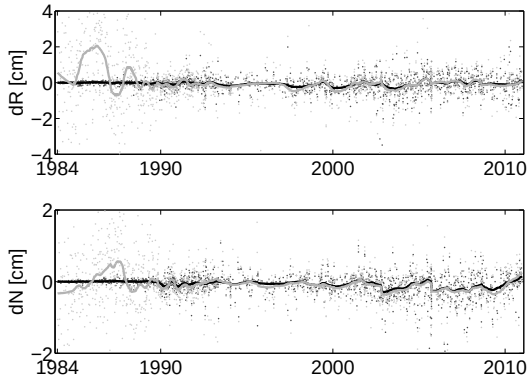

Fig. 4 Difference in station coordinates (height and north component) at station Westford for solution 2 (light grey) and solution 3 (black) w.r.t. solution 1. Bold lines are smoothed values over 100 days.

the early VLBI years. After 1990 the values for the north gradients reach systematically negative values, which reflects the atmospheric bulge above the equator since Westford is a station in the northern hemisphere. Figure 4 shows the corresponding estimates of station positions (height and north component) at station Westford for solution 2 (light grey) and solution 3 (black) w.r.t. to station positions estimated in solution 1. The unstable gradient determination in solution 2 in the early years also shows up in the station estimates and can reach a few centimeters. Since 1990 there is a good agreement between the station coordinates if gradients were estimated with or without absolute constraints and the difference to solution 1 (neglection of the troposphere asymmetry) reaches several millimeters. Mean values of the es-

Fig. 5 Global map with mean values over 1990.0 - 2011.0 for total tropospheric gradients from solution 2 (light grey) and solution 3 (black). Plotted are stations that participated in more than 20 sessions.

timated gradients over 1990.0 - 2011.0 from solutions 2 and 3 for all stations participating in more than 20 sessions are shown in Figure 5. At all stations the north-south component of the tropospheric gradient vectors points towards the equator. The unconstrained gradients from solution 2 are larger at all sites in comparison with solution 3, and the largest differences between these two solutions occur at stations Santia12 (Chile) and NRAO85_3 (West Virginia, USA) which observed only in the 90ies. Stations CTVA St. John's (Canada) and Urumqi (China) show also larger differences what is most probably caused by the small number of observations. The corresponding mean values of the estimated station heights and north components are plotted in Figure 6. The stations are sorted on the x-axis by latitude. The estimated positions are plotted w.r.t. the estimates from solution 1. The mean difference in the north component for stations in the southern hemisphere is 2.8 mm between solution 2 and solution 1, and 1.4 mm between solution 3 and solution 1. In the northern hemisphere the mean difference in the north component w.r.t. solution 1 is -0.6 mm for solution 2, and -0.4 mm for solution 3. In other words, if tropospheric asymmetry is neglected, stations are shifted towards the poles w.r.t. their real positions.

4 Conclusions

The first determination of a Terrestrial Reference Frame with the recently developed VieVS software (VieTRF10) is presented in this paper and is available at http://vievs.hg.tuwien.ac.at/vietrf10.txt. We showed a good agreement with the IVS combined solution even though the time span of data used for the determination of these two TRFs is not identical and there is also a difference in terms of a priori modeling since we corrected for atmosphere loading what was not done for the VTRF2008. Each of the seven analysis centers contributing to the VTRF2008 has also its own strategy for parametrization and time resolution of the pre-reduced parameters such as the zwd or tropospheric gradients. It was

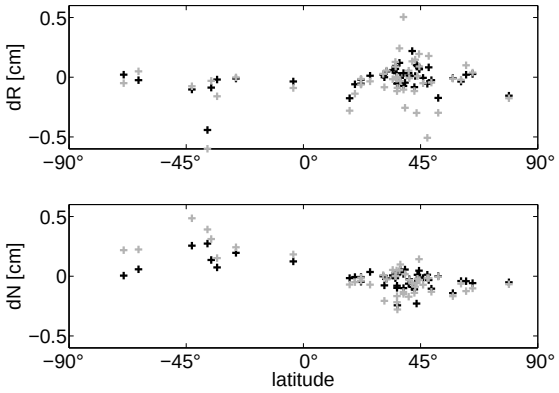

Fig. 6 Mean values over 1990.0 - 2011.0 for height and north component of stations participated in more than 20 sessions sorted by latitude. Solution 2 (light grey) and solution 3 (black) are plotted w.r.t. solution 1.

shown that handling and estimation of tropospheric gradients in the VLBI analysis has to be done carefully, especially for the early VLBI years where networks with only few stations and a small number of observations do not allow reliable gradient estimation without using absolute constraints.

5 Acknowledgements

The authors acknowledge the IVS (Schlüter and Behrend, 2007) and all its components for providing VLBI data. Hana Spicakova is grateful to Mondi Austria Privatstiftung for financial support during her Ph.D. study at TU Vienna. Tobias Nilsson works under project SCHUH 1103/3-2 Earth Rotation and Global Dynamic Processes, Forschergruppe FOR584.

References

S. Böckmann, T. Artz, and A. Nothnagel (2010). VLBI terrestrial reference frame contributions to ITRF2008. *Journal of Geodesy 84*. pp. 201-219. doi: 10.1007/s00190-009-0357-7.

J. Böhm, B. Werl, and H. Schuh (2006). Troposphere mapping functions for GPS and very long baseline interferometry from European Centre for Medium-Range Weather Forecasts operational analysis data. *Journal of Geophysical Research 111*. B02406. 9 pp. doi: 10.1029/2005JB003629.

J. Böhm, S. Böhm, T. Nilsson, A. Pany, L. Plank, H. Spicakova, K. Teke, and H. Schuh (2010). The new Vienna VLBI Software VieVS. *Proceedings of the 2009 IAG Symposium*, Series: International Association of Geodesy Symposia. Vol. 136. Geodesy for Planet Earth. Steve Kenyon,

Maria Christina Pacino and Urs Marti (ed.). ISBN 978-3-642-20337-4.

A. Fey, D. Gordon, and C. S. Jacobs (2009). The Second Realization of the International Celestial Reference Frame by Very Long Baseline Interferometry, Presented on behalf of the IERS / IVS Working Group. IERS Technical Note, No. 35, Frankfurt am Main, Germany: Verlag des Bundesamtes für Kartographie und Geodäsie, 204 p. ISBN 3-89888-918-6.

F. Lyard, F. Lefevre, T. Letellier, and O. Francis (2006). Modelling the global ocean tides: modern insights from FES2004. *Ocean Dynamics 56*. pp. 394-415. doi: 10.1007/s10236-006-0086-x.

D. S. MacMillan and C. Ma (1997). Atmospheric gradients and VLBI terrestrial and celestial reference frames. *Geophysical Research Letters 24/4*. pp. 453-456. doi: 10.1029/97GL00143.

D. D. McCarthy and G. Petit (2004). *IERS Conventions (2003)*. International Earth Rotation and Reference Systems Service (IERS). IERS Technical Note, No. 32, Frankfurt am Main, Germany: Verlag des Bundesamtes für Kartographie und Geodäsie, ISBN 3-89888-884-3.

L. Petrov and J.-P. Boy (2004). Study of the atmospheric pressure loading signal in very long baseline interferometry observations. *Journal of Geophysical Research 109*. B03405. 14 pp. doi: 10.1029/2003JB002500.

W. Schlüter, and D. Behrend (2007). The International VLBI Service for Geodesy and Astrometry (IVS): current capabilities and future prospects. *Journal of Geodesy 81/6-8*. pp. 379-387. doi: 10.1007/s00190-006-0131-z.

Common Realization of Terrestrial and Celestial Reference Frame

M. Seitz, R. Heinkelmann, P. Steigenberger, T. Artz

Abstract The realization of the International Celestial Reference System (ICRS) and the International Terrestrial Reference System (ITRS) is performed separately today. As a consequence, the two computed reference frames are not fully consistent as well as the EOP series derived accordingly. Differences exist in the network geometry, the realization of the scale, and the EOP series. The paper shows the first results of a consistent computation of CRF, TRF, and the EOP series linking both frames. The CRF is slightly influenced by the combination in two different ways: by the combination of the EOP and by the combination of the station networks. It is shown that both effects are small. The effect of combining the station networks – mainly driven by the misfits between local ties and results of space geodetic techniques – reaches up to 2 mas, but is much smaller for most of the sources. The mean difference is about 10 μas. However, a clear but small systematic can be seen. The combination of the EOP lead also to small changes in the source positions. Sources close to the celestial south pole are affected by a maximum of ± 1 mas. A further systematic effect (-0.5 mas in maximum) is detected for some of the sources with declinations between about $\pm$ 40. The reasons are not known. The integral impact of the combination on the CRF is small and not significant w.r.t. the axis stability (10 μas) and the noise floor (40 μas) of ICRF2.

Keywords CRF · TRF · EOP · combination · VLBI · GNSS · SLR

Manuela Seitz and Robert Heinkelmann
Deutsches Geodätisches Forschungsinstitut,
D-80539 München, Alfons-Goppel-Str. 11, Germany

Peter Steigenberger
Institut für Astronomische und Physikalische Geodäsie, Technische Universität München,
D-80333 München, Arcisstr. 21, Germany

Thomas Artz
Institut für Geodäsie und Geoinformation Universität Bonn,
D-53115 Bonn, Nußallee. 17, Germany

1 Introduction and Motivation

Today, the International Terrestrial and the International Celestial Reference System, ITRS and ICRS, respectively, are realized separately by applying two individual computation methods. As a consequence, the corresponding reference frames and the Earth Orientation Parameters (EOP), which are also estimated in both realizations, are not completely consistent. The left graphic of Fig. (1) illustrates the situation as it stands today. While the computation of the International Celestial Reference Frame (ICRF) is based on VLBI (Very Long Baseline Interferometry) observations only, the International Terrestrial Reference Frame (ITRF) is computed from a combination of the observation data of different space geodetic techniques, namely VLBI, SLR (Satellite Laser Ranging), GNSS (Global Navigation Satellite Systems) and DORIS (Doppler Orbitography and Radiopositioning Integrated by Satellite).

Even if consistency w.r.t. origin and orientation between the VLBI-only TRF (VTRF) – which is estimated simultaneously with the ICRF – and the ITRF is achieved by aligning the VTRF to the ITRF, inconsistencies between the two realizations exist: (i) the VLBI station networks of both realizations differ w.r.t. the scale, as the ITRF scale is derived from VLBI and SLR observations while the VTRF scale is derived from VLBI only, (ii) the station networks differ w.r.t. network geometry, as it is slightly changed by the combination, (iii) the EOP series differ significantly, as the one from ICRF computation is derived from VLBI only, while the EOP series which corresponds to the ITRF is a combined series. In order to achieve full consistency, all parameters – station coordinates, source positions and the EOP – must be adjusted together. In the right part of Fig. (1) the computation strategy for such a consistent realization is shown. The origin of the combined TRF is derived from SLR and the scale from SLR and VLBI as it is conventional for the ITRF computation (IERS, 2010). In order to avoid a deformation of the network, the orientation of the frames can be realized by no-net-rotation (NNR) conditions w.r.t. a priori reference frames, e.g. DTRF2008 (Seitz et al., 2011) and ICRF2 (IERS, 2009). In this paper a first consistent realization of both reference systems is presented and the effect of the combination on the relevant parameters, especially on the CRF, is studied.

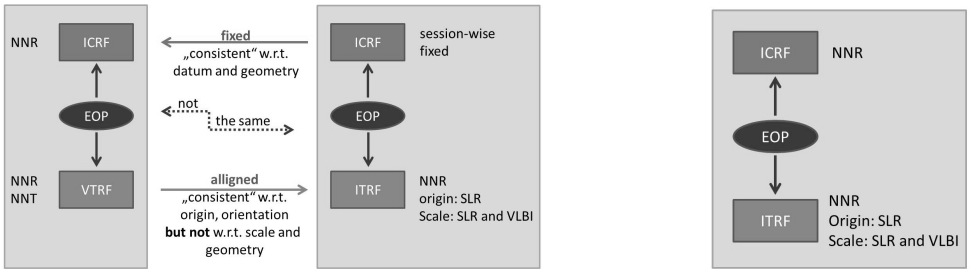

Fig. 1 Current situation for ITRS and ITRS realization (left) and a fully consistent realization (right)

2 Input data

The input data are time series of daily GPS, weekly SLR and session-wise VLBI normal equations covering 13, 14 and 23 years, respectively. They are provided by different German geodetic institutions, within the framework of the project GGOS-D (Rothacher et al., 2011). The project aims on the consistent computation of reference frames and geodetic parameters series from space geodetic techniques, striving for a very high accuracy and consistency of the resulting parameters. Table (1) gives an overview about the input data.

Table 1 Input data

	time span	resolution	institutions
VLBI	1984-2007	session-wise (24h)	combined: DGFI+IGG
GPS	1994-2007	daily	GFZ
SLR	1993-2007	weekly	DGFI

Table (2) shows which kind of parameters can be derived from the individual techniques. Including coordinates of stations and sources and the EOP series, altogether about 45,000 parameters are estimated.

Table 2 Parameters of the combined solutions as derived from the individual techniques. Brackets mean that not the parameter in an absolute sense can be derived but the first derivative in time.

	VLBI	SLR	GPS
station coordinates	x	x	x
source coordinates	x		
terrestrial pole	x	x	x
celestial pole	x		(x)
UT1-UTC	x	(x)	(x)
origin		x	
scale	x	x	

3 Computation strategy

The computation strategy applied for the analysis and combination of the data is shown in Fig. (2). The input series are analyzed with respect to discontinuities and outliers. Therefore, initially all the normal equations (NEQ) are solved and solution time series are generated. The NEQ are prepared for the combination by setting up station velocities as new parameters and transforming the VLBI EOP to 0 UT epochs. Considering the detected discontinuities and outliers, the NEQ are combined to one NEQ per technique. In a second processing step the NEQ of the different techniques are combined. Common parameters, which are combined, are the station coordinates and the EOP. As the observations of different space geodetic techniques are usually not related to common reference points, terrestrial difference vectors (so called "local ties") are introduced as pseudo-observations into the combination in order to link the station networks of the different techniques. Thus, so called co-location sites, where different techniques are operated close to each other, are very important. Figure (3) shows the global distribution of the used co-location sites. Different from station positions, station velocities and EOP can be combined directly by adding the corresponding NEQ elements.

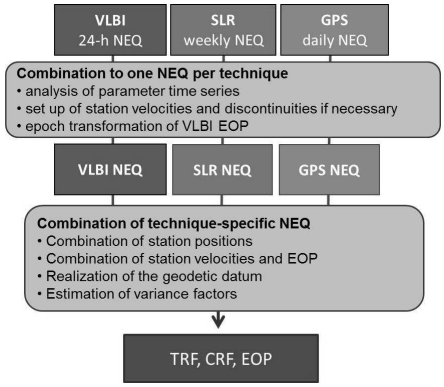

Fig. 2 Computation strategy for ICRS-ITRS realization

The geodetic datum of the TRF is realized in accordance to the IERS Conventions (IERS, 2010). The origin is realized by SLR observations, the scale is realized as a weighted mean of

VLBI and SLR contributions and the orientation is given by no-net-rotation conditions w.r.t. a previous reference frame, in this case the DTRF2008 (Seitz et al., 2011). The orientation of the CRF is realized applying no-net-rotation conditions w.r.t. ICRF2. Stable sources according to Feissel et al. (2006) are used for the generation of the condition equations. A more detailed description of the computation strategy is given in Rothacher et al. (2011).

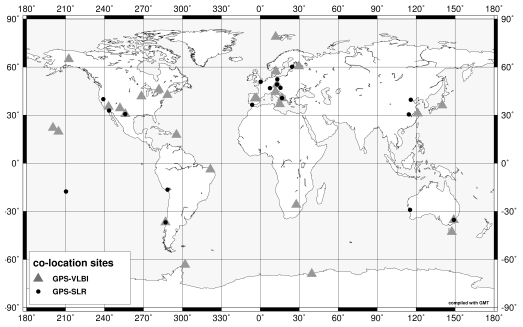

Fig. 3 Global distribution of co-location sites used.

4 Solution approaches

It must be expected that the impact of a common adjustment of CRF and TRF on the source coordinates is twofold: The combination of the EOP should lead to changes of the CRF, but also the combination of station coordinates which leads – as it is well known from ITRF computation – to small changes in the station network geometry will have an impact on the CRF. As introduced before, the EOP are handled as common parameters while station positions of different techniques are linked by introducing local ties. In order to analyze the effect of the local ties on the combined solution and especially on the CRF, three combined solutions are computed including the local tie vectors with standard deviations of 0.5, 1.0 and 2.0 mm. For comparison a VLBI-only solution is computed and in addition a combined solution is derived for which only the EOP but not the station coordinates are combined. The different solution types are summarized in Tab. (3).

Table 3 Different solution types.

Solution	Combined parameters	Standard deviation for local ties
VLBI-only	/	/
EOP combined	EOP	/
TRF-CRF 0.5	TRF, EOP	0.5 mm
TRF-CRF 1.0	TRF, EOP	1.0 mm
TRF-CRF 2.0	TRF, EOP	2.0 mm

5 Discussion of the results

The VLBI-only solution includes the positions of 2378 sources. The mean weighted differences of source coordinates w.r.t. ICRF2 are small (53 μas in declination (DE) and 3 μas in right ascension (RA·cos(DE))) and show no systematics. The differences for the stable sources are smaller: 41 and 1 μas, respectively. The solution is used in the following for comparisons.

Figure (4) shows the differences in DE and RA·cos(DE) of the 3 CRF-TRF solutions w.r.t. the VLBI-only solution. Considering all sources, the mean weighted difference is smaller than 10 μas for DE and about 1 μas for RA·cos(DE). The largest differences can be found for sources in low declinations, as it can be expected because of the declination dependency of mean source coordinate precession. The differences between the 3 solutions are very small. Remarkable is the ”bow” feature in RA·cos(DE) which is shown by some sources with latitudes between 40. This effect will be discussed later.

Looking at the differences of the stable sources, the effect on RA·cos(DE) is very small. For DE, the differences are also very small but show a systematic: The smaller the standard deviations of the local ties are the larger is a southwards shift of the sources, which itself increases towards the south pole. The WRMS in the diagrams also reflect this effect as they are computed without applying a detrend-function.

Besides the effects on the CRF also the impact of the combination on the TRF is studied. Two aspects are considered here: The combined station network shall be consistent and, at the same time, the network deformation due to the combination shall be small. Figure (5) shows the mean deformation of the station network caused by the combination and the translation parameters of the VLBI stations w.r.t. the DTRF2008 reference frame. Both are derived by a similarity transformation between the VLBI part of the combined CRF-TRF solution and the VLBI-only solution, which is aligned to DTRF2008. The mean deformation is quantified by the RMS of the station position residuals resulting from the transformation. Figure (5) shows that the mean deformation increases if the standard deviation of local ties becomes smaller. The smallest translation parameters, however, are achieved for the combined solution obtained with a standard deviation for local ties of 0.5 mm. It can be concluded, that the two contradicting aspects, the deformation of the frames and the consistency of the combined network, must be balanced.

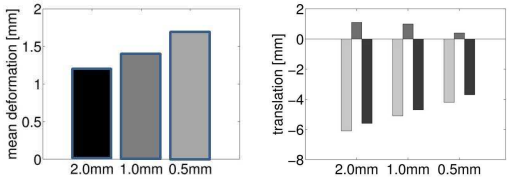

Fig. 5 Mean deformation of VLBI station network caused by combination (left) and translation of VLBI part of CRF-TRF solution w.r.t. DTRF2008 (right). The bars of one triple represent the translation in x-, y-, and z-direction.

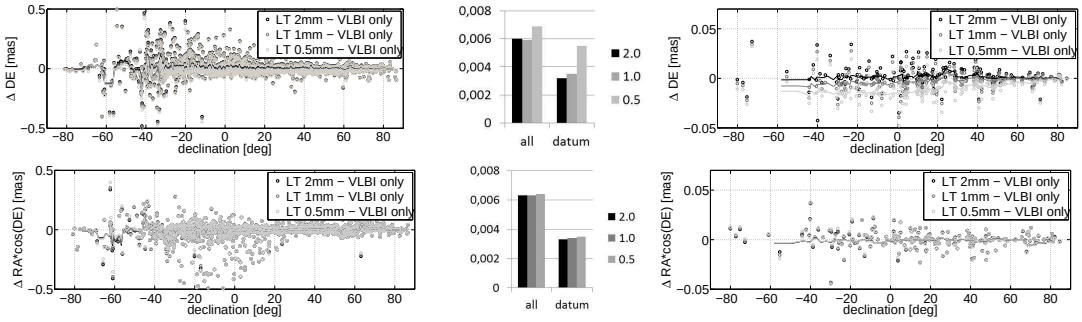

Fig. 4 Differences in DE and RA·cos(DE) of the three combined solutions with standard deviations of the local ties of 0.5, 1.0 and 2.0 mm w.r.t. the VLBI-only solution considering all sources (left) and stable sources only (right). The solid lines represent values of a moving median. The bar plots in the middle show the corresponding WRMS computed without the application of a detrend-function.

In order to separate the effect of combination of station coordinates and the effect of EOP combination on the CRF, the combined solutions are compared to a solution in which the EOP are combined but not the station coordinates. In Fig. (6) the differences in RA·cos(DE) are shown. A comparison of the figure with the left subfigure of Fig. (4) shows, that the ”bow” feature which can be seen from a comparison of the combined CRF-TRF and the VLBI-only solution vanishes if the combined CRF-TRF solution is compared to the ”EOP combined only” solution. The conclusion is, that the systematic is caused by EOP combination as it cannot be seen if two solutions with combined EOP are compared. From Fig. (6) it can also be concluded, that in particular those sources which are located close to the celestial south pole are affected by the combination of the station networks.

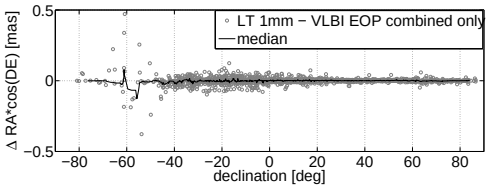

Fig. 6 Difference in RA·cos(DE) between CRF-TRF solution (exemplarily the solution with 1.0 mm standard deviations for local ties) and an ”EOP combined only” solution. The WRMS is 2.2 μas.

6 Conclusions

Presently, ICRF and ITRF are not computed fully consistent. The paper shows first results of a consistent solution of CRF, TRF and the corresponding EOP, which link both frames. Non-deforming no-net-rotation conditions are applied in order to avoid an over constraining and, thus, a deformation of the solution. While the effect of the combination of different space geodetic techniques on the station coordinates and EOP is well known from ITRF computation, the effects on the CRF are the subjects of investigation. Two different effects are investigated: the effect of the combination of EOP and the effect of the combination of station coordinates. The combination of station coordinates leads to position differences of sources on the southern hemisphere of up to 2 mas but in the most cases the differences are much smaller. The mean differences for DE and RA·cos(DE) are 10 and 1 μas, respectively. Sources with declinations between -50 and -70 show the largest effects. The effect on the stable sources does not exceed 0.08 mas. A clear systematic can only be seen for the declination of the stable sources: the lower the standard deviation of the local ties is the larger are the southwards shifts of the sources. However, the effect is very small. The maximum median value is below 0.02 mas. The combination of the EOP leads also to position differences of the sources. A systematic ”bow” feature is detected in RA for sources with declinations between about ± 40. But not all sources are affected. The reason for the effect is not yet known. Furthermore, the combination of EOP causes position changes of sources close to the celestial south pole of up to 0.8 mas. While EOP benefit from a combination, station positions can be affected by the discrepancies between local ties and the results of the space geodetic techniques. Consequently, the effect of EOP combination on the CRF is an improvement, while the effect of combination of station positions on the CRF is not clearly beneficial. Further, more detailed studies have to be done to get a better understanding of the impacts of different session types, the different co-location stations and the different EOP. However, as shown from the comparisons with the VLBI-only solution, the systematic effect of the combination on the CRF is small. The effect on the stable sources, expressed by the WRMS, is even not significant w.r.t. the axis stability of 0.01 mas specified for the ICRF2. The WRMS w.r.t. all sources is smaller than the noise floor of 0.04 mas specified for the ICRF2.

References

M. Feissel, C. Ma, A.-M. Gontier, and C. Barache (2006), Analysis strategy issues for the maintenance of the ICRF axes, *Astron and Astrophys, 451*.

IERS (2009), The Second Realization of the International Celestial Reference Frame by Very Long Baseline Interferometry, Presented on behalf of the IERS / IVS Working Group, *IERS Tech. Note 35*, Verlag des Bundesamtes für Geodäsie und Kartographie, Frankfurt am Main.

IERS (2010), IERS Conventions (2010), *IERS Tech. Note 36*, Verlag des Bundesamtes für Geodäsie und Kartographie, Frankfurt am Main.

M. Rothacher, D. Angermann, T. Artz, W. Bosch, H. Drewes, S. Böckmann, M. Gerstl, R. Kelm, D. König, R.König, B. Meisel, H. Müller, A. Nothnagel, N. Panafidina, B. Richter, S. Rudenko, W. Schwegmann, M. Seitz, P. Steigenberger, V. Tesmer, and D. Thaller (2011), GGOS-D: Homogeneously Reprocessing and Rigorous Combination of Space Geodetic Techniques, *J Geod, accepted*.

M. Seitz, D. Angermann, M. Bloßfeld, H. Drewes, and M. Gerstl (2011), The 2008 DGFI realization of ITRS: DTRF2008, *J Geod, submitted*.

Impact of A Priori Gradients on VLBI-Derived Terrestrial Reference Frames

J. Böhm, H. Spicakova, L. Urquhart, P. Steigenberger, H. Schuh

Abstract We compare the influence of two different a priori gradient models on the terrestrial reference frame (TRF) as determined from Very Long Baseline Interferometry (VLBI) observations. One model has been determined by vertical integration over horizontal gradients of refractivity as derived from data of the Goddard Data Assimilation Office (DAO), whereas the second model (APG) has been determined by ray-tracing through monthly mean pressure level re-analysis data of the European Centre for Medium-Range Weather Forecasts. We compare VLBI solutions from 1990.0 to 2011.0 with fixed DAO and APG gradients to a solution with gradients being estimated, and we find better agreement of station coordinates when fixing DAO gradients compared to fixing APG gradients. As a consequence, we recommend that gradients are constrained to DAO gradients, in particular in the early years of VLBI observations (up to about 1990), when the number of stations per session is small and the sky distribution is far from uniform. Later than 1990, the gradients can be constrained loosely and the a priori model is of minor importance.

Keywords Troposphere Gradients, Terrestrial Reference Frame, VLBI

1 Introduction

As recommended by the Conventions of the International Earth Rotation and Reference Systems Service (IERS) (Petit and Luzum, 2010), the line-of-sight delay, D_L, is expressed as a function of four parameters as follows:

$$D_L = m_h(e)D_{hz} + m_w(e)D_{wz} + m_g(e)[G_N\cos(a) + G_E\sin(a)]. \quad (1)$$

The four parameters in this expression are the zenith hydrostatic delay, D_{hz}, the zenith wet delay, D_{wz}, and a horizontal delay gradient with components G_N (north) and G_E (east). m_h, m_w, and m_g are the hydrostatic, wet, and gradient mapping functions, respectively, and e is the elevation angle of the observation direction in vacuum. a is the azimuth angle in which the signal is received, measured clockwise from north.

Horizontal gradient parameters are needed to account for the systematic component in the north-south direction towards the equator due to the atmospheric bulge (MacMillan and Ma, 1997), and they also capture the effects of random components in both directions due to the variable weather systems. Usually, those gradients are estimated in the analysis of Global Navigation Satellite Systems (GNSS) and Very Long Baseline Interferometry (VLBI) observations with the gradient mapping function m_g as part of the partial derivative.

Although it is generally not necessary to constrain those gradient estimates to a priori values in GNSS analysis, it is recommended to constrain the estimates in the early years of VLBI observations up to about 1990 (Spicakova et al., 2011) when only a few stations were observing per session and the distribution of the observations in the sky per station was far from uniform. In any case, it is advisable to constrain the gradient estimates to a realistic a priori gradient model which accounts for the atmospheric bulge. In the next sections, we describe the effect of constraining (fixing) the gradient estimates to a priori models different from zero.

2 Gradient mapping function

Two types of gradient mapping functions m_g are widely used in GNSS and VLBI software packages. On the one hand, there is the formulation by MacMillan (1995) which goes back to Davis et al. (1993) for the "wet" refractivity of air:

$$m_g = \cot(e)m_h. \quad (2)$$

Johannes Böhm, Hana Spicakova, and Harald Schuh
Vienna University of Technology, Gußhausstraße 27-29, A-1040 Vienna, Austria, johannes.boehm@tuwien.ac.at
Landon Urquhart
University of Calgary, Canada
Peter Steigenberger
Technische Universität München, Germany

This approach has the disadvantage that it is singular at the horizon. On the other hand, Chen and Herring (1997) suggest applying

$$m_g = \frac{1}{\tan(e)\sin(e)+C} \tag{3}$$

and they recommend to use $C = 0.0032$ for the estimation of total gradients (Herring, 1992). This formulation is based on a theoretical concept with an exponential decay of the horizontal gradient of refractivity with height. If used with the coefficient $C = 0.0007$ (corresponding to a scale height of 3 km) it describes the gradient mapping function for the wet part and is rather close to the formulation by MacMillan (1995) (see also Figures (1) and (2)).

Exemplarily, we determined ray-traced delays at 5, 7, 10, 15, 20, 30, 50, 70, and 90 degrees elevation towards north, east, south, and west at two sites (Wettzell in Germany, and Tsukuba in Japan) on 1 January 2008 at 0 UT. Then, we removed the azimuth-symmetric part and compared the residuals to the gradient mapping functions by scaling the latter so that they agree with the residual ray-traced delays at 5 degrees elevation. From the two samples we did not find a clear preference of one type of gradient mapping function (see Figures (1) and (2)). Furthermore (not shown here), the impact on station coordinates is at the sub-millimetre level if either using the formulation by MacMillan (1995) (Eq. (2)) or Chen and Herring (1997) (Eq. (3)) for the estimation of gradients. Thus, we used the formulation by Chen and Herring (1997) (Eq. (3)) with $C = 0.0032$ for our investigations, i.e., for mapping the a priori gradients as well as for estimating gradients, and we recommend its application in all software packages for better comparability.

3 A priori gradient models

We used two different a priori gradient models for comparison. MacMillan and Ma (1997) introduced gradients derived from data of the Goddard Data Assimilation Office (DAO) (Schubert et al., 1993). These gradients are derived by vertical integration over the horizontal gradients of refractivity, and they are provided for all VLBI sites. Secondly, Böhm et al. (2011b) determined an a priori gradient (APG) model from 40 Years Re-Analysis (ERA40) monthly mean pressure level data of the European Centre for Medium-Range Weather Forecasts (ECMWF) with a horizontal resolution of 5 degrees. North and east gradients were derived by the determination of ray-traced delays in zenith direction as well as towards north, east, south, and west at 5 degrees elevation, and by fitting those delays to the model by Chen and Herring (1997) (Eq. (3)) with the coefficient $C = 0.0032$. The north and east gradients, G_N and G_E, were then averaged over all months and expanded into spherical harmonics up to degree and order 9. This model can be downloaded from the GGOS Atmosphere Server at TU Vienna [1] and plots on APG are provided by Böhm et al. (2011b).

[1] http://ggosatm.hg.tuwien.ac.at/DELAY/SOURCE/apg.f

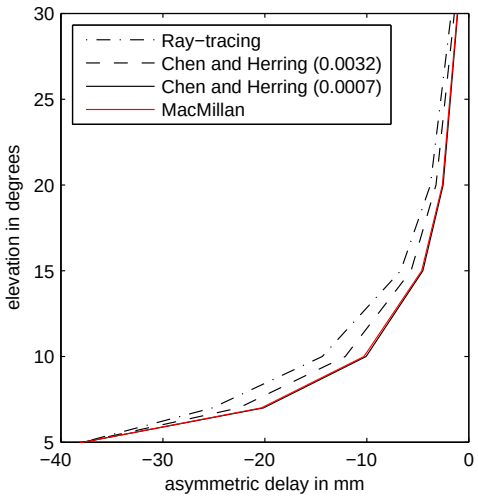

Fig. 1 Asymmetric delays towards east at station Wettzell on 1 January 2008. The gradient mapping functions were scaled to agree with the ray-traced delays at 5 degrees elevation. A coefficient C of about 0.0060 would agree best with the ray-traced delays in the range of elevations shown in the figure.

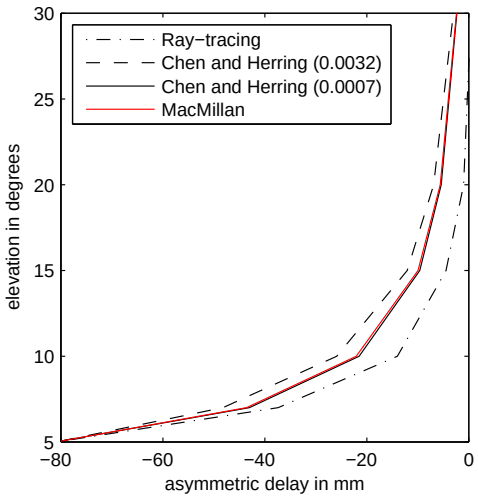

Fig. 2 Asymmetric delays towards west at station Tsukuba on 1 January 2008. The gradient mapping functions were scaled to agree with the ray-traced delays at 5 degrees elevation. A coefficient C of about -0.0030 would agree best with the ray-traced delays in the range of elevations shown in the figure.

Figure (3) shows north gradients from DAO (MacMillan and Ma, 1997) and APG (Böhm et al., 2011b) for all VLBI stations. Clearly visible is the atmospheric bulge above the equator which causes the north gradients to be slightly negative in the northern and slightly positive in the southern hemisphere. However, there

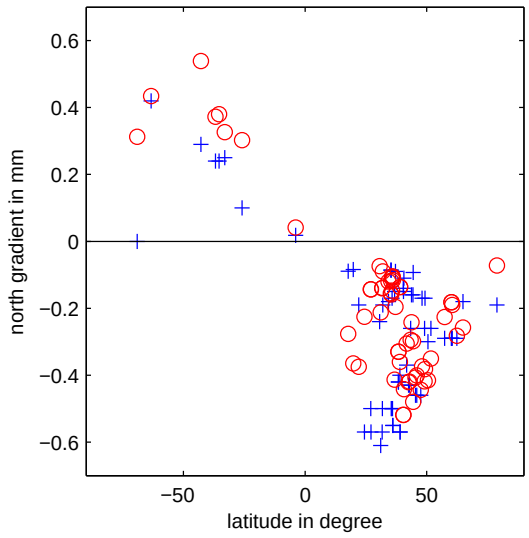

Fig. 3 North gradients in mm versus station latitude as derived from DAO by vertical integration (+) and by ray-tracing through ECMWF data as provided with APG (o).

is a quite good agreement between the gradients derived by two completely different approaches and different weather models.

4 VLBI analysis

Böhm et al. (2011b) carried out investigations with APG in the analysis of Global Positioning System (GPS) observations, and they found that the north gradients from APG are generally larger than the north gradients estimated in GPS analysis. The reason for this is not clear, but possible contributions might come from the sky distribution at the stations which is not uniform or from the downweighting of observations at low elevations (Urquhart et al., 2011). Spicakova et al. (2011) showed the importance of constraints (on zero a priori gradients) in the early years of VLBI observations up to about 1990. If those constraints are not applied, estimated gradients get unrealistically large and impact station coordinates significantly.

We compared three different VLBI solutions for the years 1990.0 to 2011.0 (Spicakova et al., 2011) obtained with the Vienna VLBI Software (VieVS) (Böhm et al., 2011a). In the first solution we estimated gradients as piecewise linear offsets every six hours with relative constraints (0.5 mm after six hours) but without absolute constraints. In the second solution we fixed the gradients to the values from APG, and in the third solution we fixed the gradients to the values from DAO. The criterion for a good a priori gradient model is that the estimated station coordinates are close to those station coordinates estimated in the first solution.

Figure (4) shows the differences in the north components with respect to the first solution. Clearly visible are the smaller differences in the station north components for DAO gradients compared to APG gradients, in particular in Asia and Europe. This is also confirmed by the station up components shown in Figure (5).

However, as soon as gradients are estimated (with no or loose constraints), it is no longer of importance which a priori gradients are used and the station coordinates agree.

5 Conclusions

We recommend using the gradient mapping function as introduced by Chen and Herring (1997) (Eq. (3)) with the coefficient $C = 0.0032$ for the mapping of a priori gradients as well as for the estimation of gradients. The application of the same gradient mapping function by different space geodetic techniques is the prerequisite for a rigorous combination of gradients.

For the analysis of VLBI sessions up to 1990, we recommend constraining the gradient estimates to DAO gradients, as introduced by MacMillan and Ma (1997). After 1990, when the number of stations per session is larger and the sky distribution with sources at the stations is more uniform, the choice of the a priori gradients is less important because gradients can be estimated reliably.

There is the plan to revise the gradient model APG by using a better resolution than just degree and order 9, or - similar to DAO - to determine those gradients for every station specifically. On the other hand, we will investigate and revive the application of the six-hourly linear horizontal gradients (Böhm and Schuh, 2007) which are available for all VLBI sites since 2006 at the GGOS Atmosphere Server.

6 Acknowledgements

We like to acknowledge the International VLBI Service for Geodesy and Astrometry (IVS) (Schlüter and Behrend, 2007) for providing their data and products, and the Austrian Weather Service (ZAMG) for granting access to the data of the ECMWF. Hana Spicakova is grateful to the Mondi Austria Privatstiftung for financial support during her PhD study at TU Vienna.

References

J. Böhm, and H. Schuh. Troposphere gradients from the ECMWF in VLBI analysis. *J Geod*, 81(6-8):403-408, doi: 10.1007/s00190-007-0144-2, 2007.

J. Böhm, S. Böhm, T. Nilsson, A. Pany, L. Plank, H. Spicakova, K. Teke, and H. Schuh. The new Vienna VLBI Software VieVS. Geodesy for Planet Earth, *Proceedings of the 2009 IAG Symposium*, Buenos Aires, Argentina, 31 August 2011 - 4 September 2009, International Association of

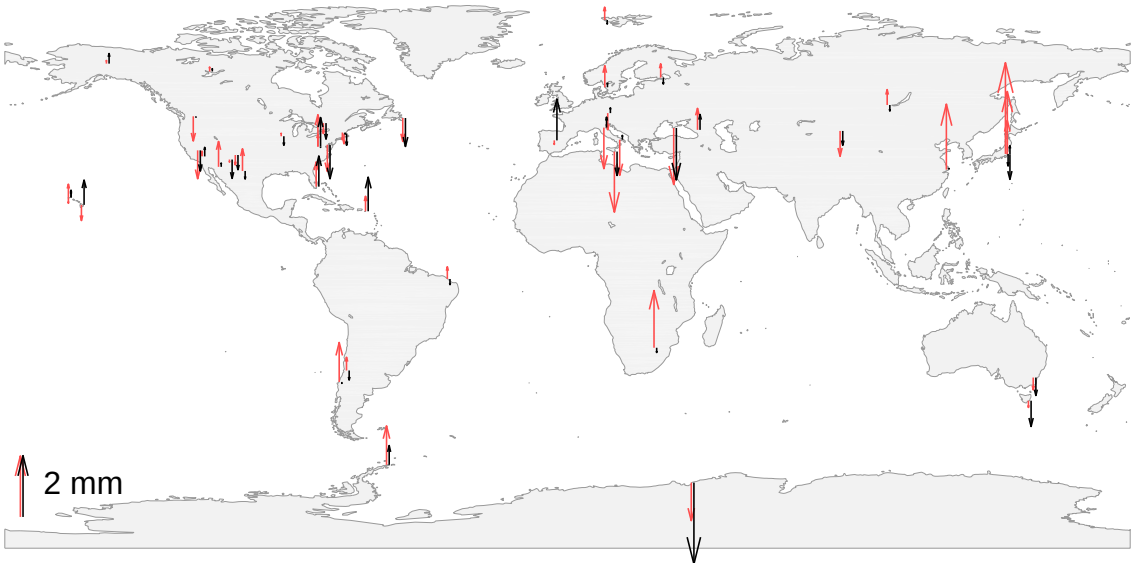

Fig. 4 Station north components with fixed APG (red) and DAO gradients (black), compared to a solution with gradients estimated.

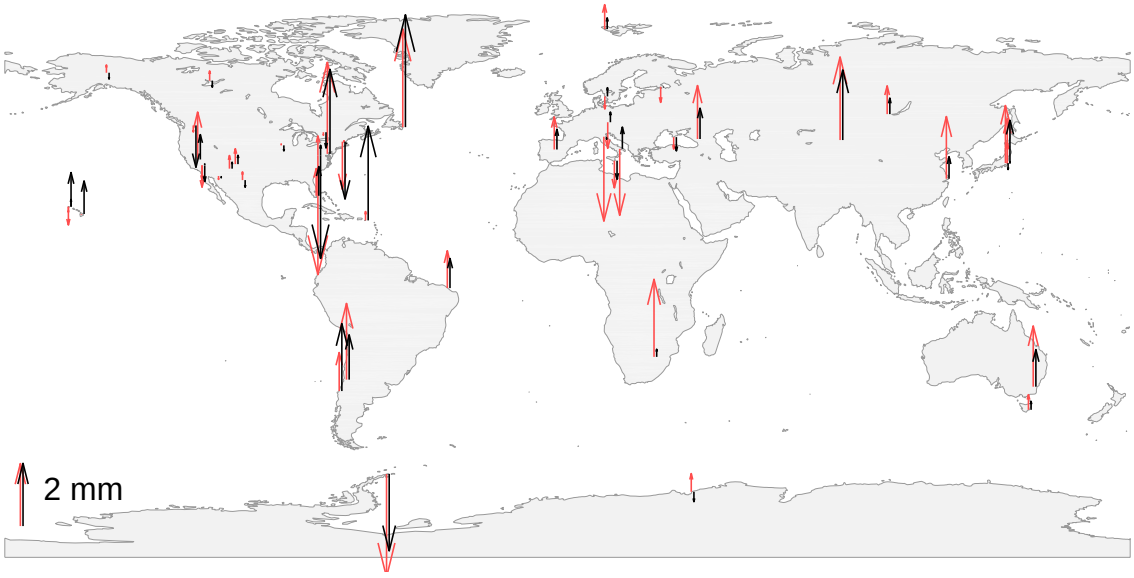

Fig. 5 Station up components with fixed APG (red) and DAO gradients (black), compared to a solution with gradients estimated.

Geodesy Symposia Series, Vol. 136, S. Kenyon, M.C. Pacino, U. Marti (eds.), ISBN 978-3-642-20337-4, 2011a.

J. Böhm, L. Urquhart, P. Steigenberger, R. Heinkelmann, V. Nafisi, and H. Schuh. A priori gradients in the analysis of space geodetic observations. Submitted to *Proceedings of the IAG Commission 1 Symposium 2010 (REFAG2010)*, Paris, France, 4-8 October 2010, International Association of Geodesy Symposia Series, X. Collileux, Z. Altamimi (eds.), 2011b.

G. Chen, and T.A. Herring. Effects of atmospheric azimuthal asymmetry on the analysis of space geodetic data. *J Geophys Res*, Vol. 102, No. B9, pp. 20489-20502, doi: 10.1029/97JB01739, 1997.

J. L. Davis, G. Elgered, A. E. Niell, and C. E. Kuehn. Ground-based measurement of gradients in the "wet" radio refractivity of air. *Radio Science*, Vol. 28, No. 6, pp. 1003-1018, doi: 10.1029/93RS01917, 1993.

T. A. Herring. Modeling atmospheric delays in the analysis of space geodetic data. In *Publications on Geodesy*, Vol. 36, *Proceedings of Refraction of Transatmospheric Signals in Geodesy*, J.C. DeMunck, Th. Spoelstra (eds.), pp. 157-164, Netherlands Geodetic Commission Publications in Geodesy, The Hague, Netherlands, 1992.

D. S. MacMillan. Atmospheric gradients from very long baseline interferometry observations. *Geoph Res Letters*, Vol. 22, No. 9, pp. 1041-1044, doi: 10.1029/95GL00887, 1995.

D. S. MacMillan, and C. Ma. Atmospheric gradients and the VLBI terrestrial and celestial reference frames. *Geoph Res Letters*, Vol. 24, No. 4, pp. 453-456, doi: 10.1029/97GL00143, 1997.

G. Petit, and B. Luzum (eds.). IERS Conventions (2010). *IERS Technical Note 36*, Frankfurt am Main: Verlag des Bundesamts für Kartographie und Geodäsie, 2010.

S. D. Schubert, J. Pjaendtner, and R. Rood. An assimilated data set for Earth science applications *Bull Am Meteorol Soc*, 74(12), pp. 2331-2342, 1993.

W. Schlüter, and D. Behrend. The International VLBI Service for Geodesy and Astrometry (IVS): current capabilities and future prospects. *J Geod*, Vol. 81(6-8):379-387, doi: 10.1007/s00190-006-0131-z, 2007.

H. Spicakova, L. Plank, T. Nilsson, J. Böhm, and H. Schuh. Terrestrial reference frame solution with the Vienna VLBI Software VieVS and implication of tropospheric gradient estimation. *Proceedings of the 20th Meeting of the European VLBI Group for Geodesy and Astrometry (EVGA)*, this issue, 2011.

L. Urquhart, F. G. Nievinski, M. C. Santos. Ray-traced Slant Factors for Mitigating the Tropospheric Delay at the Observation Level. Submitted to *J Geod*, 2011.

Application of ray-tracing through the high resolution numerical weather model HIRLAM applying the Conformal Theory of Refraction

S. Garcia-Espada, R. Haas, F. Colomer

Abstract In space geodetic techniques like VLBI and GPS, accuracy is limited by atmospheric propagation effects by neutral atmosphere in the troposphere. In recent years numerical weather models (NWM) have been applied to improve mapping functions which are used for tropospheric delay modeling in VLBI and GPS data analyses. A troposphere correction model applying ray-tracing through the Limited Area numerical weather prediction (NWP) HIRLAM 3D-VAR model and applying the Conformal Theory of Refraction is developed. The advantages of HIRLAM model are the high spatial resolution (0.2°x0.2°) and the high temporal resolution in prediction mode (every 3 hours). The advantages of the Conformal Theory of Refraction (Moritz, 1967) is that the atmospheric propagation effects are evaluated along the line of sight and the known vacuum elevation angle is used so no iterative calculations are needed. When ray-tracing through HIRLAM profiles and calculating the slant delays using the Conformal Theory of Refraction, we include the effect of an inhomogeneous atmosphere in the slant delays values.

Keywords HIRLAM, NWM, ray-tracing, Conformal Theory of Refraction

1 Introduction

The electromagnetic signals on their way through the earth's atmosphere experience propagation delays. Troposphere delays are one of the main contributors to the total error and are usually taken into account by parametrization of atmosphere delays as unknown parameters which are estimated together with the other parameters of interest in the geodetic VLBI analysis data like gradients, clocks or station positions. The propagation delays relate to the refractivity of the medium which in the so-call neutral atmosphere is influenced by temperature, pressure and humidity.

In recent years, regional-scale NWMs have improved in terms of accuracy and precision. Thus it appears to be reasonable to calculate slant delays by ray-tracing through these NWMs and to apply these slant delays as external information for the analysis of space geodetic data.

Susana Garcia-Espada and Francisco Colomer
National Geographic Institute (IGN)
Apartado 148, E-19080 Yebes (Guadalajara), Spain
Susana Garcia-Espada and Rüdiger Haas
Chalmers University of Technology,
Department of Earth and Space Science
Onsala Space Observatory, SE-43992 Onsala, Sweden

2 HIRLAM Numerical Weather Model

The HIRLAM project[1] has been established in order to provide the best available operational short-range forecasting system for the National Meteorological Services in Denmark, Finland, Iceland, Ireland, Netherlands, Norway, Spain and Sweden. Meteo-France has a research cooperation agreement with HIRLAM. The HIRLAM system is a complete NWP system including data assimilation with analysis of conventional or non-conventional observations and a limited area forecasting model with a comprehensive set of physical parametrization. The forecast model is a limited area model with a boundary relaxation scheme. The model exists both in a grid-point version and in a spectral version. Initial and boundary conditions are taken from European Centre for Medium Range Weather Forecast (ECMWF). The HIRLAM model is a synoptic scale model which means it is displaying conditions simultaneously over a broad area. It is a numerical short-range ($<$ 48 h) weather forecasting system. The advantage of the HIRLAM model are its high spatial resolution (22 km to 5 km horizontally (Fig. (1)), 16 to 60 levels vertically) and high temporal resolution (6 hours assimilation data and analysis and prediction at 00h, 06h, 12h, 18h; 3 hours cycle also available).

3 Conformal Theory of Refraction

The optical path length σ between a fixed origin and a variable point is described by the Eikonal equation, $(grad\sigma)^2 = n^2$ which

[1] Synoptic scale model HIRLAM, http://hirlam.org/

Fig. 1 HIRLAM horizontal grid.

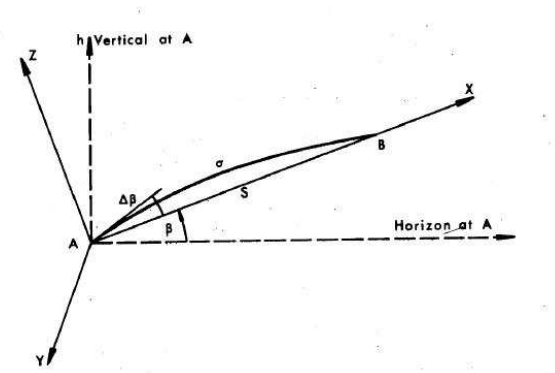

Fig. 2 Local system defined in the Conformal Theory of Refraction showing the effects of wave propagation through the atmosphere (Moritz, 1967).

is a first order partial differential equation for the optical distance σ, and corresponds to the well known principle of Fermat which states that light or other electromagnetic waves will follow the path between two points which involves the minimum travel time.

The Conformal Theory of Refraction was derived as an approximate solution of the calculation of the optical path length, and the vertical and lateral angles of refraction which include the solution of the Eikonal equation in the equations (Moritz, 1967). Figure (2) shows the local system defined by Moritz (1967) to develop the Conformal Theory of Refraction. The extra path delay can be written:

$$\Delta S = 10^{-6} \int_0^S N dX - \frac{1}{2} 10^{-12} \int_0^S [(\int_0^S \frac{dN}{dY} \varepsilon d\varepsilon)^2 + (\int_0^S \frac{dN}{dZ} \varepsilon d\varepsilon)^2] \frac{dX}{X^2}$$

where ε denotes only an integration variable along the chord (Moritz, 1967).

If we neglect the small effect of the curvature due to lateral refraction caused by the gradient $\frac{dN}{dY}$ assuming it is approximately 0, and if we replace the gradient $\frac{dN}{dZ}$ perpendicular to the chord AB, with sufficient accuracy, by the vertical gradient of refractivity like:

$$\frac{dN}{dZ} = cos\beta (\frac{dN}{dh})$$

where β is the vacuum elevation angle. Then both simplifications lead finally to the practical approximation:

$$\Delta S = 10^{-6} \int_0^S N dX - \frac{cos^2\beta}{2} 10^{-12} \int_0^S (\int_0^S (\frac{dN}{dh}) \varepsilon d\varepsilon)^2 \frac{dX}{X^2}$$

where $\frac{dN}{dh}$ stands for the vertical gradient of the refractivity N, β is the vacuum elevation angle and ε denotes only an integration variable along the chord AB (Brunner and Angus-Leppan, 1976). The main advantage is that atmospheric propagation effects are evaluated along the known chord line AB and not along the unknown wave path. The second advantage is that the vacuum elevation angle β is used so no iterative calculations are needed.

4 Application

We calculated the slant delay caused by the neutral atmosphere via ray-tracing through the numerical weather model HIRLAM applying the Conformal Theory of Refraction equation for the analysis of 15 geodetic European VLBI experiments from EURO75 (22^{nd} March 2005) to EURO89 (3^{rd} September 2007). Twelve stations were involved: Crimea in Ukraine, Dss65a in Spain; Matera, Noto, and Medicina in Italy; Metsähovi in Finland; Ny-Ålesund in Norway; Onsala in Sweden; Svetloe and Zelenchukskaya in Russia and Wettzell and Effelsberg in Germany. Badary station in Russia was also involved in EURO87 but it is not included in HIRLAM grid so we did not included it in the calculations.

We used HIRLAM files with 22 km horizontal resolution, 40 vertical levels and 6 hours time resolution (00h, 06h, 12h, 18h). We did interpolation in time for each scan of the mentioned geodetic VLBI experiments between the nearest time files. We did horizontal interpolation in the 40 km horizontal grid between the four nearest points profile around the station. We did interpolation in the vertical, we refined from 40 vertical levels to approximately 1000 layers, where the step size between them depends on the atmosphere height at each step. The atmosphere height was extrapolated to 136 km. The ray-tracing algorithm goes through the necessary number of HIRLAM vertical profiles depending on the ray (scan) elevation angle β until it crosses the complete atmosphere. For each step through the atmosphere, there is a horizontal and vertical interpolation of the ray point going through the atmosphere. Station heights were calculated over *WGS84* ellipsoid and undulations were calculated using the potential coefficient model *EGM86*. Stations heights were introduced to the HIRLAM vertical profile, in some cases it was necessary to interpolate or extrapole them in the vertical profiles, which means that the HIRLAM topography models differently the terrain topography depending on the location of the station.

To calculate the slant delay ΔS applying the Conformal Theory of Refraction (Moritz, 1967), we integrated through the elevation angle β of each observation starting at the station height.

We neglected the effect of curvature due to lateral refraction caused by $\frac{dN}{dY}$ assuming it is approximately 0. The size and number of the integration steps along the chord line of sight depend on the vacuum elevation angle β and the current height of the ray point in the atmosphere. We needed to find a compromise between the computing time and the number of integration steps, so we used approximately 250 integration steps for each ray. At each point we recalculated the angle β due to the *WGS84* ellipsoid. The calculated slant delay is azimuth angle dependence, it is the 'path delay' through the 3D inhomogeneous atmosphere through the chord line.

5 Preliminary results

We estimated zenith wet delays (ZWD) for all the stations involved in the CONT08 experiments to check that ray-tracing through HIRLAM is consistent with other techniques (Teke et al., 2010). In that case forecast and analysis HIRLAM profiles were combined, so we had a time resolution of 3 hours.

In order to check the Conformal Theory of Refraction we created a schedule in which all the scans had the same time epoch as previous estimated ZWD in CONT08 experiments and which observation elevation angle was 90° in all cases. Then, we calculated the slant delays for all scans at 90°, which is equivalent to calculate estimated ZWD. We can compare estimated ZWD through HIRLAM to the calculation of slant delays using the Conformal Theory of Refraction with an elevation angle of 90°.

Figure (3) shows time series of the differences of estimated ZWD through HIRLAM minus the calculated slant delays using the Conformal Theory of Refraction with elevation angles of 90°, for Wettzell station during CONT08 experiments. For this example, at Wettzell station the mean of the differences is 0.83 mm and the standard deviation of the mean is 0.02 mm. This differences are due to an improvement in the software. The interpolation in space was for estimated ZWD through HIRLAM assumed to be over an sphere and for the calculation of the slant delays at 90° the interpolation in space was calculated over the ellipsoid *WGS84*. For all the other stations in CONT08 we obtain values in the same order of magnitude.

In order to compare an homogeneous atmosphere versus an inhomogeneous atmosphere, we did a comparison of slant delays calculated using ray-tracing through HIRLAM model applying Raytrace software (Davis et al., 1987-1989) as presented in Garcia-Espada et al. (2010) and slant delays calculated using ray-tracing through HIRLAM model applying the Conformal Theory of Refraction explained in this paper. For the Raytrace software only one HIRLAM vertical profile is assumed as an homogeneous atmosphere around the station position. For the Conformal Theory of Refraction different vertical profiles are considered around the station position and the ray-scan crosses a different number of them depending on the corresponding elevation angle β. Figure (4) is a time series comparison between calculated slant delays for an homogeneous atmosphere versus an inhomogeneous atmosphere during EURO75 experiment for Effelsberg station. In this example, the maximum difference is 24.70 cm and the minimum differences is 5.58 cm.

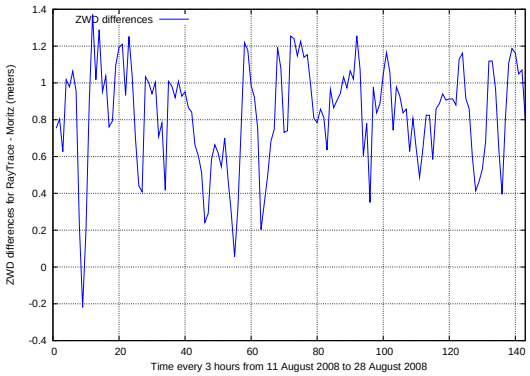

Fig. 3 Differences between estimated ZWD through HIRLAM minus calculated slant delays for scans with elevation angle 90° using the Conformal Theory of Refraction during CONT08 experiments at Wettzell station.

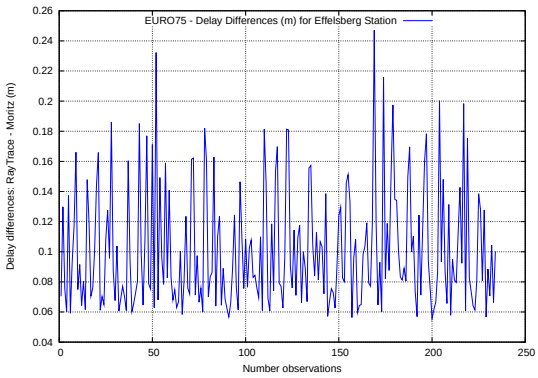

Fig. 4 Slant delays differences between Raytrace software (homogeneous atmosphere) and the Conformal Theory of Refraction (inhomogeneous atmosphere) ray-tracing through HIRLAM.

Station	# observations EURO75	Max diff (m)	Min diff (m)
Effelsberg	234	0.25	0.06
Medicina	263	0.37	0.05
Onsala60	214	0.33	0.05
Nyales20	190	0.35	0.05
Wettzell	225	0.37	0.06
Noto	164	0.29	-0.18

Table 1 Maximum and minimum differences between calculated slant delays with Raytrace software minus calculated slant delays with the Conformal Theory of Refraction for all stations involved in EURO75.

Table (1) shows as an example for EURO75, the maximum and minimum differences between calculated slant delays with Raytrace software minus calculated slant delays with the Conformal Theory of Refraction for the 6 stations involved in the experiment: Effelsberg and Wettzell in Germany, Medicina and Noto in Italy, Onsala60 in Sweden and Nyales20 in Norway.

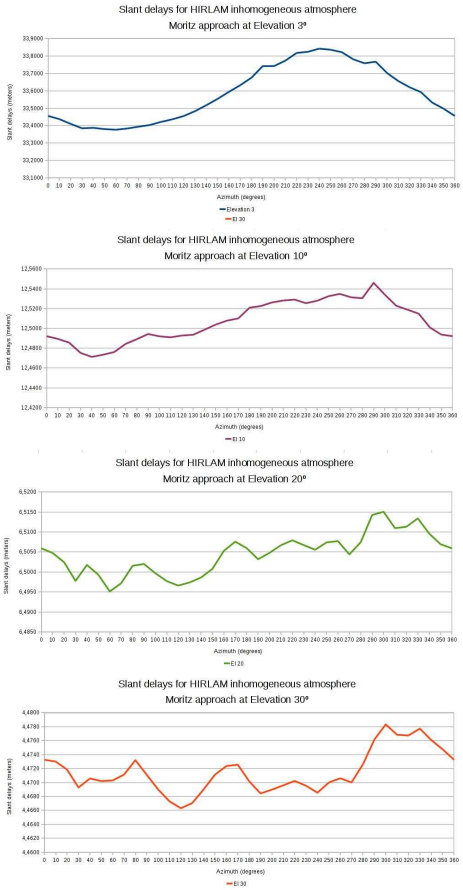

Fig. 5 Calculated slant delays for elevation angles 3°, 10°, 20° and 30° in an inhomogeneous atmosphere using the Conformal Theory of Refraction through HIRLAM for Effelsberg station (25^{th} March 2005 at 12:00 - start time for EURO75).

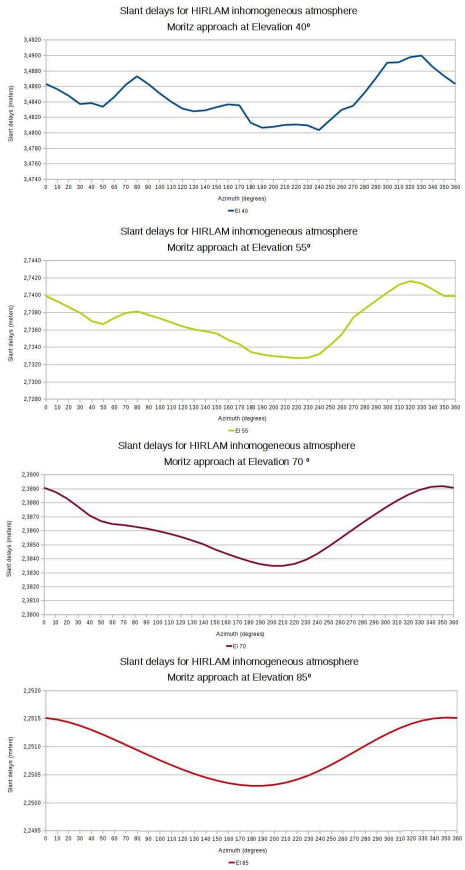

Fig. 6 Calculated slant delays for elevation angles 40°, 55°, 70° and 85° in an inhomogeneous atmosphere using the Conformal Theory of Refraction through HIRLAM for Effelsberg station (25^{th} March 2005 at 12:00 - start time for EURO75).

First preliminary results show differences between the calculated slant delays in an homogeneous and in an inhomogeneous atmosphere. The maximum differences correspond to lower elevations while minimum differences correspond to higher elevations.

Figures (5) and (6) show calculated slant delays using the Conformal Theory of Refraction ray-tracing through HIRLAM for different elevations angles for Effelsberg station during 25^{th} March 2005 at 12:00 (start time for EURO75).

6 Conclusions

We have calculated slant delays modelling an homogeneous and inhomogeneous atmosphere. While using Raytrace software approach simplifies to an homogeneous atmosphere, the Conformal Theory of Refraction approach includes the effect of an inhomogeneous atmosphere in the slant delay calculations. The differences between approaches are mainly the inhomogeneous atmosphere contributions. Comparisons of estimated ZWDs and calculated slant delays with elevation 90° using the Conformal Theory of Refraction is in the order of 1 mm level due to improvements in the interpolation software. We calculate more precisely and accurately slant delays using the Conformal Theory of Refraction. We will continue to compare calculated slant delays using the Conformal Theory of Refraction ray-tracing through HIRLAM to other NWM e.g. ECMWF and other approaches e.g KARAT. We will analyze the 15 geodetic VLBI European data using the calculated slant delays as a priori.

References

J. Böhm, H. Schuh, Vienna Mapping Functions in VLBI Analyses, *IVS 2004 General Meeting Proceedings*, p.277-281

F. K. Brunner and P.V. Angus-Leppan, On the significance of meteorological parameters for terrestrial refraction. *Unisurv G*, 25, 95-108

J. L. Davis, T.A.H. Herring and A.E. Niell, The Davis/Herring/Niell Raytrace program, 1987-1989

S. Garcia-Espada, R. Haas, and F. Colomer, Application of raytracing through the high resolution numerical weather model HIRLAM for the analysis of European VLBI, *6th IVS General Meeting Proceedings*, Hobart, Australia, 2010

T. A. Herring, Modelling atmospheric delay in the analysis of space geodetic data, *Proceedings of Symposium on Refaction of Transatmospheric Signals in Geodesy*, J.C. de Munck and T.A.Th. Spoelstra (eds.), Netherlands Geodetic Commission, Publications on Geodesy, No. 36, New Series, 157-164, 1992

T. Hobiger, R. Ichikawa, Y. Koyama, and T. Kondo, Fast and accurate ray-tracing algorithms for real-time space geodetic applications using numerical weather models, *Journal of Geophysical Research*, VOL. 113, D20302, doi:10.1029/2008JD010503, 2008

H. Moritz Application of the Conformal Theory of Refraction. *Österr. ZfV*, Sonderband 25, pages 323-334, 1967

A. E. Niell Preliminary evaluation of atmospheric mapping functions based on numerical weather models. *Physics and chemistry of the Earth*, 26, 475-480, 2001

B. Stoyanov, R. Haas, L. Gradinarsky, Calculating Mapping Functions from the HIRLAM Numerical Weather Prediction Model, In: In: IVS 2004 General Meeting Proceedings, p.471-475

K. Teke, J. Boehm, T. Nilsson, H. Schuc, P. Steigenberger, R. Dach, R. Heinkelmann, P. Willis, R. Haas, S. Garcia-Espada, T. Hobiger, R. Ichhikawa, S. Shimizu, 2010, Multi-technique comparison of troposphere zenith delays and gradients during CONT08. *Journal of Geodesy* In press

Strategy to Improve the Homogeneity of Meteorological Data in *Mark3* Databases

K. Le Bail, J. M. Gipson

Abstract Errors in modeling the troposphere is a major part of the error budget in VLBI processing, making the meteorological data very important. Summary tables of missing meteorological data point to the lack of data for important stations in the network (Zelenchukskaya during the CONT08 campaign for example). As a first step in this paper, we study the impact of erroneous meteorological data on the VLBI processing and show that they directly impact the quality of the VLBI solution: the scatter of baseline length WRMS is affected at a significant level (up to 1 mm for 10 years of data), as well as the determination of the Up component: the case of Svetloe during CONT08 shows a linear correlation of 8.9mbar/mm in the case of an offset in pressure. We analyze Westford over the period January 2002 to April 2010, using different sources of meteorological data in the processing: ECMWF, other on-site recorded meteorological data, such as a sensor associated with GPS receivers, and the default value used by *Calc/Solve*. We conclude that using a constant default value in *Calc/Solve* to replace missing meteorological data is not satisfying.

Keywords Meteorological Data, *Calc/Solve*, *Mark3* databases, VLBI processing

1 Introduction

Pressure and temperature data contribute in the VLBI processing in a very significant way. Many studies show the impact of this data via atmospheric modeling, e.g., Davis et al. (1985), Niell (1996), and more recently, Heinkelmann et al. (2009) and Nilsson et al. (2009), to cite only a few. Other studies show the discrepancy found between sensors on the same site and the importance of precise meteorological sensors and homogeneous recording of pressure and temperature, see Niell (2005).

Considering the above studies with great interest, we decided to determine what is in the *Mark3* databases. We constructed yearly tables gathering all the information on pressure and temperature. An example is given in Figure (1) for the year 2008. The crosses indicate missing meteorological data for the stations observing during the session, while the large dots indicate the presence of meteorological data in the database. The small dots indicate the station does not participate in the session. For 2008, the CONT08 campaign stands out: only eleven stations are participating continuously. In this figure, we also see that for some stations, like Fortaleza and Zelenchukskaya, two major stations in the network, more than 90% of the meteorological data is missing in 2008. In the case of Westford, the meteorological data are provided in the past years, by a sensor from the SuoMinet network (an international network of GPS receivers, *http://www.unidata.ucar.edu/data/suominet/*). The absence of data during the last trimester of 2008 show that those data have not been uploaded. When looking at the other years, the same remarks are still valid: some of the major stations are missing a large amount of meteorologic data, other stations change the source of meteorologic data. To emphasize the impact of such discrepancies, we focused on different periods. First we analyzed the eleven stations of the CONT08 campaign, and we show results for Svetloe and Zelenchukskaya. We also studied Westford from January 2002 to April 2010, considering only the R1 and R4 sessions. The results obtained are presented in section 2 of this paper. In section 3 we discuss a strategy to obtain a homogeneous data set and give conclusions of this study.

2 Impact of erroneous meteorological data in the VLBI processing

2.1 Comparison with ECMWF data and pressure offset: the case of Svetloe

Figure (2) compares the pressure found in the database with pressure from the ECMWF model (derived at the Vienna Institute for use with the VMF, Boehm and Schuh, 2004) for Svetloe. There is an offset of about 10mbar over the CONT08 period. To study the effect of this offset, we performed different simulations, subtracting a constant value (2mbar, 5mbar and 10mbar) from the pressure in the database for only Svetloe, and then we solved for station positions over the CONT08 period for the eleven stations.

Karine Le Bail and John M. Gipson
NVI Inc / NASA Goddard Space Flight Center, Greenbelt, MD 20770, U.-S.

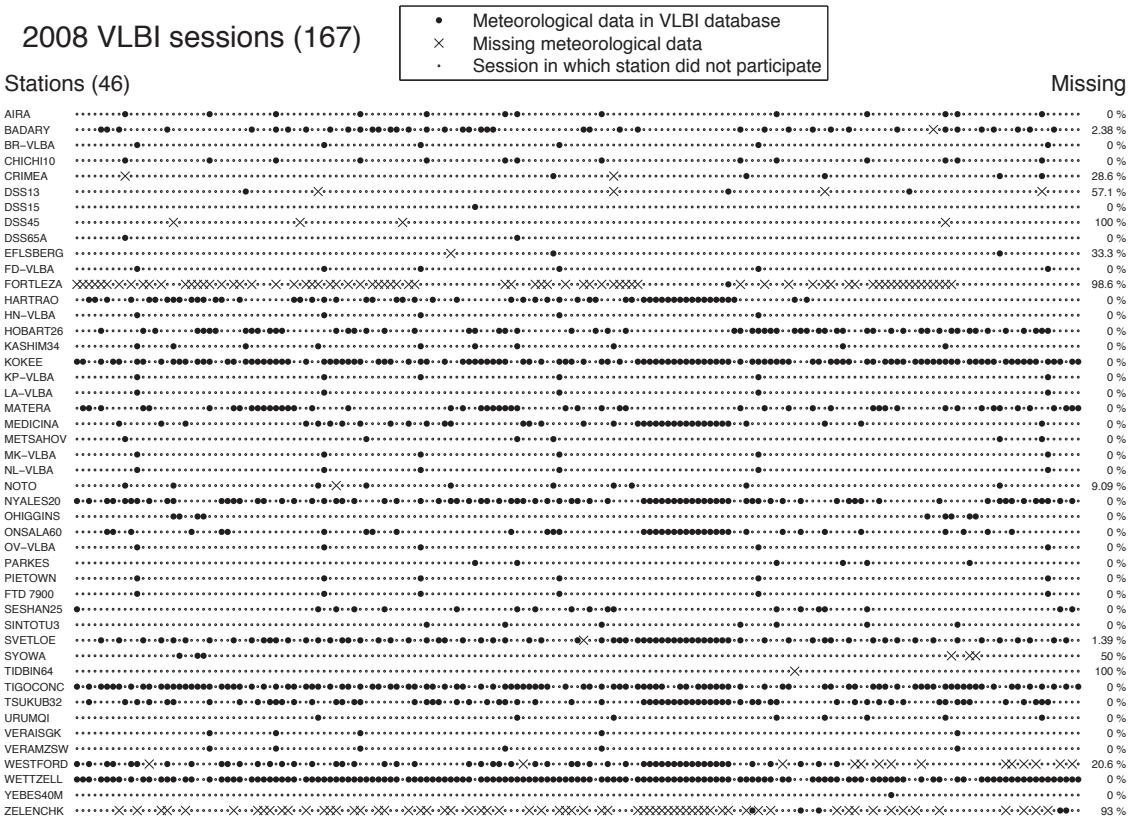

Fig. 1 Summary table of the presence of meteorological data in the *Mark3* databases for the year 2008

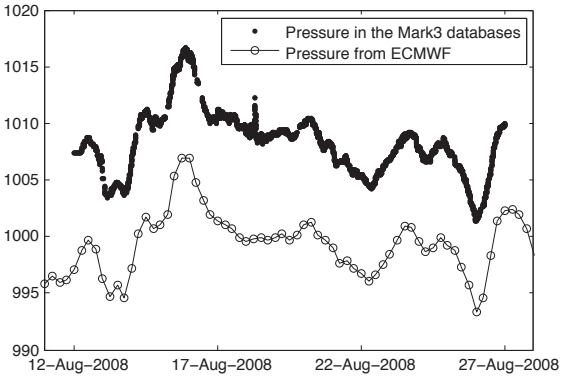

Fig. 2 Pressure in mbar for the station Svetloe during the campaign CONT08, as in *Mark3* databases and as obtained using ECMWF model

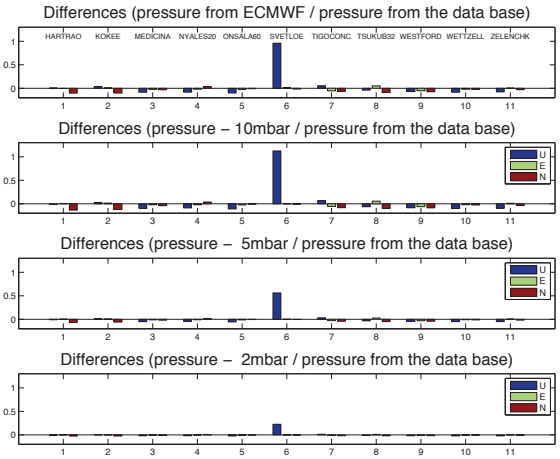

Fig. 3 Changes in position of the eleven CONT08 stations between using for Svetloe either the *Mark3* databases pressure or a modified pressure (ECMWF or biased value)

In Figure (3), we plot the differences in U, E, N determination using the pressure from the database wrt a modified pressure: 1). the ECMWF pressure, 2). the database pressure minus 10mbar, 3). minus 5mbar, 4). minus 2mbar. The major effect is on the Up component determination of Svetloe. The Figure (4) plots the differences of the Up component of Svetloe versus the difference in pressure (10mb, 5mbar and 2mbar). A straight line is estimated and perfectly fits the three points: the slope has a value of 8.9mbar/mm.

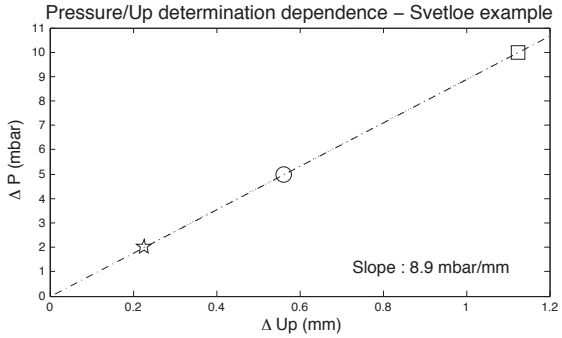

Fig. 4 Dependence in pressure and Up determination for the station Svetloe

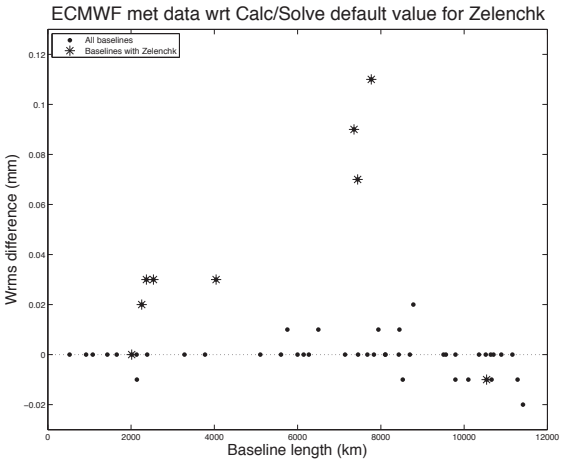

Fig. 5 Differences in WRMS between using for Zelenchukskaya the *Calc/Solve* default value pressure and using ECMWF pressure, in function of the baseline lengths during CONT08. The baselines with Zelenchukskaya are indicated with a star

2.2 *Default value in Calc/Solve*

In the case of missing data, the strategy adopted in *Calc/Solve* is to use a fixed and constant value. To quantify the effect, we studied two examples: Zelenchukskaya over a period of two weeks (CONT08) and Westford over a period of nine and a half years.

2.2.1 The case of Zelenchukskaya during the CONT08 campaign

Zelenchukskaya is studied over the CONT08 period. We compute solutions using in one case the *Calc/Solve* value, and, in the other, the ECMWF value. Figures (5) and (6) show the impact of this strategy. In Figure (5) we plot the difference in WRMS of the scatter in baseline lengths as a function of baseline length. The points in the upper half of the plot show a reduction in WRMS in using the ECMWF meteorological data rather than the default value. This improvement in WRMS is up to 0.12mm for some of the baselines. Figure (6) is the graph of differences in the Up component determination affecting the eleven stations of CONT08. The impact is mostly on the Zelenchukskaya Up component with a displacement of 0.31mm.

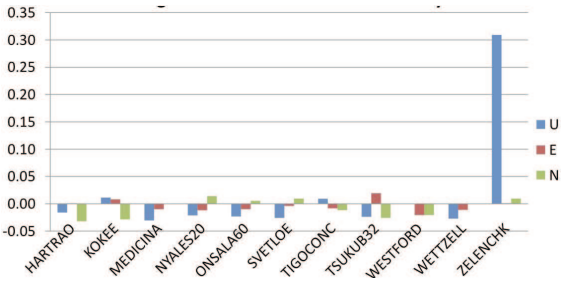

Fig. 6 Effect on using ECMWF meteorological data at Zelenchukskaya instead of the *Calc/Solve* default value. Changes in position of the eleven stations of CONT08

2.2.2 The case of Westford over the period January 2002 to April 2010

To study Westford, we use data from 351 R1 and R4 sessions from January 2002 to April 2010. The pressure and temperature are collected from 1). The *Mark3* databases, 2). The ECMWF data, and 3). The sensor of the SuoMinet network in Westford (SA01). We compare the results obtained using meteorological data from these three sets and using the default value of *Calc/Solve* when there is no meteorological data in the database. To give an idea of such differences, Figure (7) shows the data from the database and the default value (straight line) in the same plot. It is obvious that using a default value is not realistic. Once again, using meteorological data from the ECMWF or the SuoMinet sensor reduces the WRMS and changes the estimate of Up. In Figure (8), the crosses represent the baselines including Westford and in Figure (9), we plot the differences of the Up component. The differences in WRMS reaches up to 0.93mm (Badary - Westford baseline) and affects the Up component of both Badary and Westford by more than 0.1mm.

3 Discussion on a strategy proposed to obtain a homogeneous database and conclusions

In summary, meteorological data in the *Mark3* databases is not homogeneous as it contains missing, biased and inaccurate data. In some cases, the meteorological data in the database comes from another source that has been used to manually fill gaps in the time series (Westford case). This data is not necessarily consistent with existing data. Using the default value in *Calc/Solve* is not a satisfying solution either, as shown in the subsection 2.1.

For those reasons and to achieve continuity in the meteorological data, the data has to be cleaned. Two solutions are then possible.

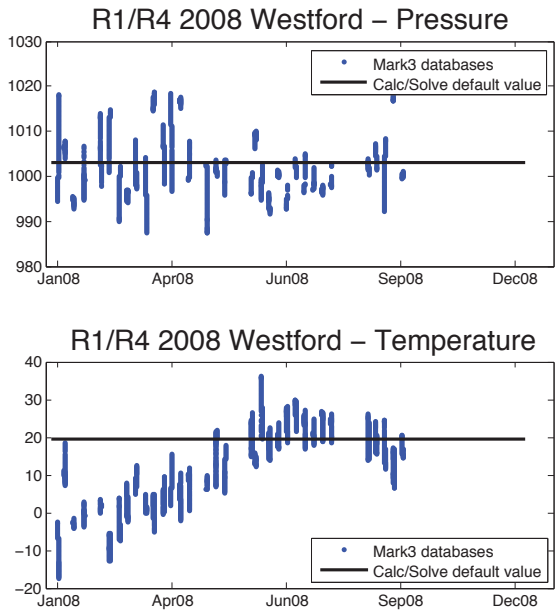

Fig. 7 Pressure and temperature values for Westford in the *Mark3* databases in 2008 and the *Calc/Solve* default value associated

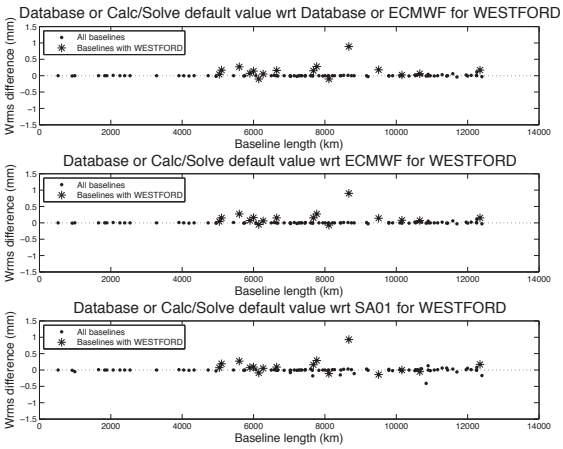

Fig. 8 Differences in WRMS between using different sources of meteorological data for Westford and using the *Mark3* values or the default value. R1 and R4 sessions from January 2002 to April 2010. The baselines with Westford are indicated with a star

The first one is to correct the *Mark3* databases to obtain a homogeneous set of meteorological data. This is a long and meticulous work that is currently underway at GSFC/NASA on the existing data. First, this consists of detecting all the bad data (by doing statistics on what is in the database, as well as comparison with other meteorological data) and to correct them with appropriate data, but also to search for accurate meteorological data in the case of missing ones.

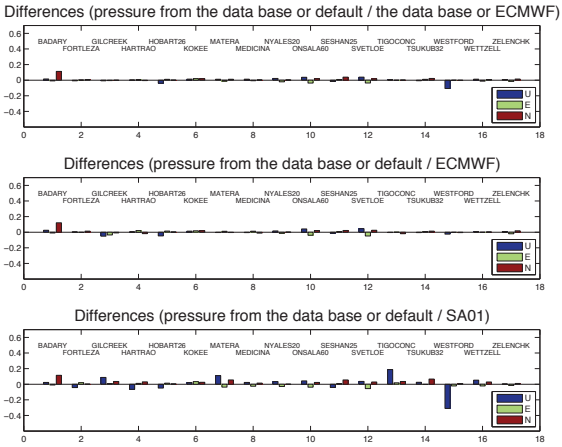

Fig. 9 Changes in VLBI stations position between, for Westford, using either the *Mark3* databases pressure or the *Calc/Solve* default value if no data in the databases, and using another set of pressure (ECMWF or meteorological sensor from the SuoMinet network at Westford)

The second solution is to have a homogeneous network of meteorological sensors associated to the point of measurement in the global network, observing and recording pressure and temperature continuously. Of course, this solution is not applicable to the existing data and database. But this supports the specification for the VLBI2010 stations, showing the importance of the two parameters pressure and temperature.

References

J. Boehm, and H. Schuh. Vienna Mapping Functions in VLBI analyses. In *Geophys. Res. Lett.*, volume 31, L01603, 2004.

J. L. Davis, T. A. Herring, I. I. Shapiro, A. E. E. Rogers, and G. Elgered. Geodesy by radio interferometry: Effects of atmospheric modeling errors on estimates of baseline length. In *Radio Science*, volume 20, pages 1593-1607, November-December 1985.

R. Heinkelmann, J. Boehm, H. Schuh, and V. Tesmer. The Effect of Meteorological Input Data on the VLBI Reference Frames. In H. Drewes, editor, *Geodetic Reference Frames*, International Association of Geodesy Symposia 134, Springer-Verlag Berlin Heidelberg, 2009.

A. Niell. Global mapping functions for the atmosphere delay at radio wavelengths. In *Journal of Geophysical Research*, volume 101(B2), pages 3227-3246, 1996.

A. Niell. SA01 (suominet) - WES2/Westford (GSOS) pressure comparison for 2005 doy 208 (2005/07/27). In *ECGVM MEMO, Massachusetts Institute of Technology, Haystack Observatory*, September 2, 2005.

T. Nilsson, and R. Haas. Impact of atmospheric turbulence on geodetic very long baseline interferometry. In *Journal of Geophysical Research*, volume 115, B03407, 2010.

Report on IVS-WG4

John Gipson

Abstract In 2007 the IVS Directing Board established IVS Working Group 4 on VLBI Data Structures. This note discusses the history of WG4, presents an overview of the proposed structure, and presents a timeline for next steps.

Keywords IVS Working Group IV, netCDF *Calc/Solve*, *Mark3* databases, VLBI processing

1 Introduction

At the 15 September 2007 IVS Directing Board meeting I proposed establishing a "Working Group on VLBI Data Structures". The thrust of the presentation was that, although the VLBI database system has served us very well these last 30 years, it is time for a new data structure that is more modern, flexible and extensible. This proposal was unanimously accepted, and the board established IVS Working Group 4 . Quoting from the IVS website (Gipson, 2007): "The Working Group will examine the data structure currently used in VLBI data processing and investigate what data structure is likely to be needed in the future. It will design a data structure that meets current and anticipated requirements for individual VLBI sessions including a cataloging, archiving and distribution system. Further, it will prepare the transition capability through conversion of the current data structure as well as cataloging and archiving softwares to the new system."

Changes to the VLBI data format affect everyone in the VLBI community. Hence it is important that the Working Group have representatives from a broad cross-section of the IVS community. Table (1) lists the original members of IVS WG4 together with their original affiliations.[1] The initial membership was arrived at in consultation with the IVS Directing Board. On the one hand, we wanted to ensure that all points of view were represented. On the other hand, we wanted to make sure that the size did not make WG4 unwieldy. The current composition and size of WG4 is a reasonable compromise between these two goals. My initial request for participation in WG4 was enthusiastic: everyone I contacted agreed to participate with the exception of an individual who declined because of retirement.

Chair	John Gipson
Analysis Center Director	Axel Nothnagel
Correlator Representatives	Roger Cappalo Colin Lonsdale
GSFC/Calc/Solve	David Gordon Leonid Petrov
JPL/Modest	Chris Jacobs Ojars Sovers
Occam	Oleg Titov Volker Tesmer
TU Vienna	Johannes Böhm
IAA	Sergey Kurdubov
Steelbreeze	Sergei Bolotin
Observatoire de Paris/PIVEX	Anne-Marie Gontier
NICT	Thomas Hobiger Hiroshi Takiguchi

Table 1 Original Membership in Working Group 4

2 History of Working Group 4

WG4 held its first meeting at the 2008 IVS General Meeting in St. Petersburg, Russia. This meeting was open to the IVS community. Roughly 25 scientists attended: 10 WG4 members, and 15 others. This meeting was held after a long day of proceedings. The number of participants and the ensuing lively discussion is strong evidence of the interest in this subject. A set of design goals, displayed in Table (2), emerged from this discussion. In some sense the design goals imply a combination and extension of the current VLBI databases, the information contained on the IVS session web-pages, and lots more information (Gipson, 2008, 2010).

John Gipson
NVI, Inc./NASA Goddard Spaceflight Center, Greenbelt, MD, 20770, USA

[1] Membership was subsequently reduced for various reasons: Colin Lonsdale resigned because of increased management responsibilities; Leonid Petrov left the Goddard VLBI group; And, most sadly the premature death of Anne-Marie Gontier.

Table 2 Key Goals of New Format

Goal	Description
Provenance	Users should be able to determine the origin of the data and what was done to it.
Compactness	The data structure should minimize redundancy and the storage format should emphasize compactness.
Speed	Commonly used data should be able to be retrieved quickly
Platform/OS /Language Support	Data should be accessible by programs written in different languages running on a variety of computers and operating systems.
Extensible	It should be easy to add new data types.
Open	Data should be accessible without the need of proprietary software.
Decoupled	Different types of data should be separate from each other.
Multiple data levels	Data should be available at different levels of abstraction. Most users are interested only in the delay and rate observables. Specialists may be interested in correlator output.
Completeness	All VLBI data required to process (and understand) a VLBI session from start to finish should be available: schedule files, email, logfiles, correlator output and final 'database'.
Web Accessible	All data should be available via the web

During the next year the WG4 communicated via email and telecon and discussed how to meet the goals that emerged from the St. Petersburg meeting. A consensus began to emerge.

The next face-to-face meeting of WG4 was held at the 2009 European VLBI in Bordeaux, France. This meeting was also open to the IVS community. At this meeting a proposal was put forward to split the data contained in the current Mark3 databases into smaller files which are organized by a special ASCII file called a wrapper. I summarized some of the characteristics and advantages of this approach. Overall the reaction was positive.

In the Summer of 2009 we worked on elaborating these ideas, and in July a draft proposal was circulated to Working Group 4 members. Concurrently I began a partial implementation of these ideas and wrote software to convert a subset of the data in a Mark3 database into the new format. This particular subset included all data in NGS cards and a little more. The subset was chosen because many VLBI analysis packages including Occam, Steelbreeze, and VIEVS can use NGS cards as input. In August 2009 we made available, via anonymous ftp, three VLBI sessions in the new format: an Intensive, an R1 and an RDV.

3 Overview of New Organization

In a paper as brief as this it is impossible to completely describe the new organization and format. Instead I briefly describe three of the key components: 1) Modularization; 3) Organize data through wrappers; 2) Storing data in netCDF files;

3.1 Modularization

A solution to many of the design goals of Table 3 is to modularize the data, that is to break up the data associated with a session into smaller pieces. These smaller pieces are organized by 'type', e.g: group delay observable; met-data; editing criteria; station names; station positions; etc. In many, though not all, cases, each 'type' corresponds to a Mark3 database L-code. Different data types are stored in different files, with generally only one or a few closely related data types in each file. For example, it might be convenient to store all of the met-data for a station together in a file. However, there is no compelling reason to store the met data together with pointing information. Splitting the data in this way has numerous advantages, some of which are outlined below. The first three directly address the design goals. The remaining are other advantages not originally specified, but are consequences of this design decision.

1. **Separable.** Users can retrieve only that part of the data they are interested.
2. **Extensible.** It is easy to add new data-types by specifying the data and file format for the new data.
3. **Decoupled.** Different kinds of data are separated from each other. Observables are separated from models. Data that won't change is separated from data that might change.
4. **Flexible.** Since different data is kept in different files, it is easy to add new data types.
5. **Partial Data Update.** Instead of updating the entire database, as is currently done, you only need to update that part of the data that has changed[2]

Data is also organized by 'scope', that is how broadly applicable it is: Does it hold for the entire session, for a particular scan, for a particular scan and station, or for a particular observation? Mark3 databases are observation oriented: all data is stored once for each observation. This results in tremendous redundancy for some data. For example, consider an $N-$station scan, with $(N-1)\times N/2$ observations, with each station participating in $N-1$ observations. Station dependent data, such as met or pointing data, will be the same for all observations involving a given station. Storing this data once per observation instead of once per scan results in an $(N-1)$ fold redundancy.

[2] This would be done by making a new version of the relevant file, keeping the old one intact.

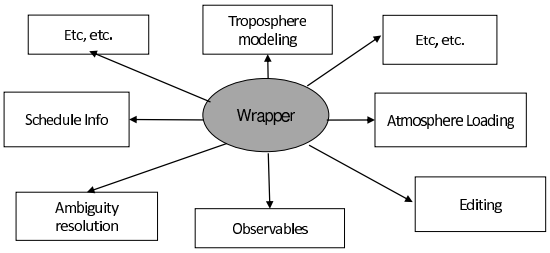

Fig. 1 Wrappers organize the data.

3.2 Organizing Data by Wrappers

The main disadvantage of breaking up the VLBI data into many smaller files is that you need some way of organizing the files. This is where the concept of a wrapper comes in. A wrapper is an ASCII file that contains pointers to VLBI files associated with a session. VLBI analysis software parses this file and reads in the appropriate data. As new data types are added, or as data is updated, new versions of the wrapper are generated. The wrapper concept is illustrated schematically in (2). The wrapper can serve several different purposes:

1. The wrapper can be used by analysis programs to specify what data to use.
2. Wrappers allows analysts to experiment with 'what if' scenario. For example, to use another analysts editing criteria all you need to do is modify the wrapper to point to to the alternative editing file.
3. Because of the general structure of the wrapper, different analysis packages can use different wrappers that point to different subsets of the VLBI data.
4. The wrapper is a convenient means of signaling to the IVS data center what information is required. In this scenario, a user writes a wrapper with pointers to the relevant files and sends it to the IVS data center. The data center packages the data in a tar file and makes it available.

3.3 netCDF as Default Storage Format

Working Group 4 reviewed a variety of data storage formats including netCDF, HCDF, CDF, and FITS. In some sense, all of these formats are equivalent since there exist utilities to convert from one format to another. Ultimately we decided to use netCDF because it has a large user community, and because several members of the Working Group have experience with using netCDF. Quoting from the Unidata web-site:[3]

> NetCDF (network Common Data Form) is a set of interfaces for array-oriented data access and a freely-distributed collection of data access libraries for C, Fortran, C++, Java, and other languages. The netCDF libraries support a machine-independent format for representing scientific data. Together, the interfaces, libraries, and format support the creation, access, and sharing of scientific data.

NetCDF data is:

- **Self-Describing**. A netCDF file includes information about the data it contains.
- **Portable.** A netCDF file can be accessed by computers with different ways of storing integers, characters, and floating-point numbers.
- **Scalable.** A small subset of a large dataset may be accessed efficiently.
- **Appendable.** Data may be appended to a properly structured netCDF file without copying the dataset or redefining its structure.
- **Sharable.** One writer and multiple readers may simultaneously access the same netCDF file.

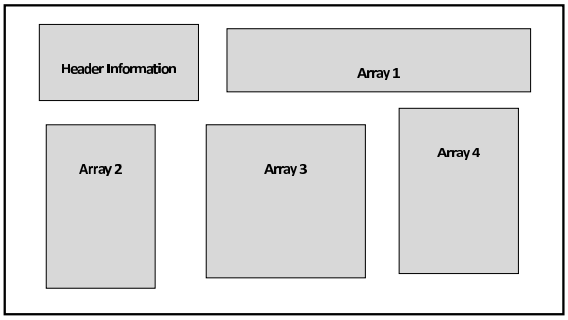

Fig. 2 A netCDF file is a container for arrays.

At its most abstract, netCDF is a means of storing arrays in files. The arrays can be of different sizes and shapes, and contain different types (in a programming language sense) of data – strings, integer, real, double, etc. Since most VLBI data is some kind of array using netCDF is a natural choice. These files can contain history entries which aid in provenance. Storing data in netCDF format has the following advantage:

1. **Platform/OS/Language Support.** NetCDF has interface libraries to all commonly used computer languages running on a variety of platforms and operating system.
2. **Speed.** NetCDF is designed for fast data access.
3. **Compactness.** Data is stored in binary format, and the overhead is low. A netCDF file is much smaller than an ASCII file storing the same information.
4. **Open.** NetCDF is an open standard, and software to read/write netCDF files is freely available.
5. **Large User Community.** There are many freely available programs to work with netCDF files.

[3] `www.unidata.ucar.edu/software/netCDF/docs/faq.html\#whatisit`

Because of the open architecture of this system, I propose calling the new format "VLBI OpenDB Format", or OpenDB for short.

4 Data Transition and Calc/Solve Issues

The starting point for most IVS-analysis packages is a "Version 4" Mark3-database[4]. A Version 4 database has all the ambiguities resolved and the data is edited to flag bad data. Version 4 databases are produced by *Calc/Solve*[5]. Hence any discussing of transitioning from Mark3 databases to OpenDB format must deal with the *Calc/Solve* transition as well.

It is useful to have an understanding of the key stages in the transformation of VLBI correlator output to a Version 4 database ready for distribution. The following describes the processing at Goddard. The details may differ at other institutions, but the fundamentals remain the same. Anytime data is added to a Mark3 database a new version is produced.

1. For each band *Dbedit* makes a Version 1 database from the correlator output. Typically this is X- and S-band, although a few sessions use other bands.
2. *Dbcal* inserts cable-cal and met, making a Version 2 database. Cable-cal and met data are used by most analysis packages.
3. *Calc* computes partials and a prioris, and creates a Version 3 database. In contrast to cable-cal and met data, although much of this information is required by *Solve*, it is not used by other analysis package.
4. *Interactive-Solve* is used to resolve ambiguities, edit the data, apply ionosphere corrections, and merge the X- and S-band database together. The Version 4 database is ready for distribution.
5. Many analysis packages use so-called "NGS cards". This is ASCII representation of a subset of the data in a Mark3 database. *Db2ngs* extracts and converts the data from the database.

By design, the Mark3 database contains almost all of the data required to analyze VLBI data.[6] However reading a Mark3 database is very slow. Because of this the Goddard VLBI group developed "superfiles" which contain a subset of the Mark3 database in binary form. Superfiles can be used in *Interactive-Solve*, but are typically used in *Global-Solve* which "stacks" individual sessions together to obtain, for example, estimates of station position and velocity, or source positions.

Since *Calc/Solve* is used to produce Version 4 databases, the IVS cannot completely transition to the OpenDB format until *Calc/Solve* is modified to handle it. A serious obstacle to modifying *Calc/Solve* is that it is operational software. We must make sure that it continues to work, and that at all stages we maintain continuity with previous versions. The conversion of *Calc/Solve* to use the new format is taking place in several steps.

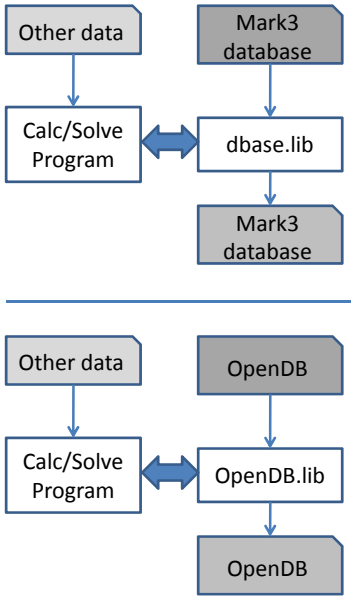

Fig. 3 Replacing dbase.lib with OpenDB.lib allows us to almost transparently produce OpenDB files.

1. To maintain compatibility with the current software, we are developing a replacement for the database library which will read and write OpenDB format. In terms of *Calc/Solve* the function calls will be identical. This minimizes changes to existing programs. This is illustrated schematically in Figure 3.
2. In the Summer of 2011 we will complete *db2OpenDB* which converts a Mark3 database into OpenDB format. Originally this just converted the data contained in NGS cards. Currently it converts about 90% of the data [7] in Mark3 databases.
3. I am modifying *Global-Solve* to use OpenDB format instead of superfiles. This process, begun in Fall 2010, should be also be complete in Summer 2011. Preliminary results indicate that there will be little, if any timing penalty. There may be even be a slight performance boost because of reduced I/O.

5 Next Steps

In the previous section I discussed the status of the *Calc/Solve* analysis software. Below I summarize the status of some other analysis packages.

[4] Perhaps in NGS card format.

[5] Here "*Calc/Solve*" refers to the entire suite of software developed to process and analyze Mark3 databases.

[6] A few notable exceptions include EOP, atmospheric loading, VMF data, and information about breaks in station position.

[7] This excludes some items obsolete or unused items such as the numerical value of π, or the speed of light.

- In the Fall of 2009 and in the Spring of 2010 the VLBI group at the Technical University of Vienna developed the interface to *VieVs*.
- Oleg Titov has begun re-writing Occam to use the new format.
- Thomas Hobiger has indicated that C5++ will be modified to use the new format.

In terms of transitioning to the new format:

1. We will make one year of VLBI data available in OpenDB format in July 2011. This will give software-developers something to work with.
2. Interfacing to the new format will give real world experience and may lead to fine-tuning of the specifications. The final specifications will be ready in Fall 2011.
3. In 2012 we will make available all VLBI data in OpenDB format.
4. We will present the final report of IVS WG4 at the 2012 General Meeting.

After the 2012 IVS General Meeting Working 4 will dissolve.

References

J. Gipson. `http://ivscc.gsfc.nasa.gov/about/wg/wg4/index.html` , 2007.

J. Gipson. IVS Working Group 4 on VLBI Data Structures. *The 5th IVS General Meeting Proceedings*, 2008.

J. Gipson. IVS Working Group 4: VLBI Data Structures. *The 6th IVS General Meeting Proceedings*, 2010.

Improved velocities of the ”Quasar” network stations

I. Gayazov, E. Skurikhina

Abstract VLBI observations performed after release of ITRF2008 have been used for improvement of velocities of the ”Quasar” network stations Svetloe, Zelenchukskaya and Badary. Obtained values of velocities being compared with those derived from GPS data show agreement within 1.5 mm/y. Baselines for VLBI antenna reference points and GPS antenna markers show the consistency within 10 mm for the epoch 2005.0 when taking into account local tie parameters.

Keywords Network stations, Coordinates and Velocities

1 Introduction

The new version of International Terrestrial Reference Frame – ITRF2008 (Altamimi et.al., 2011) is the combination of different space geodesy technique solutions with local ties at co-location sites. The agreement between local ties and space geodesy estimates of station coordinates has been carefully investigated when deriving the ITRF2008 solution. Nevertheless, for several co-location sites there were rather large discrepancies between these types of data. These discrepancies occurred not only in coordinates of co-located stations, but also in their velocities, especially for stations with short observational history.

For co-location sites which form regional networks with certain self-dependence the agreement between coordinates and velocities of various instruments at the site and local tie data is considered as definite criterion of quality. Namely in this context the Russian VLBI network ”Quasar” observatories (Badary – Bd, Svetloe – Sv, Zelenchukskaya – Zc) (Finkelstein et.al., 2008) are examined in the course of this work.

The consistency of geocentric coordinates of VLBI antenna reference points and GPS markers at the observatories of the ”Quasar” network has been tested earlier taking into account local tie parameters (Gayazov and Skurikhina, 2008). However, the velocities of co-located instruments of this network stations were derived independently in ITRF2008 and in result the additional errors arise. This is the case of co-located stations Zc and Bd of the ”Quasar” VLBI network. Differences of velocities determined in VLBI and GPS sub-frames of ITRF2008 for station Zc exceed 3 mm/y and for the Bd station differences between VLBI and DORIS results reach up to 5 mm/y (see Tab. (1)).

Therefore, VLBI observations performed after release of ITRF2008 have been used for improvement of velocities of the ”Quasar” network stations.

Station	Velocity components	ITRF2008 VLBI	ITRF2008 GPS	ITRF2008 DORIS
Sv	Vx, mm/y	-18.4	-18.2	
	Vy, mm/y	12.5	13.7	
	Vz, mm/y	8.4	9.0	
Zc	Vx, mm/y	-20.0	-22.2	
	Vy, mm/y	16.4	14.4	
	Vz, mm/y	11.6	9.2	
Bd	Vx, mm/y	-31.3		-26.2
	Vy, mm/y	-0.1		-0.1
	Vz, mm/y	-4.4		-3.8

Table 1 Comparison of velocities of the ”Quasar” network stations determined by various techniques

2 Improvement of Velocities

Regular VLBI observations at the ”Quasar” network observatories were carried out under series of IVS programs: IVS-R1, IVS-R4, EURO, VLBA, IVS-T2, IVS-Intensives. At the beginning of 2011 all diurnal sessions of VLBI observations (see Tab. (2)) with participation of these observatories have been processed by using OCCAM program package and the new series of their coordinates in ITFR2008 has been obtained (Fig. (1), (2), (3)). Velocities of VLBI antenna reference points of the observatories were calculated from these time series of coordinates.

Continuous GPS observations at the ”Quasar” network stations have more prolonged history than VLBI observations. At IGS network stations SVTL and ZECK GPS observations are

I. Gayazov, E. Skurikhina
Institute of Applied Astronomy, RAS,
Kutuzova 10, 191187 Saint Petersburg, Russia

Station	Time span	Number of sessions
Zc	2006.0 - 2011.0	161
Bd	2007.2 - 2011.0	97
Sv	2003.2 - 2011.0	218

Table 2 Data used for determination of VLBI antenna coordinates at the observatories

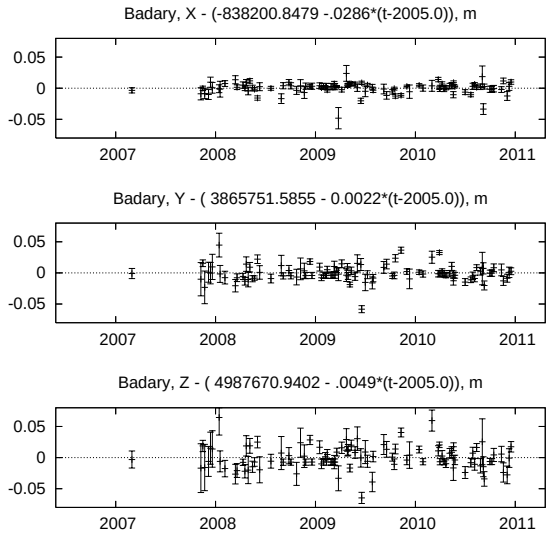

Fig. 1 Series of VLBI Antenna coordinates of the Badary station.

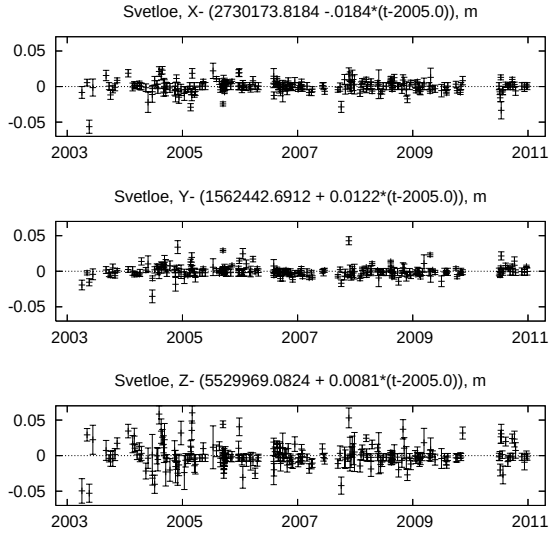

Fig. 2 Series of VLBI Antenna coordinates of the Svetloe station.

carried out beginning from 1997 and at BADG station (Bd observatory) – since 2005. Therefore there was not necessity to improve velocities of SVTL and ZECK GPS stations which have

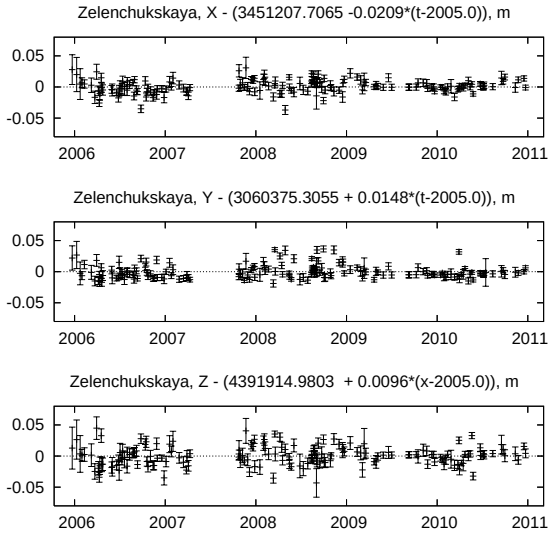

Fig. 3 Series of VLBI Antenna coordinates of the Zelenchukskaya station.

been well determined in ITRF2008. As for the velocity of the BADG station it has been derived from GPS observations at 4-year time interval (March, 2005 – March, 2009) processed using the GRAPE program package (Sharkov and Gayazov, 2009).

3 Comparison of VLBI and GPS Results

Velocities of stations of the ”Quasar” network obtained from VLBI and GPS observations are presented in Tab. (3). The comparison of data shows, that the improved velocities are in agreement at the level of 1.5 mm/y in all components, and the greatest differences are observed in height and east components (see Tab. (4)). It can also be seen from (Tab. (1)) that for Bd observatory both VLBI and GPS results are closer to values derived from DORIS data than to VLBI solution in ITRF2008.

Station	Velocity components	Technique		Differences
		VLBI	GPS	
Sv	Vx, mm/y	-18.4	-18.2	-0.2
	Vy, mm/y	12.2	13.7	-1.5
	Vz, mm/y	8.1	9.0	-0.9
Zc	Vx, mm/y	-20.9	-22.2	1.3
	Vy, mm/y	14.8	14.4	0.4
	Vz, mm/y	9.6	9.2	0.4
Bd	Vx, mm/y	-28.6	-27.3	-1.3
	Vy, mm/y	-2.2	-2.2	0.0
	Vz, mm/y	-4.9	-5.3	0.4

Table 3 Comparison of improved velocities of stations

Station	Velocity differences		
	V_N, mm/y	V_E, mm/y	V_H, mm/y
Sv	0.4	-1.2	-1.2
Zc	-0.6	-0.6	1.2
Bd	0.0	1.3	0.5

Table 4 Differences of VLBI and GPS velocities transformed to local systems

In 2010 the recurrent geodetic surveying of local tie parameters has been implemented at all observatories of the "Quasar" network. The new set of local tie parameters have been used to reduce baselines between GPS antenna markers to those for VLBI antenna reference points. The agreement of GPS baselines reduced in that way with the VLBI derived baselines serves as an additional characteristic of the network. For baselines Sv–Zc, Sv–Bd, Bd–Zc these differences referenced to the epoch 2005.0 were correspondingly equal to -3.2, -4.8, 9.7 mm.

Baseline	Sv–Zc, m	Sv–Bd, m	Bd–Zc, m
VLBI	2014661.0452	4281660.5296	4404836.1898
GPS (reduced)	2014661.0484	4281660.5344	4404836.1801

Table 5 Baselines for VLBI antennas compared with reduced baselines for GPS markers for epoch 2005.0

4 Conclusions

The level of agreement between coordinates and velocities of different space geodetic instruments and local tie data at the "Quasar" VLBI network stations has been examined. Processing VLBI and GPS observations carried out during last years has allowed to improve velocities of the network observatories in ITRF2008 and to reduce the discrepancies between VLBI and GPS results to level 1.5 mm/y. Baselines obtained from VLBI and GPS data are consistent within 10 mm for the epoch 2005.0.

References

Z. Altamimi, X. Collilieux, L. Métivier. ITRF2008: an improved solution of the international terrestrial reference frame. *J. Geodesy*, 2011. doi: 10.1007/s00190-011-0444-4.

A. Finkelstein, A. Ipatov, S. Smolentsev. The network "Quasar": 2008–2011. In A. Finkelstein, D. Behrend, editors, *Measuring the Future. Proceedings of the Fifth IVS General Meeting, Nauka*, pages 39–46. Saint Petersburg, 2008.

I. Gayazov and E. Skurikhina. Local ties between co-located Space Geodetic Instruments at Quasar network observatories. In A. Finkelstein, D. Behrend, editors, *Measuring the Future. Proceedings of the Fifth IVS General Meeting, Nauka*, pages 82–86. Saint Petersburg, 2008.

V. Sharkov and I. Gayazov. Improvement of the Badary Observatory Velocity from GPS-Observations. *IAA RAS Transactions, v.20, Nauka*, pages 496–500. Saint Petersburg, 2009 (in Russian).

Crustal movements in Europe observed with *EUROPE* and *IVS-T2* VLBI networks

N. Zubko and M. Poutanen

Abstract The comparative analysis of the *EUROPE* and *IVS-T2* geodetic VLBI sessions has been performed. The main purpose of both campaigns is to observe and accurately determine the VLBI station coordinates and their time evolution. In this analysis our interest is to understand the influence of network configuration on the estimated parameters and, also, how much the results of these two campaigns are consistent. We have used the VieVS software developing at Vienna University of Technology to analyze the *EUROPE* and *IVS-T2* sessions of 2002-2009. We have analyzed differences in station time series obtained with these two networks and the effect of network configuration and station selection. The EPN (EUREF permanent GNSS Network) and IGS (International GNSS Service) networks can be used to compare the results.

Keywords Crustal movements, *EUROPE*, *IVS-T2*

1 Introduction

The main purpose of the *EUROPE* and *IVS-T2* geodetic VLBI campaigns is to estimate Terrestrial Reference Frame (TRF). The VLBI stations participating in *IVS-T2* sessions are distributed around the world; whereas, in *EUROPE* campaign only European stations take participation. Configuration of the network evidently affects the estimated parameters. In order to show and evaluate that effect we analyze data from these campaigns.

The crustal motion in Europe observed with European geodetic VLBI network have been studied by, e.g., Haas et al. (2003), Tomasi et al. (1999). In the current work, we estimate positions of the VLBI radio antennas within *EUROPE* and *IVS-T2* networks to compare them. For the analysis we have used VieVS software (Boehm et al., 2009). From our analysis we have obtain time series of estimated positions of VLBI radio antennas for each network. Using the time series we obtain horizontal and vertical velocities for each VLBI antenna.

Nataliya Zubko and Markku Poutanen
Finnish Geodetic Institute, Geodeetinrinne 2, Masala, Finland

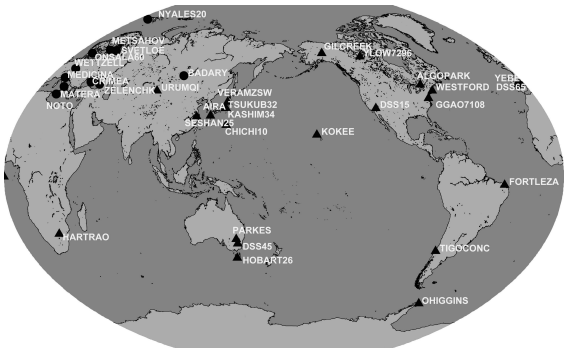

Fig. 1 *EUROPE* (shown with circles)and *IVS-T2* (shown with circles and triangles) observing networks

2 Data selection

We analyze the observation data obtained during *EUROPE* and *IVS-T2* campaigns in 2002–2009. Figure 1 presents locations of VLBI stations participating in those campaigns. In *IVS-T2* we selected sessions which included stations participating also in *EUROPE* sessions. We excluded some sessions and stations with poor quality of data. Figure 2 shows number of observation sessions for each station involved into analysis, where with grey and black bars the participations in *EUROPE* and *IVS-T2* sessions respectively are represented . We present results for all stations, contributing in more than 10 observation sessions for each campaign.

3 Results

Using VieVS software, we estimate the coordinates of VLBI radio antennas. For the analysis, the NNR and NNT conditions are applied. We choose VTRF 2008 as a reference frame. Figures 3 and 4 show time series of estimated x, y and z coordinate offsets from VTRF- 2008 and their standard deviations for some VLBI

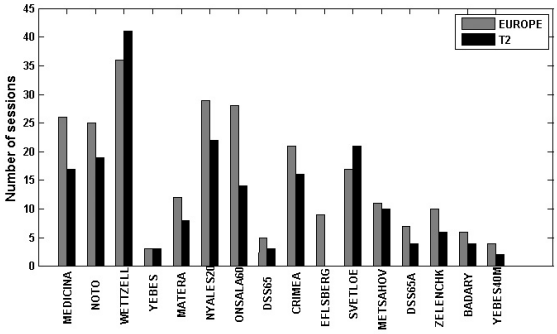

Fig. 2 Antenna's activity

stations participating in *EUROPE* and *IVS-T2* campaigns. The linear least-squares fitting is applied to the data (red lines).

The results presented in Figures 3 and 4 show that the scattering of data points in the *EUROPE* sessions is smaller than for *IVS-T2* sessions. The same holds also for the standard deviations of estimated coordinate. It can be assumed that the station movement could be estimated with higher accuracy using data from *EUROPE* campaign than the data from *IVS-T2* sessions.

As can be seen from Figures 3 and 4 the trend of the linear fit can be opposite for these networks. This can be result of difference in the network configurations; however, the uncertainty of the fit is in many cases so large that it will affect the results.

We have performed a comparative analysis of the time series obtained by VLBI and GPS techniques. Using the time series we estimate horizontal and vertical velocities for each antenna. Figures 5 and 6 show horizontal velocities obtained from VLBI data (white arrows) and from GPS data (black arrows). To minimize the reference frame related issues, motions are shown relative to station Wettzell. The GPS data for velocities presented at Figures 5 and 6 have been calculated using GPS time series [1]

As one can see in Figures 5 and 6, the velocities of Medicina, Onsala, Svetloe derived from *EUROPE* campaign are better consistent with the GPS results than from *IVS-T2*. However, for Noto station the horizontal velocity obtained with *EUROPE* VLBI data is two times higher than the speed retrieved with GPS technique. Metsähovi has participated in geoVLBI campaigns since 2005 and the small amount of data can affect the result. The VLBI results for Ny Ålesund does not agree well with GPS data. Nevertheless, for this station, the directions of motion obtained within *EUROPE* and *IVS-T2* campaigns nearly coincide.

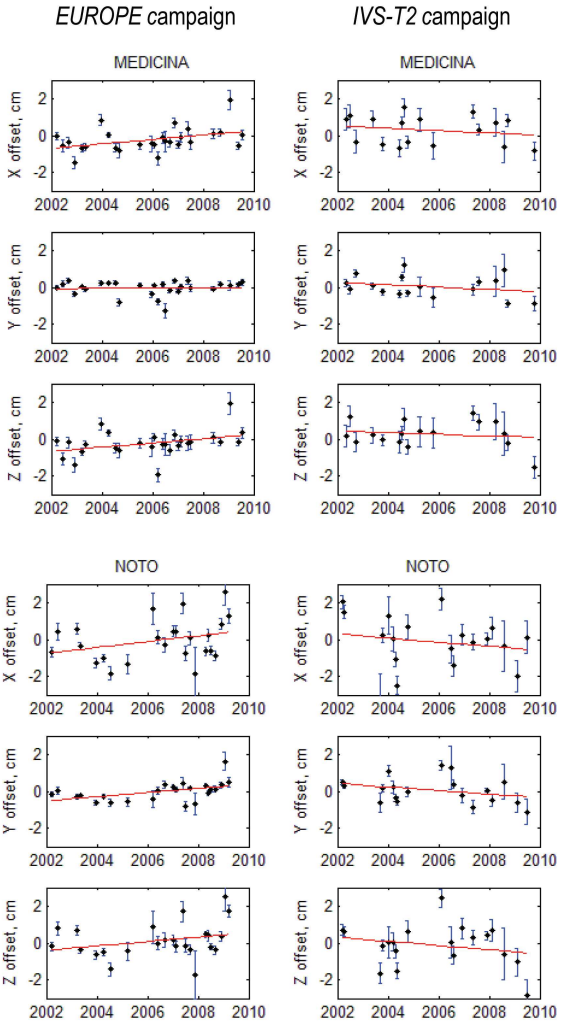

Fig. 3 X, Y, Z coordinate offsets from TRF and their standard deviations of *EUROPE* and *IVS-T2* sessions

EPN network values. We can see a network selection effect in horizontal velocities, although in many cases uncertainties of the trendline are too large to make any definite conclusion. More analysis are needed to understand the reason for differences.

4 Conclusions

We have analyzed the geodetic VLBI observation sessions, which have been collected during 8 years within *EUROPE* and *IVS-T2* campaigns. The station velocities acquired with these two networks were compared and a comparison is also made with

[1] http://sideshow.jpl.nasa.gov/mbh/series.html

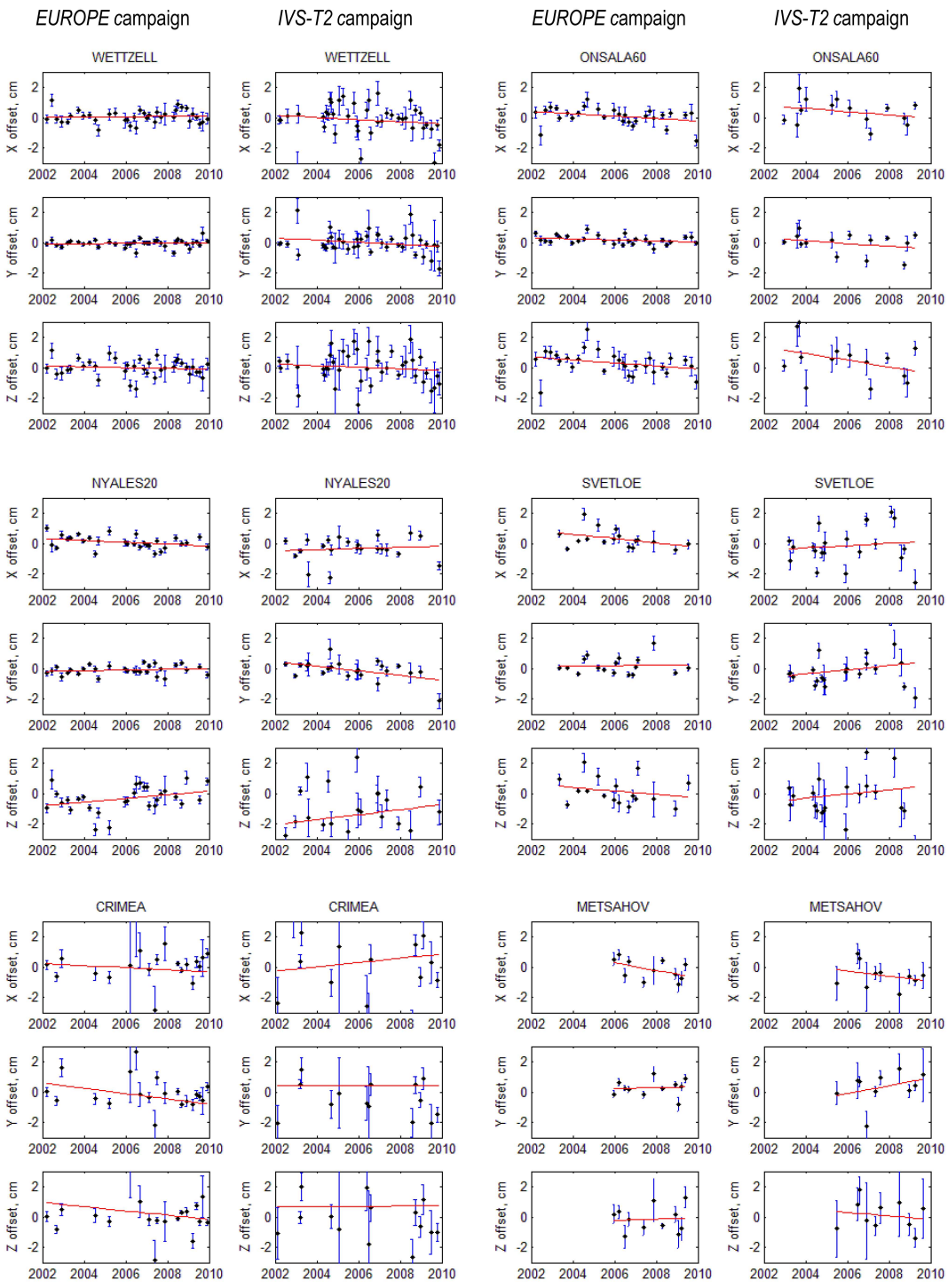

Fig. 4 X, Y, Z coordinate offsets from TRF and their standard deviations of *EUROPE* and *IVS-T2* sessions

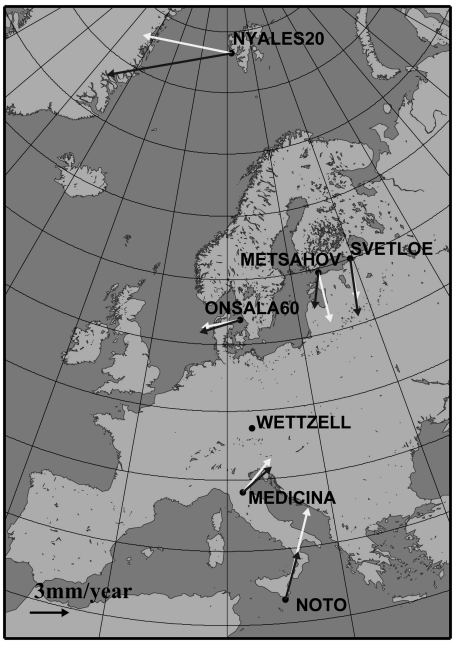

Fig. 5 Horizontal velocities derived from *EUROPE* VLBI campaign (white arrows) and GPS data (black arrows).

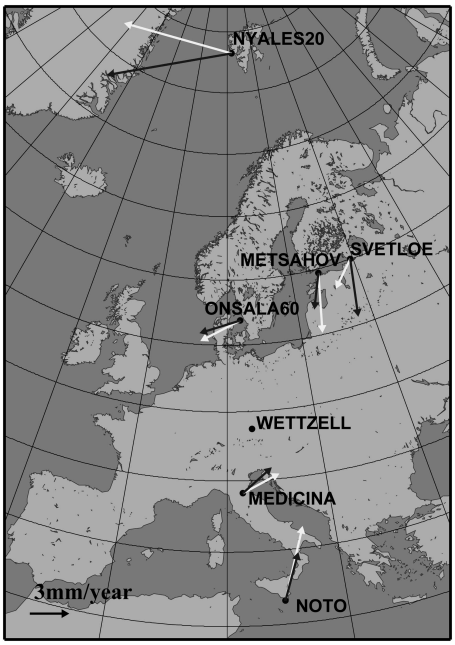

Fig. 6 Horizontal velocities derived from *IVS-T2* VLBI campaign (white arrows) and GPS data (black arrows).

References

J. Boehm, H. Spicakova, L. Plank, K. Teke, A. Pany, J. Wresnik, S. Englich, T. Nilsson, H. Schuh, T. Hobiger, R. Ichikawa, Y. Koyama, T. Gotoh, T. Kubooka, and T. Otsubo. Plans for the Vienna VLBI Software VieVS. *Proceedings of the 19th European VLBI for Geodesy and Astrometry Working Meeting*, edited by G. Bourda, P. Charlot, and A. Collioud, Bordeaux, pages 161–164, 2009.

R. Haas, A. Nothnagel, J. Campbell, E. Gueguen Recent crustal movements observed with the European VLBI network: geodetic analysis and results. *Journal of Geodynamics*, 35, pages 391414 , 2003.

P. Tomasi, M.J. Rioja and P. Sarti. The European VLBI Network activity in geodesy: crustal deformation in Europe. *New Astronomy Reviews*, pages 603–607, 1999.

Validation Experiment of the GPS-VLBI Hybrid System

Y. Kwak, T. Kondo, T. Gotoh, J. Amagai, H. Takiguchi, M. Sekido, R. Ichikawa, T. Sasao, J. Cho, T. Kim

Abstract We carried out 24-hour GPS-VLBI (GV) hybrid observation between Kashima and Koganei baseline to validate GV hybrid system on December 25, 2009. We could detect the correlation peaks of GPS signals with high signal to noise ratio(SNR) from correlation processing as well as quasar signals. GPS signals were regarded as white noise signals in correlation processing. Although effective bandwidth of GPS signal is smaller than that of geodetic VLBI observation, larger SNR of GPS signal compensates for the disadvantage in the bandwidth. However, scatters of the O-C (Observed-Calculated) of GPS data from the actual analysis results were bigger than expected thermal noise errors. In this paper, we discuss the results of the 24-hour GV hybrid observation and the causes of the larger scatters of GPS data.

Keywords VLBI, GPS, combination of space geodetic techniques, GPS-VLBI hybrid system, GPS-VLBI hybrid observation

Y. Kwak, J. Cho
Korea Astronomy and Space Science Institute, 776, Daedeokdae-ro, Yuseong-gu, Daejeon 305-348, Republic of Korea

T. Kondo, T. Gotoh, J. Amagai, M. Sekido, R. Ichikawa
Kashima Space Research Center/NICT, 893-1 Hirai, Kashima, Ibaraki, 314-0012 Japan

H. Takiguchi
Institute for Radio Astronomy and Space Research, Auckland University of Technology, Duthie Whyte Building, Level 1, 120 Mayoral Drive, Auckland 1010, New Zealand

T. Sasao
Yaeyama Star Club, 2097-2 Arakawa, Ishigaki, Okinawa, 907-0024 Japan

T. Kim
Ajou University, San 5, Woncheon-dong, Yeongtong-gu, Suwon 443-749, Republic of Korea

1 Introduction

Space geodetic techniques, Very Long Baseline Interferometry (VLBI), Global Navigation Satellite System(GNSS), Satellite Laser Ranging (SLR) and Doppler Orbitography and Radiopositioning Integrated by Satellite (DORIS), are the key techniques to construct International Reference Frame and to determine Earth Orientation Parameters(EOP). It is impossible to complete International Terrestrial Reference Frame (ITRF) and every component of EOP with sole technique. For instance, VLBI cannot determine the origin of the TRF since VLBI only measure the baselines between stations. Satellite geodetic technique itself cannot determine UT1 related to the rotation angle of the Earth, since longitude of the ascending node, one of satellite orbital elements, is correlated with UT1. For more detail, see Plag and Pearlman (2009).

To compensate those limitations, Institut Géographique National (IGN), International Earth Rotation and Reference System Service(IERS) International Terrestrial Reference System(ITRS) product centre, combines the products of all space geodetic techniques (Altamimi et al., 2002). Deutsches Geodätisches Forschungsinstitut(DGFI), IERS ITRS combination centre, also combines the normal matrices and normal vectors of all space geodetic techniques (Angermann et al., 2004).

In this paper, we approach the combination method in observation level, especially hardware step. Combination of Global Positioning System(GPS), one of GNSS techniques, and VLBI in hardware step is feasible since both techniques measure radio signal. The most efficient combination method of two techniques is to perform sampling, recording and correlation in the same manner, while maintaining advantageous characteristics for radio-wave reception in each of the observation techniques (Kwak et al., 2010b). This concept, so called GPS-VLBI(GV) hybrid system, was suggested for the first time in Kwak et al. (2008a) and evolved in Kwak et al. (2008b), Kwak et al. (2010a) and Kwak et al. (2010b). Similar approach to the observation level combination was also proposed by Dickey (2010). Tornatore et al. (2010) proceed the observation level combination in another approach.

2 GPS-VLBI Hybrid System

GV hybrid system is a novel observation method to combine VLBI and GPS techniques in observation level. In the system, VLBI antennas and GPS antennas located at the same site, simultaneously receive signals from quasars and GPS satellites, respectively. Both signals are sampled and recored in identical types of samplers and recorders that refer to identical Hydrogen maser clock. The signal processing and data generation of normal GPS observation are carried out inside commercial GPS receiver. Hence, signal transmission cable should be directly connected from the output terminal of GPS antenna to normal geodetic VLBI system in order to realize GV hybrid system. Since geodetic VLBI down-converters are dedicated to S/X band signals, an additional GPS down converter is introduced to convert original GPS L1/L2 signals to input signals for VLBI sampler. For more detail, see Kwak et al. (2010b). Both data of quasars and GPS satellites are recorded in normal geodetic VLBI data format, Mark5 or K5. In principle, VLBI type data of quasars and GPS satellites can be correlated in normal VLBI correlator. The correlation output is group delay of S/X band data for quasars, and of L1/L2 data for GPS satellites. The idea is nothing but processing an additional frequency band of radio signal in VLBI system.

3 Validation Experiment

On the basis of successful VLBI type observation of GPS (Kwak et al., 2010b), we construct 24-hour GV hybrid observation for validation of GV hybrid system. We focus on the validity of the GV hybrid system in this paper. The schedule file of geodetic VLBI observation includes the coordinates of the radio sources and stations, and observation schedule. The antenna operation program reads the observation information and adjusts the motion of a antenna to target the source. However, the schedule file of GPS does not need the coordinates of the GPS satellites since a GPS antenna is an omni-directional antenna. The start time and the end time of each observation and the position of antenna are sufficient for GPS schedule file. The 24-hour GV hybrid observation was held during 12:12:00UTC 25th to 13:00:00UTC 26th December 2009 for over 24 hours. In 24-hour geodetic VLBI session, actual observation recording time is about 8 hours since it takes time to move a big antenna to the next source from the previous source. Meanwhile, continuous 24-hour observation of GPS part is possible since it is not necessary to move a GPS antenna. The data volume generated by 24-hour GV hybrid observation is shown as Table (1) .

Owing to limitation of hard disks, we took 1-minute on and 2-minute off GPS observation strategy for every 3 minutes in this validation experiment . According to Kwak et al.(2010), 1-minute observation is enough to get high signal to noise ratio(SNR). The observation was carried out on the baseline between Kashima and Koganei, Japan(Figure (1)).

	VLBI	GPS
Bandwidth per channel(MHz)	8	32
Number of channels	12	2
Bit number(bit/sample)	1	1
Observation time(seconds)	∼ 55,800	∼ 86,400
Recording rate(Mbits/sec)	192	128
Total data volume for 24 hours(TB)	1.3	1.4
Data volume in this experiment(TB)	1.3	0.5

Table 1 Data volume per station of VLBI and GPS during 24-hour GV hybrid observation

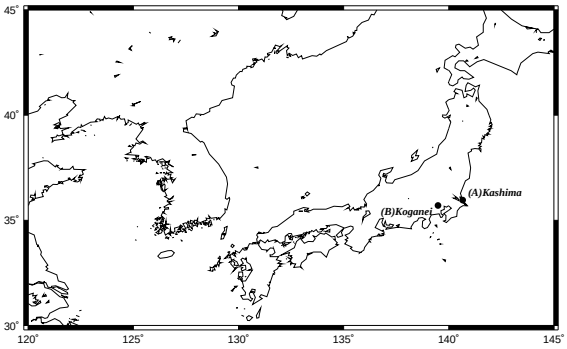

Fig. 1 A 110km Baseline between (A)Kashima and (B)Koganei

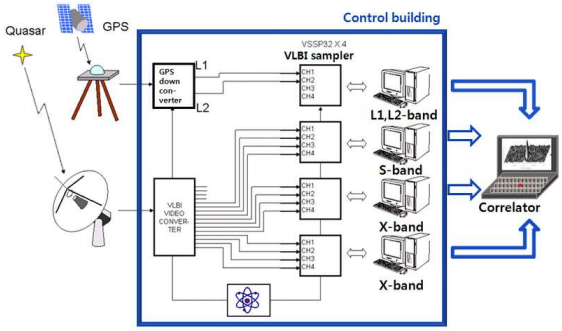

Fig. 2 A block diagram of GV hybrid system

In 24-hour GV hybrid observation, four units of K5/VSSP[1]32, developed by National Institute of Information and Communications Technology(NICT), are applied for sampling and recording data. Each K5/VSSP32 unit is able to deal with four observation channels. However, the control PC of a K5/VSSP32 unit cannot support the simultaneous observation of a quasar and GPS satellites. Hence, we set up four S-band channels in a unit, eight X-band channels in two units and GPS L1 and L2 channels in a unit(Figure (2)). While the sampling frequency of S/X band channels are 16MHz, the sampling frequency of GPS L1/L2 channels are 64MHz to cover individual channels whose main-lobe width is 20.46MHz.

The observation data are recorded in K5 data format. The K5 data format is able to be converted to Mark5 data format. In this

[1] VSSP: Versatile Scientific Sampling Processor

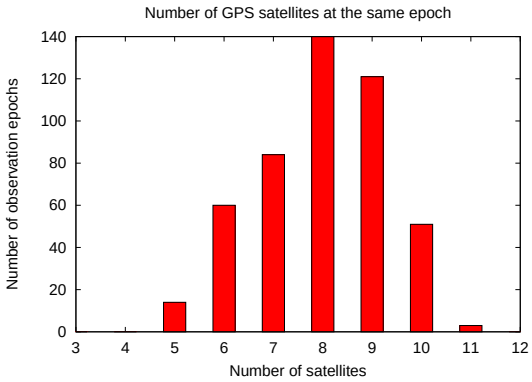

Fig. 3 Number of simultaneously observed GPS satellites above 15 degree cutoff angle in elevation

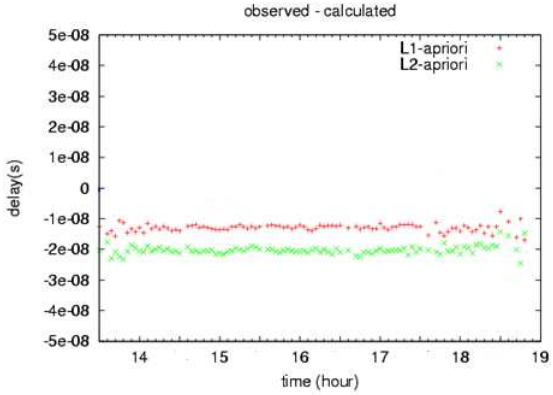

Fig. 4 Observed - Calculated (O-C) values of L1 and L2 signal of a GPS satellite, Space Vehicle(SV)01. It shows path length differences in L1 and L2 cables.

study, we take K5 data format since we make use of K5 software correlator. The K5 software correlator has also been developed by NICT (Kondo et al., 2003).

We utilize 'apri_calc', which is the VLBI a priori group delay generating program developed by NICT, to get a priori group delay of quasar. Meanwhile, we simply calculate path length difference of radio wave to obtain GPS a priori group delay. That is analogous to single difference in GPS technique. The only distinction is we take difference value from the correlation result, group delay. We make use of broadcast ephemerides of International GNSS Service(IGS) to calculate the a priori coordinate of GPS satellites. Every correlation processing is carried out for every channel. The processing time of K5 software correlator solely depends on computational performance of a processing computer. As usual VLBI data processing, bandwidth synthesis technique is applied to correlated S-band and X-band data, respectively. Because L1-band and L2-band data contain all signals of GPS satellites on the sky, the correlation processing has to be repeated the number of GPS satellites with distinctive delay values for the identical signal. We set cut-off angle 15 degree in elevation for GPS satellites to avoid severe multi-path effects. At least five satellites were on the sky, above 15 degree in elevation, during the experiment(Fig (3)).

4 Results

Final correlated data are group delays of S-band and X-band data for quasars, and of L1-band and L2-band data for GPS satellites. In this paper, we do not discuss group delays of quasars since they are the same as those of regular VLBI observation. Fig (4) shows Observed - Calculated (O-C) values of L1 and L2 signal of a GPS satellite, respectively. The reference values are ionosphere calibrated O-C of two frequencies. Both values are biased and they are about 10 nanoseconds apart. In this validation experiment, Phase/Delay Calibrator is not installed in GPS signal processing part while it is already applied in VLBI part

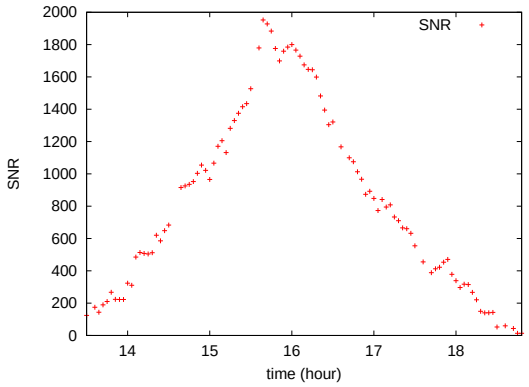

Fig. 5 Correlation peak SNR variation of L1 signal of a GPS satellite, SV01, during the observation

as usual. Therefore uncalibrated effects are obviously inserted in delay values. Phase/Delay Calibrator of GPS part should be taken into account in next version of GV hybrid system for accurate group delay. The scatters of the O-C of all GPS satellite signals are a few nanoseconds level which is considerably bigger than general uncertainty of VLBI group delay, 0.1 nanoseconds level.

Meanwhile, Fig (5) shows the SNR variation of correlation peaks of a GPS satellite L1 signal during the observation. If GPS signals are regarded as white noise, the expected errors of group delays of all GPS satellite signals are more or less 100 picoseconds for L1 signal and a few hundred picoseconds level for L2 signal.

5 Conclusions

The 24-hour GV hybrid observation was successfully carried out. GPS signals were stably sampled and recorded in VLBI system during the 24-hour experiment. Many GPS satellites show high correlation SNR which would yield 0.1 nanoseconds level of thermal noise error assuming white noise. However, actual O-C of GPS group delays show a few nanosecond level scatter.

There are several aspects that were neglected in the validation experiment. Spectral characteristic of GPS signal was not considered in correlation model. Phase/Delay Calibrator was not applied in GPS part. Phase center of GPS antenna were not took into account in this analysis. A priori group delays of GPS signal were calculated using IGS broadcast ephemerides whose declared accuracy is about 1 meter. Consequently, those factors resulted in considerable uncertainties of group delays.

Therefore, GV hybrid system will be improved and extended in various aspects,

- better correlation model considering characteristics of GPS signals such as real spectrum and code nature,
- consideration of GPS specific problems such as phase center variation and multi-path,
- better instrumentation in use of Phase/Delay Calibrator and cable ducts,
- better a priori delay model in use of precise GPS ephemerides.

In the experiment, the baseline is rather short to determine global parameters, e.g. satellite coordinates, EOP and CRF. In order to contribute to determine global parameters, especially UT1 and CRF which only VLBI technique is able to determine, for GV hybrid system, lager network of GV hybrid system is required.

References

Z. Altamimi, P. Sillard, and C. Boucher, ITRF2000: A new release of the International Terrestrial Reference Frame for earth science applications, *Journal of Geophysical Research - Solid Earth*, 107, 2214, 2002

D. Angermann, H. Drewes, M. Krügel, B. Meisel, M. Gerstl, R. Kelm, H. Müller, W. Seemüller, and V. Tesmer, ITRS Combination Center at DGFI:A Terrestrial Reference Frame Realization 2003, *Deutsche Geodätische Kommission*, 2004

J. Dickey, How and Why to do VLBI on GPS, *In International VLBI Service for Geodesy and Astrometry 2010 General Meeting Proceedings (eds. Behrend, D. and Baver, K.)*, 2010

T. Kondo, Y. Koyama, and H. Osaki, Current Status of the K5 Software Correlator for Geodetic VLBI: *IVS CRL-TDC News*, No. 23, pp.18-20, 2003.

Y. Kwak, T. Kondo, T. Gotoh, J. Amagai, H. Takiguchi, M. Sekido, R. Ichikawa, T. Sasao, J. Cho, and T. Kim, The First Experiment with VLBIGPS Hybrid System, *In International VLBI Service for Geodesy and Astrometry 2010 General Meeting Proceedings (eds. Behrend, D. and Baver, K.)*, 2010a

Y. Kwak, T. Kondo, T. Gotoh, J. Amagai, H. Takiguchi, M. Sekido, R. Ichikawa, T. Sasao, J. Cho, and T. Kim, VLBI Type Experimental Observation of GPS, *Journal of Astronomy and Space Science*, 27, pp.173-180, 2010b

Y. Kwak, T. Sasao, J. Cho, and T. Kim, New Approach to VLBI-GPS Combination, *In International VLBI Service for Geodesy and Astrometry 2006 General Meeting*, 2008a

Y. Kwak, T. Sasao, J. Cho, and T. Kim, New suggestion for VLBI-GPS combined observation, *In Asia Oceania Geosciences Society Fifth Annual Meeting*, 2008b

H.-P. Plag and M. Pearlman (eds), The Global Geodetic Observing System: Meeting the Requirements of a Global Society on a Changing Planet in 2020, Springer, 2009

V. Tornatore and R. Haas, Planning of an Experiment for VLBI Tracking of GNSS Satellites, *In International VLBI Service for Geodesy and Astrometry 2010 General Meeting Proceedings (eds. Behrend, D. and Baver, K.)*, 2010

Towards an accurate alignment of the VLBI frame and the future Gaia frame – VLBI observations of optically-bright weak extragalactic radio sources: Status and future prospects

G. Bourda, A. Collioud, P. Charlot, R. Porcas, S. Garrington

Abstract The space astrometry mission Gaia will construct a dense optical QSO-based celestial reference frame. For consistency between optical and radio positions, it will be important to align the Gaia and VLBI frames with the highest accuracy. However, the number of quasars suitable for this alignment is currently rather limited (Bourda et al., 2008). It was hence realized that the densification of the list of such objects was necessary. Accordingly, we initiated a multi-step VLBI observational project, dedicated to finding additional suitable radio sources for aligning the two frames. The sample consists of ∼450 optically-bright radio sources, which have been selected by cross-correlating optical and radio catalogs. The initial observations, aimed at checking whether these sources are detectable with VLBI, and conducted with the European VLBI Network in 2007, showed an excellent ∼90% detection rate (Bourda et al., 2010). The second step, dedicated to extracting the most point-like sources of the sample by imaging their VLBI structures, was initiated in 2008. About 25% of the detected targets were observed with the Global VLBI array during a pilot imaging experiment, revealing ∼50% of them as point-like sources on VLBI scales (Bourda et al., 2011). The rest of the sources were observed in March and November 2010 with the final imaging experiment in March 2011. And finally, the third step of this project, dedicated to measuring accurately the VLBI position of the most point-like sources of the sample, will be initiated in 2011.

Géraldine Bourda, Arnaud Collioud and Patrick Charlot
Laboratoire d'Astrophysique de Bordeaux, Université de Bordeaux, CNRS/UMR5804, 2 rue de l'Observatoire, BP89, 33271 Floirac Cedex, France

Richard Porcas
Max-Planck-Institut für Radioastronomie, Auf dem Hügel 69, 53121 Bonn, Germany

Simon Garrington
University of Manchester, Jodrell Bank Observatory, Macclesfield, Cheshire SK11 9DL, UK

Keywords VLBI observations, extragalactic radio sources, celestial reference frame, Gaia

1 Context

During the past decade, the IAU (International Astronomical Union) fundamental celestial reference frame was the ICRF (International Celestial Reference Frame; Ma et al., 1998; Fey et al., 2004), composed of the VLBI (Very Long Baseline Interferometry) positions of 717 extragalactic radio sources, measured from dual-frequency S/X observations (2.3 and 8.4 GHz). Since 1 January 2010, the IAU fundamental celestial reference frame has been the ICRF2 (IERS Technical Note 35, 2009), successor of the ICRF. It includes VLBI coordinates for 3 414 extragalactic radio sources, with a floor in position accuracy of 60 μas and an axis stability of 10 μas.

The European space astrometry mission Gaia, to be launched in March 2013, will survey all stars and QSOs (Quasi Stellar Objects) brighter than apparent optical magnitude 20 (Perryman et al., 2001). Using Gaia, optical positions will be determined with an unprecedented accuracy, ranging from a few tens of μas at magnitude 15–18 to about 200 μas at magnitude 20 (Lindegren et al., 2008). Unlike Hipparcos, Gaia will permit the realization of the extragalactic celestial reference frame directly at optical bands, based on the QSOs that have the most accurate positions. A preliminary Gaia catalog is expected to be available by 2015 with the final version released by 2020.

In this context, aligning VLBI and Gaia frames will be crucial for ensuring consistency between the measured radio and optical positions. This alignment, to be determined with the highest accuracy, requires several hundreds of common sources, with a uniform sky coverage and very accurate radio and optical positions. Obtaining such accurate positions implies that the link sources must be brighter than optical magnitude 18 (Mignard, 2003), and must not show extended VLBI structures.

In a previous study, we investigated the potential of the ICRF for this alignment and found that only 70 sources (10% of the catalog) are appropriate for this purpose (Bourda et al., 2008). This highlights the need to identify additional suitable radio sources, which is the goal of a VLBI program that we initiated four years

ago. This program has been devised to observe 447 optically-bright extragalactic radio sources, on average 20 times weaker than the ICRF sources, extracted from the NRAO VLA Sky Survey, a dense catalog of weak radio sources (Condon et al., 1998). The observing strategy to detect, image, and measure accurate VLBI positions for these sources is described in Bourda et al. (2010). In this paper, we give the status of this program and outline future prospects.

2 The observing program

2.1 VLBI detection

The initial observations, whose goal was to assess the VLBI detectability of the 447 targets, were conducted with the European VLBI Network[1] (EVN), recording at 1 Gbps in a geodetic-style dual-frequency S/X mode, in June and October 2007 (during two 48–hours experiments, EC025A and EC025B, respectively). These showed excellent detection rates of 97% at X-band and 89% at S-band. Overall, 398 sources were detected at both frequencies, corresponding to an overall detection rate of about 89% (Bourda et al., 2010). The mean correlated flux densities were also determined for each source and band by averaging over all scans and baselines detected (see Fig. (1)):

- At X-band, 432 sources were detected and the mean correlated fluxes ranged from 1 mJy to 190 mJy, with a median value of 26 mJy.
- At S-band, 399 sources were detected and the mean correlated fluxes ranged from 8 mJy to 481 mJy, with a median value of 46 mJy.

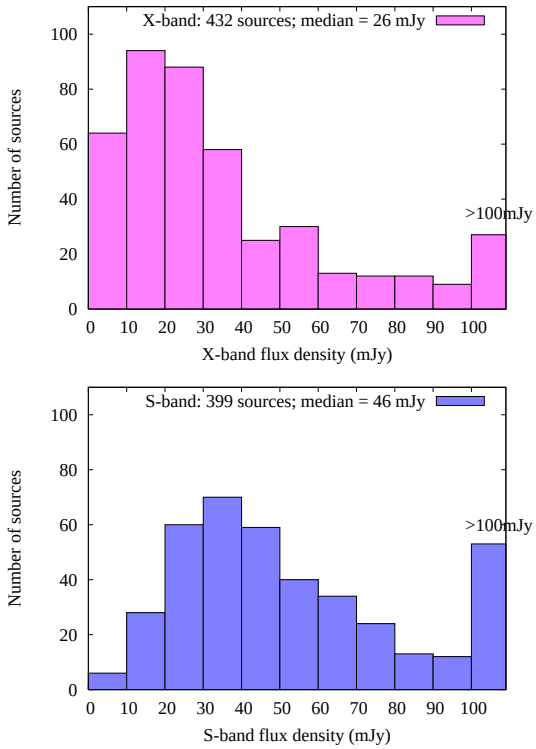

Fig. 1 Mean correlated flux density distribution, at X- and S-bands, for the sources detected in EC025A and EC025B. The corresponding median values are 26 mJy and 46 mJy, respectively.

2.2 VLBI imaging

Proceeding further with our program, the second step was targeted at imaging the sources previously detected, using the global VLBI network (EVN+VLBA; Very Long Baseline Array), recording at 512 Mbps in a geodetic-style dual-frequency S/X mode, in order to identify the most point-like sources and therefore the most suitable ones for the alignment.

A pilot imaging experiment[2] was carried out in March 2008 (during 48–hours; experiment designated GC030) to image 105 of the 398 previously detected sources. As a result, all sources were successfully imaged at both bands (Bourda et al., 2011; see http://www.obs.u-bordeaux1.fr/BVID/GC030). The total flux densities of these sources were determined at both S- and X-bands (see Fig. (2)), as well as their continuous structure indices (see Fig. (3); for a definition of the *continuous* structure index see e.g. Bourda et al., 2011). We showed that about 50% of these targets were point-like sources (i.e. 47 sources out of 105 observed had an X-band structure index < 3.0).

Additional imaging experiments[3] were then carried out with the global VLBI array to observe the remaining 290 sources, during 144 hours:

- In March 2010 (97 sources), during 48 hours;
- In November 2010 (118 sources), during 57 hours;
- In March 2011 (75 sources), during 38 hours.

We are now analyzing these three global observations in order to determine the VLBI structures of the targets and to extract the most point-like sources.

[1] The network comprised the antennas of Effelsberg, Medicina, Noto, Onsala-25m, as well as the 70-m Robledo telescope for part of the time (in October 2007).

[2] The network comprised 5 telescopes of the EVN (Effelsberg, Medicina, Noto, Onsala-25m and the South-African antenna at Hartebeesthoek), the DSN 70-m Robledo telescope for part of the time, and 9 antennas of the VLBA; the VLBA Fort Davis antenna could not observe during this experiment.

[3] The network comprised the 10 antennas of the VLBA, and five telescopes of the EVN (Effelsberg, Medicina, Onsala-25m, Yebes-40m and either Noto or the South-African antenna at Hartebeesthoek).

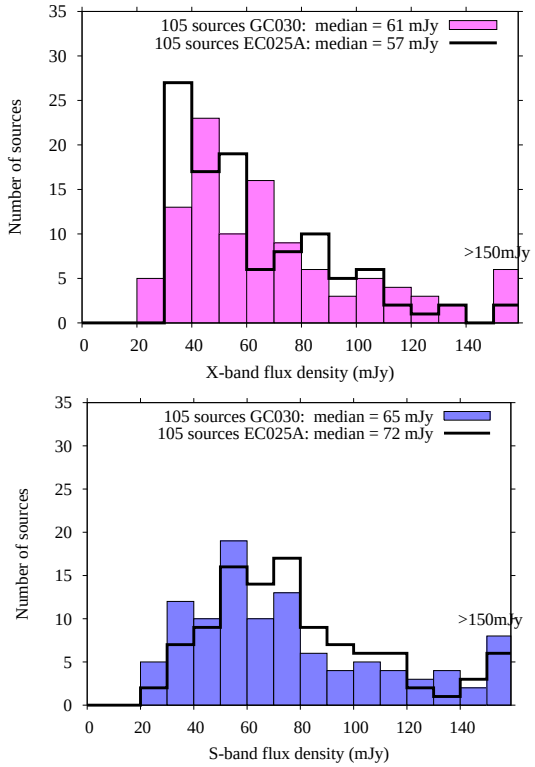

Fig. 2 Distribution of the total flux densities at X- and S-bands for the 105 sources observed during the pilot imaging experiment GC030. The corresponding mean correlated flux density distribution determined during EC025A for the same sources is plotted in black.

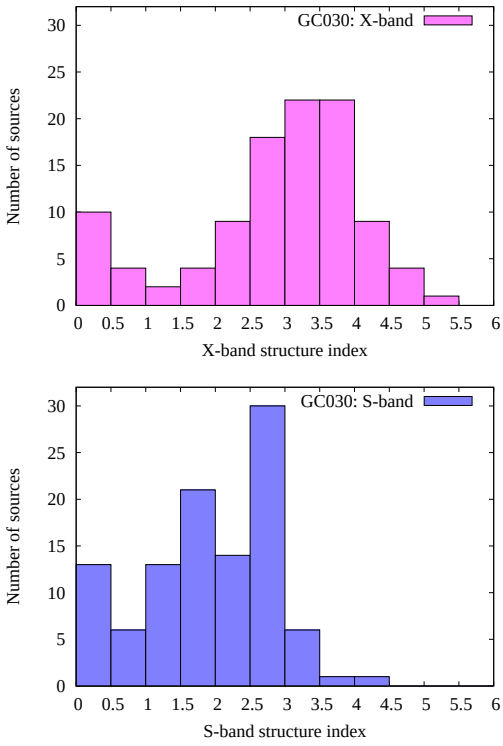

Fig. 3 Distribution of the continuous structure index at X-band (upper panel) and S-band (lower panel) for the 105 sources observed during GC030.

2.3 VLBI astrometry

The final stage of this program, dedicated to determining very accurate VLBI positions (i.e. position accuracy wanted to better than 100 μas) for the most point-like sources of the sample will begin by the end of 2011.

3 Summary and future prospects

Within the next few years, the alignment between optical and radio frames will benefit from this multi-step VLBI project. Obtaining such an alignment with the highest accuracy is essential, not only to ensure consistency between measured radio and optical positions, but also to measure directly core shifts within AGNs. This will be of great interest in the future for probing AGN jets properties.

Furthermore, while making the Gaia link possible, these new VLBI positions will also serve in the future to densify the VLBI frame at the same time.

Acknowledgements

The authors would like to thank the VLBI friends at the EVN and VLBA observing stations. This work has benefited from research funding from the European Community's sixth Framework Programme under RadioNet R113CT 2003 5058187. The EVN is a joint facility of European, Chinese, South African and other radio astronomy institutes funded by their national research councils. The VLBA is part of the National Radio Astronomy Observatory (NRAO), which is operated by Associated Universities, Inc., under cooperative agreement with the National Science Foundation.

References

G. Bourda, P. Charlot, and J.-F. Le Campion. Astrometric suitability of optically-bright ICRF sources for the alignment with the future Gaia celestial reference frame. *A&A*, 490: 403–408, 2008.

G. Bourda, P. Charlot, R. Porcas, and S. Garrington. VLBI observations of optically-bright extragalactic radio sources for

the alignment of the radio frame with the future Gaia frame. I. Source detection. *A&A*, 520: A113, 2010.

G. Bourda, A. Collioud, P. Charlot, R. Porcas, and S. Garrington. VLBI observations of optically-bright extragalactic radio sources for the alignment of the radio frame with the future Gaia frame. II. Imaging candidate sources. *A&A*, 526: A102, 2011.

J. J. Condon, W.D. Cotton, E.W. Greisen, Q.F. Yin, R.A. Perley, G.B. Taylor, and J.J. Broderick. The NRAO VLA Sky Survey. *AJ*, 115: 1693–1716, 1998.

A. L. Fey, C. Ma, E.F. Arias, P. Charlot, M. Feissel-Vernier, A.-M. Gontier, C.S. Jacobs, J. Li, and D.S. MacMillan. The Second Extension of the International Celestial Reference Frame: ICRF-EXT.1. *AJ*, 127: 3587–3608, 2004.

IERS Technical Note 35. The Second Realization of the International Celestial Reference Frame by Very Long Baseline Interferometry. Presented on behalf of the IERS / IVS Working Group, A. Fey, D. Gordon & C. Jacobs (eds.), Frankfurt am Main: Verlag des Bundesamts für Kartographie und Geodäsie, ISBN 3-89888-918-6, 204 p., 2009.

L. Lindegren, C. Babusiaux, C. Bailer-Jones, U Bastian, A.G.A. Brown, M. Cropper, E. Høg, C. Jordi, D. Katz, F. van Leeuwen, X. Luri, F. Mignard, J.H.J. de Bruijne, and T. Prusti. The Gaia mission: science, organization and present status. In W. Wenjin, I. Platais, and M. Perryman (eds), *Proceedings of IAU Symposium 248, A Giant Step: from Milli- to Micro-arcsecond Astrometry*, Cambridge University Press, pp. 217–223, 2008.

C. Ma, E.F. Arias, T. Eubanks, A.L. Fey, A.-M. Gontier, C.S. Jacobs, O.J. Sovers, B.A. Archinal, and P. Charlot. The International Celestial Reference Frame as Realized by Very Long Baseline Interferometry. *AJ*, 116: 516–546, 1998.

F. Mignard. Future Space-Based Celestial Reference Frame. In R. Gaume, D. McCarth, and J. Souchay (eds.), *Proceedings of IAU General Assembly XXV, Joint Discussion 16: The International Celestial Reference System: Maintenance and Future Realization*, pp. 133–140, 2003.

M. A. C. Perryman, K.S. de Boer, G. Gilmore, E. Høg, M.G. Lattanzi, L. Lindegren, X. Luri, F. Mignard, O. Pace, P.T. de Zeeuw. GAIA: Composition, formation and evolution of the Galaxy. *A&A*, 369: 339–363, 2001.

Single baseline GLONASS observations with VLBI: data processing and first results

V. Tornatore, R. Haas, D. Duev, S. Pogrebenko, S. Casey, G. Molera Calvés, A. Keimpema

Abstract The VLBI technique, in geodetic mode, was used to observe signals emitted by three GLONASS (GLObal NAvigation Satellite System) satellites. The baseline observing simultaneously satellites had at its ends the Medicina (32 m) and Onsala85 (25 m) radio telescopes, both equipped with L-band receivers. Several preparatory tests were necessary for obtaining good data that could be processed.
In this paper we report on the observations performed on August 16, 2010 data processing and results of the experiment. The natural radio source 3c286 was observed also as a calibrator before and after satellite observing sessions. A narrow band approach using software primarily developed for astronomical and space applications, was applied to extract the narrow band carrier.
Differential frequency on the baseline Medicina-Onsala was also evaluated to compute differential phase which was then adopted to determine satellite coordinate corrections with respect to ITRF values. Broad-band correlation was performed on the calibrator data using the DiFX software. The SFXC correlation of satellite data was performed testing near field delay model at extreme nearness; obtained results are described.

Vincenza Tornatore
Politecnico di Milano, DIIAR, Piazza Leonardo da Vinci 32, IT-20133 Milan, Italy
Rüdiger Haas
Chalmers University of Technology, Department of Earth and Space Sciences, Onsala Space Observatory, SE-439 92 Onsala, Sweden
Dmitry Duev
Joint Institute for VLBI in Europe, Oude Hoogeveensedijk 4, NL-7991 PD Dwingeloo, The Netherlands, and Lomonosov Moscow State University, GSP-1, Leninskie gory, RU-119234 Moscow, Russian Federation
Sergei Pogrebenko
Joint Institute for VLBI in Europe, Oude Hoogeveensedijk 4, NL-7991 PD Dwingeloo, The Netherlands
Simon Casey
Onsala Space Observatory, SE-439 92 Onsala, Sweden
Guifré Molera Calvés
Aalto University Metsähovi Radio Observatory, Finland-Metsähovintie 114, FI-02540 Kylmälä, Finland
Aard Keimpema
Joint Institute for VLBI in Europe, Oude Hoogeveensedijk 4, NL-7991 PD Dwingeloo, The Netherlands

1 Introduction

Reference frames of high accuracy are the basis for the analysis and interpretation of geodetic parameters and their temporal behaviour. Modern reference frames are generated by IERS (International Earth Rotation and Reference System Service) which combines solutions of the space geodetic techniques VLBI, SLR/LLR (Satellite Laser Ranging/Lunar Laser Ranging), GNSS (Global Navigation Satellite Systems) and DORIS (Doppler Orbitography and Radiopositioning Integrated by Satellite). The consistency in time of the analysis strategies for each data series but also between the different techniques is essential to obtain a reference frame of highest accuracy.
Presently the combination of different geodetic space techniques is based on local-ties at co-located stations. Local-ties are derived from local terrestrial geodetic surveys carried out at these stations. Some discrepancies between the local-ties derived from terrestrial surveys and coordinate differences derived from space-geodetic observations have been found in several studies, however the reason for the discrepancies is often not clear (Krügel and Angermann, 2005).

The tracking of GNSS satellites by VLBI sites permits the connection of both observing techniques at the satellite level (satellite co-location) and not at the station level. In this case the link depends neither on the local ties nor on the uncertainties of the GNSS reference point of the ground station antennas. The connection at the satellite level is a promising alternative to the connection at the stations. The independently estimated station coordinates at co-located sites could also allow a validation of the local ties (Thaller et al., 2011).
With this work we want to verify if from a technical point of view the estimate of a GNSS satellite coordinates (in this case in particular we observe GLONASS satellites) can be obtained using the VLBI technique. Observing GNSS signals, using the same optics as the VLBI signals (including gravitational and thermal deformations), the combination of the kinematic VLBI reference frame of natural celestial radio sources and the dynamical GNSS reference frames of satellite orbits is aided. The GNSS satellite

Satellite	Observation Interval [UT]	Emitted frequency [MHz]
PR11	11:59:50-12:14:50	1602.00
PR21	12:44:50-12:59:50	1604.25
PR13	13:29:50-13:44:50	1600.87

Table 1 Satellite observation setup

positions could be expressed with respect to the background natural radio sources. Furthermore, the connection of the VLBI TRF to the Earth's gravity field could be improved.

In Section 2 the observations of the GLONASS satellites in VLBI geodetic mode are described, in Section 3 data processing of GLONASS and calibrator data are recalled both for narrow-band and broad-band correlation, finally in Section 4 comments on present results and further developments are presented.

2 VLBI GLONASS experiment description

The VLBI observations were carried out on August 16, 2010 on the baseline Onsala-Medicina and three GLONASS satellites were tracked one by one. During the experiment the radio source 3c286 was observed as a calibrator for 5 minutes at the beginning and at the end of the whole satellite session. The GLONASS satellites observed in turn, for 15 minutes each, were PR11, PR21 and PR13. They were selected, according to the planning, among those simultaneously visible at both stations and very well distributed in the sky at each station. Then, during the observation interval, they had nor a very low elevation, which is good to decrease a bit the troposphere effect, nor a very high elevation which might have given antenna pointing problems. In order to track the satellites the 15 minutes observation interval was actually made up of 45 scans of 20 seconds each, where for about half of these 20 seconds both the telescopes were pointing at the satellite, and for the other half were moving to the new satellite location. Such re-pointing of the radio telescopes produced in the data residuals some glitches with a period of about 20 seconds. They could be avoided if a continuous tracking software could be installed in the Field System. Frequencies emitted by each satellite and the interval of observation can be found in Table (1).
During all the experiment 4 IFs were simultaneously recorded, there are 2 which were always tuned to 1610 MHz, 1 of these recorded RHCP (Right Hand Circular Polarization), the other LHCP (Left Hand Circular Polarization). The other 2 IFs, which again recorded RHCP and LHCP, were set to one of the 3 frequencies corresponding to the satellite being observed, and therefore changed during the experiment. A bandwidth of 16 MHz was observed in a way that eachone of the emitted frequencies was in the center of the bandwidth. Each RHCP had 16 MHz, as did each LHCP, therefore a combined total of 32 MHz per observed frequency, or 64 MHz total recorded bandwidth across the 2 frequencies. Additional attenuation for both RHCP and LHCP channels was applied in order to avoid saturation of the receiving systems by the strong satellite signal.
The calibrator 3c386 was observed at the starting of the satellite session for 5 minutes beginning 11:40:00 UT and for 5 minutes at the end of the satellite session beginning at 14:00 UT. For the calibrator 3c386 2 IFs were at 1592.88 MHz and 2 at 1610 MHz both RHPC and LHCP.

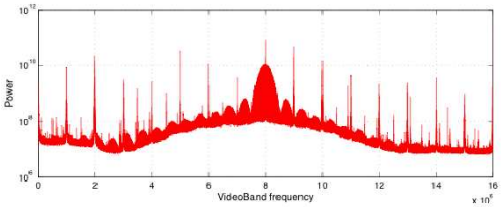

Fig. 1 Power spectrum for interval 2 (PR11) observed at Onsala radio telescope

3 Data processing of VLBI GLONASS observations

Several studies and data processing have been performed on the data recorded during the August 16, 2010 experiment.

3.1 Narrow-band correlation

The initial detection of the satellite carrier signal and subharmonics relative to the carrier was performed using the high-resolution software spectrometer, SWSpec (Wagner and Molera Calvés, 2007) and spacecraft tracking software, SCTracker (Wagner et al., 2010) developed at Metsähovi Radio Observatory in collaboration with JIVE in the framework of the Planetary Radio Interferometry and Doppler Experiments (PRIDE).

The first iteration of SWspec on data of the second interval (satellite PR11) observed with the Onsala radio telescope is shown in (Fig. (1)). The GLONASS signal is seen in the central lobe at 8 MHz. The narrow peaks spaced 1 MHz are caused by the Phase Calibrator signal from the receiver. We notice high level of power in the main and side lobes. For GLONASS satellite PR11 autocorrelation spectrum analysis we used $1.6x10^6$ DFT (Discrete Fourier Transform) points, 1-second integration time and Cosine-squared windowing, for a spectral resolution of 20 Hz over the 16 MHz bandwidth.

The SCtracker filters the satellite signal down to 8 kHz narrow bandwidth with spectral resolution of 4 Hz. The frequency detection noise is at a level of several mHz in 1 second. Results of the narrow-band signal processing were then analysed at JIVE.

After the PLL (Phase-Locked-Loop), the GLONASS signal is filtered out to a narrow band around the carrier line of 800 Hz and spectral resolution of 0.8 Hz. With such accuracy, we can extract the residual phase of the carrier tone. The phase fluctuations detected at each stations allow us to study the phase scintillation along the propagation path. We can see the results of analysis on the GLONASS data for the 4th interval (satellite PR13) obtained at Onsala radio telescope in the Fig. (2). The satellite phase with

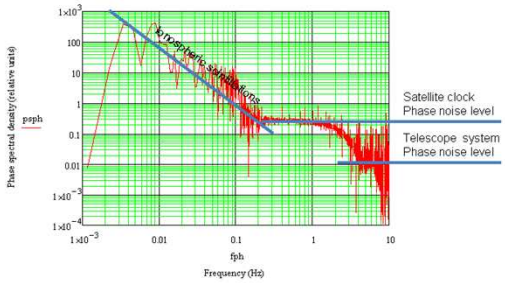

Fig. 2 Phase scintillation spectrum, as of GLONASS PR13 observations, Onsala, interval 4

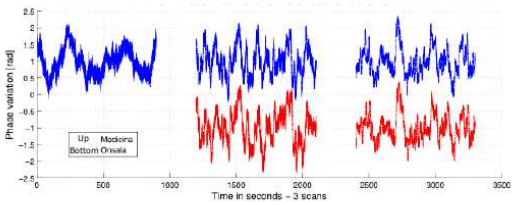

Fig. 3 Phase fluctuations for the three: GLONASS satellites PR11, PR21, PR13 observed at Medicina (top) and Onsala (bottom).

a 20 Hz sampling phase lock was extracted. The y-axis is the power spectra density of the phase scintillations and the x-axis is frequency of the phase scintillations in Hz. The phase scintillation is dominated by three components: ionosphere scintillations, GLONASS LO phase noise and receiving telescope phase noise.

The phase from the 3 satellites (PR11, PR21, PR13) observed with the Medicina and Onsala antennas on the August 16, 2010 was extracted. The H-maser clock at the antennas was used as reference. For convenience (+1) radian phase has been added to the Medicina data and (-1) radian to Onsala data. The detection of the phase was successful for 5 observation intervals out of 6. Each one elapsed 900 seconds (15 minutes). Phase fluctuations for the three satellites are shown in the Fig. (3)

The topocentric detections of the frequency/phase for Medicina and Onsala stations were reduced to the common phase centre, namely the geocentre. For this reduction, the precalculated geocentric VLBI delays of the satellite signal were used. Geometric part of the delay for GLONASS satellites is computed using the Sekido-Fukushima model (Sekido and Fukushima, 2006) for a near-field radio source. Contributions to the delay due to troposphere, ionosphere (using IGS TEC maps), and clock offsets/rates at the stations were taken into account as well (Duev et al., in press). On the baseline Onsala-Medicina the differential frequency of PR21 GLONASS carrier was then calculated. It shows a linear trend that is very close to zero (Fig. (4)). Such differential frequency was used to compute the differential phase, which was in turn adopted as a residual for the least-

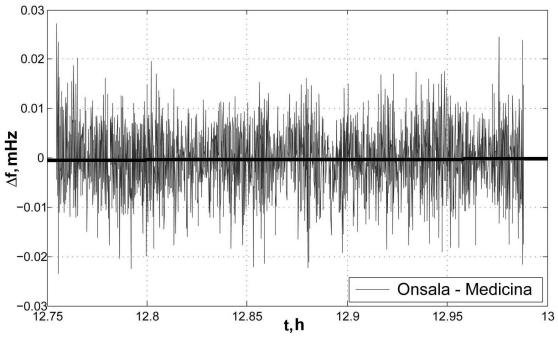

Fig. 4 Differential frequency of the GLONASS PR21 satellite carrier on the baseline Onsala-Medicina.

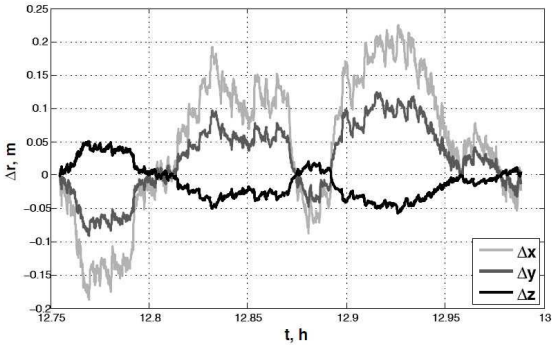

Fig. 5 Corrections to the ITRF position of the satellite PR21 on the baseline Onsala-Medicina.

squares estimation of corrections to the ITRF position of the satellite (Fig. (5)). The corrections obtained are of the order of 10 cm.

Correlation between the corrections to different coordinates is also present due to the fact that the observations were conducted only on one baseline.

3.2 Broad-band correlation

Data of August 16, 2010 experiment was processed also applying broad-band correlation. The signals of the reference source 3c286 were correlated using the DiFX software (Deller et al., 2007) in order to determine clock offsets and clock offset rates between the stations. Cross-correlation fringe and residual phase of the fringe were calculated for the calibrator radio source 3c286, as detected during our experiment on the baseline Onsala-Medicina. Clock offset calibration accuracy was at a level of 0.2ns, clock rate offset determination accuracy was better than 0.05 ps/s, phase noise at a level of 0.2 radians at 1s sampling (Tornatore et al., 2011). Also the software SFXC (http://www.jive.nl/correlator/status.html) was used to find fringes for both calibrator 3c286 (Fig. (6) top) and GLONASS satellite PR21 (Fig. (6) bottom). On the baseline Onsala-Medicina, channel 1, 16 MHz bandwidth, RCP, 16K lags

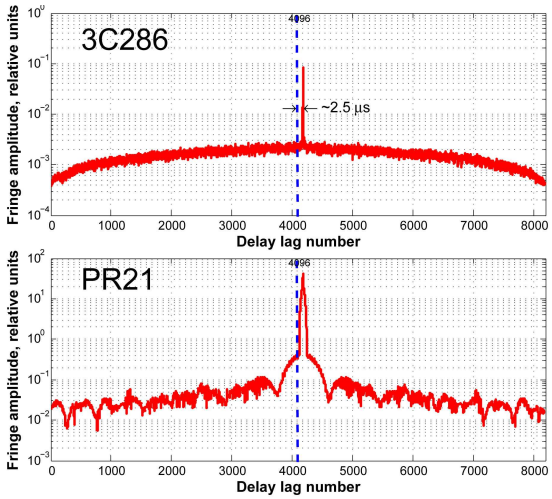

Fig. 6 Fringes for both calibrator 3c286 (top) and GLONASS satellite PR21 (bottom) on the baseline Onsala-Medicina.

with *a priori* clock offsets, averaged, vector 2s, then scalar over the full scan length. The software was run with 8000 FFT points otherwise we would miss the fringes.

Fringes were calculated also after a clock search with clock offset of 2.5 ms and clock rate offset of -1.78 ps/s, vector averaged, 10s, then scalar over the full scan length. It has to be noticed for fringes of the satellite PR21 in lag domain, that the side lobes of correlation are significantly above the noise level even at $\approx$ 100 microseconds offsets due to a high coherency of the signal. Fringes were found only in the IF correspondent to the frequency emitted by the satellite and not for the second frequency 1610 MHz. It is not clear the reason why the calibrator is not seen at 1610 MHz. Some problems are still present in the results, a bias of several nanoseconds was found in the residual delays. Currently we are busy with fine tuning of our delay model.

4 Conclusions and further developments

The obtained results show that the objectives of VLBI-observations of GNSS satellites can be achieved. To improve the present accuracy of parameter estimation additional elaboration is requested: on one hand considering the modelling part, more detailed analysis is still requested to improve delay model for near (or *very near*) field objects. On the other hand considering the observation side further experiments are encouraged in the direction of dual-frequency observations (G2/G1) to allow for ionosphere correction. Also an increasing of the number of observing telescopes, of the number of source calibrators (possibly well distributed in the sky), longer duration of observations is also expected to bring an improvement of GLONASS ephemerides accuracy from current 5 cm. Observations of other constellation satellites like for example the GPS (Global Positioning System) could also help to fix present uncertainties still present in the data or in the near field model. Together with VLBI geodetic observation mode also a phase referencing observation mode, could be attempted, even if in this case high satellite velocity could represent an obstacle to find radio source calibrators near to the satellite route.

5 Acknowledgements

This work is based on observations with the Medicina radio telescope, operated by INAF–Istituto di Radioastronomia, Italy, and the Onsala85 radio telescope, operated by the Swedish National Facility for Radio Astronomy.
The authors are thankful for personnel at the VLBI stations of Medicina and Onsala, for supporting the experiments. The author V. Tornatore wish to thank MIUR (Ministry of Education of University and Research) for supporting her participation to the 20th EVGA Meeting and 12th Analysis Workshop in the framework of the PRIN (Project of considerable National Interest, 2008) *Il nuovo di sistema di riferimento geodetico italiano: monitoraggio continuo e applicazioni alla gestione e al controllo del territorio*, national coordinator prof. F. Sansó.

References

A. T. Deller, M. Tingay,M. Bailes, C. West. DiFX: A Software correlator for very Long Baseline Interferometry using Multiprocessor Computing Environments. *The Astr. Soc. of the Pacific*, 119: 318-336, 2007.

D. A. Duev, S. V. Pogrebenko, G. Molera Calvés. A Tropospheric Signal Delay Model for Radio Astronomical Observations. *Astronomy Reports*, Vol. 55, 2011, in press.

M. Krügel, D. Angermann. Analysis of local ties from multiyear solutions of different techniques. In: Richter B, Dick W, Schwegmann W (eds) *Proceedings of the IERS workshop on site co-locations, Verlag des Bundesamts für Kartographie und Geodäsie, Frankfurt am Main, Germany*, IERS technical note, no. 33, 2005

M. Sekido, T. Fukushima. A VLBI Model for a Radio Source at Finite Distance. *J. Geodesy*, 80, 137-149, 2006.

D. Thaller, R Dach, M. Seitz, G. Beutler, M Mareye; B. Richter. Combination of GNSS and SLR observations using satellite co-locations. *J. Geodesy*, Volume 85, Issue 5, pp.257-272, 2011

V. Tornatore, R. Haas, D. Duev, S. V. Pogrebenko, S. Casey, G. Molera Calvés Determination of GLONASS satellite coordinates with respect to natural radio sources using the VLBI technique: preliminary results, *Proceedings of ETTC (European Test and Telemetry Conference) 2011, Toulouse 2011*, in press

J. Wagner, G. Molera Calvés. High-resolution spectrometer software home page, 2007 http://cellspetasklib.sourceforge.net/

J. Wagner, G. Molera Calvés, S. V. Pogrebenko. Metsähovi Software Spectrometer and Spacecraft Tracking tools, software release, GNU GPL, 2009-2010 http://www.metsahovi.fi/en/vlbi/spec/index

The Celestial Reference Frame at X/Ka-band (8.4/32 GHz)

C. S. Jacobs, J. E. Clark, L. J. Skjerve, O. J. Sovers, C. Garcia-Miro, S. Horiuchi

Abstract We have constructed an X/Ka-band (8.4/32 GHz) celestial reference frame using fifty-two 24-hour sessions with the Deep Space Network. We detected 455 sources covering the full 24 hours of right ascension and declinations down to -45 deg. Comparison of 404 X/Ka sources in common with the S/X-band (2.3/8.4 GHz) ICRF2 shows wRMS agreement of 213 microarcsec (μas) in $\alpha\cos\delta$ and 282 μas in δ. There is evidence for systematic errors at the 100 μas level. Known errors include limited SNR, lack of phase calibration, troposphere mismodelling, and limited southern geometry. Compared to X-band, Ka-band allows access to more compact source morphology and reduced core shift. Existing X/Ka data and simulated Gaia data predict a frame tie precision of 10–15 μas (1-σ, per 3-D rotation component) with anticipated improvements reducing that to 5–10 μas per component.

Keywords reference systems, celestial frame, ICRF, frame tie, Gaia, catalogs, astrometry, interferometry, VLBI, radio continuum, X/Ka-band, Ka-band, galaxies: active galactic nuclei, quasars, blazars

1 Introduction

For over three decades now, radio frequency work in global astrometry, geodesy, and deep space navigation has been done at S-band (2.3 GHz) and X-band (8.4 GHz). While this work has been tremendously successful in producing 100 μas level global astrometry (e.g., Ma et al., 2009) and sub-cm geodesy, developments made over the last decade have made it possible to consider the merits of moving to a new set of frequencies. In this paper we present global astrometric results from X/Ka (8.4/32 GHz) observations.

Advantages: Moving the observing frequencies up by approximately a factor of four has several advantages. For NASA's Deep Space Network, the driver is the potential for higher data rates for telemetry signals from deep space probes. Other advantages include 1) the spatial distribution of flux becomes significantly more compact (Charlot et al, 2010) lending hope that the positions will be more stable over time, 2) Radio Frequency Interference (RFI) at S-band would be avoided, 3) Ionosphere and solar plasma effects on group delay are reduced by a factor of 15!

Disadvantages: While these are very significant advantages, they do not come without a price. The change from 2.3 / 8.4 GHz to 8.4 / 32 GHz moves one closer to the water line at 22 GHz and thus increases the system temperature from a few Kelvins per atmospheric thickness up to 10–15 Kelvins per atmosphere or more. Thus one becomes much more sensitive to weather. Furthermore, the sources themselves are in general weaker and many sources are resolved. Also, with the observing wavelengths shortened by a factor of 4, the coherence times are shortened so that practical integration times are a few minutes or less—even in relatively dry climates. The shorter wavelengths also imply that the antenna pointing accuracy requirements must be tightened by the same factor of 4. The combined effect of these disadvantages is to lower the system sensitivity. Fortunately, advances in recent years in recording technology make it feasible and affordable to offset these losses in sensitivity by recording more bits. Thus while most of the X/Ka data presented in this paper used the same overall 112 Mbps bit rate as previous S/X work, recent data were taken at 448 Mbps with an increase to 2048 Mbps hoped for within the next year or two.

This paper is organized as follows: We will describe the observations, modelling, and present the results. Next, we will estimate the accuracy by comparing to the S/X-based ICRF2 (Ma et al., 2009) including a look at zonal errors. This will be complemented by a discussion of the error budget and the potential for improving the geometry of our network by adding a southern

C.S. Jacobs, J.E. Clark, L.J. Skjerve, and O.J. Sovers
Jet Propulsion Laboratory, California Institute of Technology, 4800 Oak Grove Dr., Pasadena CA 91109.

C.Garcia-Miro
Ingenieria y Servicios Aeroespaciales,
Instituto Nacional de Técnica Aeroespacial/NASA
Madrid Deep Space Communication Complex,
Paseo del Pintor Rosales, 34 bajo, E-28008 Madrid, Spain

S. Horiuchi
C.S.I.R.O. Astronomy and Space Science/NASA,
PO Box 1035, AU Tuggeranong ACT 2901, Australia

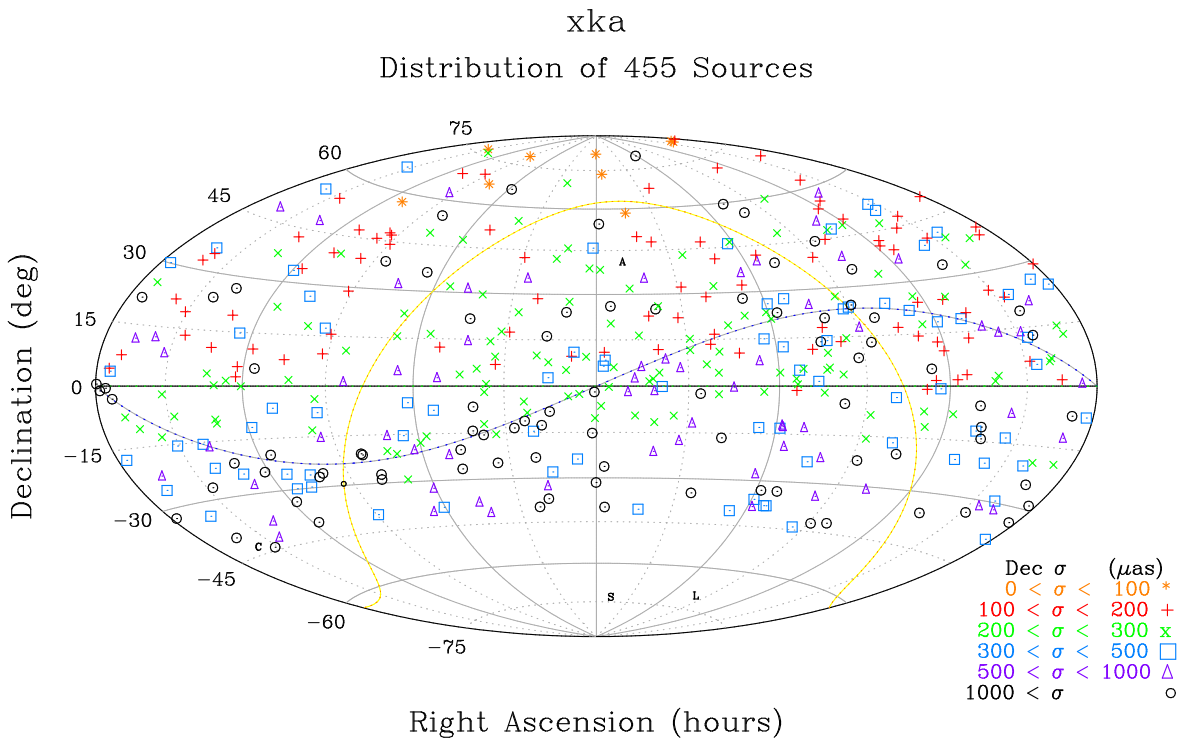

Fig. 1 Distribution of 455 X/Ka-band sources detected to date. Symbols indicate 1-σ formal declination uncertainties as defined in the legend at lower right. $(\alpha, \delta) = (0, 0)$ is at the center. The ecliptic plane is indicated by the sinusoidal curve. The galactic plane is indicated by the Ω-shaped curve. Note the trend for decreasing declination precision moving southward. Local galactic neighborhood indicated by A, C, S, L: Andromeda, Centaurus-A, Small & Large Magellanic clouds (none observed at X/Ka).

station. Lastly, we will discuss the potential for linking the X/Ka radio frame and the Gaia optical frame.

2 The VLBI Observations

The results presented here are from fifty-two Very Long Baseline Interferometry (VLBI) observing sessions of ∼24 hour duration done from July 2005 until September 2010 using NASA's Deep Space Stations (DSS) 25 or DSS 26 in Goldstone, California to either DSS 34 in Tidbinbilla, Australia or DSS 54 or DSS 55 outside Madrid, Spain to form interferometric baselines of 10,500 and 8,400 km length, respectively. We recorded VLBI data simultaneously at X-band (8.4 GHz) and Ka-band (32 GHz). Initially, sampling of each band was at 56 Mbps while more recent passes used 160/288 Mbps at X/Ka. Each band used a spanned bandwidth of ∼360 MHz. The data were filtered, sampled, and recorded to the Mark4 or Mark5A VLBI systems. The data were then correlated with the JPL BlockII correlator (O'Connor, 1987) or the JPL SOFTC software correlator (Lowe, 2005). Fringe fitting was done with the FIT fringe fitting software (Lowe, 1992). The measurements covered the full 24 hours of right ascension and declinations down to −45 deg. Individual observations were about 1 to 2 minutes in duration.

3 Modelling

The above described set of observations were then modelled using the MODEST software (Sovers et al., 1998). A priori Earth orientation was fixed to the MHB nutation model (Mathews et al., 2002) and the empirically determined UT1-UTC and Polar Motion of the Space 2008 series (Ratcliff et al., 2010). The celestial frame was aligned to the ICRF2 defining sources (Ma et al., 2009) using a no-net-rotation constraint (Jacobs et al, 2010). Station velocities were estimated; station locations were estimated with a 1 cm constraint per component to a decades-long S/X-band VLBI solution.

4 Results

In all, we detected 455 extragalactic radio sources which covered the full 24 hours of RA and Declinations down to −45 deg. In Fig. (1) these sources are plotted using Hammer's (1892) equal-area projection to show their locations on the sky. RA= 0 is at the center. The ecliptic plane is shown by the sinusoidal-shaped curve and the Galactic plane is indicated by the Ω-shaped curve. The source symbols indicate the 1-σ formal declination uncertainties with the value ranges indicated in the figure's legend.

Note that the declination precision drops as one moves toward the south. This is a result of having significantly less data on the California to Australia baseline combined with the need to observe sources closer to the horizon as declination moves south, thus incurring greater error from higher system temperatures and tropospheric mis-modelling.

5 Accuracy: X/Ka vs. S/X comparisons

Experience shows that formal uncertainties tend to underestimate true errors. An independent estimate of position errors was obtained by comparing our X/Ka-band positions to the S/X-based ICRF2. For 404 common sources, the weighted RMS (wRMS) differences are 213 μas in $\alpha\cos\delta$ and 282 μas in δ.

6 Zonal Errors

Section 5 gave a measure of overall coordinate agreement. We now turn to X/Ka−S/X differences which are systematically correlated as a function of position on the sky. The slopes of α and δ differences vs. α and δ:

$\Delta\alpha\cos\delta$ vs. $\alpha = 3.5 \pm 1.7$ μas/hr
$\Delta\delta$ vs. $\alpha = 1.8 \pm 1.2$ μas/hr
$\Delta\alpha\cos\delta$ vs. $\delta = 0.4 \pm 0.5$ μas/deg
$\Delta\delta$ vs. $\delta = 1.1 \pm 0.9$ μas/deg

The most significant slope is $\Delta\alpha\cos\delta$ vs. α at 2.1σ. Note that the use of full correlations had a significant effect on the determination of these slopes. Fig. (2) shows in detail the declination differences vs. declination in the sense (X/Ka − S/X).

7 Discussion of Error Budget

Having assessed the size of errors in our positions using the much larger ICRF2 S/X data set as a standard of accuracy, we now discuss the major contributions to the errors in the X/Ka measurements: SNR, instrumentation, and troposphere. The trend of the weighted RMS group delay vs. the Ka-band SNR shows that for SNR $<$ 15 dB, the thermal error dominates the error budget. For higher SNRs, troposphere and instrumentation errors become more important. Binning of wRMS delay vs. airmass thickness shows that troposphere is not the dominant error due to the generally low SNRs just mentioned. However, the phase rates (which carry much less weight in the fit) are dominated by errors from tropospheric mismodelling, thus hinting that troposphere will become more important as our SNR improves with increased data rates. Lastly, we have errors from un-calibrated instrumentation. A proto-type phase calibrator was developed in order to calibrate the signal path from the feed to the sampler (Hamell et al., 2003). Test data indicate an approximately diurnal instrumental effect with ∼180 psec (5.4cm) RMS. Although the data themselves can be used to estimate instrumental parameters which partially characterize this effect, operational phase calibrators are being built in order to make direct reliable calibrations of the instrumentation .

8 Southern Geometry Simulation

Besides the three classes of measurement errors described above, our reference frame suffers from a very limited geometry—we have only one station in the southern hemisphere. In order to better understand this limitation, we simulated the effect of adding a second southern station (Bourda et al., 2010). Data from 50 real X/Ka sessions were augmented by simulated data for 1000 group delays each with SNR = 50 on a ∼9000 km baseline: Australia to S. America or S. Africa. The resulting solution extended Declination coverage to the south polar cap region: −45 to −90 deg. Precision in the south cap region was ∼200 μas (1 nrad) and in the mid south precision was 200–1000 μas, all with just a few days observing. We conclude that adding a second southern station would greatly aid our X/Ka frame's accuracy. In fact, the resulting four station network should compete well in astrometric accuracy with the historical S/X network and its ICRF2.

9 Potential frame tie to Gaia optical frame

The Gaia mission (2012 launch) is expected to measure 10^9 objects with 10s of μas precision including 500,000 quasars of which ∼ 2000 are expected to be both optically bright ($V < 18$) and radio loud (30–300+ mJy).

We have 336 sources with optical counterparts (Veron-Cetty & Veron,, 2010) with visual (500–600 nm) magnitude, V, bright enough to be detected by Gaia ($V < 20$ mag). Of these, 130 are bright by Gaia standards ($V < 18$).

Description	Magnitude range	Number	Percent
Bright	$0 < V < 18$	130	29 %
Detectable	$18 < V < 20$	206	45 %
Undetectable	$20 < V$	51	11 %
Unmeasured	V unknown	68	15 %

Table 1 Optical magnitude categories of X/Ka sources

Using existing X/Ka-band position uncertainties and simulated Gaia uncertainties (corrected for ecliptic latitude, but not for V−I color), we did a covariance study which predicts that the 3-D rotation between the X/Ka frame and the Gaia frame could be estimated with a precision of 10–15 μas per rotation angle (1-σ). The result is dominated by X/Ka uncertainties which have potential for a factor of two or more improvement by the time of the final Gaia catalog in 2021. Thus a frame tie precision of 5–10 μas may be possible.

Angle	Formal Uncertainty
R_x	± 16 μas
R_y	± 13 μas
R_z	± 11 μas

Table 2 Estimated precision of X/Ka to Gaia frame tie

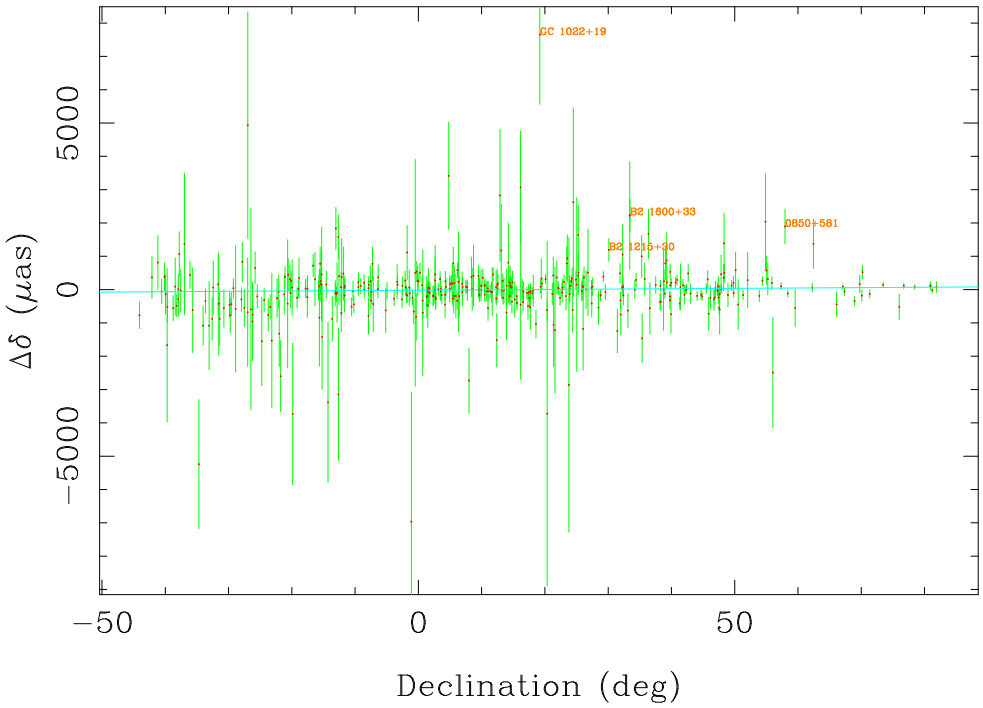

Fig. 2 Declination differences vs. declination for X/Ka − S/X-based ICRF2. The slope is 1.1 ± 0.9 μas/deg.

10 Conclusions

A celestial frame at X/Ka-band (8.4/32 GHz) has been constructed with 455 sources. For the 404 sources common to X/Ka and the S/X-based ICRF2, we find positional agreement of 213 μas (1 nrad) in $\alpha\cos\delta$ and 282 μas (1.4 nrad) in δ. Improvements in data rates and instrumental calibration are projected to allow better than 200 μas (1 nrad) accuracy within the next few years. Simulations of adding another southern station predict better than 200 μas accuracy for the southern polar cap within a very short time of adding data from an all southern baseline. This gives hope that better than 100 μas accuracy over the full sky might be achieved within a few years of adding a southern baseline. Lastly, simulations of the X/Ka sources with optical counterparts bright enough to be detectable by the Gaia mission show potential for a frame tie with 5–15 μas precision and reduced systematic errors from source structure and core shift compared to S/X-band.

11 Acknowledgements

This paper is dedicated to our colleague Lyle J. Skjerve who passed on to the next life while this paper was in preparation. He is missed. The research described herein was performed at the Jet Propulsion Laboratory of the California Institute of Technology, under a contract with the National Aeronautics and Space Administration. Government sponsorship acknowledged.

References

G. Bourda, P. Charlot, and C.S. Jacobs, (2010) 'Future Radio Reference Frames and Implications for the Gaia Link,' Proc. of ELSA Conference: Gaia at the Frontiers of Astrometry, Sevres, France.
`tphip.obspm.`r/gaia2010/IMG/pdf/Poster_Bourda.pdf

P. Charlot, D. A. Boboltz, A. L. Fey, E. B. Fomalont, B. J. Geldzahler, D. Gordon, C. S. Jacobs, G. E. Lanyi, C. Ma, C. J. Naudet, J. D. Romney, O. J. Sovers, and L. D. Zhang, (2010), 'The Celestial Reference Frame at 24 and 43 GHz II. Imaging, AJ, 139, 5, 1713. doi: 10.1088/0004-6256/139/5/1713
`http://iopscience.iop.org/1538-3881/139/5/1713/`

R. Hamell, B. Tucker, & M. Calhoun, (2003), 'Phase Calibration Generator,' NASA JPL IPN Prog. Report, 42-154, pp. 1–14.
`tmo.jpl.nasa.gov/progress\_report/42-154/154H.pdf`

E. Hammer, (1892) 'Über die Planisphäre von Aitow und verwandte Entwürfe, insbesondere neue flächentreue ähnlicher Art,' Petermanns Mitt., 38, pp. 85–87.

C. S. Jacobs, M. B. Heflin, O. J. Sovers, and J. A. Steppe, (2010), 'CRF Rotational Alignment Significantly Altered by RA-Dec Correlations,' IVS 2010 Gen. Meeting Proc., eds. D. Behrend & K. D. Baver, NASA/CP-2010, IVS Analysis Session, Hobart, Tasmania, Australia.
`tp://ivscc.gsc`.nasa.gov/pub/general-meeting/2010/presentations/GM2010_AW_jacobs.pdf

S. T. Lowe, (1992) *Theory of Post-BlockII VLBI Observable Extraction*, JPL Pub. 92-7, Pasadena CA.
trs.asa.gov/archive/nasa/casi.ntrs.nasa.gov/19940009399_1994009399.pdf

S. T. Lowe, (2005) *SOFTC: A Software VLBI Correlator*, JPL section 335 internal document, Pasadena, CA.

C. Ma et al., (2009), editors: A. L. Fey, D. Gordon & C. S. Jacobs, IERS Tech Note 35: 'The 2nd Realization of the ICRF by VLBI,' IERS, Frankfurt, Germany, Oct. 2009.
http://www.iers.org/nn_11216/IERS/EN/Publications/TechnicalNotes/tn35.html

P. M. Mathews, T. A. Herring, and B. A. Buffet, (2002), 'Modeling of Nutation and Precession: New nutation series for Nonrigid Earth and Insights into the Earth's Interior,' JGR, 107, B4, 10.1029/2001JB000390.
w.agu.org/journals/jb/jb0204/2001JB000390/

T. O'Connor, (1987) *Introduction to the BlockII Correlator hardware*, JPL internal publication, Pasadena CA.

J. T. Ratcliff and R.S. Gross, (2010), *Combinations of Earth Orientation Measurements: Space 2008, COMB2008, and POLE 2008*, JPL Publication 10-4, Pasadena CA. http://hdl.handle.net/2014/41512

O. J. Sovers, J. L. Fanselow, & C. S. Jacobs, (1998), 'Astrometry, Geodesy with Radio Interferometry: Expts., Models, Results,' Rev. Mod. Phys., 70, 4, 1393–1454.
link.aps.org/doi/10.1103/RevModPhys.70.1393
doi: 10.1103/RevModPhys.70.1393

Veron-Cetty & Veron, (13th ed.), A&A, 51, Feb. 2010.
vizier.cfa.harvard.edu/viz-bin/VizieR?-source=VII/258

The first VLBI detection of the secular aberration drift

O. Titov, S. B. Lambert

Abstract We present the first detection of the Galactic aberration in 8-GHz astrometric observations of extragalactic radio sources by geodetic VLBI. We analyzed the full geodetic VLBI observational data base to derive source proper motion and we fitted dipolar and quadrupolar vector spherical harmonics coefficients to the velocity field. Our results are in good agreement with theoretical prediction and constitute the first observation of this very tiny effect.

Keywords Galaxy, Secular aberration

1 Introduction

The Solar system rotates around the center of the Milky Way in about 250 million years at a distance of about 8.4 kpc Reid et al. (2009). This motion should result in an aberration drift of distance bodies as seen from the Earth of about $V^2/R \sim 5.4$ microseconds of arc per year (μas/yr) (e.g., Kovalevsky, 2003). In the extragalactic source proper motion field, such an effect should appear as a tiny dipolar pattern pointing towards the Galactic center ($\alpha = 266^\circ, \delta = -29^\circ$). Although predicted, the dipole was never observed. Gwinn et al. (1997) studied extragalactic source proper motions obtained from analysis of 16 years of VLBI observations but no significant dipole was found. MacMillan (2005) investigated another six years of data without success. Titov and Malkin (2009) found a dipole but with wrong direction and magnitude compared to the prediction. In Titov, Lambert and Gontier (2011), we report on the first detection of the dipole in source proper motions. Hereafter, we present some key points of this study.

Oleg Titov
Geoscience Australia, PO Box 378, Canberra, 2601, Australia
Sébastien Lambert
Observatoire de Paris, Département Systèmes de Référence Temps Espace (SYRTE), CNRS UMR 8630, Université Pierre et Marie Curie, 75014 Paris, France

2 Secular aberration drift

An extensive description of the analysis configuration was given in Titov et al. (2011). The main points were that (i) we processed about 5,000 sessions in independent mode with the Solve package, (ii) all classical geodetic and nuisance parameters were estimated, and (iii) source coordinates were loosely constrained by a no-net rotation with respect to the ICRF2 (Ma et al. 2009). The latter point appeared to be the key of the problem. In VLBI analysis softwares, the user can strengthen or loose the constrain (i.e., weighting the constraint equations) by specifying a σ. In classical solutions, one usually takes a σ equivalent to allowing the sources to stay within circles of a few milliarc seconds around the a priori position. We increased the circle radius to about an arc second. Indeed, the effect of the secular aberration drift on the celestial reference frame is to slowly deformating the axes. A too tight constraint would obviously impeach the axes to deform, and the dipole would simply be destroyed! Also, we removed 39 sources showing significant non linear positional variations due to large-scale variations in their structure (including 3C 84, 3C 273B, 3C 279, 3C 345, 3C 454.3, and 4C 39.25) from the constraint.

This analysis provided us with source coordinate time series. It is worth noting that this analysis strategy to obtain coordinate time series is very different from the analysis configuration used in many other works related to, e.g., source selection for stable frame definition (see, e.g., (see, e.g., Lambert and Gontier, 2009; Ma et al., 2009). Compared to the cited works, our strategy is essentially characterized by a much looser constraint and results in much noisier series. The rms of our coordinate time series is higher than those of Lambert and Gontier (2009) by typically a factor of 5.

Then, we used weighted least-squares to fit source proper motions to coordinate time series after a clean-up to remove large outliers. We kept time series of 555 sources with a sufficiently large observational history after 1990. At this stage of the work, it is interesting to look at the distribution of proper motions versus the right ascension for the 40 most observed sources: a systematic clearly shows up (Fig. (1)).

Finally, we applied weighted least-squares again to fit dipolar and quadrupolar vector spherical harmonics coefficients to the velocity field. The dipole components are reported in

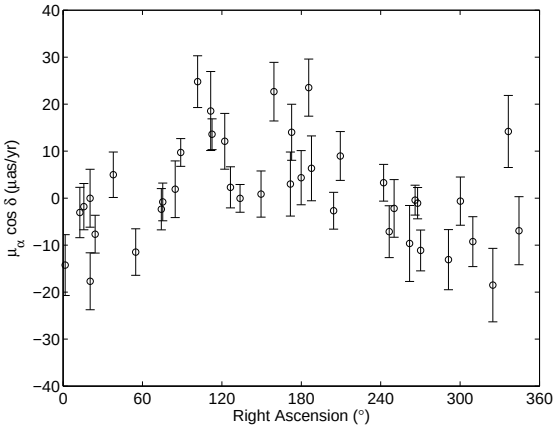

Fig. 1 Distribution of velocities of the 40 most observed sources in right ascension: a pattern is already visible.

Figs. (2)–(3). It is of amplitude 8.0 ± 2.0 μas/cy for the 40 most observed sources, and 6.4 ± 1.5 μas/cy for the 555 sources, and it points towards ($\alpha = 241 \pm 12^\circ$, $\delta = -28 \pm 12^\circ$) and ($\alpha = 263 \pm 11^\circ$, $\delta = -20 \pm 12^\circ$), respectively. Within error bars, the dipole direction contains the Galactic center.

A number of tests were done to check that we really observed the Galactic aberration. We analyzed various sets of radio source proper motions by selecting sources of structure indices lower than 2.5 (most compact sources) and ICRF2 defining sources (i.e., sources of high positional stability and low structure index). No significant departure to previous values was noticed.

As mentioned in the previous section, the NNR constraint is a fundamental point in our work. We made solutions with tightened constrained and found that the dipole moved off the Galactic center, towards a point situated around the same right ascension but in the Northern hemisphere. The reason of this systematics was not understood but should be investigated in the future. It probably raises a consequence of the network dissymmetry.

3 Quadrupolar pattern and cosmology

The quadrupole harmonics may come from an anisotropy of the expansion of the Universe (or equivalently of the Hubble constant H_0) or primordial, low frequency gravitational waves. In the latter assumption, the amplitude of the quadrupole component is linked to the limit energy density of gravitational waves (see, e.g., Gwinn et al., 1997). These gravitational waves have periods longer than the observational time span of $\sim$30 years (corresponding to frequencies less than 10^{-9} Hz). Their wavelength can even be comparable to the size of the Universe. From the analysis of the 555 source proper motions, we found a marginally statistically significant quadrupole component of amplitude 6.4 ± 3.6 μas/yr (see Fig. (4)). The resulting higher limit of the gravitational wave energy density is $0.0042h^{-2}$ where $h = H_0/100$ km/s.

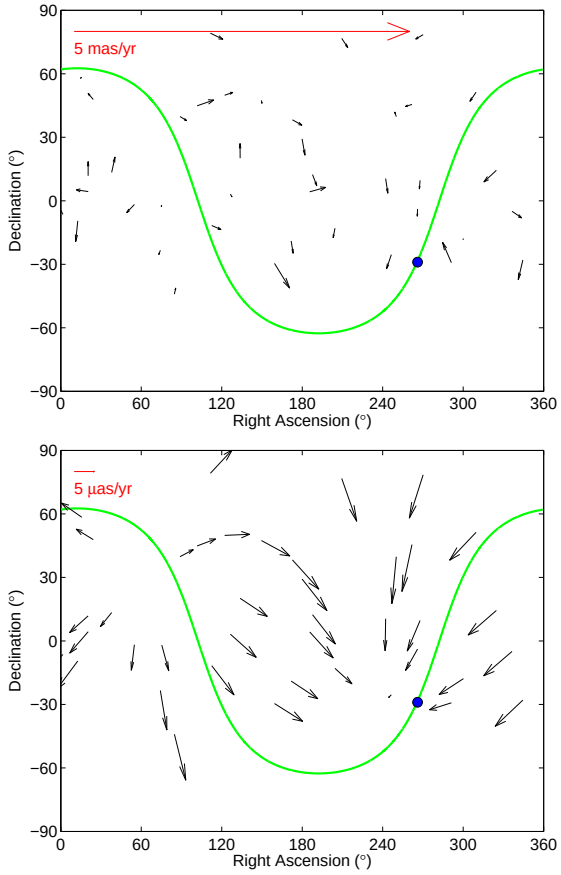

Fig. 2 Velocities and dipole pattern obtained from the 40 most observed sources. Solid line with dot shows the Galactic plane and the Galactic centre.

4 Concluding remarks

This study showed that VLBI has now accumulated accurate enough data to detect the Galactocentric acceleration through its effect on distant radio source positions. It turns out that in the future, VLBI realizations of the celestial reference system should correct source coordinates for this effect, possibly by providing source positions, together with a corrective formula.

The European optical astrometry mission Gaia, scheduled for 2012, should be able to determine the components of the acceleration vector with a relative precision of 10%. To improve the VLBI determination of the Galactocentric acceleration and to confirm the significance of the quadrupole systematics, more proper motions of extragalactic radio sources need to be measured over the next decade. Concentrating on sources showing a high positional stability and having a low structure index would reduce unwanted effects of intrinsic motion caused by the relativistic jets and other modification of the source structure. In addition, it is necessary to run a dedicated program to measure the redshift of the reference radio sources using large optical fa-

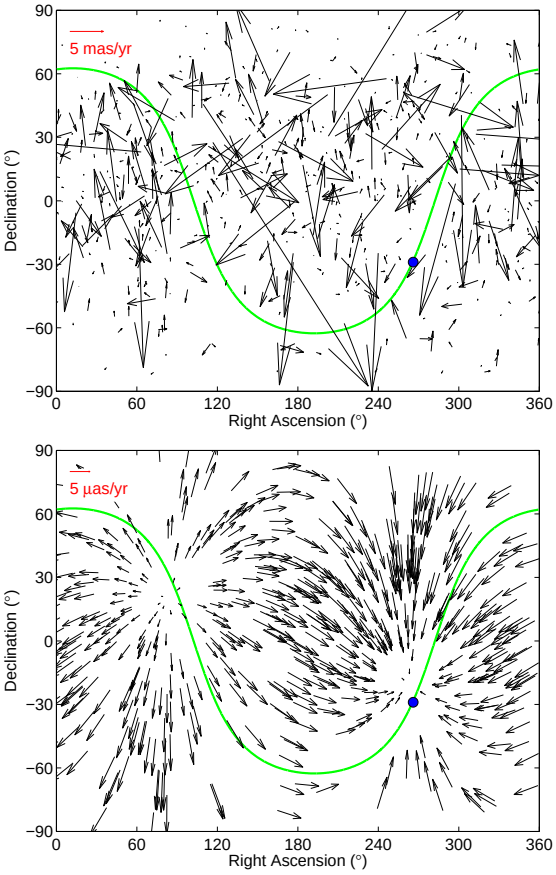

Fig. 3 Velocities and dipole pattern obtained from the 555 sources. Solid line with dot shows the Galactic plane and the Galactic centre.

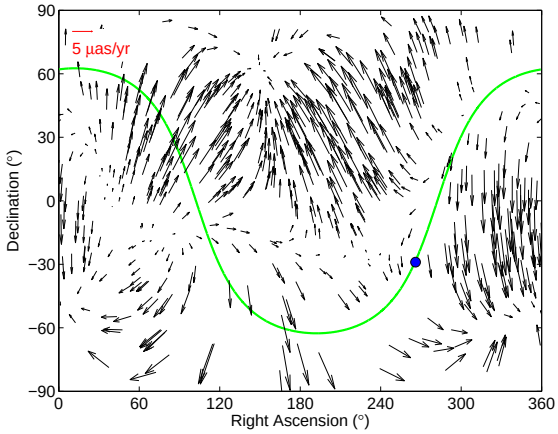

Fig. 4 Quadrupole pattern obtained from the 555 sources. Solid line with dot shows the Galactic plane and the Galactic centre.

cilities, especially in the southern hemisphere (see the paper by Titov et al. in this volume).

This study proves that VLBI is a powerful technique for geodesy, astrometry, and astrophysics, including cosmology. In addition to the wise analysis strategy employed by the authors, the key point of their success is the constant effort of the VLBI community (now concretely gathered around the IVS) for more than 30 years for maintaining, replacing, repairing antennas, scheduling and operating observations, and correlating data.

This paper is published with the permission of the CEO, Geoscience Australia.

References

C. R. Gwinn, T. M. Eubanks, T. Pyne, et al. Quasar Proper Motions and Low-Frequency Gravitational Waves. *Astrophys. J.*, 485, 87, 1997

J. Kovalevsky. Aberration in proper motions. *Astron. Astrophys.*, 404, 743, 2003

S. B. Lambert, A.-M. Gontier. On radio source selection to define a stable celestial frame. *Astron. Astrophys.*, 493, 217, 2009

C. Ma, E. F. Arias, G. Bianco, et al. The second realization of the International Celestial Reference Frame by very long baseline interferometry. In: A.L. Fey et al. (Eds.), International Earth Rotation and Reference Systems Service (IERS) Technical Note 35, Bundesamt für Kartographie und Geodäsie, Frankfurt am Main, 2009

D. S. MacMillan. Quasar Apparent Proper Motion Observed by Geodetic VLBI Networks. In: J. Romney & M. Reid (Eds.), Future Directions in High Resolution Astronomy: The 10th Anniversary of the VLBA, ASP Conference Proceedings, San Francisco: Astronomical Society of the Pacific, 477, 2005

M. J. Reid, K. M. Menten, X. W. Zheng, et al. Trigonometric Parallaxes of Massive Star-Forming Regions. VI. Galactic Structure, Fundamental Parameters, and Noncircular Motions. *Astrophys. J.*, 700, 137, 2009

O. Titov. Systematic effects in the radio source proper motion. In: G. Bourda et al. (Eds.), Proc. 19th European VLBI for Geodesy and Astrometry (EVGA) Working Meeting, 14, 2009

O. Titov, S. B. Lambert, A.-M. Gontier. VLBI measurement of the secular aberration drift. *Astron. Astrophys.*, 529, A91, 2011

Optical spectra of southern flat-spectrum IVS radio sources

O. Titov, D. Jauncey, H. Johnston, R. Hunstead, L. Christensen

Abstract About 1200 radio quasars are observed regularly by the International VLBI Service, IVS, to define and maintain the International Celestial Reference Frame, ICRF. We have presented evidence for large scale systematic proper motions, dipole and quadrupole effects, at a level in excess of 10 μas/year. This result presents a serious challenge to the standard cosmologies. However, we are concerned that our estimates of the spherical harmonics may be influenced by the paucity of IVS quasars with known redshifts in the south. We estimate that 100–150 new redshifts uniformly distributed in the south will remove these concerns. In this paper we present the results of spectroscopic observations of 47 southern IVS radio sources with the 3.58-meter NTT telescope.

Keywords radio sources, red shift, optical spectra, emission lines

1 Introduction

From 1998 through 2009 the initial International Celestial Reference Frame (ICRF1) was based on a catalogue of 608 radio VLBI source positions. Of those, 212 were so-called 'defining' sources that were used to establish the orientation of the ICRS axes (Ma et al., 1998). The Second ICRF catalogue (ICRF2) was adopted in 2009. It comprises 295 'defining' radio sources with an accuracy of about 40 μas (Fey, Gordon and Jacobs, 2009). The main uncertainty in the reference frame is caused by intrinsic structure in the radio sources (MacMillan and Ma, 2007). Apparent motions for some radio sources have been found to reach several hundred μas/year (Feissel-Vernier, 2003) due to the well-known ejections of internal jets, rather than "real" proper motion. If we assume that jet orientation is random to our line of sight, then all the apparent motions should also be random. For a large sample of quasars their positional variations are expected to be uncorrelated over the sky, and therefore not produce any systematic patterns. However, systematic effects in the apparent motions of radio sources have been predicted theoretically. The galactocentric acceleration of the Solar system barycentre should cause a first order vector spherical harmonic of magnitude 5 μas/year. This dipole effect has now been confirmed to be 6.4 ± 1.5 μas/year (Titov, Lambert and Gontier, 2011). This estimate well matches to the theoretical prediction, and confirms that the measured proper motions are realistic.

Primordial gravitational waves (GW) in the early Universe may produce second order vector spherical harmonics of electric and magnetic types (Gwinn et al., 1997). Generalized expression for the proper motion in the frame of general relativity has been published by Kristian and Sachs (1966) who found that in an expanding Universe the apparent proper motion of distant objects may increase with distance. This means that any dependence of the quadrupole systematic amplitude on redshift, if found, could be used as an independent astrometric test of the ΛCDM model. If the estimated magnitude of the quadrupole increases systematically with redshift, it will serve as indirect confirmation of the GW hypothesis. Titov, Lambert and Gontier (2011) found a limit on the GW power density of as much as $\Omega_{\rm GW} = 0.0042 \pm 0.0004\, h^{-2}$, where $h = H_0/(100\ {\rm km/s/Mpc})$ is the normalized Hubble constant. The quadrupole increases systematically with redshift but the observed magnitude is not statistically significant.

From a theoretical point of view, if the observed radio sources are distributed evenly around the sky, the parameters of the vector spherical harmonics will be separated properly. However, the real distribution of the reference quasars is uneven. This leads to a correlation between the estimated parameters and, as a result, potentially biases the estimates (Titov and Malkin, 2009). Individual apparent motion of radio sources, induced by the effect of intrinsic structure, would exaggerate this problem if the number of quasars were not sufficient.

Oleg Titov
Geoscience Australia, PO Box 378, Canberra, 2601, Australia
David Jauncey
CSIRO Astronomy and Space Science, ATNF & Mount Stromlo Observatory, Cotter Road, Weston, ACT 2611, Australia
Helen Johnston and Richard Hunstead
Sydney Institute for Astronomy, School of Physics, University of Sydney, NSW 2006, Australia
Lise Christensen
Technische Universität Munich, Excellence Cluster Universe, Boltzmannstr. 2, D-85748 Garching

The total number of the radio sources included in the IVS astrometric program exceeds 4,000, though only $\sim$ 1,000 radio sources are observed on a regular basis. By July 2010 the database of the radio source physical characteristics (Titov and Malkin, 2009) comprised 4261 objects, mostly quasars, but there is a serious deficit in the southern hemisphere of candidate sources for which VLBI observations have been made, as well as a significant lack of optical identifications for the existing candidate radio sources. By July 2010, of the 2211 objects with measured redshifts only 781 are in the southern hemisphere and only 129 with declination south of -40°. Lack of redshifts in the south can cause difficulties in analysis of the apparent proper motions of the reference radio sources.

2 Observation and data analysis

Spectroscopic observations were performed in 2010 August in Visitor Mode at the NTT using the ESO Faint Object Spectrograph and Camera (EFOSC) system with grism #13 covering the wavelength range 3685–9315Å. We selected radio sources with missing redshifts in a range of magnitudes. The finding charts were prepared using the Aladin system and the SuperCosmos Sky Survey (SSS). The seeing during observations was typically $0\farcs8$–$1\farcs5$ although occasionally as high as $4''$. The spectral resolution was 21Å. After setting up on each object we observed for an initial 15 minutes with further integrations if no obvious emission line was seen on the first exposure; individual spectra were later combined. Wavelength calibration was performed using the spectrum of a He/Ne/Ar lamp.

Fig 1 shows typical spectra of quasars with strong emission lines (IVS B1505−304 and B2354−251). The spectrum of IVS B1505−304 is dominated by a broad Ly-α line with clear associated absorption. Ly-β emission is also visible closer to the blue end of the spectra. Its redshift is estimated as $z = 3.400$, and the reduced spectrum of is shown in Fig 2. In the spectrum of IVS B2354−251 (Fig 3) it is easy to recognize the C IV and C III] emission lines (near 4200Åand 5200Å, respectively). The third line, Mg II, is almost obscured by the sky absorption at 7600Å. Its redshift is estimated as $z = 1.614$.

Data reduction was performed with the IRAF software suite using standard procedures for spectral analysis. After removing the bias and pixel-to-pixel gain variations from each frame, we then removed cosmic rays using median filtering, as implemented in the IRAF task SZAP. The separate exposures were combined and a single spectrum extracted. The resulting one-dimensional spectrum was calibrated in wavelength, and then flux-calibrated using the spectrum of a spectrophotometric standard taken with the same instrumental setup. Because the observing conditions were not photometric, the resultant flux calibration should be taken as approximate.

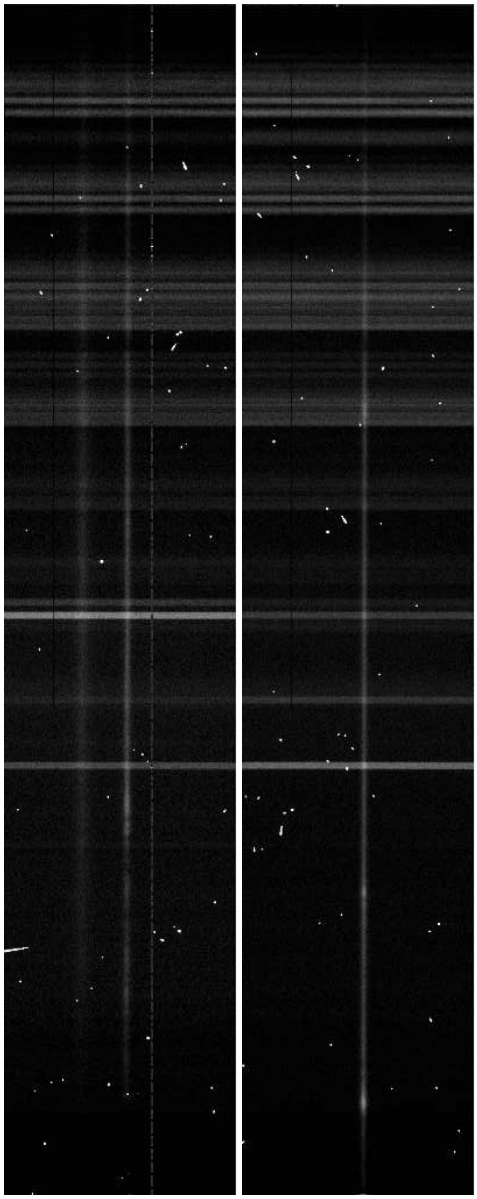

Fig. 1 Unprocessed spectra of IVS B1505−304 (left) and B2354−251 (right). The wavelength range is from 3685Å at the bottom to 9315 Åat the top. Vertical lines across the centre of the images represent continuum spectrum of the objects, and bright spots indicate positions of emission lines.

3 Radio-optical identification

Proper identification of extragalactic radio sources can be also verified by comparison of their coordinates at optical and radio wavelengths. While for the most of the targets the differences are less than $0\farcs3$, the four targets (IVS B1647−296, B1748−253, B1822−173, B2300−307) have larger radio-optical differences

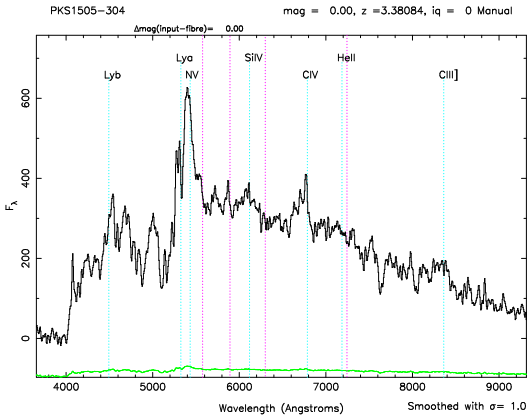

Fig. 2 Calibrated spectrum of IVS B1505−304

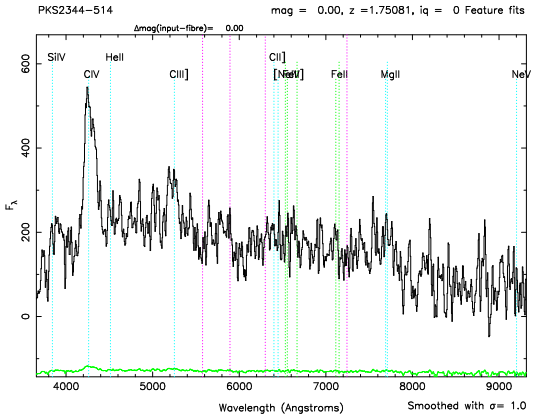

Fig. 3 Calibrated spectrum of IVS B2354−251

0.″5–5″. Spectra of these four objects are stellar with a set of known absorption lines, confirming them as Galactic stars. Three of them lie very close to the Galactic plane; however, the fourth object known as IVS B2300−307 has a Galactic latitude $b = -66°$. We believe that in this case the radio source is completely obscured by the 16th magnitude foreground star, in spite of a difference in position of 3.6″. Expected magnitude of the radio source is about 20 or greater. Separation of the star and the radio source counterpart in the optical may be possible under perfect observing conditions (seeing $\leq 0.''8$). A second attempt to measure spectrum of this radio source is highly desirable.

The radio source IVS B1923+210 represents a special case for identification. This object (see Fig 4, object 3) has been previously observed at the 6-meter telescope in Russia, and no spectral lines were found (Maslennikov et al., 2010). For the current campaign we observed all three optical objects located nearby the source of radio emission (coordinates are 19h 25m 59.6s +21d 06m 26s for the reference frame J2000) on Fig 4. All three spectra are shown in Fig 5. The spectra of stars 1 and 2 both show the Ca II triplet which establish their identity. Object 3, which is coincident with the radio position, shows no stellar absorption features although the S/N is poor. There are also no obvi-

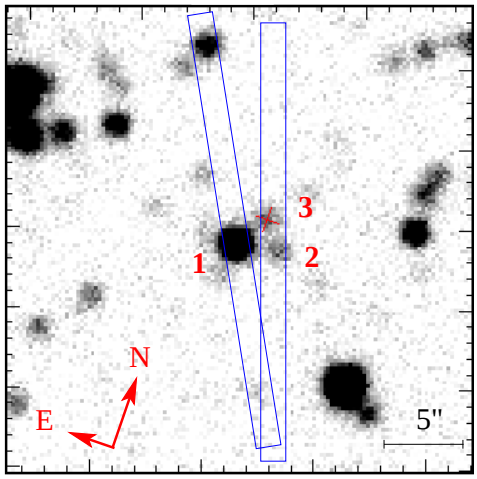

Fig. 4 Finding chart for quasar IVS B1923+210, marked as #3 here

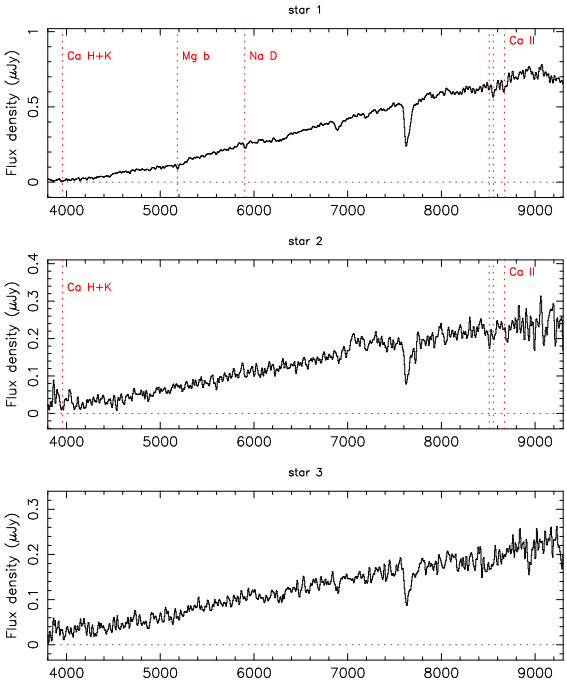

Fig. 5 Spectrum of the radio source IVS B1923+210 and two close stars

ous emission lines. The combination of a radio-optical coincidence and featureless spectrum is sufficient to suggest this as a probable BL Lac object. It is worth noting that in NED database IVS B1923+210 is known as a source of 16^m, which appears to be referring to star 1 in Fig. 4. The magnitude of the proposed counterpart to IVS B1923+210 is about 20^m.

4 Conclusions

We performed spectroscopic observations of 47 radio sources in the Southern Hemisphere and measured 31 new redshifts, with two sources having $z > 3$. At least two emission lines were confidently identified for each object. Due to successful detection of the emission lines for the faintest targets we could argue that our methodology was efficient. When the redshifts of QSOs are determined, it is critical to know which lines are used, because some high ionisation lines are shifted in velocity relative to the systemic redshift. The shifts of high ionisation lines can be typically up to 1000 km/s, while lines such as [OIII] 5007, and also the Mg II 2800 doublet are generally closer to the systemic redshift.

Nine objects had featureless spectra, and, they were considered as possible BL Lac sources. For one source, IVS B1707−038, previously known as a BL Lac, three emission lines were identified with confidence ($z = 1.923$). There were eight ICRF2 defining radio sources in this run. Five of them (IVS B1659−621, B1758−651, B1815−553, B2236−572 and B2344−514) were confirmed as extragalactic sources. Source IVS B1631−810 was confirmed as a BL Lac source with a featureless spectrum. Two other sources, IVS B0107−610 and B1443−162, were scanned in bad weather conditions and no confident emission lines were found in their spectra. A detailed paper about the program results is under preparation.

5 Acknowledgment

This paper is based on observations collected at the European Organisation for Astronomical Research in the Southern Hemisphere, Chile (058.A-0855(A)). Two of us, Oleg Titov and David Jauncey, were supported by a travel grant from ANSTO in their Access to Major Research Facilities Program (AMRFP) (reference number AMRFP 10/11-O-04) to come to La Silla.

6 Concluding remarks

This paper is published with the permission of the CEO, Geoscience Australia.

References

M. Feissel-Vernier. Selecting stable extragalactic compact radio sources from the permanent astrogeodetic VLBI programs. *A&A*, 403:105–110, 2003.

A. L. Fey, D. Gordon and C. S. Jacobs. *ICRF2 (2009)*. The Second Realization of the International Celestial Reference Frame by Very Long Baseline Interferometry. Alan L. Fey, David Gordon and Christopher S. Jacobs (eds.), International Earth Rotation and Reference Systems Service (IERS). IERS Technical Note, No. 35, Frankfurt am Main, Germany: Verlag des Bundesamtes für Kartographie und Geodäsie, ISBN 3-89888-918-6, 2009, 294 pp., 2009.

C. Gwinn. et al. Quasar Proper Motions and Low-Frequency Gravitational Waves *AJ*, 485:87–91, 1997.

J. Kristian, and R. K. Sachs. Observations in Cosmology. *ApJ*, 143:379–399, 1966.

C. Ma. et al. The International Celestial Reference Frame as realized by Very Long Baseline Interferometry. *AJ*, 116:516–546, 1998.

D. S. MacMillan, and C. Ma. Radio Source Instability in VLBI Analysis. *JoG*, 81:443–453, 2007.

K. Maslennikov, A. Boldycheva, Z. Malkin Z., and O. Titov. Measurement of redshifts of selected radio sources. *Astrophysics*, 53:147–153, 2010.

O. J. Sovers, J.L. Fanselow and C.S. Jacobs. Astrometry and Geodesy with Radio Interferometry: Experiments, Models, Results. *Rev. Mod. Phys.*, 70:1393–1454, 1998.

O. Titov, and Z. Malkin. Effect of asymmetry of the radio source distribution on the apparent proper motion kinematic analysis. *A&A*, 506:1477–1485, 2009.

O. Titov, S.Lambert and A.-M. Gontier. VLBI measurement of the secular aberration drift. *A&A*, 529:A91, 2011.

PSRπ: A large VLBA pulsar astrometry program

A. T. Deller

Abstract Obtaining pulsar parallaxes via relative astrometry (also known as differential astrometry) yields distances and transverse velocities that can be used to probe properties of the pulsar population and the interstellar medium. Large programs are essential to obtain the sample sizes necessary for these population studies, but they must be efficiently conducted to avoid requiring an infeasible amount of observing time. This paper describes the PSRπ astrometric program, including the use of new features in the DiFX software correlator to efficiently locate calibrator sources, selection and observing strategies for a sample of 60 pulsars, initial results, and likely science outcomes. Potential applications of high-precision relative astrometry to measure source structure evolution in defining sources of the International Celestial Referent Frame are also discussed.

Keywords pulsars, techniques: interferometric

1 Introduction

Due to their unique combination of high density, high magnetic field and high angular momentum, pulsars provide a rich laboratory for investigating phenomena in the fields of nuclear physics, particle physics, gravitational physics and many others (see e.g., Lorimer, 2008, and references therein). However, studies of pulsars are hampered by the uncertainty in distance–dependent quantities introduced by the reliance on dispersion measure (DM) distance estimates. Due to the highly non–uniform distribution of ionized material in the ISM on sub-kpc scales, the correspondence between a pulsar's DM and its distance often remains uncertain, despite the development of detailed models of the ionized interstellar medium (e.g., the TC93 model; Taylor & Cordes 1993, and the NE2001 model; Cordes & Lazio 2002). Although distances estimated from the TC93 and NE2001 models are generally assumed to be accurate to within 20%, previous astrometric pulsar observations have shown that much greater errors are sometimes possible for individual objects (e.g., a factor of 4.5 error in the distance for PSR J0630–2834; Deller et al., 2009), and systematic biases are likely (Lorimer et al., 2006).

Thus, independent distance measures to pulsars are vital, both to enable the confident estimation of distance–dependent parameters for individual pulsars and to refine DM–based distance models for the remainder of the pulsar population. Whilst distance estimates can also be provided from associations with other astrophysical objects (e.g. Camilo et al., 2006) or annual geometric parallax measurements made via timing (e.g., Hotan et al., 2006), parallax measurement using Very Long Baseline Interferometry (VLBI; e.g., Chatterjee et al., 2009) is the most widely applicable technique and has provided the most accurate distance measurements (Deller et al., 2008).

The PSRπ program is using the Very Long Baseline Array (VLBA[1]) to undertake a large pulsar astrometry program, taking advantage of the VLBA's relatively large field of view to observe "in–beam" calibrators for the best astrometric accuracy. Taking advantage of this capability requires the identification of suitable calibrator sources, which was the first (now largely complete) phase of the PSRπ project. The second phase, which is underway now, involves astrometric observations for 60 pulsars spread over a 1.5 year period. A third phase, not yet approved, would expand the program to 200 pulsars once the ongoing VLBA sensitivity upgrade is complete[2].

In this paper, preliminary results of the PSRπ program are presented, including the success of the in–beam calibrator search program and the verification of identified calibrators in initial astrometric epochs. The current status of the program and plans for the next 18 months are presented, along with the expected program outcomes. Finally, new techniques for and applications of high precision astrometric datasets are discussed, including the potential for direct and accurate measurement of μas–level variation in the structure of sources which define the International Celestial Reference Frame (ICRF).

ASTRON, Oude Hoogeveensedijk 4, 7991 PD Dwingeloo, The Netherlands

[1] The VLBA is operated by the National Radio Astronomy Observatory as a facility of the National Science Foundation, operated under cooperative agreement by Associated Universities, Inc.

[2] The VLBA sensitivity upgrade program is described at http://www.vlba.nrao.edu/memos/sensi/

2 In–beam calibrator search observations

The steep spectrum exhibited by most pulsars dictates that a large astrometric survey using current VLBI facilities must observe at relatively low frequency ($\sim$1.6 GHz) where enough pulsars are sufficiently bright. At these frequencies, the predominant source of systematic contribution to astrometric error is the differential ionosphere between the calibrator and target sources, and so minimising the calibrator–target angular separation is the most important consideration for obtaining accurate astrometry (e.g., Chatterjee et al., 2004). An "in–beam" calibrator, which can be observed contemporaneously with the pulsar target, is always preferred. However, on average the distance to a known VLBI calibrator source is $\sim 2^\circ$, much greater than the primary beam width of a 25m antenna (such as is used in the VLBA). Thus, suitably bright and nearby compact calibrators must be identified prior to the astrometric program. The 1σ sensitivity of a single VLBA baseline at 1.6 GHz is 1.7 mJy in 5 minutes at the current maximum bandwidth of 128 MHz; this will improve to 0.8 mJy at the 512 MHz bandwidth to become available in 2011. Thus, if a S/N ratio of 10 is required at each of the VLBA's 10 stations, calibrators of peak flux density $\geq$6 mJy can be used currently, while those $\geq$3 mJy will become available with future higher bandwidths.

In the past, this "in–beam search" operation was time–consuming, due to the need to identify sources likely to be compact before snapshot VLBI observations were used to determine their true flux one at a time. However, a new "multifield" mode of the DiFX software correlator (Deller et al., 2011) enables all known sources within the telescope primary beam to be inspected at VLBI resolution simultaneously, meaning only a single snapshot observation is required, regardless of the number of candidates. The VLBA can reach a 1σ sensitivity of 300 μJy in less than 4 minutes on–source, and so phase–referenced VLBI observations can quickly and reliably detect all VLBA in–beam calibrators that will be useful at current or future data rates.

The first phase of the PSRπ project is a search for in–beam calibrators around potential astrometric targets. Figure (1) shows an example of the pointing layout used, with known background sources identified by circles. In each case, the observations were referenced to the nearest known suitable VLBA calibrator (defined here as R) using the following scan sequence:

R-P1-P2-R-P3-P4-R-P1-P2-R-P3-P4-R

Two minute scans on each target pointing were used, for a total on–source time of four minutes per pointing. Generally, five target pulsars with relatively small angular separations were grouped and observed sequentially in a single observation to minimise calibration overhead. Correlation was performed using the DiFX software correlator (Deller et al., 2011) with one phase centre placed on each known source. Sources were extracted from the FIRST survey (Becker et al., 1995) where available, and the NVSS survey (Condon et al., 1998) in areas not covered by FIRST. Correlation was performed with a spectral resolution of 4 kHz to avoid bandwidth smearing, but the output visibilities were averaged in time to 4 second resolution and in frequency to 1 MHz resolution.

Currently, the in–beam search observations for PSRπ are nearly complete, with 77 hours of observing time expended searching around 200 pulsars. Over 7000 potential calibrators have been imaged, with 530 detected in our VLBI maps at $> 9\sigma$. One or more satisfactory in–beam calibrators were found for 97% of sources, with the remainder largely being lost due to scattering in the Galactic plane. The detection rate was comparable for FIRST and NVSS sources; although the FIRST catalog is more compact on average, it also contains objects fainter than our VLBI detection threshold, so this is not surprising. These observations were optimized to locate sufficiently bright in–beam calibrators, and so the raw results in terms of VLBI detection fractions should be interpreted with caution.

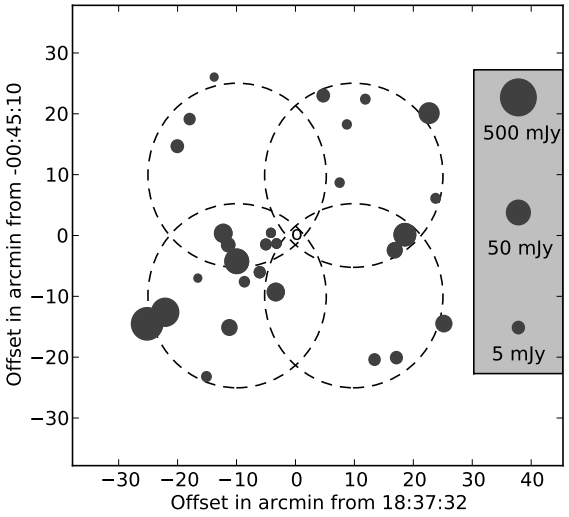

Fig. 1 The pointing pattern used to search for in–beam calibrators. The dashed lines show the half–power point of the VLBA beam, an open circle represents the pulsar and the filled circles show the background NVSS sources. The circle diameter is proportional to the logarithm of the NVSS integrated flux density. This example shows the field surrounding PSR J1837-0045.

3 Astrometric scheduling

Of the sources with one or more sufficiently bright in–beam calibrator candidates, 110 were selected for exploratory astrometric observations. The exploratory phase is used to confirm the suitability of both the pulsar and the in–beam calibrators, since the pulsar flux density is often uncertain and the snapshot observations provide limited constraints on source morphology. From these observations, 60 sources will be selected for full astrometric observations encompassing 8 epochs over 1.5 years.

For both exploratory and final astrometric observations, pulsars are grouped in pairs to minimise calibration overhead and improve *uv* coverage. Each pulsar is observed in two groups of phase referenced scans, with 30 minutes of on–source time per group. The remainder of the time was spent slewing or on exter-

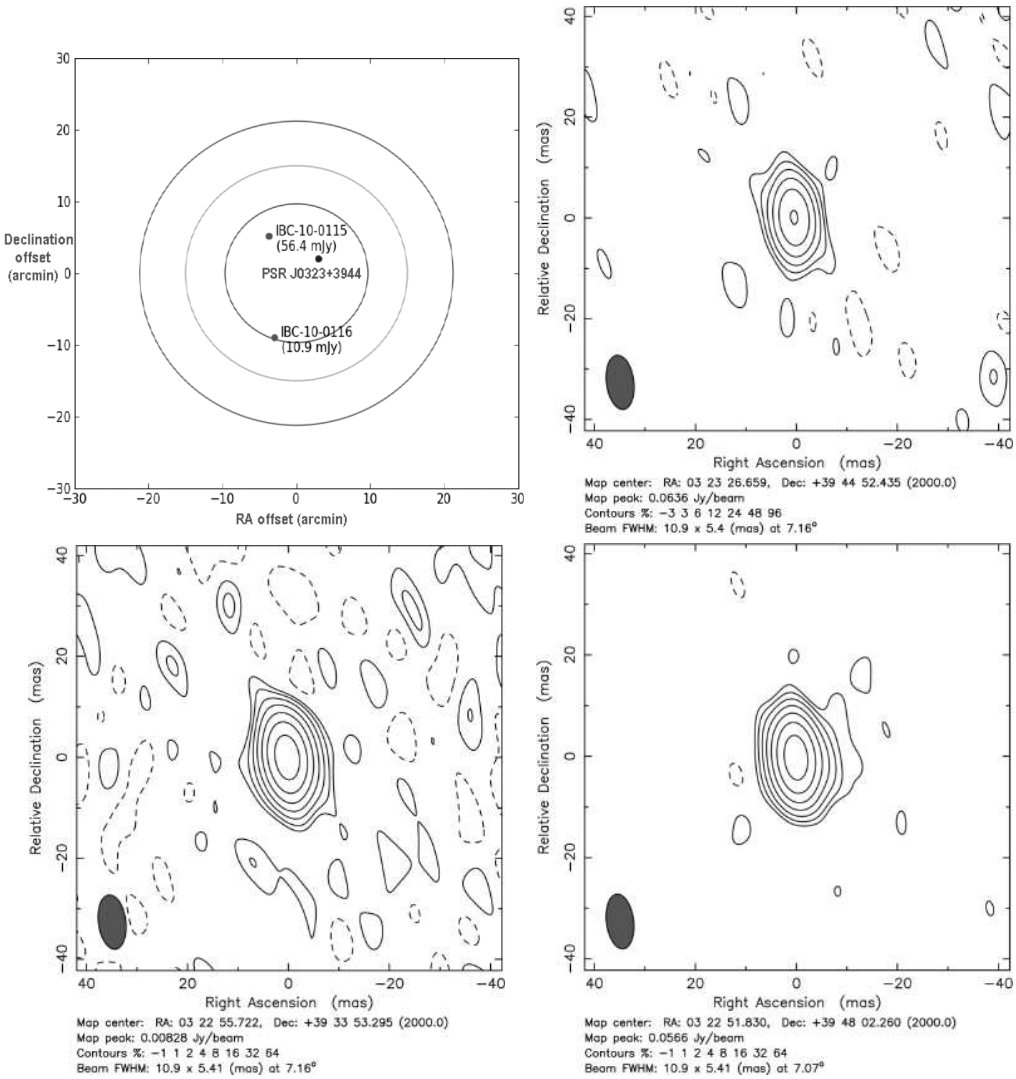

Fig. 2 Results from the first astrometric epoch on PSR J0323+3944. Clockwise from top left: the pointing setup (concentric circles showing the 75%, 50% and 25% response points of the beam), the pulsar detection from a gated correlation, the primary inbeam calibrator, and the secondary inbeam calibrator.

nal calibrator sources. Matched filtering (Deller et al., 2007) is applied when correlating pulsar data, using pulsar ephemerides obtained from pulsar timing. Figure (2) shows the pointing setup and the VLBI detections of the source PSR J0323+3944 and its two in–beam calibrators.

Several possibilities exist for taking advantage of the fortunate case of multiple in–beam calibrator sources. The simplest is to re–reduce the datasets using each calibrator independently (Chatterjee et al., 2009). This provides robustness against calibrator variability, but cannot easily take advantage of the partially independent results. A more sophisticated approach is to appropriately weight the calibrator visibilities and coherently sum them. This averages over the partially independent atmospheric errors, and also reduces the random component of the solution error because of the improved S/N. Sources too faint to provide solutions in isolation can then be used in the sum, but each source must be accurately modeled in order to be added coherently. Furthermore, if any of the included sources varies in position then the sum and the astrometric results may be adversely affected.

A third, and ideal, possibility is that three or more calibrators would be used to solve for a calibration plane, rather than point, above each antenna at regular intervals in the observation. Whilst it is presently challenging to obtain sufficiently high signal to noise observations on three or more calibrators, it may be possible for a small number of PSRπ targets, and future high–sensitivity, wide–field instruments such as the Square Kilometre Array (SKA) should use this approach routinely. Further op-

portunities offered by multi–source astrometric datasets are discussed in Section (5) below.

4 PSRπ outcomes

The completion of the first phase of PSRπ will bring about a six–fold increase in the number of pulsars with a parallax measured to an accuracy of 50μas or better. Combined with the small number of existing accurate pulsar distance measures, this will give a moderately sized ($\sim$70 objects) pool of pulsars with reliable distance measurements which can be used for unbiased investigations of the pulsar luminosity and velocity functions. The significant increase in the number of accurate distance measures will also be used as part of the next major upgrade to the Galactic electron density distribution model, following NE2001 (Cordes & Lazio, 2002). The addition of a large number of new sightlines with accurate electron column density measurements will enable a significant improvement to the model, both in terms of removing systematic biases in the large scale structure, and including many refinements in the form of small scale under– and over–densities within several kpc of the solar system.

Finally, in a sample of 60 pulsars, it is expected that a significant number of unexpected and interesting results will be uncovered based on individual pulsars. These could take the form of high velocity pulsars (e.g., Chatterjee et al., 2005), associations with supernova remnants (e.g., Thorsett et al., 2002), revision to measurements of high–energy emission (e.g., Deller et al., 2009), or breaking degeneracies in pulsar timing models (e.g., Deller et al., 2008).

5 Novel applications of multi–source astrometric datasets

Studying the structural evolution of calibrator sources at the μas level is challenging using absolute astrometry (Titov et al., 2011), and is practically impossible for faint sources. However, source structure evolution is likely to become the limiting factor for extremely precise astrometry using future instruments such as the SKA, and so understanding its characteristics is a topic of considerable importance. Relative astrometry offers the precision necessary to probe this regime, but the use of a single calibrator–target pair leaves an ambiguity as to the source of any variability. Multiple–source datasets, however, offer an opportunity to break this degeneracy.

Overcoming the usual limitations of sensitivity and the ionosphere is difficult; discerning evolution at the level of 10 μas or below would limit the angular separation to a maximum of 5' (which dictates the use of sub–mJy targets) and require a S/N ratio of several hundred (meaning an image rms of $\sim$10 μJy must be obtained). Although challenging, such observations are possible today using the European VLBI Network or the High Sensitivity Array.

Such an observing program could be used to monitor the source structure stability of a small sample of ICRF sources, allowing better estimation of the level at which source structure evolution contaminates the ICRF (by using the ICRF source as a calibrator and investigating the correlated motion of the other in–beam sources). This could be undertaken commensally with other astrometric projects using these calibrators. However, it would be necessary to obtain a deep image of the field around the source with a lower resolution instrument to first identify the potential VLBI sources.

6 Conclusions

The PSRπ program, which will measure 60 pulsar parallaxes to an accuracy of better than 50 μas, is underway with the VLBA. A new capability of the DiFX software correlator has been used to greatly speed up the identification of the in–beam calibrators necessary to reach this level of accuracy, with over 7,000 potential targets imaged using less than 80 hours of observing time. Once completed, the PSRπ program will provide the necessary information for a substantial improvement in the Galactic electron density distribution model, and the improved distance information for the pulsar population (both directly for some pulsars and through the model refinement for the remainder) will be used to update models of the pulsar velocity and luminosity distributions. Finally, the PSRπ dataset will provide opportunities to explore calibration techniques relevant to future interferometers such as the SKA.

References

R. H. Becker, R. L. White, & D. J. Helfand, 1995, ApJ, 450, 559
F. Camilo, S. M. Ransom, B. M. Gaensler, P. O. Slane, D. R. Lorimer, J. Reynolds, R. N. Manchester, & S. S. Murray, 2006, ApJ, 637, 456
S. Chatterjee, W. F. Brisken, W. H. T. Vlemmings, W. M. Goss, T. J. W. Lazio, J. M. Cordes, S. E. Thorsett, E. B. Fomalont, A. G. Lyne, & M. Kramer, 2009, ApJ, 698, 250
S. Chatterjee, J. M. Cordes, W. H. T. Vlemmings, Z. Arzoumanian, W. M. Goss, & T. J. W. Lazio, 2004, ApJ, 604, 339
S. Chatterjee, W. H. T. Vlemmings, W. F. Brisken, T. J. W. Lazio, J. M. Cordes, W. M. Goss, S. E. Thorsett, E. B. Fomalont, A. G. Lyne, & M. Kramer, 2005, ApJL, 630, L61
J. J. Condon, W. D. Cotton, E. W. Greisen, Q. F. Yin, R. A. Perley, G. B. Taylor, & J. J. Broderick, 1998, AJ, 115, 1693
J. M. Cordes & T. J. W. Lazio, 2002, ArXiv e-prints, 0207156
A. T. Deller, W. F. Brisken, C. J. Phillips, J. Morgan, W. Alef, R. Cappallo, E. Middelberg, J. Romney, H. Rottmann, S. J. Tingay, & R. Wayth, 2011, PASP, 123, 901
A. T. Deller, S. J. Tingay, M. Bailes, & J. E. Reynolds, 2009, ApJ, 701, 1243
A. T. Deller, S. J. Tingay, M. Bailes, & C. West, 2007, PASP, 119, 318

A. T. Deller, J. P. W. Verbiest, S. J. Tingay, & M. Bailes, 2008, ApJL, 685, L67
A. W. Hotan, M. Bailes, & S. M. Ord, 2006, MNRAS, 369, 1502
D. R. Lorimer, 2008, Living Reviews in Relativity, 11, 8
D. R. Lorimer, A. J. Faulkner, A. G. Lyne, R. N. Manchester, M. Kramer, M. A. McLaughlin, G. Hobbs, A. Possenti, I. H. Stairs, F. Camilo, M. Burgay, N. D'Amico, A. Corongiu, & F. Crawford, 2006, MNRAS, 372, 777
J. H. Taylor & J. M. Cordes, 1993, ApJ, 411, 674
S. E. Thorsett, W. F. Brisken, & W. M. Goss, 2002, ApJL, 573, L111
O. Titov, S. B. Lambert, & A.-M. Gontier, 2011, A&A, 529, A91+

Index of authors